



National Library of Canada

Cataloguing Branch
Canadian Theses Division

Ottawa, Canada
K1A 0N4

Bibliothèque nationale du Canada

Direction du catalogage
Division des thèses canadiennes

NOTICE

The quality of this microfiche is heavily dependent upon the quality of the original thesis submitted for microfilming. Every effort has been made to ensure the highest quality of reproduction possible.

If pages are missing, contact the university which granted the degree.

Some pages may have indistinct print especially if the original pages were typed with a poor typewriter ribbon or if the university sent us a poor photocopy.

Previously copyrighted materials (journal articles, published tests, etc.) are not filmed.

Reproduction in full or in part of this film is governed by the Canadian Copyright Act, R.S.C. 1970, c. C-30. Please read the authorization forms which accompany this thesis.

**THIS DISSERTATION
HAS BEEN MICROFILMED
EXACTLY AS RECEIVED**

AVIS

La qualité de cette microfiche dépend grandement de la qualité de la thèse soumise au microfilmage. Nous avons tout fait pour assurer une qualité supérieure de reproduction.

S'il manque des pages, veuillez communiquer avec l'université qui a conféré le grade.

La qualité d'impression de certaines pages peut laisser à désirer, surtout si les pages originales ont été dactylographiées à l'aide d'un ruban usé ou si l'université nous a fait parvenir une photocopie de mauvaise qualité.

Les documents qui font déjà l'objet d'un droit d'auteur (articles de revue, examens publiés, etc.) ne sont pas microfilmés.

La reproduction, même partielle, de ce microfilm est soumise à la Loi canadienne sur le droit d'auteur, SRC 1970, c. C-30. Veuillez prendre connaissance des formules d'autorisation qui accompagnent cette thèse.

**LA THÈSE A ÉTÉ
MICROFILMÉE TELLE QUE
NOUS L'AVONS REÇUE**



UNIVERSITÉ D'OTTAWA
UNIVERSITY OF OTTAWA

ADSORPTION OF GAS MIXTURES ON SILICA GEL

by

Denis Viateur Gravelle

A thesis submitted to the School of Graduate Studies
in partial fulfillment of the requirements for the
degree of Ph.D. in Chemical Engineering

UNIVERSITY OF OTTAWA
OTTAWA, CANADA, 1975

ABSTRACT

Adsorption isotherms of some gaseous mixtures and their pure constituents have been determined experimentally with a Cahn electrobalance assembly. The investigation was carried out at subatmospheric pressures and at temperatures ranging from -10°C to 50°C . The three binary systems adsorbed by silica gel were $\text{C}_2\text{H}_4 - \text{C}_2\text{H}_6$, $\text{CO}_2 - \text{C}_2\text{H}_6$ and $\text{C}_3\text{H}_8 - \text{CO}_2$.

An exact thermodynamic relationship, representing the equilibrium between the gas phase and the adsorbed gas, has been used to obtain thermodynamic properties on the adsorbed phase which cannot be measured directly.

Fugacity equations relating the equilibrium between the gas phase and the adsorbed phase have been obtained from a rigorous thermodynamic treatment. Description of measured phase equilibria has been successfully accomplished when these equations are combined with the analog of the Redlich-Kwong equation of state.

Following a procedure analogous to that employed by Chang and Lu in vapor-liquid equilibrium studies, the coefficients of the equation of state for the adsorbed phase have been obtained from the isotherms for the pure components.

The mixing rules employed in vapor-liquid equilibria have been extended to gas adsorption equilibria. These rules require the critical properties of the gases, an interaction constant, and two coefficients to be obtained from pure component

adsorption isotherms constituting the binary mixture considered.

The results obtained from our proposed method for predicting adsorption equilibria agree well with the experimental values. The difference between the calculated and measured values of the equilibrium properties for the binary systems investigated in this work are summarized in the following table:

SYSTEM	ΔP %	$\Delta \sigma$ %	ΔX %	Overall %
$\text{CO}_2 - \text{C}_2\text{H}_6$	5.06	2.88	5.26	4.40
$\text{C}_2\text{H}_4 - \text{C}_2\text{H}_6$	3.86	3.72	3.37	3.63
$\text{C}_3\text{H}_8 - \text{CO}_2$	10.69	1.28	7.10	6.33

ACKNOWLEDGEMENT

The author is indebted to his research supervisor, Professor Benjamin C.-Y. Lu, for his guidance and encouragement given throughout the course of this investigation, for his readiness to discuss problems, and for his gratuity in sharing his wide experience in both academic and administrative matters. The author has known Professor Lu through his undergraduate and graduate teachings of chemical engineering thermodynamics and his supervision of an undergraduate and Master's thesis. The author feels that mutual understanding and friendship has evolved throughout the years of studies in this department, and sincerely hopes that this association will continue on for years to come.

The author has appreciated greatly the helpful discussions proffered by the members of the Department of Chemical Engineering. He is also grateful to Dr. S.-D. Chang for pointing out in the early stages of this work the possible analogies existing between gas adsorption with vapor-liquid equilibrium studies. He is thankful to Dr. Jim L. Argo for his enthusiastic participation in bringing out constructive criticisms to the final draft of this thesis.

The author wishes to extend his thanks to Mr. Frank Giacobbi for his assistance in administrative matters and to Mr. G. Gasperetti for his assistance in constructing and improving the experimental assembly.

Financial support provided by the National Research Council of Canada through a bursary and an operating grant to Professor Lu, and an Ontario Graduate Fellowship are gratefully acknowledged.

Many thanks are extended to Mlle Diane Boisvenue who has spent countless hours in typing this thesis.

Finally, I wish to express my sincere admiration to my wife, Hélène, whose faith, love and courage have contributed in many ways to make this study possible.

TABLE OF CONTENTS

	ABSTRACT	i
	ACKNOWLEDGEMENT	iii
	LIST OF FIGURES	xi
	LIST OF TABLES	xvii
	NOMENCLATURE	xxi
	INTRODUCTION	1
CHAPTER I	LITERATURE SURVEY OF GAS-SOLID EQUILIBRIA	5
I.A	Measured Adsorption Isotherms	5
I.B	Experimental Methods for the Determination of Gas-Solid Equilibria	6
I.B.1	Manometric Method	8
I.B.2	Gravimetric Method	9
I.C	Correlation and Prediction Methods	12
I.C.1	Brunauer - Emmett - Teller Equation - (BET)	12
I.C.2	Isosteric Heat of Adsorption	17
I.C.3	Equation of State	18
I.C.4	Redlich-Kwong Equation of State	22
I.C.5	Ideal Adsorbed Solution Theory	27
I.C.6	Pitzer's Correlation	28
CHAPTER II	THERMODYNAMIC CONSIDERATIONS OF GAS-SOLID EQUILIBRIA	30

Table of Contents (Cont'd)

II.A	Phase Equilibria From Exact Thermodynamic Relationship	30
II.A.1	The Adsorbed Phase	31
II.A.2	Gibbs Adsorption Isotherm	32
II.A.3	Equilibrium Conditions	33
II.A.4	Evaluation of γ and x_1	35
II.B	Thermodynamic Equations for the Fugacity	38
II.B.1	Mixed Adsorbate Fugacity	39
II.B.2	Fugacity of a Component in the Mixed Adsorbate	42
II.B.3	Experimental Fugacities	44
II.C	Adsorbed Phase Equation of State	47
II.C.1	Gibbs Adsorption Isotherm	48
II.C.2	Spreading Pressure	49
II.C.3	Gas Phase Pressure	50
II.C.4	Analog of the Redlich-Kwong Equation of State	51
II.C.4.a	de Boer's Parameter Evaluation Method	52
II.C.4.b	Temperature Dependence of the Characteristic Parameters	53
II.C.5	Fugacity of Pure Adsorbate	54
II.C.6	Component Fugacity in Mixed Adsorbate	56
II.C.6.a	Mixing Rules	56
II.C.6.b	Fugacity Equation	59

Table of Content (Cont'd)

CHAPTER III	EXPERIMENTAL STUDY OF GAS-SOLID EQUILIBRIA	61
III.A	Materials	62
III.A.1	Gas Supply	62
III.A.2	Adsorbent	63
III.A.2.a	Surface Activation	63
III.A.2.b	Specific Surface Area	66
III.B	Gravimetric Adsorption System	68
III.B.1	Apparatus	68
III.B.1.a	Cahn Electrobalance Assembly	72
III.B.1.b	Vacuum Unit	72
III.B.1.c	Pressure Measuring Unit	73
III.B.1.d	Feed and Flow-thro Unit	74
III.B.1.e	Temperature Control and Measurement Unit	74
III.B.2	Calibration	76
III.B.2.a	Cahn RG Electrobalance	76
III.B.2.b	Precision Pressure Gage	78
III.B.2.c	Temperature Measurement	80
III.B.3	Experimental Procedure	80
III.B.4	Equilibration	84
III.B.5	Experimental Results	85
III.B.6	Reproducibility of Adsorption Equilibria	86
III.B.7	Hysteresis	96
III.B.8	Correction Factors	97

Table of Contents (Cont'd)

III.B.8.a	Buoyancy Effects	99
III.B.8.b	Thermomolecular Flow	99
III.C	Volumetric Adsorption System	101
III.C.1	Apparatus	101
III.C.2	Calibration	104
III.C.2.a	Bulb Volume	104
III.C.2.b	Manifold and Dead Space Volume	105
III.C.2.c	Gas Partitioner	106
III.C.2.d	Temperature Calibration	111
III.C.3	Experimental Procedure	111
III.C.4	Experimental Results	113
III.C.5	Reproducibility	114
CHAPTER IV	CORRELATION AND PREDICTION OF GAS-SOLID EQUILIBRIA	119
IV.A	Experimentally Determined Adsorption Isotherms	121
IV.A.1	Specific Surface of the Adsorbent	121
IV.A.2	Empirical Representation of the Adsorption Isotherms	122
IV.A.3	Data Comparison with the Literature	124
IV.A.3.a	Adsorption Isotherms	124
IV.A.3.b	Heat of Adsorption	124

Table of Contents (Cont'd)

IV.A.4	Spreading Pressure Calculation	130
IV.B	Pure Component Adsorption	130
IV.B.1	Ideal Values of the Parameters α and β	132
IV.B.2	Evaluation of the Parameters by the Method of de Boer	135
IV.B.3	Evaluation of the Parameters by the Method of Chang-Lu	141
IV.B.4	Some Correlations Considered for α and β	151
IV.B.4.a	Characteristic Parameter Correlation	151
IV.B.4.b	Compressibility Factor Correlation	156
IV.C	Mixed Adsorption Equilibria	163
IV.C.1.a	Measured Phase Equilibria with the Gravimetric Method	163
IV.C.1.b	Measured Phase Equilibria with the Manometric Method	168
IV.C.2	Ideal Adsorption Solution Theory	178
IV.C.3	Analog of the Redlich-Kwong Equation of State	182
IV.C.3.a	Adsorbed Phase Equilibria Prediction	182
IV.C.3.b	Measured Pure Component Properties	186
IV.C.3.c	Measured Mixture Properties	189
IV.C.3.d	Comparison Between Measured and Calculated Phase Equilibria	190
IV.C.3.e	Prediction of Gas Adsorption at Elevated Pressures	211

Table of Contents (Cont'd)

IV.C.3.f	Practical Application	216
IV.C.3.g	Results of the Prediction of Gas-Solid Equilibria	220
CHAPTER V	SUMMARY AND CONCLUSIONS	224
	BIBLIOGRAPHY	231
	APPENDICES	238

LIST OF FIGURES

I.1	Approach Underlying this Investigation.	4
I.2	Manometric Adsorption System.	10
I.3	Gravimetric Adsorption System.	11
I.4	Useful Characteristics of the Methods Employed in the Measurement of Phase Equilibria.	15
III.1	Gravimetric Adsorption Apparatus.	69
III.2	Strip Chart Recorder Trace of an Equilibrium Determination.	82
III.3.1	Adsorption Isotherm at 263.2°K for C ₃ H ₈ - CO ₂ and CO ₂ - C ₂ H ₆ Systems.	87
III.3.2	Adsorption Isotherm at 273.2°K for C ₃ H ₈ - CO ₂ and CO ₂ - C ₂ H ₆ Systems.	88
III.3.3	Adsorption Isotherm at 298.2°K for C ₃ H ₈ - CO ₂ and CO ₂ - C ₂ H ₆ Systems.	89
III.3.4	Adsorption Isotherm at 323.2°K for C ₃ H ₈ - CO ₂ System.	90
III.4	Adsorption Isotherm Reproducibility at 273.2°K for C ₂ H ₆ on the Same Sample.	91
III.5	Adsorption Isotherm Reproducibility at 273.2°K for C ₂ H ₄ on Different Samples.	93
III.6	Adsorption Isotherm Reproducibility at 298.2°K for C ₂ H ₄ and C ₂ H ₆ on the Same Sample.	94

List of Figures (Cont'd)

III.7	Mixture Adsorption Isotherm Reproducibility at 298.2°K for C ₃ H ₈ and CO ₂ on the Same Sample.	95
III.8	Isobaric Adsorption-Desorption for the System C ₃ H ₈ - CO ₂ .	98
III.9	Buoyancy Correction.	100
III.10	Manometric Adsorption Apparatus.	102
III.11	Strip Chart Recorder Trace of the Gas Partitioner Calibration for 74.94% Propane with Carbon dioxide.	107
III.12.	Gas Partitioner Calibration for C ₃ H ₈ - CO ₂ Mixture.	109
III.13	Gas Partitioner Calibration for CO ₂ - C ₂ H ₆ Mixture.	110
IV.1	Adsorption of C ₃ H ₈ at 750 mmHg.	123
IV.2	Adsorption Isosteres for CO ₂ .	127
IV.3	Isosteric Heat of Adsorption for CO ₂ .	128
IV.4	Entropy of Adsorption for CO ₂ .	129
IV.5	Prediction of π for CO ₂ at 273.2°K Using Different Equations of State - Ideal Values of α and β .	134
IV.6	Selection of β by de Boer's Method.	136
IV.7	Prediction of π for CO ₂ at 273.2°K - Method of de Boer Applied to the Redlich-Kwong Analog.	138

List of Figures (Cont'd)

IV.8	Prediction of π for CO_2 at 323.2°K Using Different Equations of State.	139
IV.9	Prediction of π for CO_2 at 263.2°K Using Different Equations of State.	140
IV.10	Pressure Dependent α and β of the Redlich-Kwong Equation Analog at 273.2°K for CO_2 - Method of Chang-Lu.	143
IV.11	Temperature Dependent α at 750 mmHg - Method of Chang-Lu.	144
IV.12	Temperature Dependent β at 750 mmHg - Method of Chang-Lu.	145
IV.13	Temperature Effect on π -dependent α for C_2H_6 .	146
IV.14	Temperature Effect on π -dependent β for C_2H_6 .	147
IV.15	Temperature Effect on π -dependent α for CO_2 .	148
IV.16	Temperature Effect on π -dependent β for CO_2 .	149
IV.17	π -dependent β for CO_2 and C_2H_6 at 273.2°K .	150
IV.18	Reduced Temperature Effect on Ω_a with ω .	153
IV.19	Reduced Temperature Effect on Ω_b with ω .	154
IV.20	Reduced Temperature Dependence of Ω_b for Different Adsorbates.	155

List of Figures (Cont'd)

IV.21	Adsorbed Phase Compressibility Factors, Z , and Acentric Factor, ω , for Different Adsorbates at 750 mmHg.	157
IV.22	Temperature Effect on the Pressure Dependent Z for C_3H_8 .	158
IV.23	Temperature Dependent Z for Different Adsorbates at 750 mmHg.	159
IV.24	Reduced Temperature Dependent Z for Different Adsorbates.	160
IV.25	Reduced Pressure Dependent Z for Different Adsorbates.	161
IV.26	Reduced Temperature Effect on Z with ω .	162
IV.27	Effect of Y on the Temperature Dependent X for the System $C_3H_8 - CO_2$ at 750 mmHg.	165
IV.28a	Composition Diagram for $C_2H_4 - C_2H_6$ and $CO_2 - C_2H_6$ at $263.2^\circ K$ and 750 mmHg - Gravimetric Method.	167
IV.28b	Composition Diagram for $CO_2 - C_2H_6$ and $C_3H_8 - CO_2$ at $263.2^\circ K$ and 750 mmHg - Gravimetric Method.	167
IV.29	Comparison Between Two Methods of Measuring Phase Equilibria for $CO_2 - C_2H_6$ at $273.2^\circ K$ and 342.1 mmHg.	172

List of Figures (Cont'd)

IV.30	Comparison Between Two Methods of Measuring Phase Equilibria for $\text{CO}_2 - \text{C}_2\text{H}_6$ at 273.2°K and 390.18 mmHg.	173
IV.31	Comparison Between Two Methods of Measuring Phase Equilibria for $\text{C}_3\text{H}_8 - \text{CO}_2$ at 273.2°K and 329.3 mmHg.	174
IV.32	Comparison Between Two Methods of Measuring Phase Equilibria for $\text{CO}_2 - \text{C}_2\text{H}_6$ at 273.2°K and 329.3 mmHg.	175
IV.33	Effect of Y on the Temperature Dependent Moles Adsorbed for $\text{C}_3\text{H}_8 - \text{CO}_2$ at 273.2°K and 350 mmHg.	176
IV.34	Comparison Between Two Methods of Measuring Molar Compositions (X-Y) for $\text{C}_3\text{H}_8 - \text{CO}_2$ at 273.2°K and 350 mmHg.	177
IV.35	Average Deviation in Adsorbed Phase Composition with Temperature.	179
IV.36a	Comparison Between Calculated and Measured Composition Diagram for $\text{C}_3\text{H}_8 - \text{CO}_2$ at 263.2°K and 300 mmHg - Ideal Adsorption Solution Theory.	180
IV.36b	Comparison Between Calculated and Measured Composition Diagram for $\text{C}_2\text{H}_4 - \text{C}_2\text{H}_6$ at 298.2°K and 300 mmHg - Ideal Adsorption Solution Theory.	181

List of Figures (Cont'd)

IV.37	Supporting Data for the Prediction of Mixed Equilibria using the Analog of the Redlich-Kwong Equation of State.	187
IV.38	Pure Component Supporting Data of C ₂ H ₄ at 298.2°K for Phase Equilibrium Predictions.	188
IV.39	Temperature Dependence of C _{ij} for Different Binary Mixtures.	194
IV.40	Comparison Between Calculated and Measured Phase Equilibria for C ₂ H ₄ - C ₂ H ₆ at 298.2°K and $\frac{\pi A}{RT} = 0.250$ - Our Proposed Method.	208
IV.41	Comparison Between Calculated and Measured Phase Equilibria for C ₂ H ₄ - C ₂ H ₆ at 298.2°K and $\frac{\pi A}{RT} = 0.771$ - Our Proposed Method.	210
IV.43	Comparison Between Calculated and Measured Phase Equilibria for C ₂ H ₄ - C ₂ H ₆ at 298.2°K and $\frac{\pi A}{RT} = 1.101$ - Our Proposed Method.	215
IV.42	Proposed Methods for the Evaluation of α and β at Elevated Pressures.	212
IV.44	Comparison Between Calculated and Measured Phase Equilibria for C ₂ H ₄ - C ₂ H ₆ at 298.2°K and 300 mmHg - Our Proposed Method.	217
IV.45	Comparison Between Calculated and Measured Phase Equilibria for C ₂ H ₄ - C ₂ H ₆ at 298.2°K and 750 mmHg - Our Proposed Method.	218

LIST OF TABLES

I.1	Literature Survey of Gaseous Adsorption on Silica Gel.	7
I.2	General Properties of the Manometric and Gravimetric Methods used in the Study of Phase Equilibria.	13
I.3	Ideal Adsorbate Interaction Parameters.	21
III.1	Precision Pressure Gage Calibration Chart.	79
III.2	Measured Adsorption Equilibrium Data.	83
III.3	Measured Adsorption Isotherms of Binary Systems Obtained with the Cahn Electrobalance Assembly.	242
III.4	Corrected Adsorption Isotherms of Binary Systems Measured with the Cahn Electrobalance Assembly.	264
III.5	Gas Partitioner Calibration Data.	108
III.6	Equilibrium Gas Phase Composition Analysis.	115
III.7	Measured Mixture Adsorption by the Manometric Method.	115½
IV.1	Specific Surface Area of Silica Gel.	240
IV.2	Pure Component Adsorption Isotherms with Spreading Pressure.	264

List of Tables (Cont'd)

IV.3	A Comparison of Predicted Spreading Pressures using Different Equations of State.	133
IV.4	Parameters of the Analog of the Redlich-Kwong Equation of State Obtained by the Method of de Boer.	137
IV.5	Parameters of the Analog of the Redlich-Kwong Equation of State Obtained by the Method of Chang-Lu and Compressibilities of the Adsorbed Phase.	276
IV.6	Measured Values of the Adsorbed Phase Properties in Binary Mixtures.	292
IV.7	Adsorbed Phase Compositions at 750 mmHg.	166
IV.8	Measured Phase Equilibria for the System $\text{CO}_2 - \text{C}_2\text{H}_6$ at 273.2°K using the Manometric Method.	170
IV.9	Measured Phase Equilibria for the System $\text{C}_3\text{H}_8 - \text{CO}_2$ at 273.2°K using the Manometric Method.	171
IV.10	Phase Equilibrium Prediction for all Systems, Temperatures and Spreading Pressures	192
IV.11	Temperature Dependent Values of $C_{ij} - C_{ij,opt}$	103

List of Tables (Cont'd)

IV.12	Spreading Pressure and Temperature Dependence of C_{ij} for the System $C_3H_8 - CO_2$.	195
IV.13	Per cent Deviation for all T and π for Each System in P, σ and X.	196
IV.14	Comparison Between Calculated and Measured Phase Equilibria when Vapor- Liquid Interaction Constant is Extended to Gas-Solid Equilibria.	199
IV.15	Comparison Between Calculated and Measured Phase Equilibrium Data — Computer Output.	205
IV.16	Prediction of Phase Equilibrium Data — Computer Output.	206
IV.17	Comparison Between Calculated and Measured Phase Equilibria for the System $C_2H_4 - C_2H_6$ at $298.2^\circ K$ and $\frac{\pi A}{RT} = 0.25$.	207
IV.18	Comparison Between Calculated and Measured Phase Equilibria for the System $C_2H_4 - C_2H_6$ at $298.2^\circ K$ and $\frac{\pi A}{RT} = 0.771$.	109
IV.19	Comparison Between Calculated and Measured Phase Equilibria for the System $C_2H_4 - C_2H_6$ at $298.2^\circ K$ and $\frac{\pi A}{RT} = 1.014$.	214

List of Tables (Cont'd)

IV.20	Comparison Between Calculated and Measured Phase Equilibria at 298.2°K for the Binary System C ₂ H ₄ - C ₂ H ₆ .	219
IV.21	Results of the Predictions Methods in Gas-Solid Equilibria.	223

NOMENCLATURE

a	Parameter in Equation I.21
b	Parameter in Equation I.22
c	Parameter in Equation I.1
f	Fugacity
h	Parameter in Equations I.19, II.61
k	Constant defined in Equations II.78, II.78a
k_{ij}	Interaction constant employed in Equations I.37, II.78
$k_{ij,ads}$	Negative value of the interaction constant, k_{ij} , employed in Equation II.78
m	Mass of gas adsorbed
n	Moles of gas adsorbed
n'	Parameter in Equation I.1
v	Molar volume
x	Molar composition of gas adsorbed
y	Molar composition of gas
A	Specific surface area of the adsorbent
A^2	Parameter in Equations I.21, II.60
B	Parameter in Equations I.21, II.60
C_{ij}	Interaction constant in Equations I.44, IV.77
G	Gibbs free energy
K	Limiting slope (Equation II.37)
K'	Integration constant in Equation II.53
M	Molecular weight of an adsorbed mixture (Equation II.13)

Nomenclature (Cont'd)

P	Gas pressure
Q_{st}	Isosteric heat of adsorption
R	Universal gas constant
S	Entropy
T	Temperature
V	Volume
V'_m	Parameter in Equation I.1
X	Molar composition of gas adsorbed
Y	Molar composition of gas adsorbed
Z	Compressibility factor (Equations I.19, I.29, II.65)
α	Parameter of Equations II.62, II.52
β	Parameter of Equations II.63, II.52
σ	Molar area of gas adsorbed
$\theta = \beta/\sigma$	Fraction β/σ , or b/v
π	Spreading pressure
μ	Chemical potential
ϕ	Fugacity coefficient
ω	Acentric factor
Ω_a, Ω_b	Parameters in Equations I.21 and I.22

Superscripts

o	Standard state
.	Solution property
*	Low pressure property

Nomenclature (Cont'd)

Subscripts

d	Dead space
e	Equilibrium conditions
g	Gas phase
i	Initial conditions
i, j, 1, 2	Component identification
ij	Mixture property
m	Manifold
L	Liquid phase
V	Vapor phase

INTRODUCTION

Purification and recovery of industrial gases by physical adsorption as a separation process is today done on a large scale (1). Engineering design of adsorbers for separating gas mixtures requires among other things, pure component isotherms for each material present and a method for predicting the adsorptive properties of a mixture from the pure component isotherms (2). In many instances, experimental data on adsorption isotherms are not always available in the desired region of temperature, pressure and composition. These data are not only necessary for equipment design; they are also needed to test theories or to work on an equation of state. Ultimately, one must turn to predictive or correlative techniques to obtain the surface properties. The accuracy of a predictive method for mixed gas, adsorption phase equilibria requires a basis for comparison, free from any mathematical modeling. Thus a certain "brand" of data are needed which are readily obtained from a well designed experimental technique and can satisfy a fundamental thermodynamic relationship (3).

The objectives of this thesis were to set-up an experimental apparatus capable of yielding data satisfying an exact thermodynamic relation, and to work on an equation of state capable of predicting mixed gas adsorption equilibria from a knowledge of the pure component adsorption isotherms only.

Adsorption isotherms have been determined

experimentally for the binary systems of $C_2H_6 - C_2H_4$, $C_2H_6 - CO_2$ and $CO_2 - C_3H_8$ with their pure constituents on silica gel for temperatures ranging from $50^\circ C$ to $-10^\circ C$. The investigation was carried out at subatmospheric pressures using a Cahn electro-balance to measure the total mass adsorbed at the corresponding system pressure. These data were employed to calculate the surface properties using an exact thermodynamic relation.

The calculated adsorbed phase properties of the binary mixtures for the systems $C_3H_8 - CO_2$ and $CO_2 - C_2H_6$ at $0.0^\circ C$ have been verified with a constant volume apparatus equipped with a recirculating pump.

The prediction of the surface properties of a mixture can be obtained by applying a) the ideal solution theory or b) an equation of state to the adsorbed phase. An expression for the ideal adsorbed solution theory, analogous to Raoult's law in vapor-liquid equilibria, has been used to compute the surface properties and the Redlich-Kwong equation of state usually applied to the liquid or vapor phase has been extended to the adsorbed phase. The predicted surface properties obtained from these two correlations were compared with those obtained using the exact thermodynamic relation.

The general format of the subject matter of this thesis is as follows.

A review and discussion of the pertinent literature are first presented in Chapter I. In Chapter II, some thermodynamic considerations of gas-solid equilibria are developed

which lead to a statement of a very useful exact thermodynamic relation, and to the derivation of equations necessary for the calculation of pure and mixed adsorbed phase properties. The description of the equipment and procedures employed in the study of gas-solid equilibria, and the experimental results form the subject of Chapter III. In Chapter IV, we present a discussion of the results of the correlation of experimentally determined isotherms, and of the predictive methods for the calculation of the adsorbed phase properties. Chapter V summarizes the work done in this investigation with some concluding remarks. The general approach followed in this investigation is presented in Figure I.1.

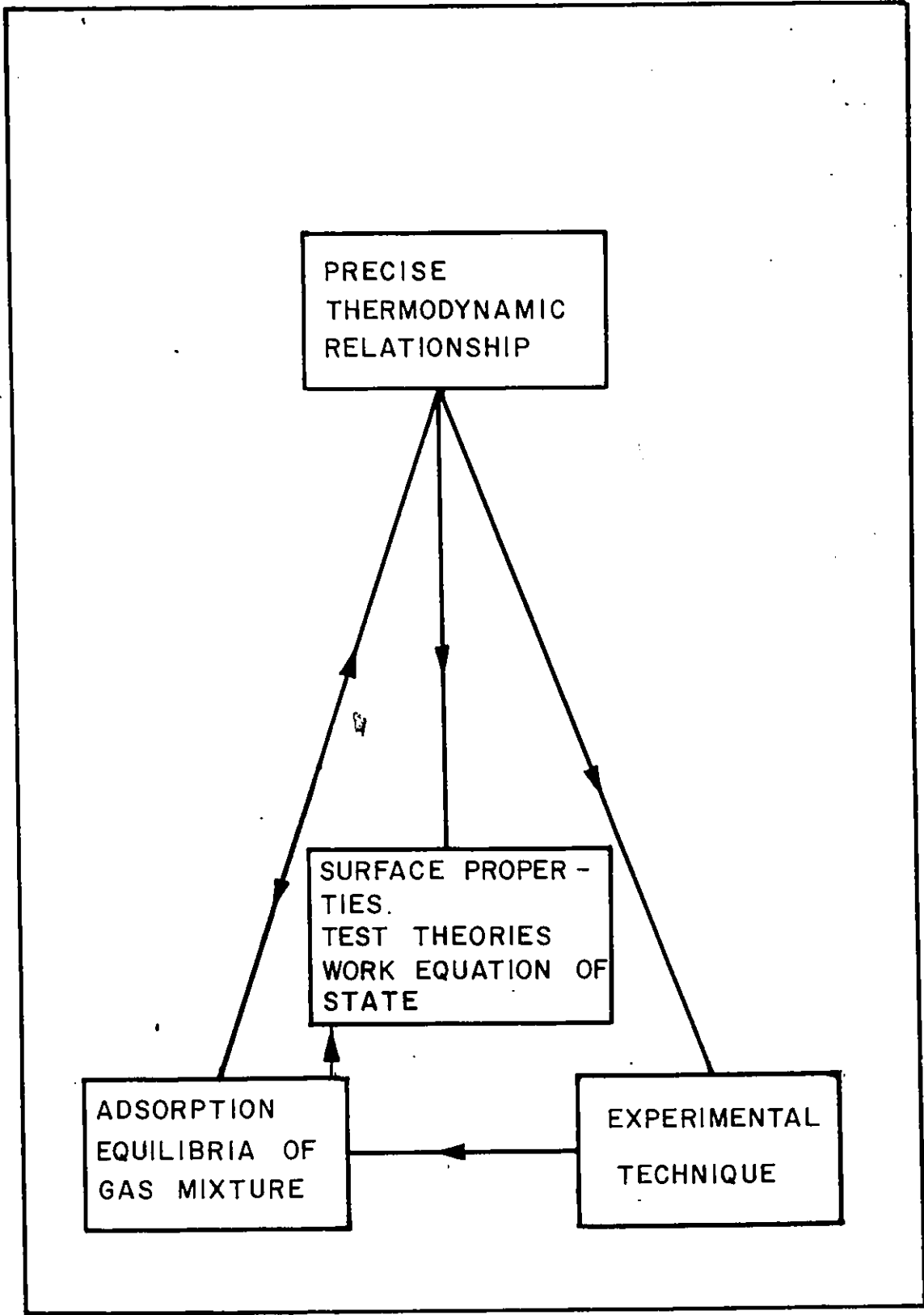


Figure I.1 Approach Underlying this Investigation

CHAPTER I

LITERATURE SURVEY OF GAS-SOLID EQUILIBRIA

Presented in this chapter is a brief survey of the work that has been done on the determination of adsorption isotherms of pure gases and their mixtures on silica gel. Experimental methods for the measurement of gas-solid equilibria are then discussed in the light of their usefulness to this work. Finally, the correlative and predictive methods pertinent to this investigation for the prediction of phase equilibria are reviewed.

I.A Measured Adsorption Isotherms

Physical adsorption has been extensively studied and a comprehensive review of the subject has been done by Young and Crowell (4), Ross and Oliver (5), Flood (6, 7) and others (8) as mentioned in a recent review on the subject (2). Presented in this work is only a brief, selective, survey of the adsorption of gases and their mixtures on silica gel, in particular, for those systems investigated in this work.

The references of Table I.1 are taken from an updated survey (2) and an examination of it leads to the following comments.

Sufficient tabular and graphically reported data for the adsorption of the pure components C_3H_8 , C_2H_6 and C_2H_4 are available covering the pressure range investigated by the

authors, although fewer isotherms are available. Measured data for CO₂ have been obtained only at low temperatures. Furthermore, most of these data were obtained by different workers, hence probably on different grades of silica gel.

The pressure range investigated for the adsorption of mixtures is limited to a few reported isotherms. Data for the binary system C₂H₆ - C₂H₄ are reported graphically and analytically at 25°C and at pressures of 0.33 and 1.3 atm. In many cases the isothermal data reported were not at exactly the same pressure. Data available for C₃H₈ - CO₂ at 0°C and 760 mmHg, however, were found to be unreliable (17).

The scarcity of the adsorption data on silica gel commands the need for more equilibrium data covering a wider temperature range for pressures ranging from 15 to 750 mmHg. The scarcity is especially true for mixtures.

Such data taken on the same sample under controlled laboratory conditions can be used to expand our knowledge about the adsorption process, viz. to permit the correlation of phase equilibria of multicomponent systems through an equation of state and finally to test theories involving phase equilibria prediction.

I.B Experimental Methods for the Determination of Gas-Solid Equilibria

This section is a brief survey of the

TABLE I.1

LITERATURE SURVEY OF GASEOUS ADSORPTION ON SILICA GEL

Pure Component Adsorption Isotherms

Component	Temperature °C	Pressure Range mmHg	Author	Reported Form	Year
C ₃ H ₈	-35	15-732	Maslan(9)	Tabular	1972
	-20	17-762	Maslan(9)	Tabular	1972
	0	25-754	Maslan(9)	Tabular	1972
	25	5-775	Lewis(10)	Tabular	1950
	100	96-753	Lewis(12)	Tabular	1950
	0	16-762	Lewis(12)	Tabular	1950
	40	10-768	Lewis(12)	Tabular	1950
C ₂ H ₄	25	14-764	Lewis(11)	Tabular	1950
	0	2-745	Lewis(12)	Tabular	1950
	40	10-764	Lewis(12)	Tabular	1950
C ₂ H ₆ , C ₃ H ₈	25	10-760	Lewis(13)	Graphical	1950
CO ₂	-195	0-700	Brunauer(15)	Graphical	1937

Mixed Adsorption Isotherms

C ₂ H ₆ -CO ₂	0	760	Jelinek(16)	Tabular	1953
	30	760	Jelinek(16)	Tabular	1953
CO ₂ -C ₃ H ₈	0	760	Jelinek(16)	Tabular	1953
	25	762-774	Lewis(13)	Tabular	1950
	40	770-776	Lewis(13)	Tabular	1950
C ₂ H ₆ -C ₂ H ₄	25	760-230	Lewis(14)	Correlation	1950

techniques employed in the measurement of the adsorption of gases on solids. It is not a comprehensive review on the subject. The advantages associated with each method, which are of value to this investigation, are pointed out.

The two principal approaches are classified as the gravimetric and the manometric methods. The measurable quantities associated with the gravimetric method are the total system pressure and the total mass of gas adsorbed while those with the manometric method are the total gas pressure and the volume of the adsorbed phase. The composition of the gas phase is required when dealing with gaseous mixtures. The temperature of the adsorption cell is also an important controlled variable. The temperature and gas composition are quantities that need to be measured in both techniques.

I.B.1 Manometric Method

In the manometric method, the number of moles of a pure adsorbed gas is calculated from accurate measurements of the pressure, volume and temperature. In addition, the gas phase compositions are needed for mixtures.

The principle underlying this method is the following. The pressure, volume and temperature of a quantity of gas adsorbed is measured and the number of moles present calculated. This material is then brought into contact with the adsorbent and, when constant pressure and temperature readings show the system

to have attained equilibrium, the number of moles remaining in the gas phase is again calculated. The difference between the initial and final values of the number of moles represents the gas transferred to the adsorbed phase.

The accurate determination of the number of moles unadsorbed at equilibrium depends on a precise knowledge of the "dead space" or the space surrounding the adsorbent particles. The dead space volume is usually evaluated by expansion measurements using helium, whose adsorption is assumed to be negligible (4).

The manometric apparatus is illustrated schematically in Figure I.2.

I.B.2 Gravimetric Method

The adsorbent is located at the bottom of an isothermal well in a light bucket suspended from a weighing assembly. The amount of gas adsorbed is obtained directly from the measurements of the weight gained by the adsorbent at equilibrium. The two measurements of final pressure and the quantity of gas adsorbed are independent of each other, unlike in the manometric method where the equilibrium pressure is used in the calculation of the amount adsorbed. The calibration of the weighing mechanism is done by adding known weights to the sample container.

Figure I.3 illustrates schematically the main components found in this adsorption apparatus.

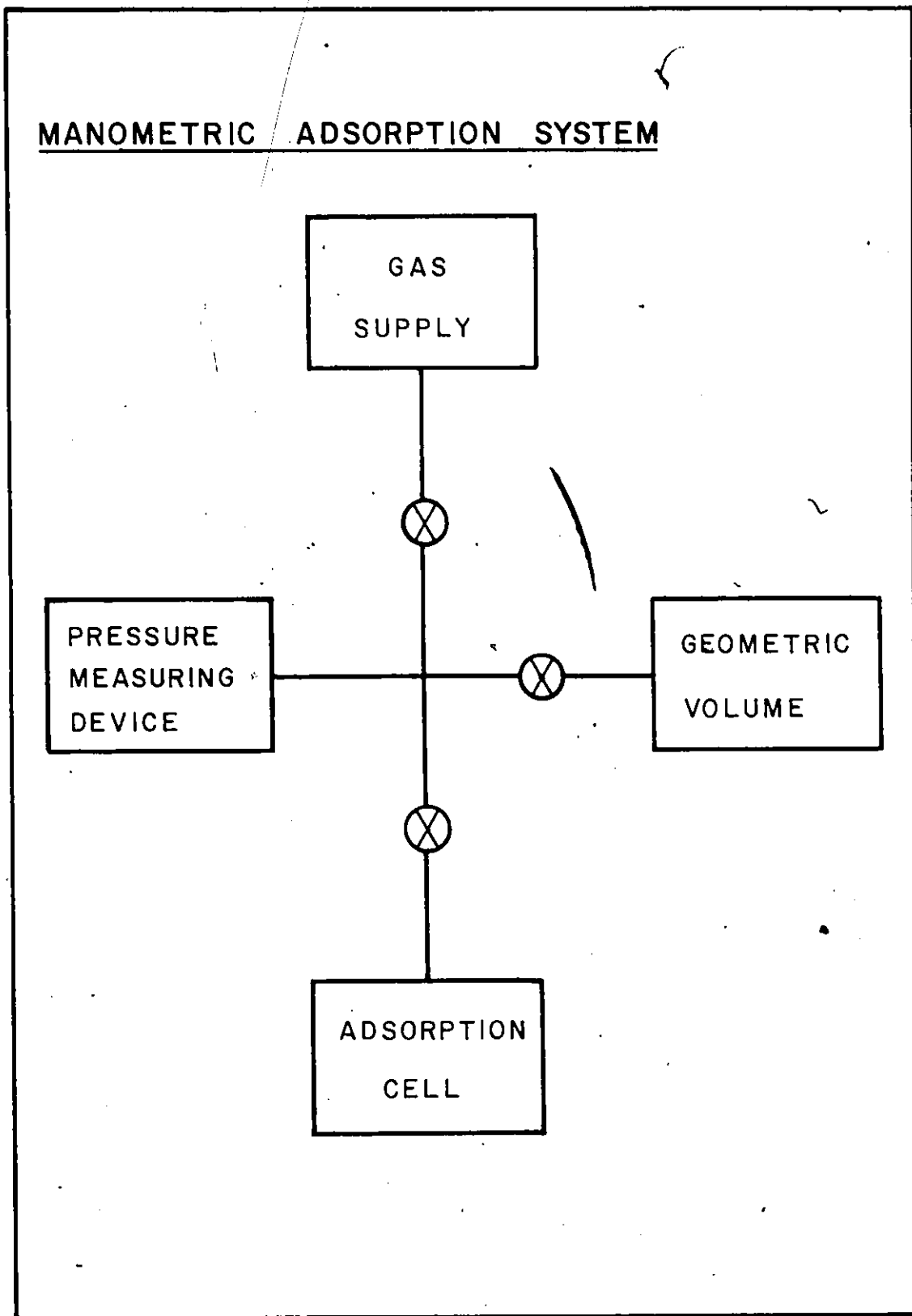


Figure I.2 Manometric Adsorption System

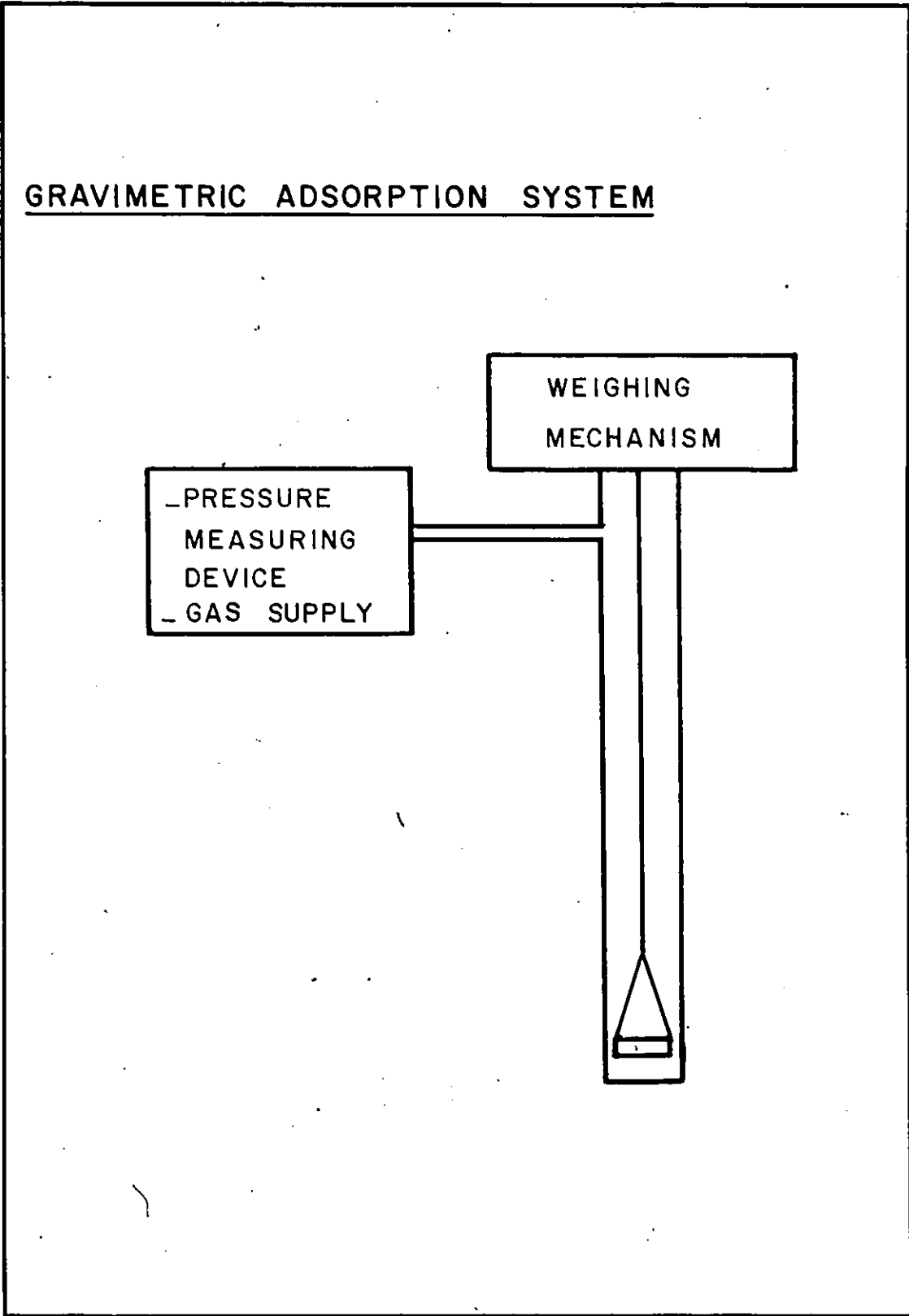


Figure I.3 Gravimetric Adsorption System

Each method has its advantages and inconveniences; both methods have been employed in this investigation. The properties of each method are listed in Table I.2. A gravimetric method, when properly adapted, yields data satisfying an exact thermodynamic relation which is used to calculate the surface properties. These calculated surface properties are then readily verified with a manometric method. This general approach is illustrated schematically in Figure I.4.

I.C Correlation and Prediction Methods

The main items recalled in this section are the different forms of the Brunauer, Emmett and Teller equation (22) and the method for measuring the heat of adsorption from gas adsorption isotherms. Also presented are some of the existing equations of state, such as the Redlich and Kwong (18) equation, and the application of the ideal solution theory (19, 20) to the adsorbed phase. Also, a correlation developed by Pitzer (21) is reviewed.

I.C.1 Brunauer - Emmett - Teller Equation - (BET) - (22)

The BET equation for the isothermal adsorption can be expressed in the form

TABLE I.2

GENERAL PROPERTIES OF THE MANOMETRIC AND GRAVIMETRIC
METHODS USED IN THE STUDY OF PHASE EQUILIBRIA

Manometric

1. Calibration of the volumes in the apparatus are needed because they are required in the calculation of the adsorption of gases.
2. Cumulation of errors are possible because there is an interrelation between the pressure and temperature through the ideal gas law for each equilibrium calculation.
3. Larger samples are needed so as to observe with accuracy the equilibration in the system.
4. Static method is preferred because the measurement of the dosage volume is required.
5. The number of moles of a mixture adsorbed is calculated directly by applying a mass balance and using the ideal gas law.

TABLE I.2 (CONTINUED)

Gravimetric

1. Calibration of the weighing mechanism is easy and flexible.
2. Measurement of the pressure and mass adsorbed are independent of each other.
3. More data are measured in a shorter time and attainment of equilibrium is directly observed.
4. Lends itself easily to "flow-thro" systems.
5. Measures the total mass adsorbed thus the number of moles of a mixture adsorbed are not directly measured.

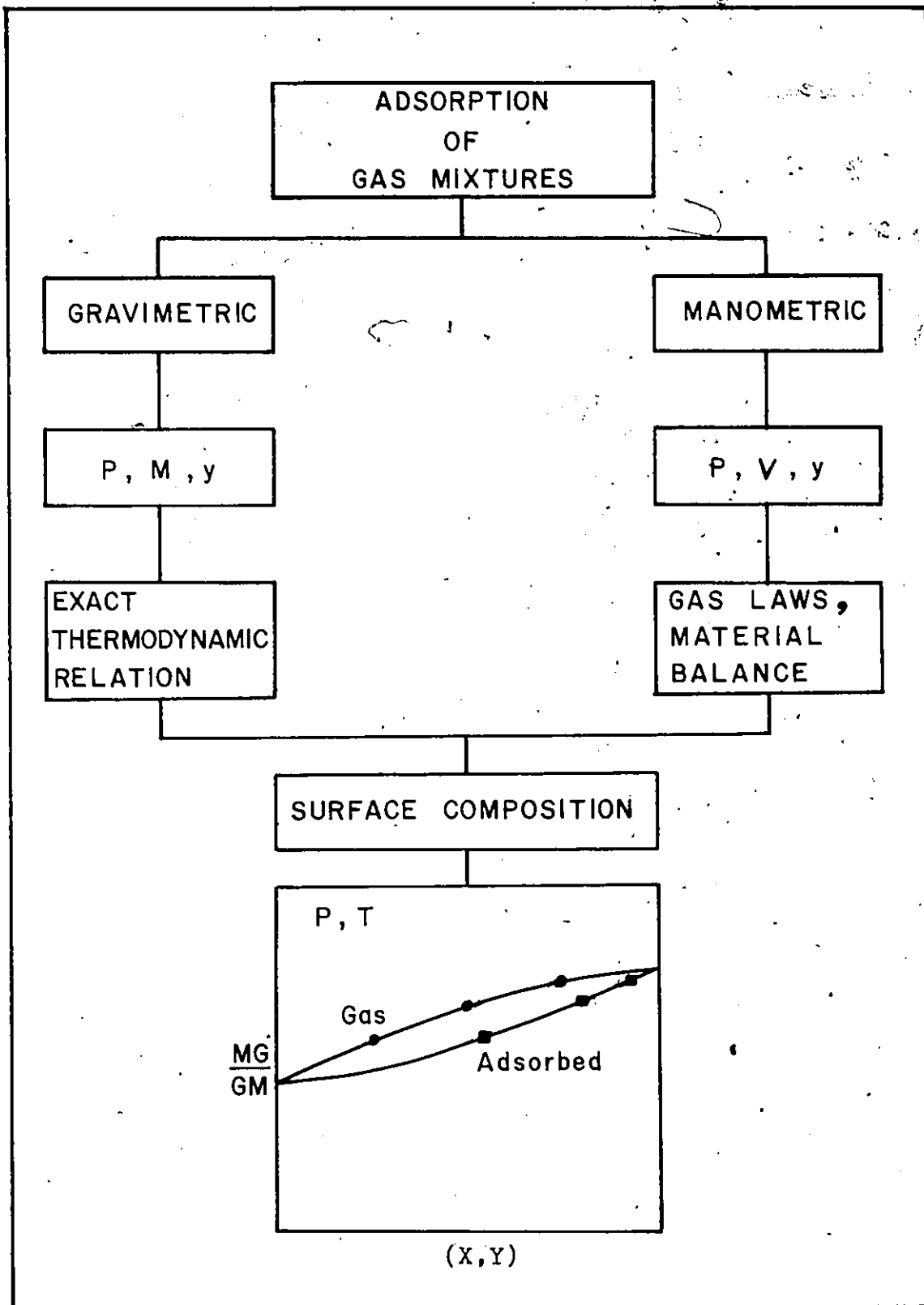


Figure I.4 Useful Characteristics of the Methods Employed in the Measurement of Phase Equilibria

$$V = \frac{V_m cr}{1-r} \left[\frac{1-(n'+1)r^{n'} + nr^{n'+1}}{1+(c-1)r - cr^{n'+1}} \right] \quad \text{I.1}$$

where $r = P/P_0$ relative adsorbate pressure
 V amount of gas adsorbed
 V_m amount of gas necessary to form monolayer
 c related to the heat of adsorption of a monolayer (E_1) and the heat of liquefaction (E_2) by the relation

$$RT \ln c = E_1 - E_2$$

n' number of layers to which the gas is limited

P_0 vapor pressure of liquid nitrogen at 77.4°K.

For the purpose of calculating the specific surface area, Equation I.1 is commonly used in one of its two limiting forms, one of which is the Langmuir equation (8)

$$\frac{r}{V} = \frac{1}{V_m c} + \frac{r}{V_m} \quad n' = 1 \quad \text{I.2}$$

and the other is known of the infinite layers BET equation (22)

$$\frac{r}{V(1-r)} = \frac{1}{V_m c} + \frac{c-1}{V_m c} r \quad n' = \infty \quad \text{I.3}$$

For $n' > 3$ and $x < 0.25$, Equation I.3 is a fair approximation to Equation I.1 provided $c \gg 1$. On the other hand,

Equation I.2 can be used only for isotherms which have an n' value very close to unity.

By a simple algebraic transformation, the n -layer BET Equation I.1 can be put into a more convenient form (23)

$$V = \frac{V_m c \phi(n', r)}{1 + c \theta(n', r)} \quad \text{I.4}$$

where

$$\phi(n', r) = \frac{r(1 - r^{n'}) - n'r^{n'}(1 - r)}{(1 - r)^2} \quad \text{I.5}$$

and

$$\theta(n', r) = \frac{r(1 - r^{n'})}{1 - r} \quad \text{I.6}$$

The Equation I.4 may be rearranged in a linear form

$$\frac{\phi(n', r)}{V} = \frac{1}{V_m c} + \frac{\theta(n', r)}{V_m} \quad \text{I.7}$$

The slope of Equation I.7 is $1/V_m$ while the intercept is $1/V_m c$.

The value of n' is usually selected until Equation I.7 yields a best straight line as directed by the method of least-squares (23, 24).

I.C.2 Isosteric Heat of Adsorption

The isosteric heat of adsorption, Q_{st} , is defined by an

application of the Clausius-Clapeyron equation of the adsorption isostere (65). It is defined by the following equation

$$\left(\frac{\partial P}{\partial T}\right)_{n,A} = \frac{Q_{st}}{T(V_g - V_a)} \quad \text{I.8}$$

in which V_g and V_a are, respectively, the molar volumes of the gas phase and the adsorbed phase. Neglecting the molar volume adsorbed compared with that in the gas phase and assuming the gas to be ideal, Equation I.8 becomes

$$\frac{\partial \ln P}{\partial \left(\frac{1}{T}\right)}_{n,A} = - \frac{Q_{st}}{R} \quad \text{I.9}$$

The isosteric heat, Q_{st} , is a differential molar quantity (4, 65) which varies with the degree of surface coverage, hence with the amount of gas adsorbed, n . It is related to the differential molar entropy of the adsorbed phase (65) \tilde{S}_a , by the following equation,

$$Q_{st} = T \Delta S = T(S_g - \tilde{S}_a) \quad \text{I.10}$$

in which S_g and \tilde{S}_a are, respectively, the molar entropy of the gas phase at temperature T and the differential molar entropy of the adsorbed phase, $(\partial S / \partial n)_{T,A}$ (4).

I.C.3 Equation of State

For a given isotherm, a two-dimensional equation of

state for a pure adsorbed component can take the following form (5):

$$\pi = \frac{RT}{\beta} F(\theta, T) \quad \text{I.11}$$

in which

$$\theta = \frac{\beta}{\sigma} \quad \text{I.12}$$

in which β represents the area of an adsorbed molecule. The adsorbed phase quantities are somewhat different from those of a three-dimensional phase (gas phase). The spreading or surface pressure is represented by the symbol π , whereas, the molar area of the adsorbed phase is represented by σ . The latter is defined by the equation

$$\sigma = \frac{A}{n} \quad \text{I.13}$$

where A and n are, respectively, the specific surface area of the adsorbent and the number of moles of gas adsorbed (moles of adsorbate).

The function $F(\theta, T)$ for various mathematical models of a mobile adsorbed film (5) are listed in the following table.

TYPE	F(θ , T)	
Ideal-gas law	a	I.14
Volmer (25)	$\frac{\theta}{1 - \theta}$	I.15
Hill-de Boer (5)	$\frac{\theta}{1 - \theta} - \frac{a\theta^2}{RT^{1.5} \beta(1 + \theta)}$	I.16

The constants a and β are terms introduced in the equation of state that provide corrections for non-ideality of the adsorbate. It should be noted that the Hill-de Boer equation is the analog of the van der Waals equation of state. The two-dimensional constants a and β are not identical to the customary van der Waals constants a and b for gases but are directly related to the three-dimensional constants a and b by Equations I.17 and I.18

$$a_{id} = a \left(\frac{9}{256b} \right)^{1/3} \quad \text{I.17}$$

and

$$\beta_{id} = 2b \left(\frac{9}{256b} \right)^{1/3} \quad \text{I.18}$$

The constants a and b are listed in Table I.3 along with a_{id} and β_{id} for the adsorbed phase of the components studied in this

TABLE I.3

IDEAL ADSORBATE INTERACTION PARAMETERS

Components	a cm ³ mole ⁻² x10 ⁻¹²	b cm ³ mole ⁻¹	a _{id} cm ² molecule ⁻² x10 ³⁰	β _{id} cm ² molecule ⁻¹ x10 ¹⁶
Ethane	5.49	63.8	153	21.7
Ethylene	4.48	57.1	132	20.0
Propane	8.70	84.4	222	25.8
Carbon dioxide	3.61	42.7	115	16.4

work (5).

The subscript 'id' is used to distinguish the ideal values of α and β from the values obtained from experimental isotherms. Equations I.17 and I.18 hold for simple and ideal situations in which the adsorbed molecules have identical interactions to those in the gas phase.

I.C.4 Redlich-Kwong Equation of State

The equation of Redlich and Kwong is generally recognized as the best simple equation available to represent properties in both the gas and liquid state (26).

The original form of the equation given by Redlich and Kwong (18) is represented in Equations I.19 to I.24

$$Z = \frac{1}{1-h} - \frac{A^2}{B} \left[\frac{h}{1+h} \right] \quad \text{I.19}$$

$$h = \frac{BP}{2} \quad \text{I.20}$$

$$A^2 = \frac{\Omega_a T_c^{2.5}}{T^{2.5} P_c} = \frac{a}{R^2 T^{2.5}} \quad \text{I.21}$$

$$B = \frac{\Omega_b T_c}{T P_c} = \frac{b}{RT} \quad \text{I.22}$$

$$\Omega_a = 0.42748 \quad \text{I.23}$$

$$\Omega_b = 0.08664 \quad \text{I.24}$$

The dimensionless constants Ω_a and Ω_b of Equations I.23 and I.24 are found by equating to zero the first two derivatives of pressure with respect to volume at the critical point. Severe restrictions are placed on the use of Equations I.10 to I.24 for predicting pure component adsorption. Studies by Chang and Lu (27) into the temperature dependence of the parameters a , b or Ω_a , Ω_b allows us to obtain a better prediction when Equation I.19 is used.

The evaluation of the parameters Ω_a and Ω_b was conducted with the following set of equations. At equilibrium, the fugacity coefficient of the vapor and the liquid phases are equal,

$$\phi_{i,L} = \phi_{i,V} \quad \text{I.25}$$

in which the quantity $\phi_{i,L}$ for a pure component is evaluated from Equation I.26

$$\ln \phi_L = Z_L - 1 - \ln Z_L - \ln(1-h_L) - (A^2/B) \ln(1-h_L) \quad \text{I.26}$$

A similar expression can be written for the vapor phase.

The combination of Equation I.26 with Equations I.19, I.20 and I.25 yields

$$\ln(Z_L \phi_V) + 1 - Z_L + \ln(1-h_L) + \frac{(1 - Z_L(1-h_L))(1+h_L)}{h_L(1-h_L)}$$

$$\ln(1+h_L) = 0$$

As will be seen in a later section, an expression for the adsorbed phase analogous to Equation I.19 is useful in obtaining

values of a and b from the knowledge of the adsorbed phase compressibilities and the application of the criteria of equilibrium.

A useful form in which the original equation of Redlich and Kwong may be written is by combining it with Equations I.20, I.21 and I.22,

$$P = \frac{RT}{v - b} - \frac{a}{\sqrt{T} v(v + b)} \quad \text{I.28}$$

where v is the molar volume contained in the Equation I.29

$$P v = Z RT \quad \text{I.29}$$

Equation I.28 may further be transformed (5) in terms of the general expression of Equation I.11 by the substitution,

$$\theta = b/v \quad \text{I.30}$$

hence,

$$P = \frac{RT}{b} F(\theta, T) \quad \text{I.31}$$

where

$$F(\theta, T) = \frac{\theta}{1 - \theta} - \frac{a \theta^2}{RT^{1.5} b(1 + \theta)} \quad \text{I.32}$$

The Redlich-Kwong equation lends itself to the evaluation and prediction of the P-v-T properties in mixtures provided

a good set of mixing rules is available. A widely used set is written in Equations I.33 to I.42. Equations I.33 to I.36 follow the proposal of Redlich-Kwong (18).

$$b = \sum x_i b_i \quad \text{I.33}$$

$$a = \sum \sum x_i x_j a_{ij} \quad \text{I.34}$$

in which

$$b_i = \Omega_{bi} RT_{ci}/P_{ci} \quad \text{I.35}$$

and

$$a_{ij} = \Omega_{aij} R^2 T_{cij}^{2.5}/P_{cij} \quad \text{I.36}$$

The evaluation of T_{cij} , P_{cij} and Ω_{aij} , proposed by Chueh and Prausnitz (28), are carried on by the following Equations I.37, I.38 and I.39.

$$T_{cij} = (T_{ci} T_{cj})^{0.5} (1 - k_{ij}) \quad \text{I.37}$$

$$P_{cij} = Z_{cij} RT_{cij}/V_{cij} \quad \text{I.38}$$

and

$$\Omega_{aij} = (\Omega_{ai} + \Omega_{aj})/2 \quad \text{I.39}$$

The Lorentz relationship is used to calculate V_{cij} (27).

$$V_{cij} = \frac{1}{8} \left[V_{ci}^{1/3} + V_{cj}^{1/3} \right]^3 \quad \text{I.40}$$

The correlation between the compressibility factor Z_{cij} and the acentric factor was studied by Pitzer and his co-workers (21) and is represented in the Equations I.41 and I.42

$$Z_{cij} = 0.291 - 0.08 w_{ij} \quad \text{I.41}$$

in which

$$w_{ij} = (w_i + w_j)/2 \quad \text{I.42}$$

Simpler mixing rules can also be used by retaining only the Equations I.33 and I.34 in which

$$a_{ij} = \sqrt{a_i a_j} \quad \text{I.43}$$

This suggestion comes from Bertholet (26).

The mixture energy constant, a_{ij} , defined by Zudkevitch (30) is given by the following expression,

$$a_{ij} = \sqrt{a_i a_j} (1 - C_{ij}) \quad \text{I.44}$$

in which C_{ij} , the interaction constant, represents the deviation

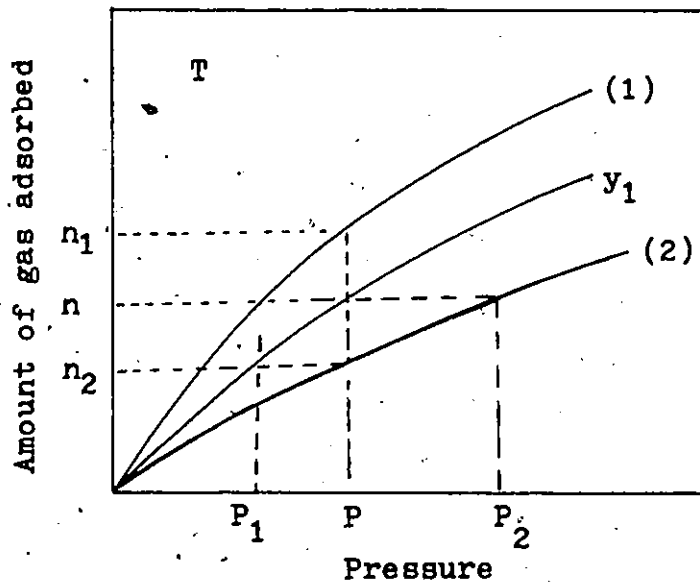
from the standard Redlich-Kwong mixing rules for a_{ij} .

I.C.5 Ideal Adsorbed Solution Theory

The relation expressing the equilibrium between a liquid and its vapor is given by Raoult's Law,

$$P y_i = p_i x_i \quad \text{I.45}$$

At a given temperature and pressure, P , the vapor pressure for component i is p_i , x_i and y_i are respectively the mole fraction of i in the liquid and vapor phase. Kidnay and Myers (19, 20) extended Equation I.45 to represent properties of the adsorbed phase. The symbols retain the same meaning except for p_i which becomes the vapor pressure exerted by the adsorbate at T and P . They are schematically illustrated in the following figure.



For a binary system, the adsorbed molar phase composition is easily calculated by

$$x_1 = \frac{P - p_2}{p_1 - p_2} \quad \text{I.46}$$

while the composition in the vapor is obtained by

$$y_1 = \frac{p_1 x_1}{P} \quad \text{I.47}$$

The molar area for the adsorbed phase is given by Equation I.48

$$\sigma = \sum \sigma_i x_i \quad \text{I.48}$$

where

$$\sigma_i = \frac{A}{n_i} \quad \text{I.49}$$

Rearranging the latter two equations yields for a binary mixture

$$\frac{1}{n} = \frac{x_1}{n_1} + \frac{x_2}{n_2} \quad \text{I.50}$$

I.C.6 Pitzer's Correlation

The well-known three-parameter correlation of Pitzer and his co-workers (21) expresses the compressibility factor Z ,

as a function of the reduced temperature T_r , reduced total pressure P_r and the acentric factor, ω .

$$\frac{PV}{RT} = Z(T_r, P_r, \omega) \quad \text{I.51}$$

in which Pitzer defined the acentric factor as

$$\omega = -\log\left(\frac{P_s}{P_c}\right)_{T_r = 0.7} - 1.0 \quad \text{I.52}$$

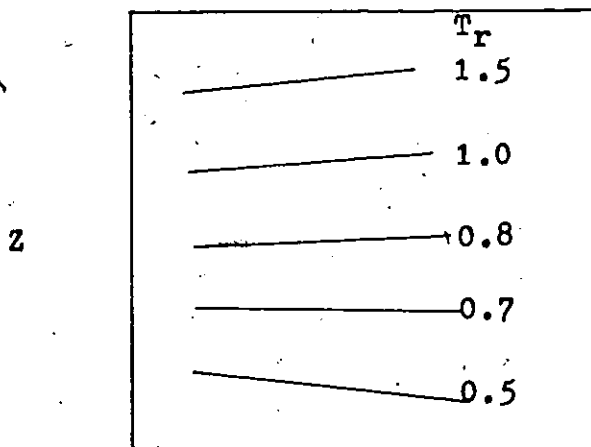
It is a measure of the deviation of the intermolecular potential from simple spherical molecules.

The compressibility factor function is usually expanded as a power series in the acentric factor,

$$Z = Z_{(0)} + \omega Z_{(1)} + \omega^2 Z_{(2)} + \dots \quad \text{I.53}$$

where $Z_{(0)}$, $Z_{(1)}$, etc, are each functions of T_r and P_r .

The following schematic diagram illustrates the sort of data needed to evaluate $Z_{(i)}$.



CHAPTER II

THERMODYNAMIC CONSIDERATIONS OF GAS-SOLID EQUILIBRIA

The object of the first section is to show that the thermodynamic theory of homogeneous phases can be extended to that of the adsorbed layer. This gives the possibility of calculating the molar surface properties of the adsorbed phase entirely from a knowledge of gravimetric adsorption data.

In the second part, rigorous expressions of thermodynamics are obtained which enable the calculation of the fugacities of the adsorbed phase. These expressions are primarily useful in the determination of the adsorbed phase molar properties through an equation of state.

The equations of state form the subject of the last section, in which the analog of the Redlich-Kwong equation is emphasized. This equation is particularly useful in the prediction of phase equilibria between the gas and adsorbed phase when properly combined with the fugacity equations developed earlier in the previous section.

II.A Phase Equilibria From Exact Thermodynamic Relationship

In the study of phase equilibria of mixed gas adsorption, a state of equilibrium must exist between the bulk gas phase and the adsorbed phase. For this reason, the adsorbed film is

treated as an open system so that the equations of thermodynamics can be successfully applied to the adsorbate.

A fundamental property relation for a homogeneous three-dimensional fluid phase treated as an open system is

$$d(nG) = -(nS) dT + (nV) dP + \sum (\mu_i dn_i) \quad \text{II.1}$$

where G , S and V are the molar Gibbs free energy, entropy, and volume. The chemical potential of species i is denoted by μ_i , and n_i is the number of moles of species i . The total number of moles is given by $n = \sum n_i$.

II.A.1 The Adsorbed Phase

The adsorbate is treated as a two-dimensional phase. It represents the real interfacial region separating the solid surface of the adsorbent and the bulk gas phase. This layer has been defined by Willard Gibbs as a region where the gas phase properties gradually change in a direction of the solid surface. The extent of the sphere of influence of the gas phase abnormalities in the region of the solid surface are not known with precision. However, for the purpose of thermodynamic analysis, the interfacial region can be treated as a two-dimensional phase having its appropriate properties; namely, the molar area, σ and the spreading pressure, π .

An analog expression of Equation II.1 applied to the

adsorbed phase becomes:

$$d(nG) = -(nS) dT + (n\sigma) d\pi + \sum(\mu_i d n_i) \quad \text{II.2}$$

It is easily seen that P and V of Equation II.1 have been replaced respectively by π and σ of Equation II.2.

The molar area has been defined earlier as $\sigma = A/n$. The assumption usually made is that the interfacial area or the specific surface area measured is an independent variable.

II.A.2 Gibbs Adsorption Isotherm

The differential Equation II.2 represents a basic relation interconnecting the primary thermodynamic variables of the two-dimensional phase. Its usefulness lies in the fact that the Gibbs free energy, G, is a function made up of directly measurable quantities.

The relationship between the chemical potential, μ_i , and the Gibbs function is given by

$$nG = \sum(\mu_i n_i) \quad \text{II.3}$$

Differentiation of Equation II.3 leads to the following differential equation

$$d(nG) = \sum(\mu_i d n_i) + \sum(n_i d\mu_i) \quad \text{II.4}$$

and comparison with Equation II.2 yields

$$(nS) dT - (n\sigma) d\pi + \sum (n_i d\mu_i) = 0 \quad \text{II.5}$$

Since $n_i = n x_i$ where x_i is the mole fraction of i in the adsorbed phase, Equation II.5 may be written as

$$S dT - \sigma d\pi + \sum (x_i d\mu_i) = 0 \quad \text{II.6}$$

which is the Gibbs-Duhem equation for the two-dimensional phase.

Adsorption studies are usually carried out isothermally since temperature is an easily controlled thermodynamic variable. Thus the restriction of Equation II.6 to constant temperature leads to the Gibbs adsorption isotherm;

$$-\sigma d\pi + \sum (x_i d\mu_i) = 0 \quad \text{II.7}$$

Exploited to its fullness, Equation II.7 provides a perfect example of the role of thermodynamics (3).

II.A.3 Equilibrium Conditions

The properties of the adsorbate may be determined from the assumption that the two-dimensional phase is always in equilibrium with the bulk gas phase. With this condition, the chemical potential of each species present are the same in both the gas phase and the adsorbate. This criterion is

expressed by

$$\mu_{i, g} = \mu_i \quad \text{II.8}$$

where $\mu_{i, g}$ is the chemical potential of species i in the gas phase in contact with the adsorbed phase.

For any small change in the conditions of equilibrium, the Gibbs adsorption isotherm takes the form of

$$-\sigma d\pi + \sum (x_i d\mu_{i, g}) = 0 \quad \text{II.9}$$

It is well-known, that for an ideal gas in which $\mu_{i, g}^{\circ}$ is a function of temperature only (31)

$$\mu_{i, g} = \mu_{i, g}^{\circ} + RT \ln y_i P \quad \text{II.10}$$

in which y_i is the mole fraction of i in the gas phase at system pressure P . The universal gas constant is represented by R . The substitution of Equation II.10 into Equation II.9 gives a general expression for the Gibbs adsorption isotherm;

$$-\frac{\sigma}{RT} d\pi + d \ln P + \sum (x_i d \ln y_i) = 0 \quad \text{II.11}$$

The variables of Equation II.11, known from experimental observations, are the system pressure P , the composition in the gas phase, y_i , and the total amount of gas adsorbed which is given by

$$m = n M \quad \text{II.12}$$

5

in which M is the average molecular weight of the adsorbed phase and it is calculated from

$$M = x_1 M_1 + (1 - x_1) M_2 \quad \text{II.13}$$

For a binary system the molecular weights of the two components are represented respectively by M_1 and M_2 .

II.A.4 Evaluation of π , σ and x_i

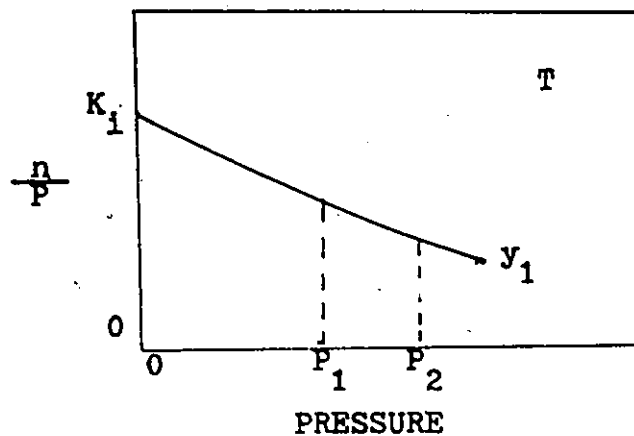
The variables that cannot be measured directly are the adsorbed film composition and the spreading pressure. However, by imposing certain restrictions on the Gibbs adsorption isotherm of Equation II.11 these variables may be calculated.

If the gas phase is held at a constant composition, Equation II.11 may be integrated between the limits of 0 to P for the gas pressure and from 0 to π for the spreading pressure, yielding an expression for the calculation of the spreading pressure

$$\frac{\pi A}{RT} = \left[\int_0^P \frac{n}{P} dP \right]_{T, y_i} \quad \text{II.14}$$

The data needed for the calculation of π is the total weight of adsorbate as a function of the gas phase pressure while the gas phase composition is held constant by some 'flow-thro' mechanism. This leads to a constant gas phase composition

adsorption isotherm. The data needed for the determination of π are schematically illustrated in the following figure.



The integral of Equation II.14 can be solved graphically and is represented by the shaded area of an n/P versus P plot or analytically by a function $n = f(P)$. The symbol K_i denotes the limiting slope which may also be evaluated either graphically or analytically from a plot of n versus P .

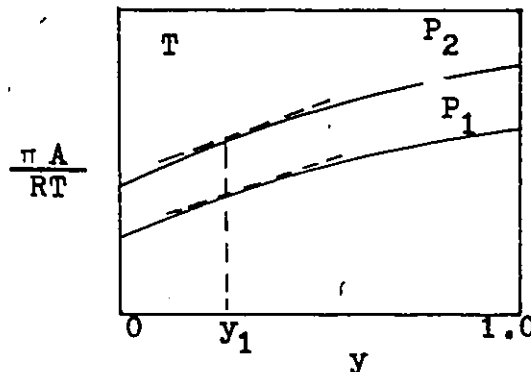
In the calculation of the spreading pressure, some difficulties are encountered because the number of moles adsorbed from a mixture of gases are not known. This arises because the molar composition in the film is unknown and may be obtained by combining the Equations II.12 and II.13.

$$n = \frac{m}{x_1 M_1 + (1 - x_1) M_2} \quad \text{II.15}$$

On the other hand, an expression for the calculation of x_1 is readily obtained by the restriction of Equation II.11 to a constant pressure operation. For a binary system

$$x_1 = y_1 + \frac{y_1 (1 - y_1)}{n} \left[\frac{\partial \left(\frac{\pi A}{RT} \right)}{\partial y_1} \right]_{T, P} \quad \text{II.16}$$

The required data for the evaluation of Equation II.16 is schematically shown in the following figures.



Several constant gas composition isotherms with their pure component isotherms are needed over the pressure range investigated. At a given pressure, the spreading pressures are calculated from the experimental observations of each curve and plotted against the gas phase composition. In this way the partial differential of Equation II.16 can be calculated and a value of x_1 is obtained.

The computation of the quantity $\frac{\pi A}{RT}$ of Equation I.14 is met with no difficulties when dealing with a pure component adsorption because the number of moles adsorbed is readily calculated. However, in the calculation of the moles adsorbed for a mixture, an initial value for x_1 at low pressure has been derived by van Ness (3) in terms of the limiting slope of each pure component adsorption

isotherm and the mole fraction in the gas phase. For a binary mixture

$$x_1 = \frac{y_1 K_1}{y_1 K_1 + y_2 K_2} \quad \text{II.17}$$

in which the limiting slope, K_1 , will be defined by Equation II.37 in Section II.B.3.

II.B Thermodynamic Equations for the Fugacity

The purpose of the following section is to show that rigorous expressions of thermodynamics can be derived to evaluate either the fugacity of the pure adsorbate, f_1 , or the fugacity of a component in a mixed adsorbate, f_1 . The usefulness of the fugacities lies in the fact that they can be written in terms of measurable properties of an adsorbed phase in equilibrium with its gas phase. Subsequently, they provide a means for calculating parameters which are part of an equation of state.

Transformations consisting in combining the fugacity equations with the analog of the Redlich-Kwong equation are useful to obtain important properties for both pure and mixed isotherms.

When this transformation is applied to the pure component fugacity equation, the characteristic parameters of the analog of the Redlich-Kwong equation can be calculated at a given pressure and temperature from the pure component adsorption

isotherm.

Furthermore, this transformation can lead to an analytical expression of the fugacity of a component in the adsorbate, \hat{f}_i .

This relation is very useful in the calculation of the film molar composition and the associated molar area at a given T and π .

II.B.1 Mixed Adsorbate Fugacity

The basic relation interconnecting the primary thermodynamic variables has been presented earlier in Equation II.2

$$d(nG) = -(nS) dT + (n\sigma) d\pi + \sum(\mu_i d n_i) \quad \text{II.2}$$

The fugacity of a mixed adsorbate is defined so as to satisfy the following two equations (31) in which μ^0 is a function of temperature only:

$$G = \mu = \mu^0 + RT \ln f \quad \text{II.19}$$

and

$$\lim_{\pi \rightarrow 0} \left[\frac{f}{\pi} \right] = 1 \quad \text{II.20}$$

Restricting Equation II.2 to one mole at constant temperature and composition

$$dG = \sigma d\pi \quad \text{II.21}$$

Combining Equations II.19 with II.21, the following relationship is obtained

$$\left[\frac{\partial \ln f}{\partial \pi} \right]_{T, x} = \frac{\sigma}{RT} \quad \text{II.22}$$

In Equation II.22, as the pressure approaches zero, the behavior of the adsorbate approaches that of an ideal gas adsorbed; namely, the fugacity of the mixed adsorbate equals the spreading pressure of the mixed adsorbate

$$f^* = \pi^*$$

thus satisfying the relation II.20.

For one mole of adsorbate at a fixed temperature and composition, Equation II.22 reduces to

$$d \ln f = \frac{\sigma}{RT} d \pi \quad \text{II.23}$$

When the Equation II.23 is integrated between the limits of the ideal and actual state of both f and π the following relation is obtained,

$$\ln \frac{f}{f^*} = \frac{1}{RT} \int_{\pi^*}^{\pi} \sigma d \pi \quad (T, x) \quad \text{II.24}$$

A residual property emphasizes the difference between an ideal-gas analog property and the actual one. The residual

molar area $\Delta\sigma'$ is defined by

$$\Delta\sigma' = \sigma' - \sigma = \frac{RT}{\pi} - \sigma \quad \text{II.25}$$

in which the quantity RT/π is the molar area; σ' , is given by the ideal-gas analog equation. The integration of Equation II.24 with the substitution of Equation II.25 gives the following expression,

$$\ln\left(\frac{f}{\pi}\right) = -\frac{1}{RT} \int_0^{\pi} \Delta\sigma' d\pi \quad \text{II.26}$$

The compressibility factor defined by the Equation II.27

$$\pi\sigma = ZRT \quad \text{II.27}$$

may also be written as

$$Z = \frac{\pi\sigma}{RT} = \frac{\sigma}{RT/\pi} = \frac{\sigma}{\sigma'} \quad \text{II.28}$$

The residual molar area can be related to the compressibility factor by a simple manipulation; namely,

$$\frac{\Delta\sigma'}{RT} = \frac{1-Z}{\pi} \quad \text{II.29}$$

Equation II.26 together with Equation II.29 becomes

$$\ln \left[\frac{f}{\pi} \right] = \left[\int_0^{\pi} (Z - 1) \frac{d\pi}{\pi} \right]_{T, x} \quad \text{II.30}$$

Equation II.30 is rigorous at constant temperature and composition. It expresses the relationship between the mixed adsorbate fugacity, f , the spreading pressure, π , and the compressibility factor of the adsorbed phase, Z . It is convenient when an equation of state expresses Z as an explicit function of π . However, it is more convenient to express Z as an explicit function of the molar area, $\sigma = A/n$. A change of variables of the Equation II.30 with the use of Equation II.27 yields the following expression

$$\ln f = \int_0^{\sigma} (Z - 1) \frac{d\sigma}{\sigma} + (Z - 1) + \ln \left(\frac{RT}{\sigma} \right) \quad \text{II.31}$$

The Equation II.31 is also valid for a pure component; namely, $f = f_1$ and Z and σ are pure component properties. It is understood that Equations II.19 and II.20 are defined for a pure component.

II.B.2 Fugacity of a Component in the Mixed Adsorbate

The fugacity of a component in the mixed adsorbate is defined by the following two relations which must be satisfied

$$\bar{G}_1 = \mu_1 = \mu_1^{\circ} + RT \ln \hat{f}_1 \quad \text{II.32}$$

and

$$\lim_{\pi \rightarrow 0} \left[\frac{\hat{f}_i}{x_i \pi} \right] = 1 \quad \text{II.33}$$

The quantity $n \ln f$ is an extensive property at constant temperature (29) and therefore can be expressed in terms of π , n_i by the following differential equation

$$d(n \ln f) = \left[\frac{n \partial (\ln f)}{\partial \pi} \right]_{T, n} d\pi + \sum \left[\frac{\partial (n \ln f)}{\partial n_i} \right]_{T, \pi, n} d n_i \quad \text{II.34}$$

The term in the first square bracket is easily identified with Equation II.22. The term in the second square bracket is related to the fugacity of a component in the adsorbate, \hat{f}_i , and is included in Equation II.35

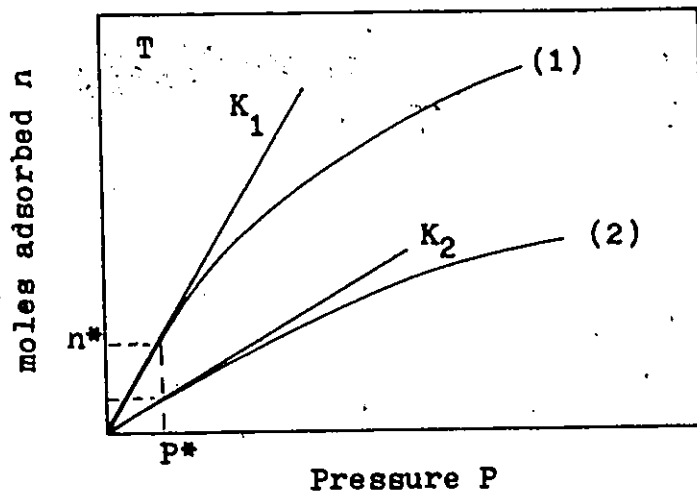
$$d(n \ln f) = \frac{n\sigma}{RT} d\pi + \sum \left[\ln \frac{\hat{f}_i}{x_i} d n_i \right] \quad \text{II.35}$$

Dividing by dn_i at constant T , A , n_j , $j \neq i$, and substituting Equation II.27 for π , followed by Equation II.31 for f yields an expression for the fugacity of a component in a mixed adsorbate in terms of the composition, x_i , and the molar area of the adsorbed phase. This rigorous expression is written as

$$\ln \hat{f}_i = \int_{\sigma}^{\infty} \left[\left(\frac{\partial n Z}{\partial n_i} \right)_{T, A, n_j} - 1 \right] \frac{d\sigma}{\sigma} + \ln \left(\frac{x_i RT}{\sigma} \right) \quad \text{II.36}$$

II.B.3 Experimental Fugacities

The slope of the tangent of an adsorption isotherm is designated by K and is illustrated in the following schematic diagram. The limiting slope can approximate the isotherm when the tangent passes



through the origin and a point close to the origin, (n^*, P^*) .

(3). The asterisk represents a condition where $P \rightarrow 0$. The limiting slope is represented in the following equation

$$K = \frac{1}{A} \frac{n^*}{P^*} \quad \text{II.37}$$

The quantity K characterizes a specific interaction between a particular adsorbed species and the adsorbent. It is generally considered a temperature-dependent parameter.

In mixed adsorption phase equilibria, the criteria of equilibrium is expressed in terms of the component fugacities

$$\hat{f}_i = \hat{f}_{i, g} \quad \text{II.38}$$

The integration of the differential of the logarithmic form of Equation II.38 at constant temperature from an equilibrium state of pure i at very low pressure p_i^* , π_i^* , to a final equilibrium state of i in a mixed adsorption system in which the conditions are specified for the composition of both phases, x_i , y_i , at system pressure, P , temperature, T , and spreading pressure, π , yields (3).

$$\hat{f}_i(\pi) = \frac{\pi_i^*}{P_i^*} \hat{f}_{i, g}(P) \quad \text{II.39}$$

With the assumptions that the gas phase behaves ideally at P , the two-dimensional gas obeys the analog of the ideal-gas law and Equation II.37, valid, the equation of equilibrium becomes

$$\hat{f}_i(\pi) = K_i RT y_i P(\pi) \quad \text{II.40}$$

For the pure adsorbate, at the same temperature and spreading pressure, Equation II.40 becomes

$$f_i(\pi) = K_i RT p_i(\pi) \quad \text{II.41}$$

Thus, the fugacities of Equations II.40 and II.41 can be calculated from the experimental adsorption isotherm at the desired

condition.

The fugacity coefficient of a pure substance in the gas phase is expressed in the following relation

$$\phi_{i, g} = \frac{f_{i, g}}{P} \quad \text{II.42}$$

An analogous expression for the fugacity coefficient in the adsorbed phase is defined in Equation II.43

$$\phi_i = \frac{f_i}{\pi} = \frac{K_i RT p_i}{\pi} \quad \text{II.43}$$

Equation II.43 was obtained by substituting Equation II.41.

The fugacity coefficient of a component in a gas mixture is usually defined by

$$\hat{\phi}_{i, g} = \frac{\hat{f}_{i, g}}{y_i P} \quad \text{II.44}$$

The fugacity of a mixed component i has already been expressed in terms of gas phase and adsorbed phase properties, in Equation II.40. Combining it with a relation analogous to Equation II.44 yields for the adsorbed phase

$$\hat{\phi}_i = \frac{\hat{f}_i}{x_i \pi} = \frac{K_i RT y_i P}{x_i \pi} \quad \text{II.45}$$

The integrated form of Equation II.31 expressed in terms of the fugacity coefficient of a pure component combined

with Equation II.43 produces an analytical expression, $F(h) = 0$, for the calculation of the characteristic parameters of any equation of state, $\pi(T, \sigma)$.

Similarly, when the integrated form of Equation II.36 is expressed in terms of the fugacity coefficient of a component in an admixture together with Equation II.45 it yields a function $F(x_i, \sigma) = 0$ which can be solved for x_i and σ . The function $F(x_i, \sigma) = 0$ is evaluated from knowledge of the calculated characteristic parameters of the components constituting the mixture adsorbed.

II.C Adsorbed Phase Equation of State

An equation of state for a three-dimensional phase is a mathematical relation between volume, pressure, temperature, and composition for a mixture. In general, for a one-component system, they are pressure explicit rather than volume explicit; that is,

$$P = F(T, V) \quad \text{II.46}$$

This concept can be extended to the adsorbed phase whereby a two-dimensional equation of state takes the form

$$\pi = F(\sigma, T) \quad \text{II.47}$$

An equation of state should be equally applicable to

both phases; namely, the gas phase in equilibrium with the adsorbed phase. It is a generally accepted fact that for an equation of state to relate the thermodynamic properties of vapor-liquid equilibrium, it must be easy to use, have few constants to evaluate, and be extendable to represent the properties of a mixture. Above all it must satisfy the Gibbs-Duhem equation (32).

II.C.1 Gibbs Adsorption Isotherm

In a two-dimensional equation of state, the Gibbs adsorption theorem must be satisfied and should describe the $\pi - \sigma - T - x$ behavior of an adsorbate. For a pure component, the Gibbs adsorption isotherm, Equation II.11, can be written in the form of Equation II.48,

$$d \ln P = \frac{\sigma d\sigma}{RT} - \frac{d\pi}{d\sigma} \quad \text{II.48}$$

which relates explicitly $P = F(\pi, \sigma)$.

An adsorption isotherm, $n = f(P)$, can be calculated if a two-dimensional equation of state of the form of Equation I.11,

$$\pi = RT F(\sigma, T) = \frac{RT}{B} F(\theta, T) \quad \text{II.49}$$

is substituted into Equation II.48.

II.C.2 Spreading Pressure

The spreading pressure is calculated from Equation II.49. The function $F(\theta, T)$ has been mentioned earlier in Equations I.14, I.15 and I.16.

The ideal gas law analog, Equation I.14 and Volmer Equation I.15 assume no interaction among the adsorbed molecules; however, the latter includes a correction for the effect of molecular size in the term β . Corrections for non-ideality are also included in the Hill-de-Boer Equation I.16 and in the analog of the Redlich-Kwong Equation I.32 in terms α and β . Equation I.32 for the adsorbed phase becomes

$$F(\theta, T) = \frac{\theta}{1-\theta} - \frac{\alpha\theta^2}{RT^{1.5}\beta(1+\theta)} \quad \text{II.50}$$

The quantities α and β retain the theoretical significance of the van de Waals interaction constants, a , and the size constant, b .

The spreading pressure equation in terms of the analog of the Redlich-Kwong equation may be written

$$\pi = \frac{RT}{\beta} \left[\frac{\theta}{1-\theta} - \frac{\alpha\theta^2}{RT^{1.5}\beta(1+\theta)} \right] \quad \text{II.51}$$

Substituting $\theta = \beta/\sigma$ into Equation II.51 gives

$$\pi = \frac{RT}{\sigma - \beta} - \frac{\alpha}{T^{1/2}\sigma(\sigma + \beta)} \quad \text{II.52}$$

which has the form of Equation II.47, $\pi = P(\sigma, T)$.

II.C.3 Gas Phase Pressure

The Gibbs adsorption isotherm expresses an equilibrium between the adsorbate and the bulk gas phase. Substitution of an equation of state of the form given by Equation II.49 into Equation II.48 yields an equation of state explicit in measurable properties such as the pressure function of the total amount adsorbed at a given temperature - in terms of an adsorption isotherm.

The analog of the Redlich-Kwong equation is used to illustrate this transformation. Taking the derivative of π with respect to σ at constant temperature and substituting into the Gibbs adsorption isotherm and integrating yields

$$P = K' \left(\frac{\theta}{1-\theta} \right) \exp \left(\frac{\theta}{1-\theta} \right) \exp \left[- \frac{\alpha}{\beta RT^{1.5}} \left(\frac{\theta}{1+\theta} + \ln(1+\theta) \right) \right]$$

II.53

in which K' is an integration constant.

Isotherm equations corresponding to the equations of state mentioned earlier are listed below

Type of Equation of State	Isotherm Equation	
Ideal-gas	$P = K \cdot \theta$	II.54
Volmer	$P = K \cdot \frac{\theta}{1-\theta} \exp\left(\frac{\theta}{1-\theta}\right)$	II.55
Hill-de Boer	$P = K \cdot \frac{\theta}{1-\theta} \exp\left(\frac{\theta}{1-\theta} - \frac{2a\theta}{RT\beta}\right)$	II.56

II.C.4 Analog of the Redlich-Kwong Equation of State

Equation II.53 expresses the relationship between P , σ and T ; all of which are measurable properties of an adsorption isotherm. The parameters a and β are readily calculated and when substituted in Equation II.53 provide a means for evaluating the spreading pressure.

The parameters a and β can be determined from the adsorption isotherms by employing different approaches. One has been suggested by de Boer (33); the other, is the method proposed in this work.

In the analog of the Redlich-Kwong equation, the characteristic parameters Ω_a and Ω_b are respectively related to a and β . Using equations analogous to Equations I.21 and I.23 in which a and b are replaced by a and β , yields the following equations

$$a = \frac{\Omega_a R^2 T_c^{2.5}}{P_c} \quad \text{II.57}$$

$$\beta = \frac{\Omega_b RT_c}{P_c} \quad \text{II.58}$$

In the correlation of Ω_a and Ω_b or of a and β , the critical constants of the gas phase may be used because little is known about the adsorbed film critical values.

II.C.4.a de Boer's Parameter Evaluation Method

The approach developed by de Boer and Kruyer on the Hill-de Boer equation to solve for the constants a and β can be extended to solve those of the Redlich-Kwong equation analog.

Equation II.53 may be transformed by taking the logarithm on both sides of the expression and regrouping the terms as shown in Equation II.59,

$$\ln \left[P \left(\frac{1-\theta}{\theta} \right) \right] - \frac{\theta}{1-\theta} = \frac{-a}{\beta RT^{1.5}} \left[\frac{\theta}{1+\theta} + \ln(1+\theta) \right] + \ln K' \quad \text{II.59}$$

When the left member of Equation II.59 is brought on an Y-axis and the term in parenthesis on the right side of Equation II.59 is brought on an X-axis, an optimization procedure can be used to determine the parameters a , β and K' , by the method of least-squares. The value of β giving a minimum sum of squares of deviation in Y can be selected (33).

The slope of the linear plot of Equation II.59 is $-\alpha/\beta RT^{1.5}$ while the intercept gives $\ln K'$ for a value of β .

II.C.4.b Temperature Dependence of the Characteristic Parameters

The original equation proposed by Redlich and Kwong is more useful to show the temperature dependence of α and β , or of Ω_a and Ω_b of Equations I.21 and I.22. Written in terms of the adsorbed phase properties, Equations I.9 to I.22 become

$$Z = \frac{1}{1-h} - \frac{A^2}{B} \left(\frac{h}{1+h} \right) \quad \text{II.60}$$

in which

$$h = \frac{B\pi}{Z} = \frac{BRT}{\sigma} \quad \text{II.61}$$

$$A^2 = \frac{\Omega_a T_c^{2.5}}{T^{2.5} P_c} = \frac{\alpha}{R^2 T^{2.5}} \quad \text{II.62}$$

and

$$B = \frac{\Omega_b T_c}{T P_c} = \frac{\beta}{RT} \quad \text{II.63}$$

In Equation II.61, the compressibility factor, Z , is related to the molar area σ with the spreading pressure π by the familiar equation

$$\pi \bar{v} = ZRT \quad \text{II.64}$$

The compressibility factor is readily determined from experimental data using Equation II.14 rearranged in the form

$$Z(P, T) = \left[\frac{1}{n(P)} \int_0^P \frac{n}{P} dP \right]_T \quad \text{II.65}$$

II.C.5 Fugacity of Pure Adsorbate

The analog of the Redlich-Kwong Equation II.52 can be easily written in the form

$$Z-1 = \frac{\beta}{\sigma - \beta} - \frac{\alpha}{RT^{1.5} (\sigma \beta)} \quad \text{II.66}$$

which when substituted into Equation II.31 and upon integration yields an expression for the mixed adsorbate fugacity

$$\ln f = \ln \left(\frac{RT}{\sigma - \beta} \right) - \frac{\alpha}{RT^{1.5} \beta} \ln \left(\frac{\sigma + \beta}{\sigma} \right) + Z - 1 \quad \text{II.67}$$

The fugacity of a mixed adsorbate and the fugacity of a pure adsorbate are equally represented by Equation II.67. If the quantities α, β, σ and Z are properties of a pure adsorbate, i , Equation II.67 becomes

$$\ln f_i = \ln \left(\frac{RT}{\sigma_i - \beta_i} \right) - \frac{\alpha_i}{RT^{1.5} \beta_i} \ln \left(\frac{\sigma_i + \beta_i}{\sigma_i} \right) + Z_i - 1 \quad \text{II.68}$$

This equation is incomplete without the following set of equations, in which μ_i^0 is a function of temperature only (31)

$$G_i = \mu_i = \mu_i^0 + RT \ln f_i \quad \text{II.69}$$

and

$$\lim_{\pi_i \rightarrow 0} \left[\frac{f_i}{\pi_i} \right] = 1 \quad \text{II.70}$$

The subscripts of Equation II.68 will be removed for ease of presentation. The substitution of the pure adsorbate fugacity defined by Equation II.68 into Equation II.43, which represents the fugacity coefficient of a pure adsorbed species, reduces to Equation II.71

$$\ln \phi = \ln \left(\frac{RT}{\sigma - \beta} \right) - \ln \pi - \frac{\alpha}{RT^{1.5} \beta} \ln \left(\frac{\sigma + \beta}{\sigma} \right) + Z - 1 \quad \text{II.71}$$

Substituting Equations II.60, II.61, II.62 and II.63 into Equation II.71 gives

$$\ln \phi = Z - 1 - \ln 2 - \ln(1-h) - \frac{A}{B} \ln(1+h) \quad \text{II.72}$$

The combination of Equation II.72 with equation of the fugacity coefficient, Equation II.43, results in Equation II.73

$$\ln(KP^{\sigma}) + 1 - Z + \ln(1-h) + \left(\frac{(1-Z(1-h))(1+h)}{(1-h)h} \right) \ln(1+h) = 0 \quad \text{II.73}$$

Equation II.73 has the form $F(h) = 0$ and h can be solved analytically; hence, the parameters Ω_a and Ω_b or α and β are readily calculated for each point of a pure component adsorption isotherm.

II.C.6 Component Fugacity in Mixed Adsorbate

II.C.6.a Mixing Rules

When Equation II.66 is employed, say in the calculation of π , for a pure adsorbate, no problems are encountered as to what the values of α_i and β_i are. However, when this equation is applied to a mixed adsorbate, the values of α and β can only be arrived at by combination rules that take into account the presence of other components simultaneously adsorbed. In Equation II.66, the parameters α and β are generally considered composition - dependent only. They can be evaluated with a set of mixing rules which contain the pure component characteristic constants α_i and β_i obtained directly from the pure component adsorption isotherms.

If the parameters α and β are, respectively proportional to the size of a molecule and to the intermolecular interaction, then it is customary to use the following mixing rules,

$$\beta = \sum x_i \beta_i \quad \text{II.74}$$

and

$$\alpha = \sum \sum x_i x_j \alpha_{ij} \quad \text{II.75}$$

The measure of average molecular diameters is given by Equation II.74 while Equation II.75 interprets α_{ij} as an interaction between pairs of molecules. For the same chemical species— $i=i$ or $j=j$ — $\alpha_{ii}=\alpha_i$ and $\alpha_{jj}=\alpha_j$. However, for $i \neq j$, the geometric-mean assumption for α_{ij} is generally considered:

$$\alpha_{ij} = \sqrt{\alpha_i \alpha_j} \quad \text{II.76}$$

The quantity α_{ij} is the most significant in the estimate of α and improvement in the correlation can be obtained by considering an analog expression, defined by Zudkevitch (30) in Equation I.44, and is similarly defined for the adsorbed phase in Equation II.77.

$$\alpha_{ij} = \sqrt{\alpha_i \alpha_j} (1 - C_{ij}) \quad \text{II.77}$$

More sophisticated mixing rules for α_{ij} can be defined by Equations I.35 to I.42. Combination of these yields an expression very similar to Equation II.77,

$$\alpha_{ij} = k(1 - k_{ij})^{1.5} \quad \text{II.78}$$

Equation II.78 is derived by substituting Equations I.37 to I.42 into Equation I.36. For a binary system,

$$a_{12} = \frac{\left(\frac{\Omega_{a1} + \Omega_{a2}}{2}\right) \left[\sqrt{T_{c1} T_{c2}} (1 - k_{12})\right]^{1.5} \frac{1}{8} (V_{c1}^{\frac{1}{3}} + V_{c2}^{\frac{1}{3}})^3 R_1^2}{\left[0.291 - 0.08 \left(\frac{\omega_1 + \omega_2}{2}\right)\right] R}$$

Rearranging the above equation yields a relation similar to Equation II.78 in which

$$k = \frac{(\Omega_{a1} + \Omega_{a2}) \left(\sqrt{T_{c1} T_{c2}}\right)^{1.5} (V_{c1}^{\frac{1}{3}} + V_{c2}^{\frac{1}{3}})^3 R_1^2}{\left[4.656 - 0.64 (\omega_1 + \omega_2)\right] R}$$

In the above equation, Ω_{ai} may be expressed in terms of a using Equation II.57

$$\Omega_{ai} = \frac{a P_{ci}}{R_1^2 T_{ci}^{2.5}} \quad \text{II.57}$$

It follows that

$$k = \left[\frac{a_1 P_{c1}}{T_{c1}^{2.5}} + \frac{a_2 P_{c2}}{T_{c2}^{2.5}} \right] \left[\frac{(\sqrt{T_{c1} T_{c2}})^{1.5} (V_{c1}^{\frac{1}{3}} + V_{c2}^{\frac{1}{3}})^3}{\left[4.656 - 0.64 (\omega_1 + \omega_2)\right] R} \right] \quad \text{II.78a}$$

Therefore k is a constant function of the critical properties of the gas phase and the characteristic parameters α and β evaluated at a given temperature and pressure of a pure adsorbate.

II.C.6.b Fugacity Equation

When the analog of the Redlich-Kwong equation of state, Equation II.66, together with the mixing rules of Equations II.74 and II.75, are substituted into the rigorous expression for the fugacity of a component i in the mixed adsorbed phase, Equation II.36, yields

$$\begin{aligned} \ln \hat{f}_i = & \ln \left[\frac{x_i RT}{\sigma - \beta} \right] + \frac{\beta_i}{\sigma - \beta} - \frac{2}{RT^{1.5}} \frac{\sum_j (x_j \alpha_{ij})}{\beta} \ln \left(\frac{\sigma + \beta}{\sigma} \right) \\ & + \frac{\alpha \beta_i}{RT^{1.5} \beta^2} \left[\ln \left(\frac{\sigma + \beta}{\sigma} \right) - \frac{\beta}{\sigma + \beta} \right] \end{aligned} \quad \text{II.79}$$

Equation II.80 results from a transformation of Equation II.79 by the substitution of

$$\hat{\phi}_i = \frac{\hat{f}_i}{x_i \pi}$$

yielding

$$\begin{aligned} \ln \phi_i = & \ln \left[\frac{RT}{\pi(\sigma - \beta)} \right] + \frac{\beta_i}{\sigma - \beta} - \frac{2}{RT^{1.5}} \frac{\sum_j (x_j \alpha_{ij})}{\beta} \ln \left(\frac{\sigma + \beta}{\sigma} \right) \\ & + \frac{\alpha \beta_i}{RT^{1.5} \beta^2} \left[\ln \left(\frac{\sigma + \beta}{\sigma} \right) - \frac{\beta}{\sigma + \beta} \right] \end{aligned} \quad \text{II.80}$$

Equations II.79 and II.80 are equivalent and the substitution of Equation II.45 in either of them yields an analytical expression capable of providing the film properties; namely, x_i and σ of an adsorbed mixture. This function, $F(x_i, \sigma) = 0$ is defined by Equation II.81.

$$-\ln \left[\frac{K_i y_i P}{x_i} \right] + \ln(\sigma - \beta) - \frac{\beta_i}{\sigma - \beta} + \frac{2 \sum_j (x_j \alpha_{ij})}{RT^{1.5} \beta} \ln \left(\frac{\sigma + \beta}{\sigma} \right)$$

II.81

$$- \frac{\alpha \beta_i}{RT^{1.5} \beta^2} \left[\ln \left(\frac{\sigma + \beta}{\sigma} \right) - \frac{\beta}{\sigma + \beta} \right] = 0$$

The function $F(x_i, \sigma) = 0$ of Equation II.81 is an equilibrium expression which relates the properties of a gas phase mixture to those of an adsorbed phase mixture provided the analog of the Redlich-Kwong equation of state is used to represent the adsorption isotherms of the components adsorbed. The quantities α_i and β_i are readily obtained from Equation II.73, $F(h) = 0$, at the desired experimental conditions. Furthermore, the quantity K_i can also be evaluated from the experimental observations in Equation II.37. In Equation II.73, the quantity Z is evaluated from Equation II.65. The mixing rules of Equations II.74, II.75, together with Equation II.76 or some modifications of it, can be employed to calculate the values of π and σ .

CHAPTER III

EXPERIMENTAL STUDY OF GAS-SOLID EQUILIBRIA

This chapter is devoted to the experimental methods employed in this work for the study of phase equilibria between the adsorbate and the gas phase composed either of a pure gas or of a mixture of gases. The attainment of good quality adsorption isotherms requires gases of research grade quality and an adsorbent able to provide reproducible adsorption isotherms. The gases employed and their binary mixture composition, the procedure followed for the activation of silica gel, and the measurement of the specific surface area of the adsorbent are described in Section A. The usefulness of the exact thermodynamic relationship, discussed earlier, was verified using a Cahn Electrobalance Assembly described in Section B. The thermodynamic properties of the adsorbed phase calculated using the exact thermodynamic relationship were compared with adsorption equilibria of gas mixtures obtained from an independent experimental approach. A constant volume adsorption apparatus was set-up specifically for that purpose and is described in Section C.

III.A Materials

III.A.1 Gas Supply

All gases, pure and mixtures, were provided by Matheson Co. Ltd. and were used without further purification.

Pure components specifications as provided by Matheson Co. Ltd. are the following:

<u>Component</u>	<u>Minimum Purity %</u>
Ethane	99.9
Ethylene	99.5
Carbon dioxide	99.995
Propane	99.5

Mixture molar compositions of the mixtures and their specifications, as provided by Matheson Co. Ltd. are the following:

<u>Mixture</u>	<u>% Heavy Component</u>		
	25%	50%	75%
$C_2H_6-C_2H_4$	$26.35 \pm 0.1\%$	$50.42 \pm 0.1\%$	$75.47 \pm 0.1\%$
$C_2H_6-CO_2$	$25.92 \pm .05\%$	$49.60 \pm .05\%$	$75.22 \pm .05\%$
$CO_2-C_3H_8$	$23.85 \pm 0.3\%$	$45.27 \pm 0.2\%$	$74.94 \pm 0.1\%$

III.A.2 Adsorbent

III.A.2.a Surface Activation

A commercial grade silica gel (25 mesh), supplied by Chromatographic Specialties, was the adsorbent used throughout this investigation.

Silica gel is usually prepared (34) by treating sodium silicate of a suitable concentration with an acid such as hydrochloric acid, or with certain salts, such as ferric chloride. The gelatinous mass thus formed is broken up, washed free from salts and dried until the gel becomes hard and glassy in appearance. The water content at this stage will vary with the method of preparation but is nearly always well above five per cent. Finally, the gel is heated to a moderately high temperature (150°C to 400°C), usually in a current of dry air. This process, known as activation, decreases still further the water content of the gel and increases greatly its adsorptive capacity. It becomes evident that the properties of silica gel will vary according to the method of preparation by the manufacturer. Generally the exact details are not provided thus making the silica gel history unknown.

Silica gel must be activated reproducibly if consistent adsorption equilibria are to be obtained not only on the same sample but on different samples of the same source. Careful control of the factors affecting activation are necessary if

successive portions of the gel are to be activated to the same extent.

No experiments were performed to find the ideal activation temperature-time-pressure relationship on silica gel. However, a systematic approach was developed after carefully analysing the methods employed by different researchers.

It is generally agreed upon that the activation temperature runs from 150°C to 400°C (35). Recent work shows that the surface area of the gel did not vary significantly with the degassing temperature between 140 and 250°C (36,37). In their investigation, all samples were degassed at 140°C . Further evidence (38) shows that the gel surface area passes through a maximum value around 200°C . Others (34) have associated heat of wetting with the temperature of activation and water content. A maximum was noted at 300°C . While activating the surface, the water condensed in the gel present in the capillary spaces or adsorbed on the surface will be liberated. However, excess heating will cause the gel structure to partially collapse due to the loss of water which constitute an integral part of the framework of the gel. This will decrease the pore volume and the activity. It follows that the selection of a proper activation temperature is important so that the physical nature of the adsorbent will not change through reactivation.

In this investigation, all samples were thermally treated at 140°C . A large quantity of silica gel was taken from the stock supply to last throughout the duration of the experiment.

The supply was placed in a shallow glass evaporating dish and laid in a muffle furnace set at 140°C for 48 hours. The effect of this treatment on the final physical properties of silica gel have been investigated, (35). This has the effect of removing any excess moisture and above all to have a gel of uniform pore characteristics. Upon completion of heating, the portion was placed in a CaCl_2 desiccator at room temperature. This insures uniformity of water content before the final activation treatment.

The stock supply was left in the desiccator at least 48 hours before the first gel samples were taken for activation treatment.

Gel samples of 0.1 gram were taken from the desiccator and placed into the pan of the gas adsorption apparatus. All samples were evacuated to 10^{-4} mmHg and thermally activated at 140°C , before each adsorption isotherm run. It has been reported (34) that the length of time of heating is immaterial provided that a minimum of 30 minutes is observed. In this work, a constant weight was observed after 45 minutes.

It has been found in the investigation that the reproducibility of the data was possible if the gas was introduced into the apparatus while the sample temperature was at 140°C . Also, for a new sample, it was found advantageous to fill the apparatus with the gas to 760 mmHg after the first heat treatment under vacuum. The gas was left overnight before actually starting the isothermal run.

III.A.2.b Specific Surface Area

The adsorption equilibrium equation of Brunauer, Emmett and Teller (22) is seldom applied to pure component data without consideration of the theoretical significance of the coefficients.

The BET relationship provides a valuable means for the estimation of the surface area of certain adsorbents because it can describe the amount of adsorbate required for monolayer coverage (32). It was the first to give good agreement with the experimental data for all types of vapor-on-solid adsorption and made possible the calculation of a reasonably accurate value for the area of the adsorbent (23). The description of the theory is presented in detail by Flood (39), while a brief survey of the general types of equipment and the more important interpretation problems of the BET surface area determination are also considered by Flood (40).

Investigators in many laboratories have used the BET theory as a research tool and as a means for routine measurement of surface areas. In this work, this theory is used in conjunction with two different gravimetric procedures used to make these measurements. The first method employed involves a gravimetric method originally devised by McBain (41). The McBain-Bakr balance consists of a helical quartz spring suspended in a tube. The spring supports a small bucket made of some inert material in which the sample is held. The tube may be surrounded by a heating element for degassing the sample at constant temperature.

The temperature of the adsorption may be controlled by means of a bath around the tube. The pressure may be measured on a mercury manometer. The amount of adsorption which occurs is proportional to the difference in extension of the spring before and after adsorption. Spring extensions are measured with the aid of a cathetometer or traveling microscope. The spring is calibrated with small known weights. This type of balance has been used in this work to measure only the specific surface area of the adsorbent and to compare the value with that obtained from an electrobalance.

The other type of gravimetric procedure for adsorption measurements is the beam-type vacuum balance. One of the first to use this type of the electronic thermobalance was Rhodin (42). In this work, a Cahn electrobalance (43) was used and is described in greater details in III.B. The theory and principles of operation of the Cahn electrobalance have been described in the literature (44, 45). Briefly, the deflection of the beam of the balance is translated into an electrical signal proportional to the deflection. This signal can be measured or fed into a recording system. It has the advantage of continuously recording the amount adsorbed; thus, the establishment of equilibrium is easily determined. The Cahn electrobalance was used in the measurement of the specific surface area and of the adsorption isotherms of pure and mixed gases.

III.B Gravimetric Adsorption System

III.B.1 Apparatus

A Cahn recording electrobalance Model RG was used to measure gravimetrically adsorption equilibrium. The gravimetric adsorption system and accessories are shown schematically in Figure III.1. The balance was modified slightly by coiling the feed line down around the hangdown tube of the balance. The feed line at one end of the apparatus together with a Cartesian manostat at the other end made it possible to obtain adsorption isotherms for gas mixtures of constant composition with pressure as the dependent variable.

The Cahn electrobalance assembly schematically shown in Figure III.1 can be divided into five assemblies or units and are as follows:

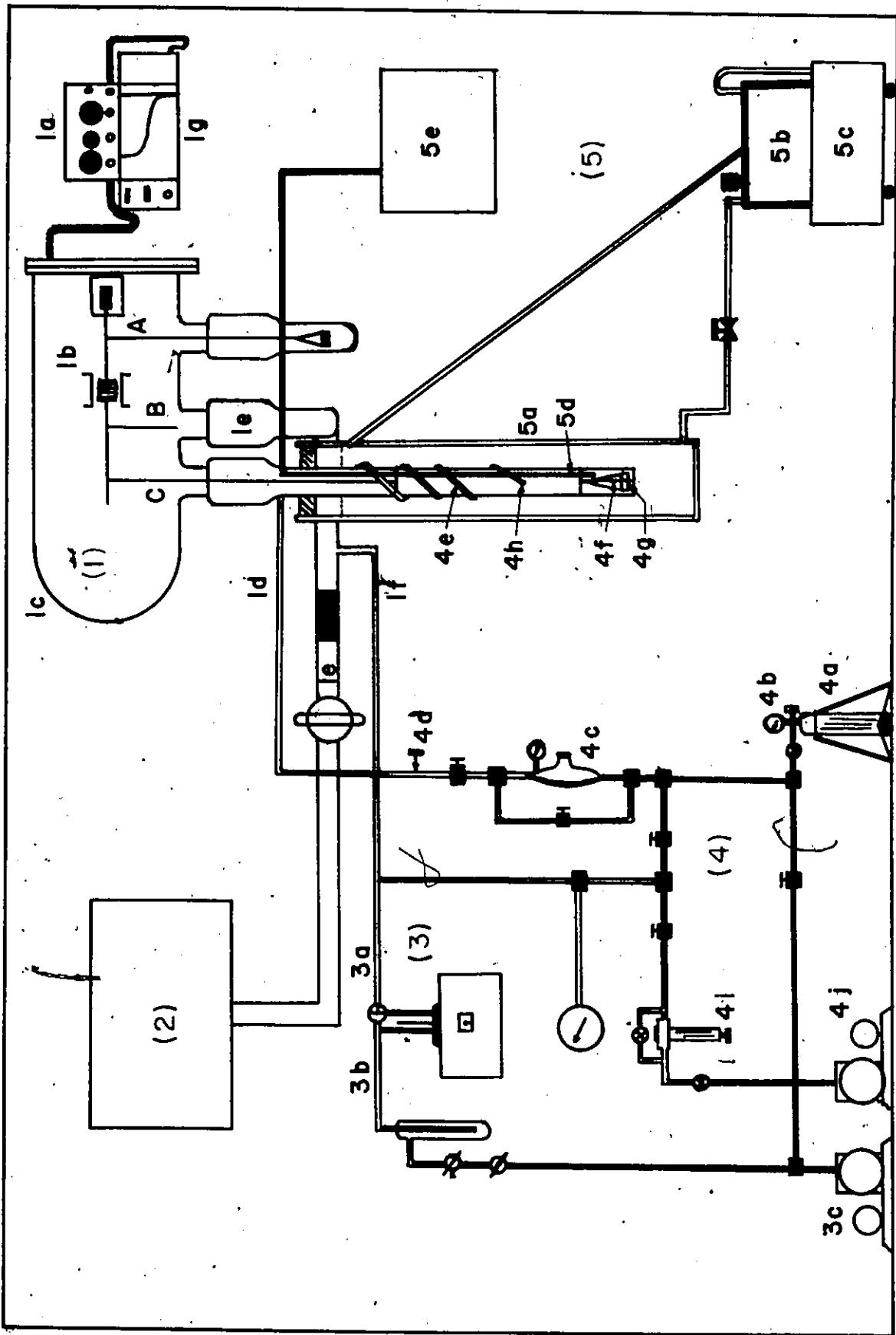


Figure III.1 GRAVIMETRIC ADSORPTION APPARATUS

LEGEND OF FIGURE III.1

1. Cahn electrobalance unit
 - a. Cahn recording electrobalance
 - b. Weighing mechanism
 - c. #2005 glass vacuum bottle
 - d. Feed line
 - e. Vacuum take-off tube
- A,B,C. Loops
2. Vacuum unit
3. Pressure measuring unit
 - a. Pressure port
 - b. Reference port
 - c. Vacuum pump
4. Feed and flow-thro unit
 - a. Gas cylinder
 - b. Pressure regulator
 - c. Low pressure regulator
 - d. Needle valve
 - e. Feed line
 - f. Feed line
 - g. Sample Vessel
 - h. Sealed perforation
5. Temperature Control and Measurement Unit
 - a. Insulated bath
 - b. Thermostatic bath

Legend of Figure III.1 (Cont'd)

- c. Refrigerating unit
- d. Thermocouple
- e. Potentiometer and Galvamometer

- 1) Cahn electrobalance unit
- 2) Vacuum unit
- 3) Pressure measuring unit
- 4) Feed and flow-thro unit
- 5) Temperature control and measurement unit

III.B.1.a Cahn Electrobalance Assembly

The gravimetric adsorption assembly consists of a Cahn Recording Electrobalance coupled with a Weighing Mechanism located in a #2005 Glass Vacuum Bottle. The vacuum bottle is mounted horizontally in the bottle holder firmly held to the balance stand which is placed on a sturdy bench top. The feed line is wound around the sample tube which is connected to the vacuum bottle at the left-hand joint while the reference tube is connected at the right-hand joint. The center joint serves for connecting the vacuum takeoff tube.

The pressure transducer and the adsorbate outlet line are attached to the side arm of the vacuum takeoff tube. The vacuum system is connected to the Kovar end of the takeoff tube. A Westronic recorder Model MT presents a continuous weight-change curve when coupled with the Recording Electrobalance.

III.B.1.b Vacuum Unit

A POPE Porta-Vac high vacuum system is used in connection

with the Cahn Electrobalance Assembly. The Porta-Vac is capable of producing vacuum as high as 10^{-6} torr. Once the condensable vapors have been removed, a vacuum of 10^{-4} torr is obtained within 10 minutes while a vacuum of 10^{-5} torr is obtained within 30 minutes. The apparatus is first evacuated with an auxiliary vacuum pump before branching it to the Porta-Vac unit - the large volume of gas would be a nuisance to the mercury diffusion pump which is operating in good steady-state conditions. The vacuum system is also equipped with a cold trap.

III.B.1.c Pressure Measuring Unit

A Model 144 Precision Pressure Gage with a standard fused quartz bourdon capsule is used to measure accurately the absolute pressure from 0 to 760 mmHg. The open type bourdon capsule gave an absolute pressure readout on a digital counter. The capsule has two ports; the reference port is adjusted to a vacuum while the pressure port is connected to the apparatus. The transducer is easily zeroed when there is equal vacuum on both ports. Conversion to pressure units was obtained by multiplying the mechanical counter reading by the capsule constant.

A cabinet Model 144 houses a temperature control unit and an optical transducer unit is mounted on a motor-driven precision gear assembly for digital readout.

The capsule consists of a fused quartz bourdon tube in a Pyrex envelope which protects the bourdon tube and provides a

means of evacuating the volume around it.

III.B.1.d Feed and "Flow-thro" Unit

The feed unit consists of a gas cylinder equipped with a pressure regulator and autoclave valves. A low pressure regulator controls the flux to a needle valve which in turn regulates the flow rate into the apparatus at about 1cc/min. The needle valve is a Flow Controller Model 8744. The gas temperature is brought to that of the cell by coiling the path down around the hangdown tube's exterior. The feed line extends down vertically into the adsorption cell, just below the metallic pan holding the silica gel, through a sealed perforation along the hangdown tube. The gas exits through the vacuum takeoff tube. A Cartesian Manostat regulates the system pressure very efficiently and once set, produces no pressure fluctuations as indicated by the pressure transducer. The flow-thro unit is finalized with a continuously operating vacuum pump located in a fume hood.

III.B.1.e Temperature Control and Measurement Unit

The adsorption cell is held at a constant temperature by circulating liquid through an insulated cylindrical container placed around the hangdown tube. The temperature is regulated by a P.M. Tamson Thermostatic Bath Model TE3 equipped with a circulation pump. Methanol is used as the medium for maintaining

constant temperature conditions for temperatures below 15°C while water is used for ambient temperatures or over. A valve regulates the outlet flow of the fluid. The liquid returns to the bath by gravity. All lines are insulated. A contact thermostat together with a quartz heater and a cooling coil provide excellent temperature control. When working at ambient temperatures, tap water line and a needle valve in series with the bath cooling coil are used. For lower temperatures, a Portable Bath Cooler Model PBC-2 is used instead of the bath cooling coil. This unit will enable the bath to be controlled at temperatures down to -20°C or lower. In use, the PBC-2 evaporator coil is placed near the bath heater and the fluid return line to minimize temperature gradient. This provides good heat exchange between the coil and bath medium and adequate agitation across the coil. This is indicated by no frost build up along the coil hose and external line.

Temperature measurements are made with a copper-constantan thermocouple placed vertically along the hangdown tube. The tip of the thermocouple extends down to the pan position. This thermocouple is used in conjunction with a Leeds K-3 potentiometer and a Tinsley galvanometer. The reference junction employed is an ice-water mixture.

The contact thermostat is adjusted to give the required constant adsorption cell temperature as indicated by the thermocouple voltage reading on the potentiometer. Frequent readings indicated excellent temperature control.

III.B.2 Calibration

III.B.2.a Cahn RG Electrobalance

Two types of weights were used with the balance: calibrating weights and tare weights.

Calibrating weights are of class M and are the most accurate available (46). They were used for calibration and as substitution weights in tare procedures. They are metric weights designed for use as reference standards for investigations demanding a high degree of constancy over a period of time. Tolerance for class M weights up to 5 grams have been so selected that corrections for the individual weights may be neglected. The tolerance on all class M weights, from 1 to 500 mg, is 0.0054 mg.

Tare weights are of class C and are relatively inaccurate. They are made of the usual weighing materials and are as stable and constant in weight as the others. They are intended to tare loop C.

Before proceeding with the calibration of the balance, the weighing Assembly is disconnected from the electrical output of the Control Unit so that the recorder base line can be set with its own zero control. The maximum sample weight variation expected during adsorption should be known in advance. The change in the weight of the silica gel sample to be encountered during the experimental runs should be investigated before the

calibration is carried out. The range in the change of weight of the sample is limited by the lowest weight produced in the activation process and by the maximum possible adsorption of the heaviest gas at the lowest system temperature and at maximum total pressure. This procedure permits the use of the same calibration range throughout the entire experimental investigation.

The beam is balanced by a 100 mg tare weight on loop C and a 100 mg calibrating weight on loop A. The latter is known as the substitution weight. Suppose the maximum variation upon adsorption will not exceed 20 mg; then a 10 mg calibrating weight is placed in the pan of loop A and a 10 mg tare weight is placed on loop C. The Mass dial of the Control Unit is set at 50% of the selected maximum variation. The balance beam axis is first roughly set horizontally. This is done by either removing or adding tare weights on loop C. The RECORDER RANGE control is turned down until the recorder is near full scale and adjustment of weights on loop C is continued until the recorder is again near zero.

The recorder is then set accurately to zero with the 50% Control Dial. The 10 mg calibrating weight is removed and the mass dial set to 0.0000. The recorder is set exactly to zero with the 0% Control Dial. The calibrating weight is replaced back on the pan, the mass dial set back to 50% and the recorder is reset to zero with the 50% Control Knob. The above procedure is repeated until the last step shows no change. The calibrating weight is removed and thus the recorder span is

calibrated to give a 1 mg full-scale recorder deflection.

The calibrating weight and substitution weight are removed from the pan. The sample is placed into the pan. Its weight should slightly exceed that of the substitution weight. The total weight of the sample is equal to the substitution weight plus the MASS dial reading provided the recorder is set to the base line prior to each reading. The total weight is in mass units, the smallest division being 0.001 mg.

III.B.2.b Precision Pressure Gage

The pressure transducer had been calibrated at 44.0°C . The calibration chart accompanying the instrument is shown in Table III.1. The actual operating temperature of the quartz tube capsule was 44.3°C . The slight deviation from the set point temperature does not change the sensitivity of the capsule span since one degree centigrade change gives a 0.013% decrease in gage reading.

The pressure transducer was calibrated for a pressure range of 25 psia, however, it was used only up to 14.7 psia. This corresponds to a readout span of 120,000 divisions. The smallest division of the gage is 0.001 which corresponds to 0.000012 psia or 0.006 mmHg.

Precision instruments for the calibration of the pressure transducer were not available. However, the average deviation in the readings of a Heise pressure gage and a mercury manometer

TABLE III.1

PRECISION PRESSURE GAGE CALIBRATION CHART

Operating pressure range	0-24.5 PSIA	
Capsule thermometer reading during calibration	44.0 Degree C	
Serial Number	2021	
Model Number	144	
Type	1	
True Corrected Pressure PSIA	Pressure Gage Reading	Tube Constant PSIA/Degree
0.0000	0.000	
1.2241	10.057	0.12172
2.4533	20.143	0.12179
3.6824	30.238	0.12178
4.9115	40.333	0.12177
6.1357	50.391	0.12176
7.3648	60.441	0.12185
8.5939	70.536	0.12184
9.8181	80.588	0.12183
11.0422	90.638	0.12183
12.2763	100.777	0.12182
13.5005	110.832	0.12181
14.7296	120.925	0.12181
15.9537	130.991	0.12179

read with a cathetometer, reveal readings which are respectively 2 mmHg above and 0.5 mmHg below those of the pressure transducer. The precision of the Heise pressure gage is 2.5 mmHg while that of the mercury manometer is 0.06 mmHg.

In this work, the pressures are read only on the pressure transducer and are reported in mmHg.

III.B.2.c Temperature Measurement

The thermocouple was calibrated against ice-water bath. The potentiometer reading was + 0.0005 millivolt. For a copper-constantan thermocouple, this is equivalent to + 0.014 °C. The smallest division on the K-3 potentiometer is 0.0005 millivolt which is equivalent to 0.014 °C.

III.B.3 Experimental Procedure

The experimental observations measured at equilibrium are the system pressure and the total mass consisting of the mass of the sample plus the amount adsorbed. The adsorption well temperature was verified for each observation. The feed composition of the gas mixture was also noted for each isotherm.

The Gravimetric Adsorption System and accessories described in III.B.1 were set according to Figure III.1. The balance was calibrated using substitution weight as described in III.B.2.a. The substitution weight was replaced by a silica gel

sample obtained from the desiccator. The hangdown tube was adjusted to the vacuum bottle. Treatment of the silica gel sample was performed as in III.A.2.a.

When a constant weight of the sample was indicated upon the strip chart recorder, the adsorption experiment was started.

The valve leading to the vacuum system was closed and immediately the first dose of the adsorbate was bled slowly into the adsorption assembly until the required initial pressure was obtained. The furnace was removed from the hangdown tube, which was left to cool, and the constant temperature well was placed up around it.

The needle valve was opened and the Cartesian manostat adjusted to give the required pressure. The first observations of pressure and mass were made at equilibrium as indicated by the constant trace upon the strip chart recorder. The recorder pen was reset to the base line and the total mass of the adsorbate-adsorbent was recorded as the sum of the substitution weight and the mass dial reading. An illustrative example of a sequence of measurements of mass adsorbed is seen in Figure III.2 for $C_3H_8 - CO_2$ at $-10.0^\circ C$. A second dose of gas was admitted into the system and the whole procedure repeated as many times as needed to complete the isotherm.

A list of typical observations and calculations for the adsorption of 23.85% C_3H_8 with CO_2 on silica gel at $-10.0^\circ C$ is seen in Table III.2.

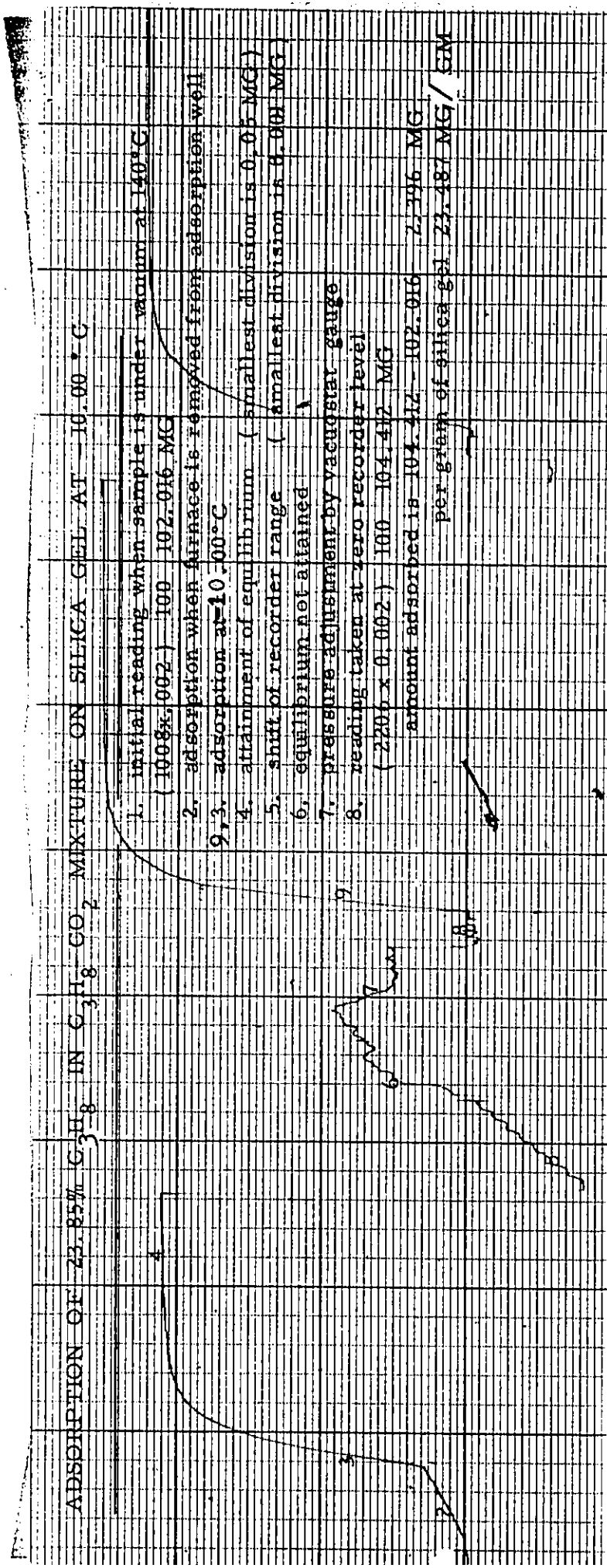


Figure III.2 Strip Chart Recorder Trace of an Equilibrium Determination

TABLE III.2

MEASURED ADSORPTION EQUILIBRIUM DATA

SpecificationsDate: 27/10/72System: C₃H₈ (0.2385) - CO₂ (0.7515)Temperature: -10.0°CPressure Gauge Temperature: 44.3°CTemperature Conversion: -0.380 MV = -10.00°CPressure Conversion: 0.1218 psid/gauge readingWeight Conversion: 100 + (0.002 MG/gauge reading)

Weight of Adsorbent measured:

in Vacuo + 140°C: 1008 102.016 MGinitial Pressure + 140°C: 1143 102.286 MGObservations

Cell Temperature (millivolt)	PRESSURE		WEIGHT			
	Gauge	cmHg	Gauge	Total	MG	MG/GM
0.380	5.691	3.581	2206	104.412	2.396	23.487
0.3805	19.488	12.271	3477	106.954	4.938	48.404
0.3815	39.134	24.637	4605	109.210	7.194	70.518
0.3800	65.202	41.072	5642	111.284	9.268	90.848
0.3805	95.200	59.959	6529	113.058	11.042	108.238
0.381	117.827	74.203	7116	114.232	12.216	119.126

III.B.4 Equilibration

Constant mass provides the indication that equilibrium has been achieved. This means that temperature and adsorption equilibrium have been reached. Since the quantity of gas adsorbed is a function of temperature, a constant mass recorded, within the sensitivity of the electrobalance, indicates the sample has reached a constant temperature. The sample tube is constructed from Pyrex glass, with a mid-section being Kovar tube, using glass to metal seals. The main purpose of the metal section is to insure that the adsorbate in the environment of the sample is maintained at the temperature of the constant temperature bath. Thus the heat of adsorption generated during the adsorption process can be dissipated away by convection and radiation (43). Different researchers (10, 49) working on adsorption of gases on silica gel claim that the equilibrium position is achieved by circulation for 15 minutes when the change in pressure approaches zero (49) while others (10) recorded the final pressure after 10 to 15 minutes. In our work, equilibrium conditions were reached within 10 to 15 minutes at higher pressures while 30 to 45 minutes were needed for the first dose. In the latter case, the temperature equilibration is longer because the sample had just been reactivated. The rate of heat transfer is not a problem for pressures higher than 25 mmHg (50).

Changes in total weight measured were less than ± 0.0005 mg for 15 minutes following a new dose. The precision of the

electrobalance was 0.001 mg. During that small interval of time, no pressure changes were observed. However, for longer periods of time, changes of pressure were observed and were due to room temperature changes. During the determination of an entire isotherm (6 hours) the adsorption well temperature fluctuations measured were $\pm 0.014^{\circ}\text{C}$ which corresponds on the potentiometer to 0.00025 mV. The smallest division on the potentiometer is 0.0005 mV or 0.014°C .

III.B.5 Experimental Results

The pressure-mass-temperature-gas phase composition (P-m-T-y) equilibria on 25 mesh silica gel were determined experimentally for the following systems:

Ethane - ethylene

Ethane - carbon dioxide

Carbon dioxide - propane

Pure component and mixture isotherms were investigated at -10°C , 0.0°C , 25.0°C and 50°C for pressures ranging from 25 mmHg to 760 mmHg. The gas phase molar compositions were roughly 25%, 50% and 75% for the three mixtures and are listed earlier in Section III.A.1.

The total number of observations made, including verifications arising from cross-plot correlations and duplications

for testing the reproducibility of the curves and testing for hysteresis, add up to 375.

Adsorption equilibria of pressure-mass adsorbed (P-m) are presented in Tables III.3 in Appendix I. The reported data were found to be reproducible on different samples of silica gel of the same stock. Adsorption and desorption experiments indicated no hysteresis effects. Buoyancy effects and thermomolecular flow were considered. The corrected isotherms are listed in Tables III.4 in Appendix I. The corrected data for the binary mixtures with their pure components for the systems $\text{CO}_2 - \text{C}_2\text{H}_6$ and $\text{C}_3\text{H}_8 - \text{CO}_2$ are plotted together in Figures III.3. The isotherms at 263.2°K , 273.2°K and 298.2°K are respectively plotted in Figures III.3.1, III.3.2 and III.3.3. The system $\text{C}_3\text{H}_8 - \text{CO}_2$ at 323.2°K is plotted in Figure III.3.4. The experimental data points of Figures III.3 were taken from Tables III.4 in Appendix I. The solid curves were obtained from the BET correlation of the corrected data of Tables III.4 in Appendix I.

III.B.6 Reproducibility of Adsorption Equilibria

It was possible to reproduce adsorption equilibrium data within the limits of the experimental error provided the silica gel sample was appropriately treated as described in III.A.2.a.

The two sets of ethane adsorption equilibria at 0.0°C

Figure III.3.1 Adsorption Isotherm at 263.2°K for C₃H₈-CO₂ and CO₂-C₂H₆ Systems

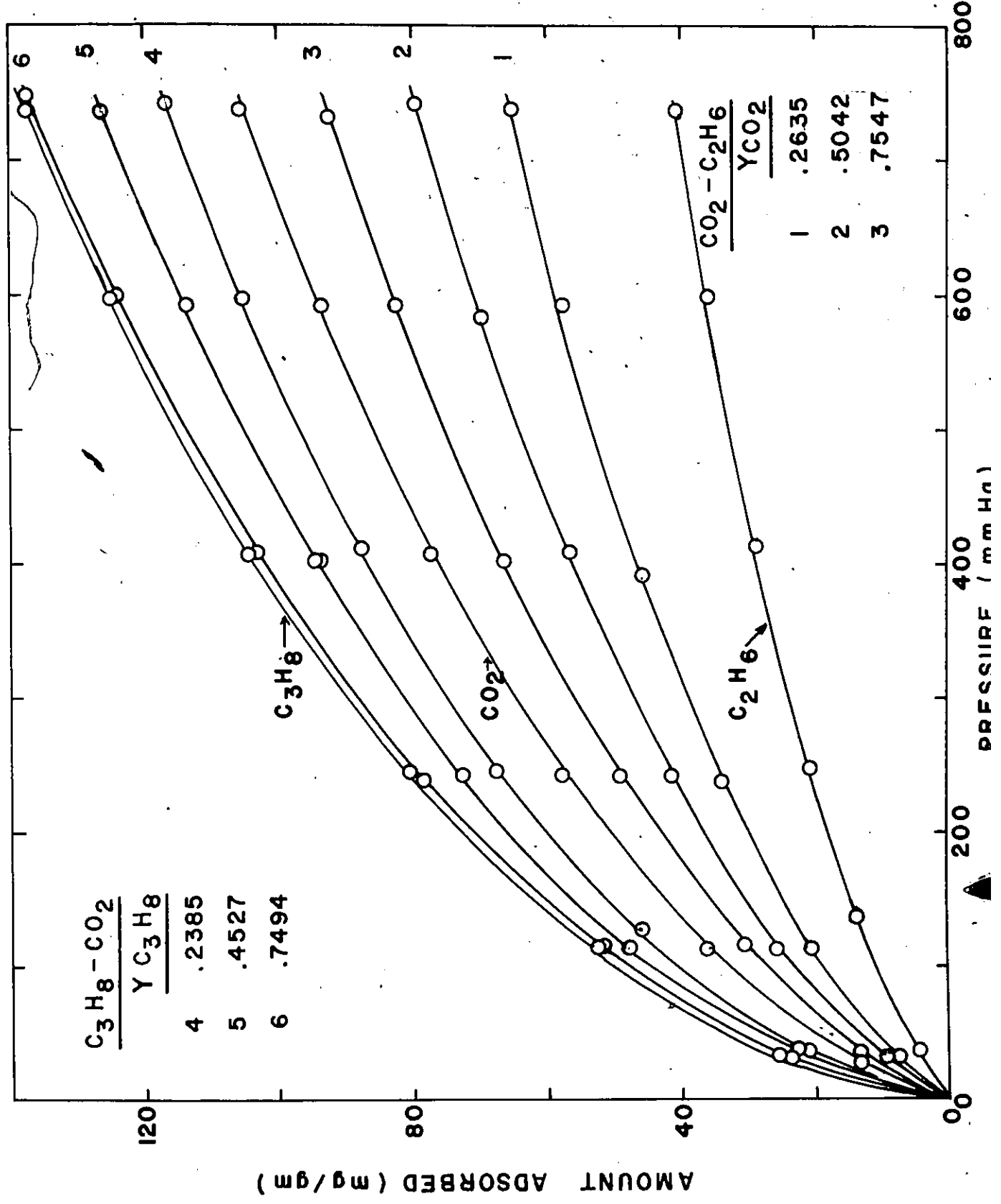


Figure III.3.2. Adsorption Isotherm at 273.2°K for C₃H₈-CO₂ and CO₂-C₂H₆ Systems

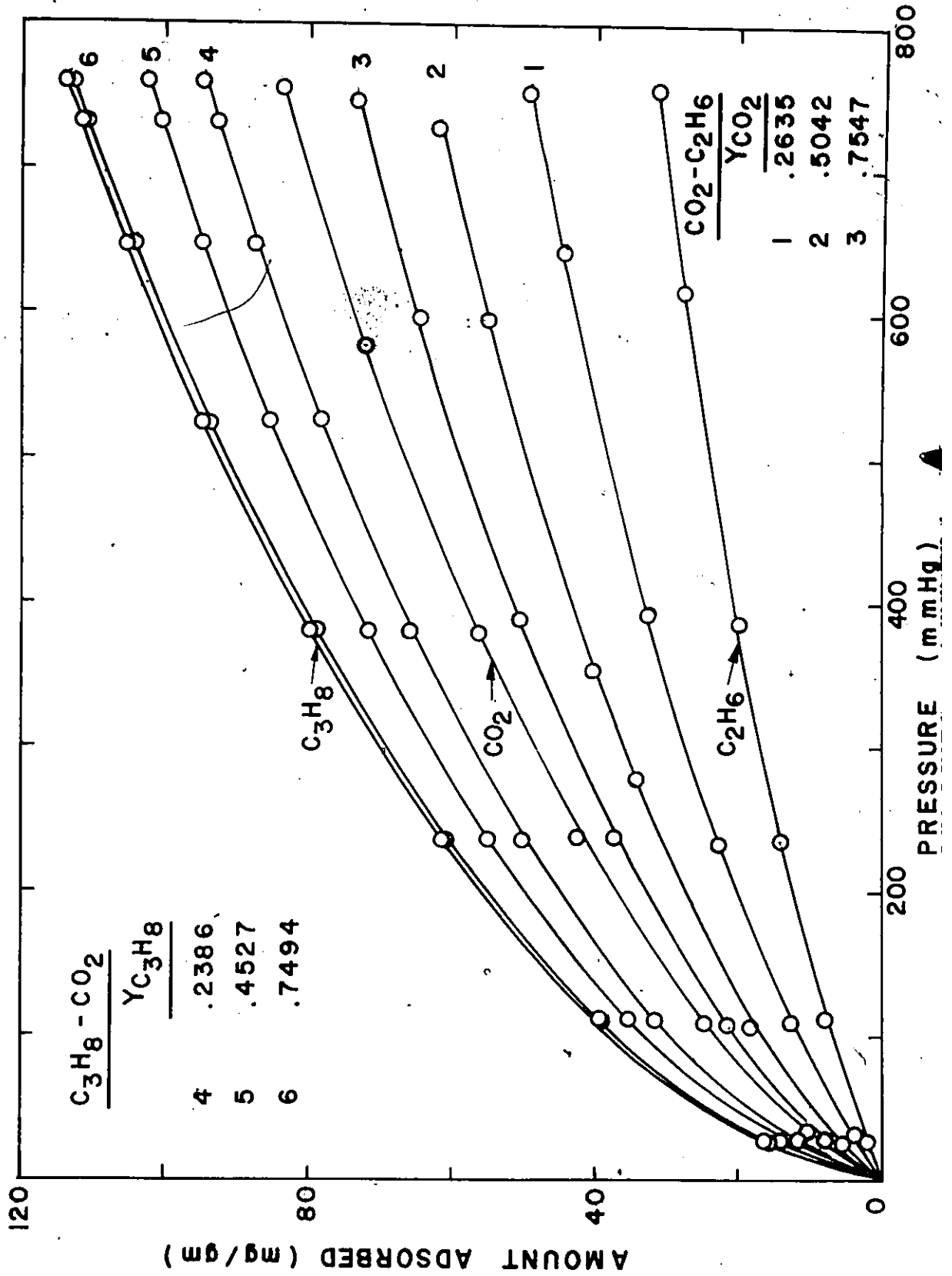


Figure III.3.3 Adsorption Isotherm at 298.2°K for C₃H₈-CO₂ and CO₂-C₂H₆ Systems

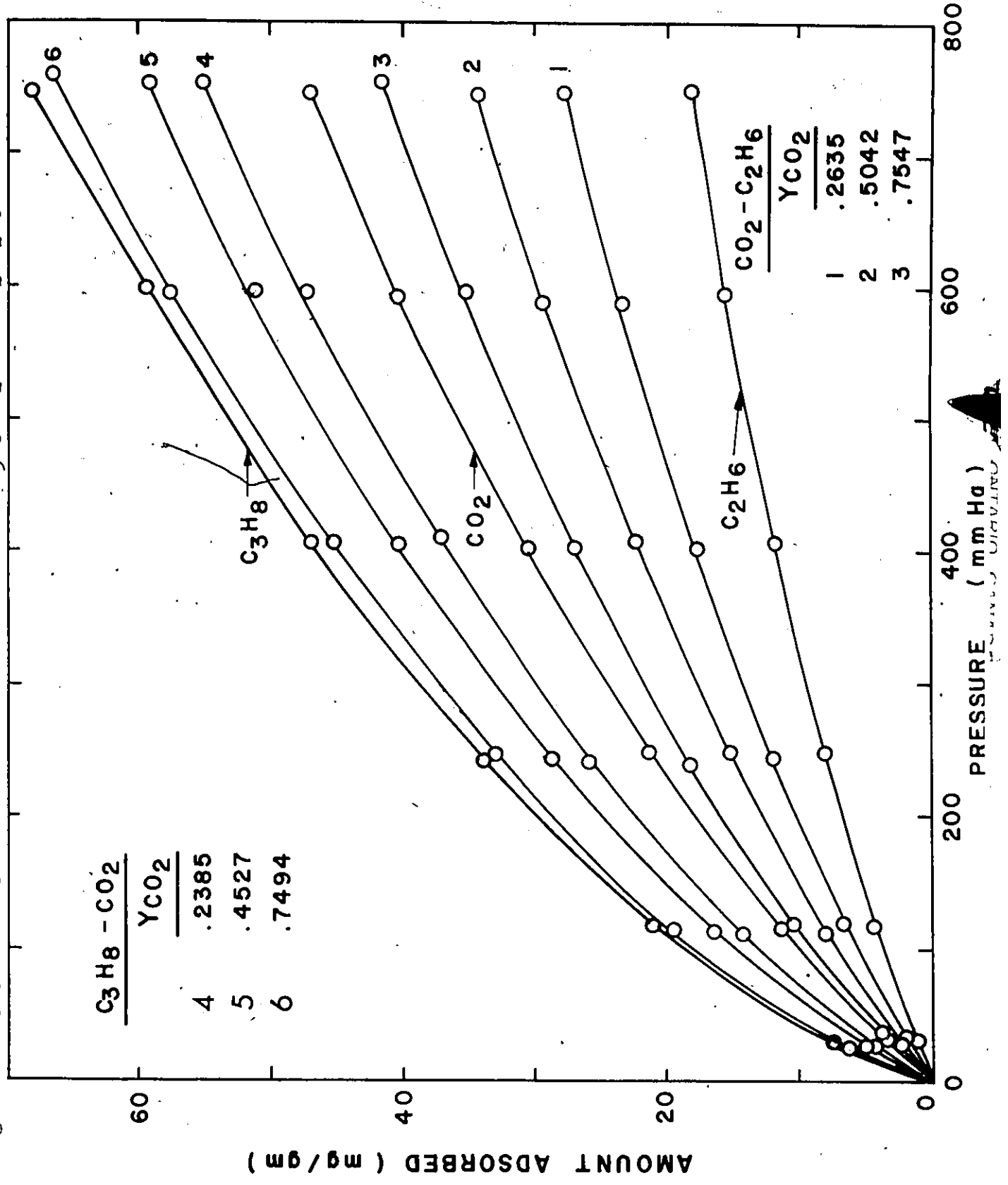
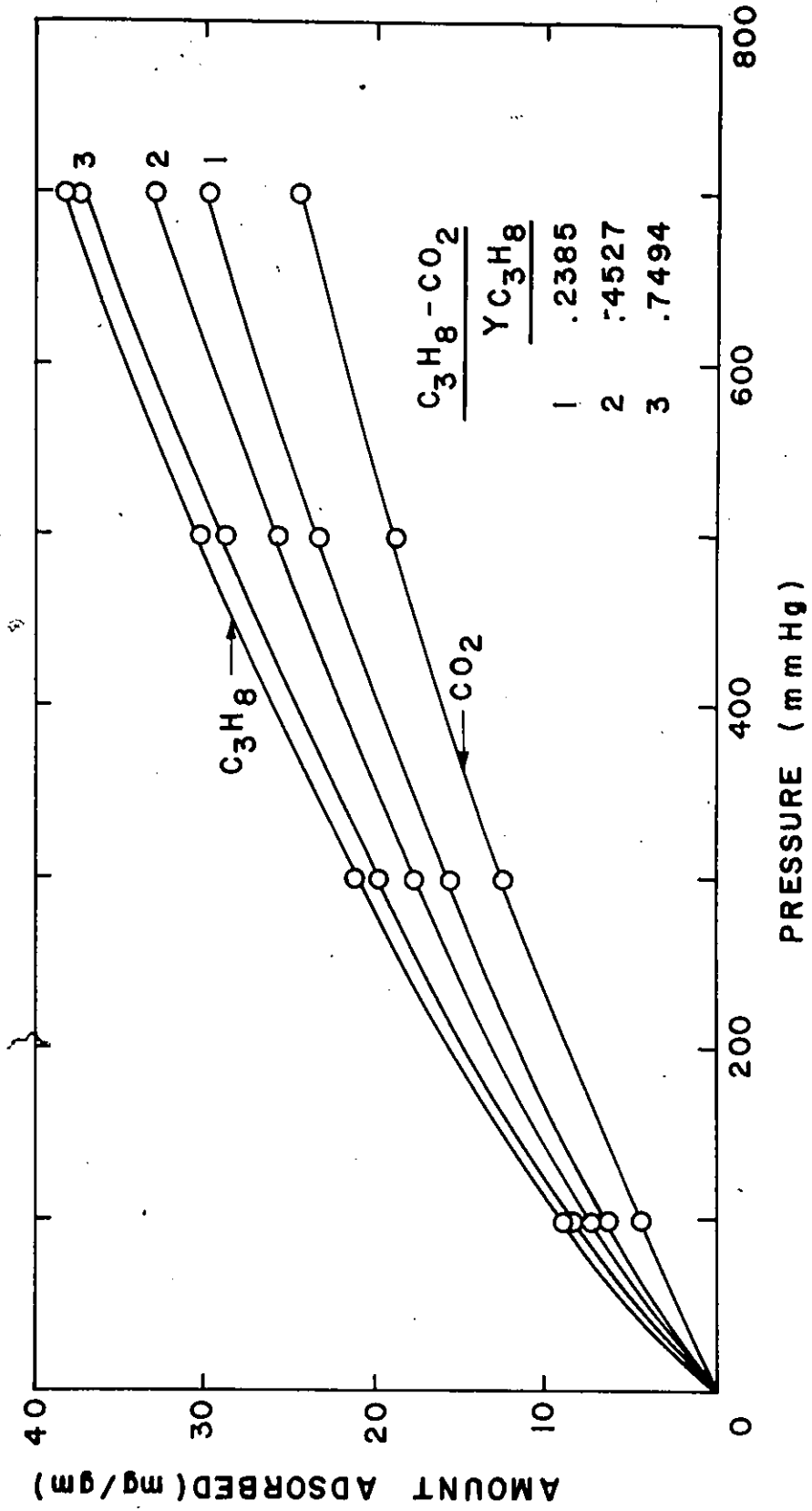


Figure III.3.4 Adsorption Isotherm at 323.2°K for C₃H₈-CO₂ System



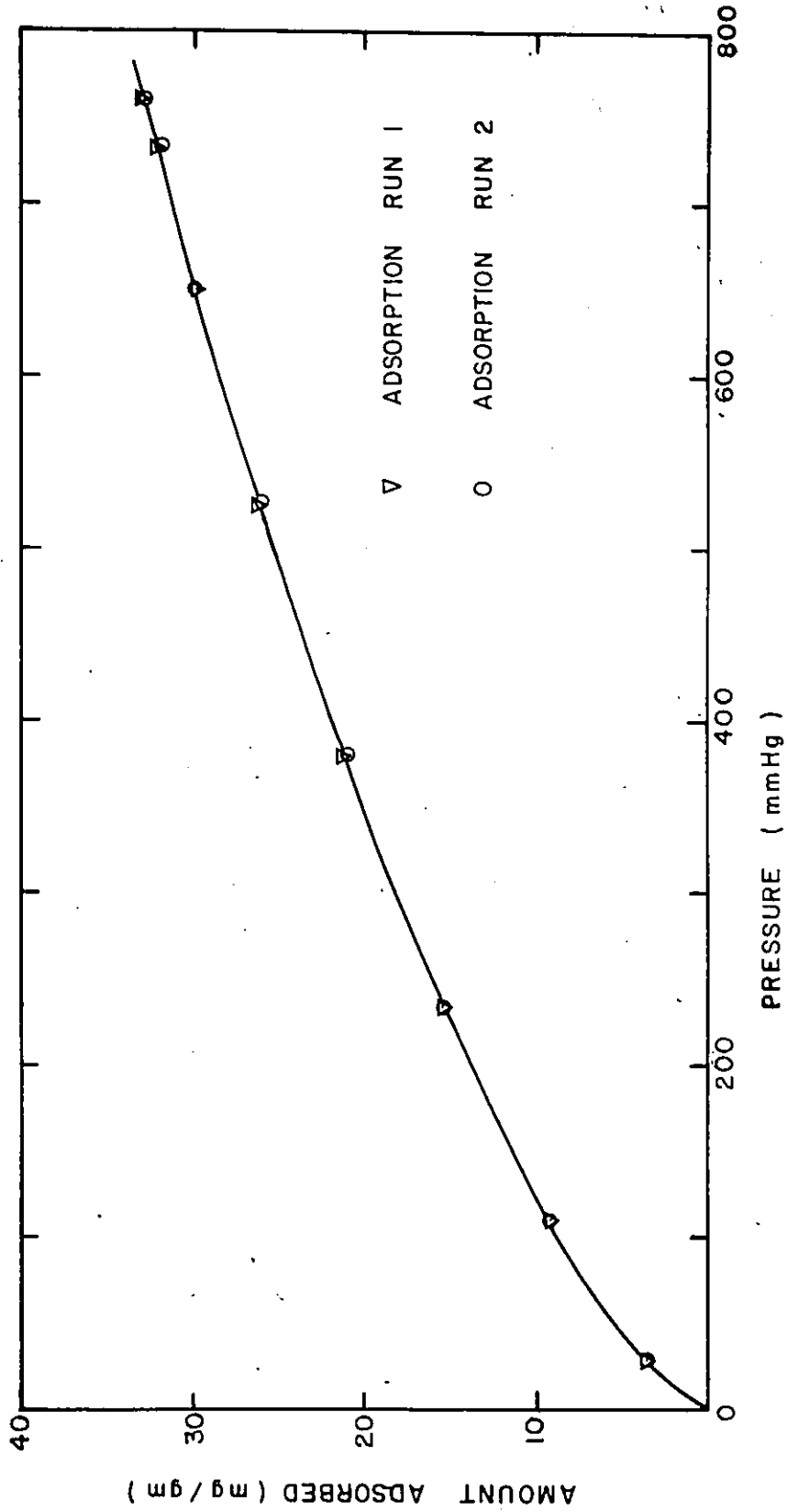


Figure III.4 Adsorption Isotherm Reproducibility at 273.2°K for C₂H₆ on the Same Sample



on the same sample #10 obtained on different occasions illustrate the degree of reproducibility and is seen in Figure III.4. The average per cent deviation in weight adsorbed per gram adsorbent is 0.61%.

It was also possible to reproduce the data on different silica gel samples #2, #8 and #10 of different weights. Adsorption equilibria were measured for ethylene at 0.0°C on these different sample weights at intervals of several months and are illustrated in Figure III.5. The average per cent deviation in the amount adsorbed per gram of sample is 0.98% for samples #8 and #10.

Adsorption equilibria for these two components were also repeated at 25°C on the same silica gel sample results are plotted in the Figure III.6.

Mixture adsorption equilibria were repeated for the system $\text{CO}_2 - \text{C}_3\text{H}_8$ on #18 silica gel sample, at 25°C and are plotted in Figure III.7.

As stated earlier, class M weights were used for the calibration of the electrobalance. The tolerance on all class M weights, from 1 to 500 mg, is 0.0054 mg (46). When measuring an adsorption equilibrium point, two readings of the mass are required; the first is for the initial mass of the adsorbent, m_1 , and the second is the mass of the adsorbent plus that of the gas adsorbed m_2 . The smallest division on the mass dial vernier is 0.001 mg. However, the duplication of an adsorption point was not within 0.002 mg since there are other factors that must be accounted for, such as, the exact pressure duplication and

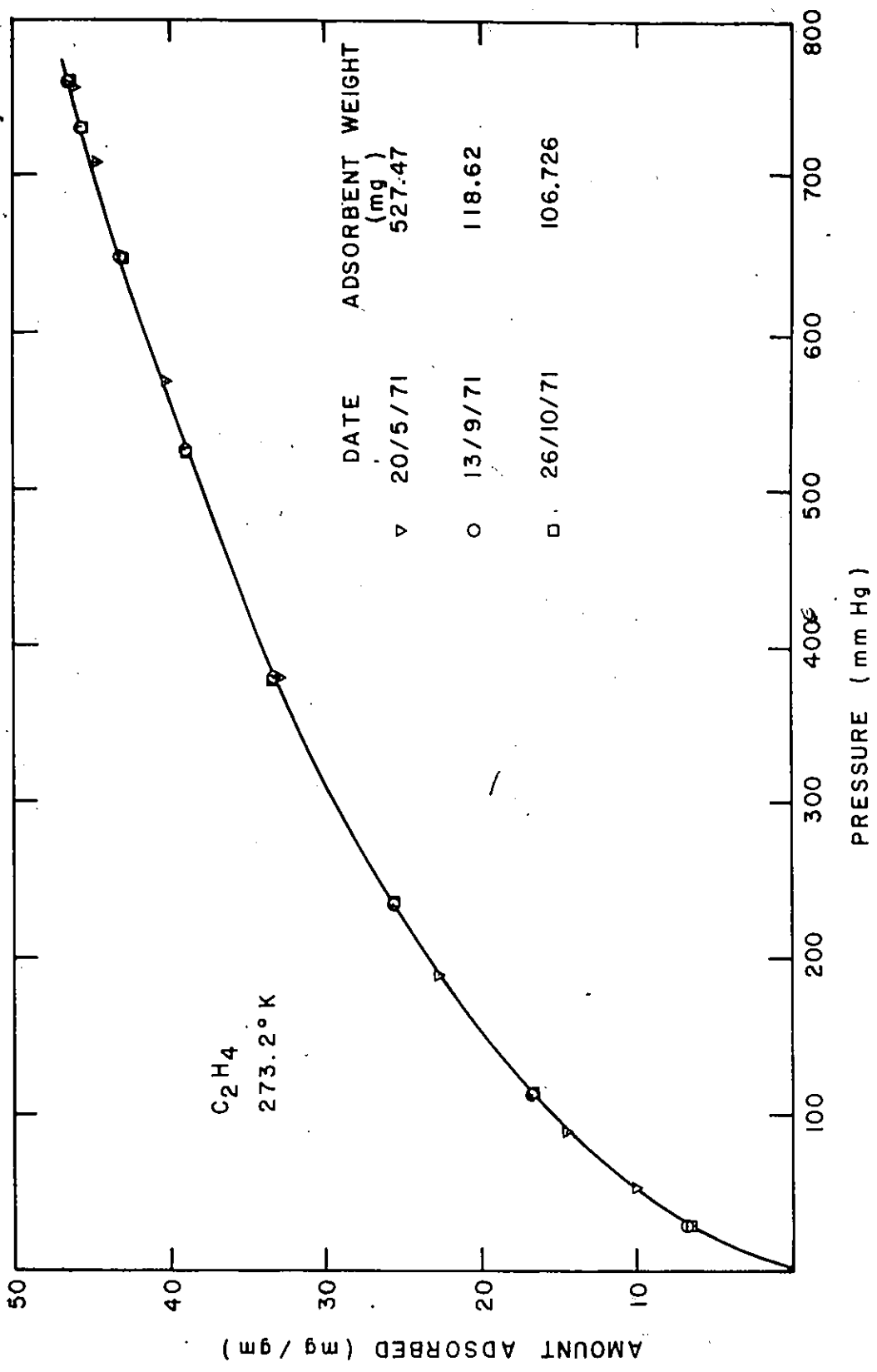


Figure III.5 Adsorption Isotherm Reproducibility at 273.2°K for C₂H₄ on Different Samples



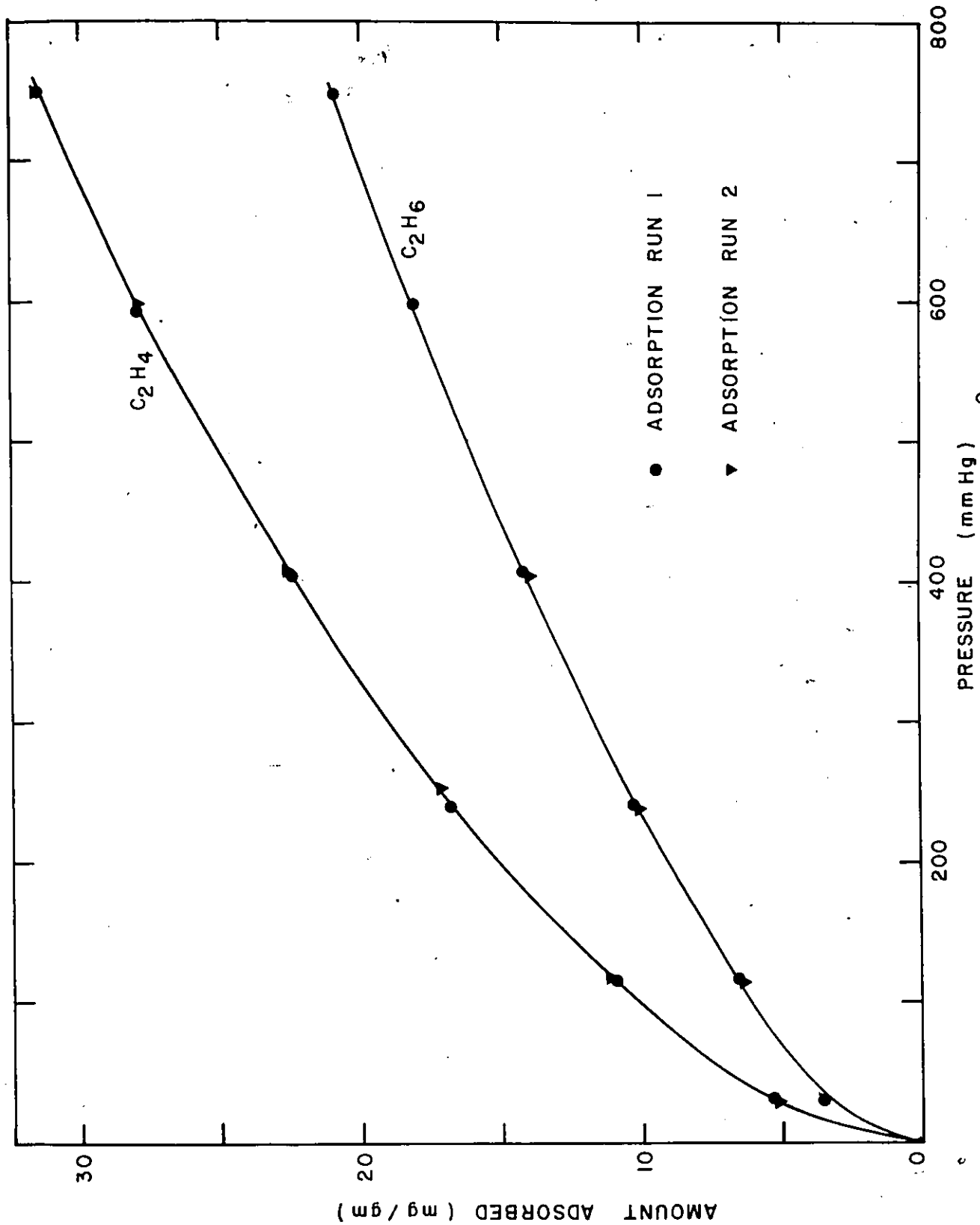
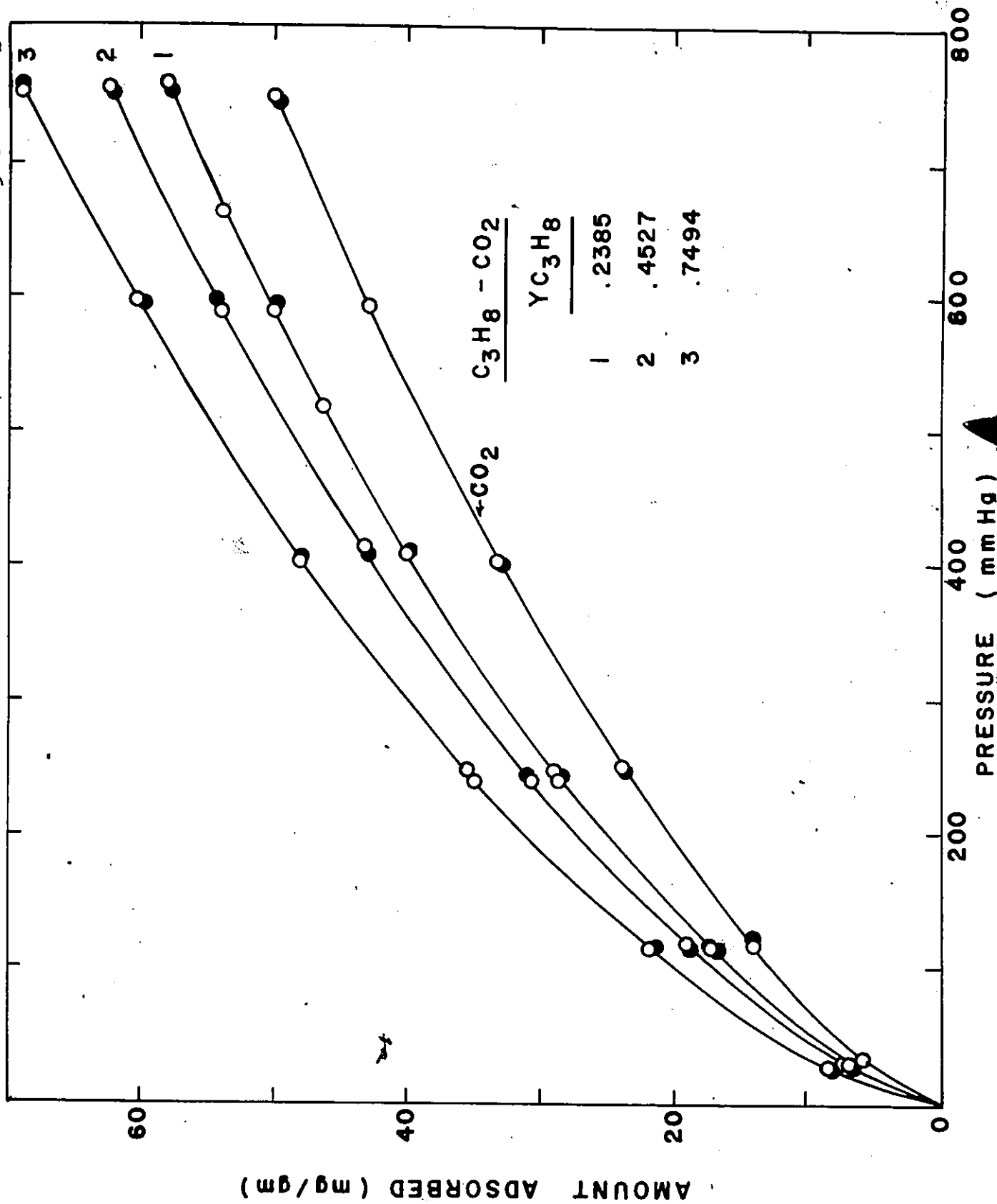


Figure III.6 Adsorption Isotherm Reproducibility at 298.2°K for C₂H₄ and C₂H₆ on the Same Sample

Figure III.7 Mixture Adsorption Isotherm Reproducibility at 298.2°K for C₃H₈ and CO₂ on the Same Sample



temperature regulation. Since each pressure duplication was within 0.2 cmHg, one can expect the amount adsorbed to be slightly different for each corresponding pressure. Temperature regulation at low temperature was more difficult than at higher temperature. The presence of external circulation of the bath liquid and room temperature fluctuations made it more difficult to regulate the bath temperature over long periods of time. Reproducibility of the initial weight of the adsorbent was satisfactory.

III.B.7 Hysteresis

Experiments were performed to study the possible hysteresis effect in the adsorption-desorption equilibria of the systems investigated in this work. They were carried out with the intent to verify the consistency of an individual isotherm and also that of several isotherms for a given system. The former consists of desorbing the gas following an isothermal adsorption run. The latter was performed by doing an isobaric adsorption-desorption experiment for the temperature range investigated.

Isothermal desorption showed no trace of hysteresis. These observations were taken at random for most of the systems investigated. It was found unnecessary to perform the desorption experiments on all runs due to the molecular similarities of the pure components and their mixtures for the temperature and pres-

sure range studied. To supplement this statement, a typical system of $\text{CO}_2 - \text{C}_3\text{H}_8$ - Silica gel system at 700 mmHg was studied for a temperature range from -22°C to $+50^\circ\text{C}$. Comparison was also made with previously determined isotherms by graphically interpolating at $P = 700$ mmHg.

The agreement between the measured isobaric equilibrium points and the values interpolated from isothermal plots is satisfactory. The graphical interpolation reveals that the average deviation in temperature is $\pm 0.15^\circ\text{K}$ while that for the mass adsorbed per gram of adsorbent is $\pm 0.5\%$. These values were estimated on larger graph paper and the results are plotted in Figure III.8.

III.B.8 Correction Factors

Correction factors, determined from blank experiments, are sometimes significant. The total load on the balance during blank experiments should be identical to that used during actual measurements (47). The source of the mass corrections considered in this work arise from the combined effect of buoyancy and to the spurious effects caused by thermal molecular flow. In the latter case, much larger weight than any weight change have been observed (48). As the pressure is increased, say to 10 mmHg, the effect of thermomolecular flow is much less and the effect of buoyancy predominates. The buoyancy effect has been found to be present at higher pressures while the thermomolecular effects

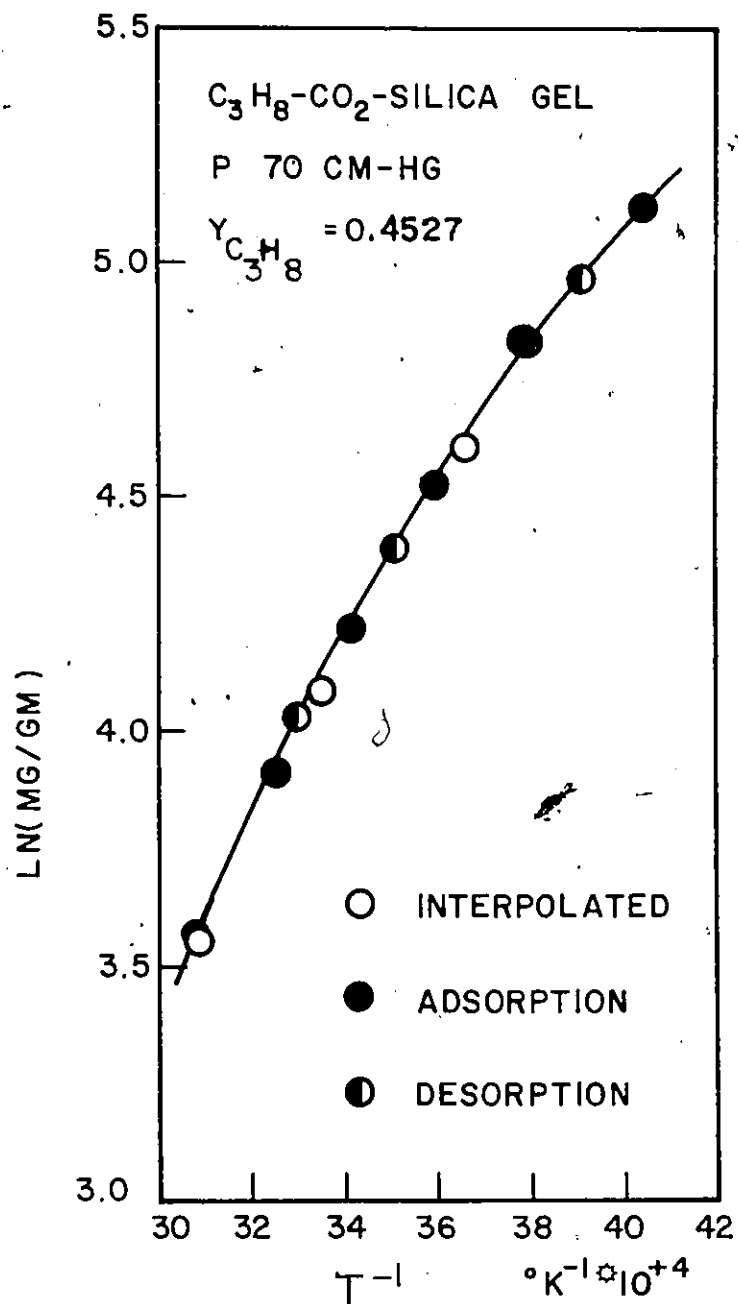


Figure III.8 Isobaric Adsorption-Desorption
for the System $C_3H_8-CO_2$

have been found at high vacuum and higher temperature.

III.B.8.a Buoyancy Effects

Usually there is an unequal upthrust on the sample or counterweight side of the beam (44). Equal upthrust is achieved if we have identical suspension wires and pans, in identical sample tubes, immersed in the same constant temperature bath. This is usually not the case. There is still likely to be a difference in volume of the sample and the counterweight. Buoyancy effects were investigated using a blank run. This consists of a series of mass measurements at a series of pressures covering the pressure and temperature range investigated. The results of the investigation are plotted in Figure III.9 as the ratio of mass of the tare weight to the pressure of the gas employed in the system against the temperature of the adsorption well.

III.B.8.b Thermomolecular Flow

At high temperatures and low pressures there exists an aerodynamic effect due to a thermomolecular effect. This anomalous behaviour has been the subject of intensive study. At these pressures, the mean free path of the molecules are longer than the tube diameter. When the molecules hit the suspension wire and pan a decrease in weight is observed. In this work, thermo-

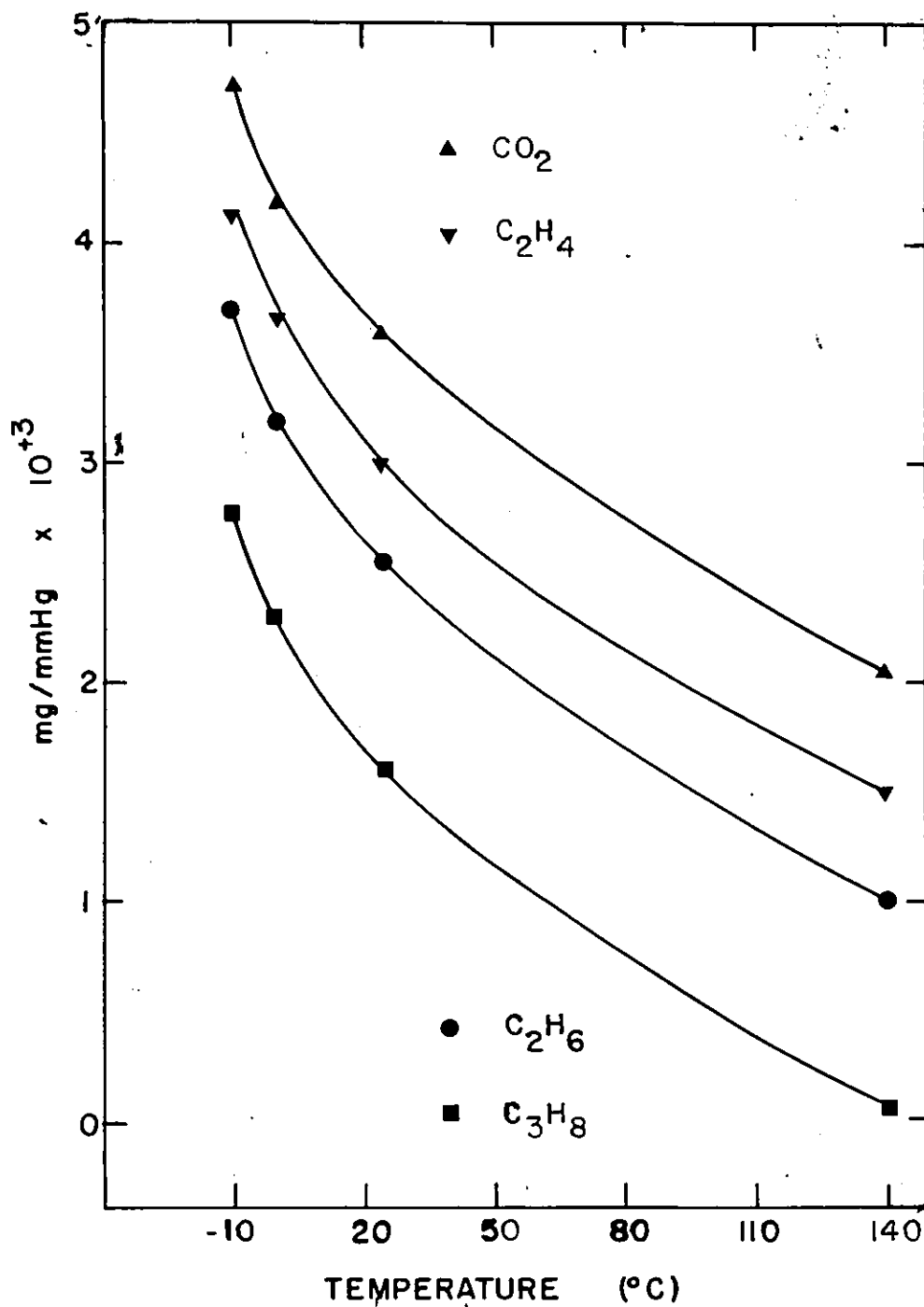


Figure III.9 Buoyancy Correction

molecular effects have been found to occur while reactivating the sample at 140°C and 10^{-4} mmHg. As soon as the gas was introduced to give a pressure of 10 mmHg, there was observed a spontaneous increase in weight for either a blank experiment or an actual sample. No noticeable adsorption took place at this temperature. However, adsorption followed once the furnace had been removed. The change in weight on the same sample has been found to be very reproducible. A value of $0.2199 \text{ mg} \pm 0.002$ based on 33 reactivations followed by an isothermal adsorption has been measured. The corrected isotherms are presented in Tables III.4 in Appendix I.

III.C Volumetric Adsorption System

III.C.1 Apparatus

A versatile Porta-Vac High Vacuum System was used as the manometric apparatus to measure adsorption equilibria. A schematic diagram is shown in Figure III.10. A gas recirculation path was achieved by installing a recirculation pump. Along this circuit, connections were made to a pressure gauge, an adsorption cell, a gas supply-line, a calibrated bulb and a gas partitioner. Accessories such as vacuum pumps, a recorder, a furnace, dewar flask and a thermometer were also needed.

The recirculation of the gas was effected with an electro-magnetic pump installed in the closed circuit. It is capable of retaining a high vacuum and has been used vapor-liquid

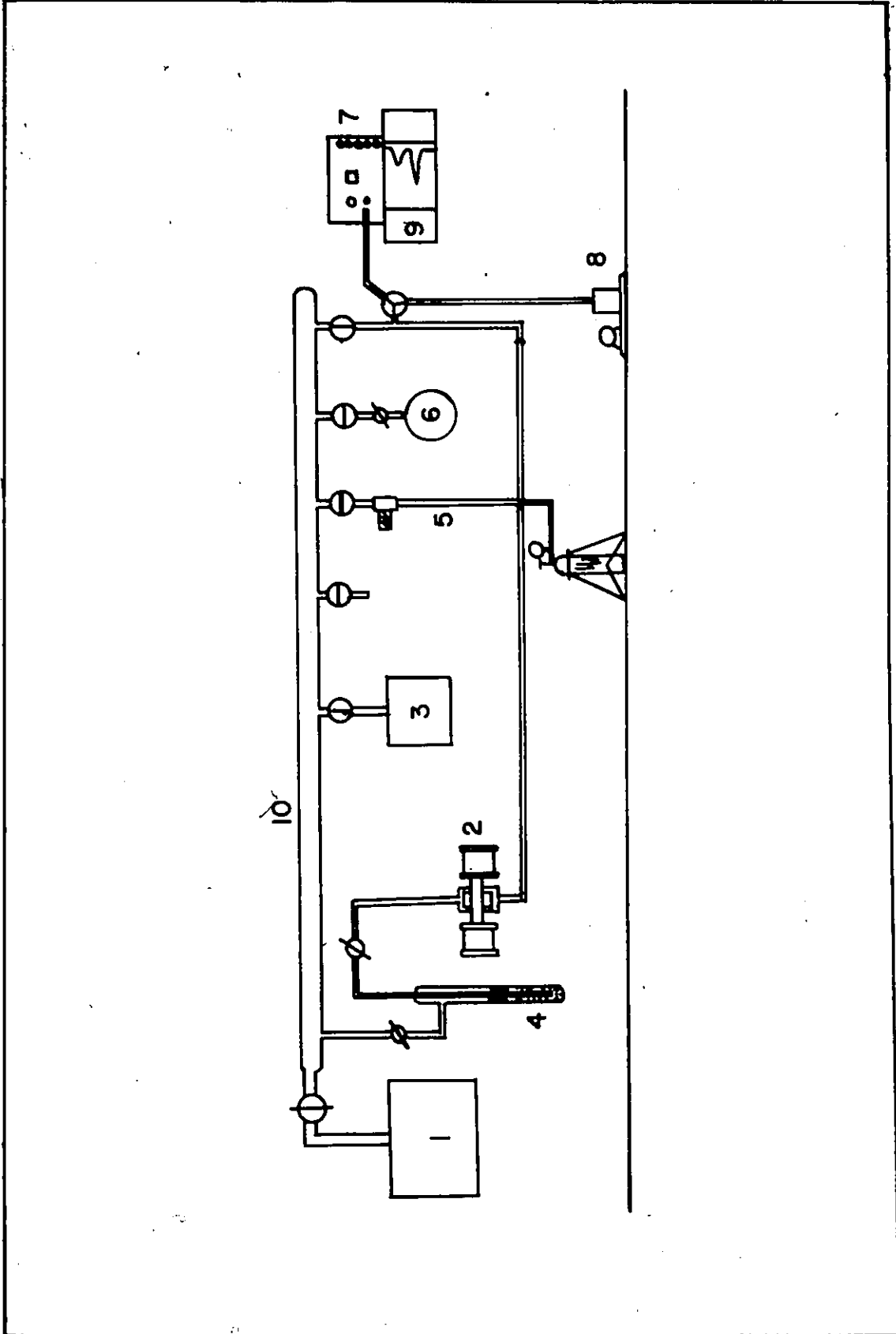


Figure III.10 MANOMETRIC ADSORPTION APPARATUS



LEGEND OF FIGURE III.10

1. Porta-Vac High Vacuum System
2. Recirculation Pump
3. Pressure Gage
4. Adsorption Cell
5. Gas Supply Line
6. Calibrated Bulb
7. Gas Partitioner
8. Vacuum Pump
9. Strip Chart Recorder
10. Manifold

equilibria (55). The system pressure was measured with a Precision Pressure Gauge described earlier in Section III.B. The adsorbent was placed in a glass cell capable of containing more than 10 grams of silica gel. Its geometry is essentially simple and is shown without further details in Figure III.10. The gas supply rate into the manifold was regulated by means of a needle valve and the gas cylinders were equipped with a pressure regulator. The manifold volume and dead-space of the apparatus were determined with the use of a calibrated one-litre capacity glass bulb. Analyses of gas samples were performed with a Fisher Model 25-V Gas partitioner coupled with an MT Westronic Recorder. Reactivation of the silica gel was made with a furnace regulated at 140°C by a Variac voltage regulator. Room temperature was measured on a thermometer with readings to the nearest tenth of a centigrade degree.

III.C.2 Calibration

III.C.2.a Bulb Volume

The volume of a clean, dry one-litre glass bulb was measured by weighing distilled water contained within it. Compensation for density of the distilled water and for buoyancy of air was taken into consideration. A value of 1.0875 ± 0.0001 was calculated as the bulb volume. A 2°C change in room temperature would give a $\pm 0.005\%$ deviation in the calculated volume.

III.C.2.b Manifold and Dead Space Volume

The calibration of the manifold and dead space volume was achieved by the expansion of helium gas. Essentially, the method consists in expanding the gas into the calibrated glass bulb from the manifold, then into the adsorption cell. The calculation of the manifold volume, V_m , and dead space, V_d , were done using the ideal gas law. The results of different determination for V_m and V_d are listed in the following table.

Calibration of Manifold and Dead Space Volume

Sample Weight (gm)	Manifold Volume		Dead Space Volume	
	V_m (litre)	deviation $\pm(\%)$	V_d (litre)	deviation $\pm(\%)$
9.372	0.7491	0.02	0.1201	0.25
7.799	0.7468	0.07	0.1203	1.2
16.543	0.7489	0.13	0.1187	0.3
11.025	0.7510	0.01	0.1199	0.05

An average value for the manifold volume is 0.7489 \pm 0.0011 litre (\pm 0.15%). The values in the 3rd and 5th columns are based on 3 gas expansions for each sample weight. In the calculation of phase equilibria, the value of the manifold

volume employed was 0.7489 litre. As for the dead space volume, the value corresponding to the sample weight was used.

III.C.2.c Gas Partitioner

Analyses of the gas mixtures were made with a Gas Partitioner Model 25V in conjunction with a Westronic Recorder Model MT-1. The gas sample was carried through a six-foot column, packed with 30-40 mesh silica gel, by helium at a flow rate of 80 cc/min and at a pressure of 20 psig. The chromatographic column was held at 55°C and the cell current was set at 5 milliamperes. The retention time for C₂H₆, CO₂ and C₃H₈ were respectively, 5, 6 and 23 minutes. The elution time remained stable throughout the experimental runs. The gas partitioner cell sensitivity for peak height trace was set at 25/25 and 10/10 for the analysis of CO₂ - C₂H₆ and CO₂ - C₃H₈ mixtures respectively. The gas chromatograph was calibrated against standard mixtures received from the Matheson Company Ltd. (see III.A.1). A typical trace of the calibration for 74.94% propane with carbon dioxide is seen on Figure III.11. Peak height ratio with corresponding mole fraction ratio are listed in Table III.5 for CO₂ - C₃H₈ and for C₂H₆ - CO₂. Graphical results are seen in Figure III.12 for CO₂ - C₃H₈ and in Figure III.13 for C₂H₆ - CO₂ as mole fraction ratio versus peak ratio of the constituents.

Synthetic mixtures were prepared from the pure constituents using the Porta-Vac apparatus. The purpose was to verify

74.94% PROPANE IN PROPANE - CARBON DIOXIDE

- I Injection No. 1
- II Injection No. 2
- I.1 Injection No. 1 for CO_2 (1)
- I.2 Injection No. 1 for C_3H_8 (2)
- II.1 Injection No. 2 for CO_2 (1)
- II.2 Injection No. 2 for C_3H_8 (2)

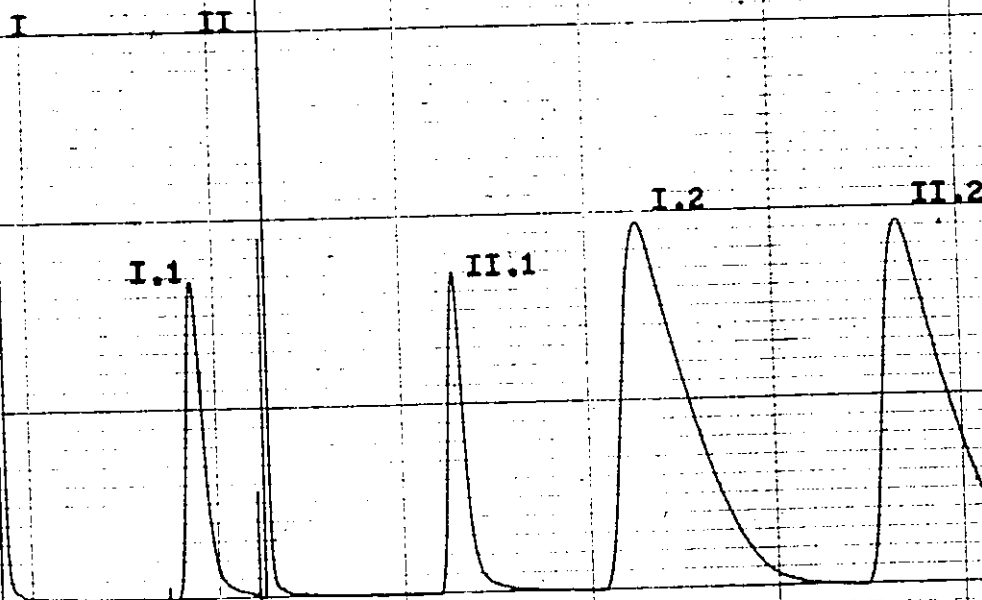


Figure III.11 Strip Chart Recorder Trace of the Gas Partitioner Calibration for 74.94% Propane with Carbon Dioxide

TABLE III.5

GAS PARTITIONER CALIBRATION DATA

C ₃ H ₈ - CO ₂ System	
$Y_{C_3H_8}$	$\frac{Y_{C_3H_8}}{Y_{CO_2}}$
	$\frac{P_{C_3H_8}}{P_{CO_2}} \left(\frac{10}{10} \right)$
0.2385	0.3132
0.4527	0.9354
0.7494	2.9904
	1.3374 ± 0.0161
CO ₂ - C ₂ H ₆ System	
Y_{CO_2}	$\frac{Y_{CO_2}}{Y_{C_2H_6}}$
	$\frac{P_{CO_2}}{P_{C_2H_6}} \left(\frac{25}{10} \right)$
	$\frac{Y_{C_2H_6}}{X_{CO_2}}$
	$\frac{P_{C_2H_6}}{P_{CO_2}} \left(\frac{25}{25} \right)$
0.2592	0.3499
0.4960	0.9841
0.7522	2.0529 ± 0.0026
	1.2386 ± 0.0072
	0.3294
	0.6674 ± 0.0025

Y: gas mole fraction

P: peak height in inches

$\left(\frac{25}{10} \right)$, etc.: gas chromatograph sensitivity

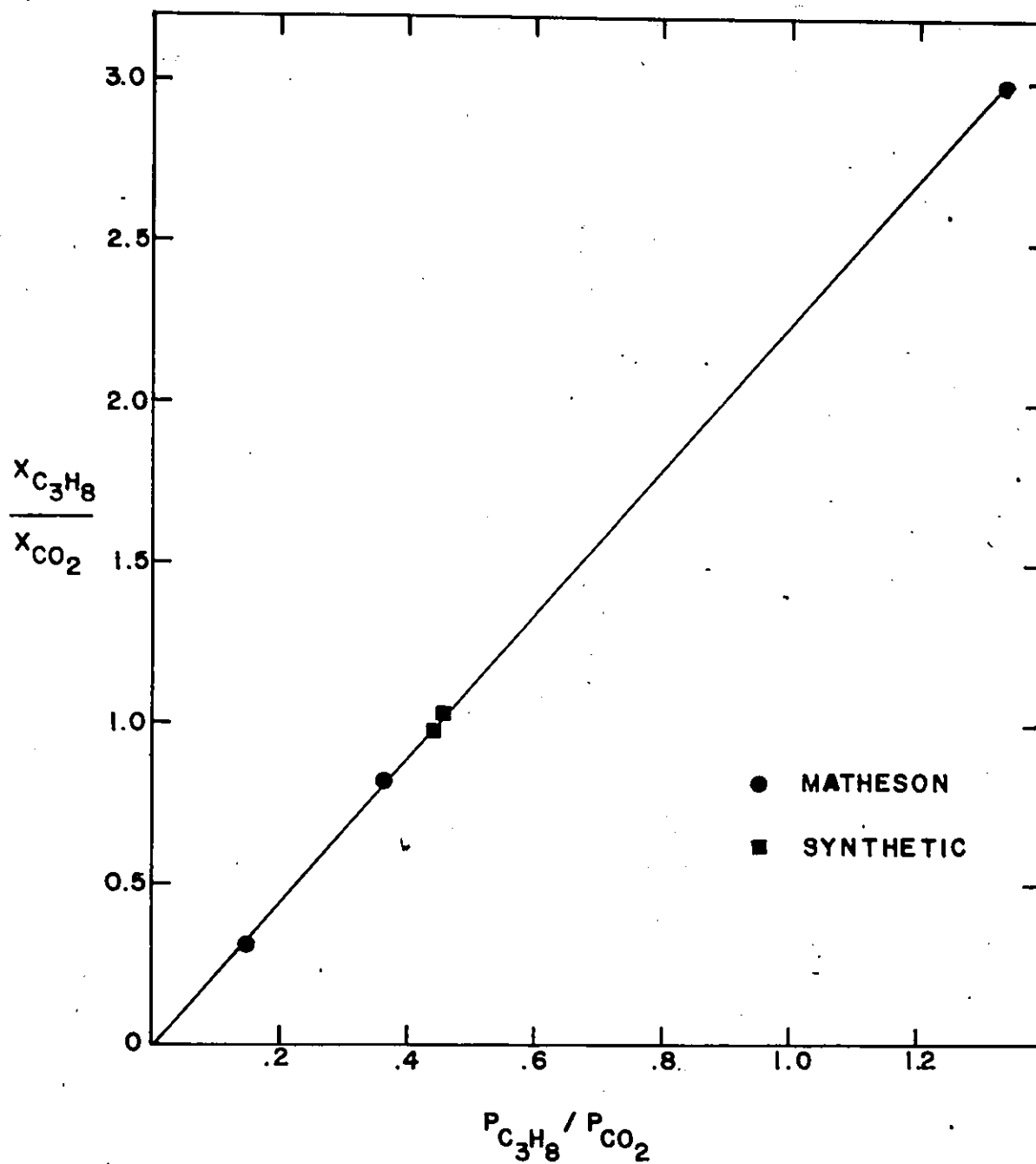


Figure III.12 Gas Partitioner Calibration for C_3H_8 - CO_2 Mixture

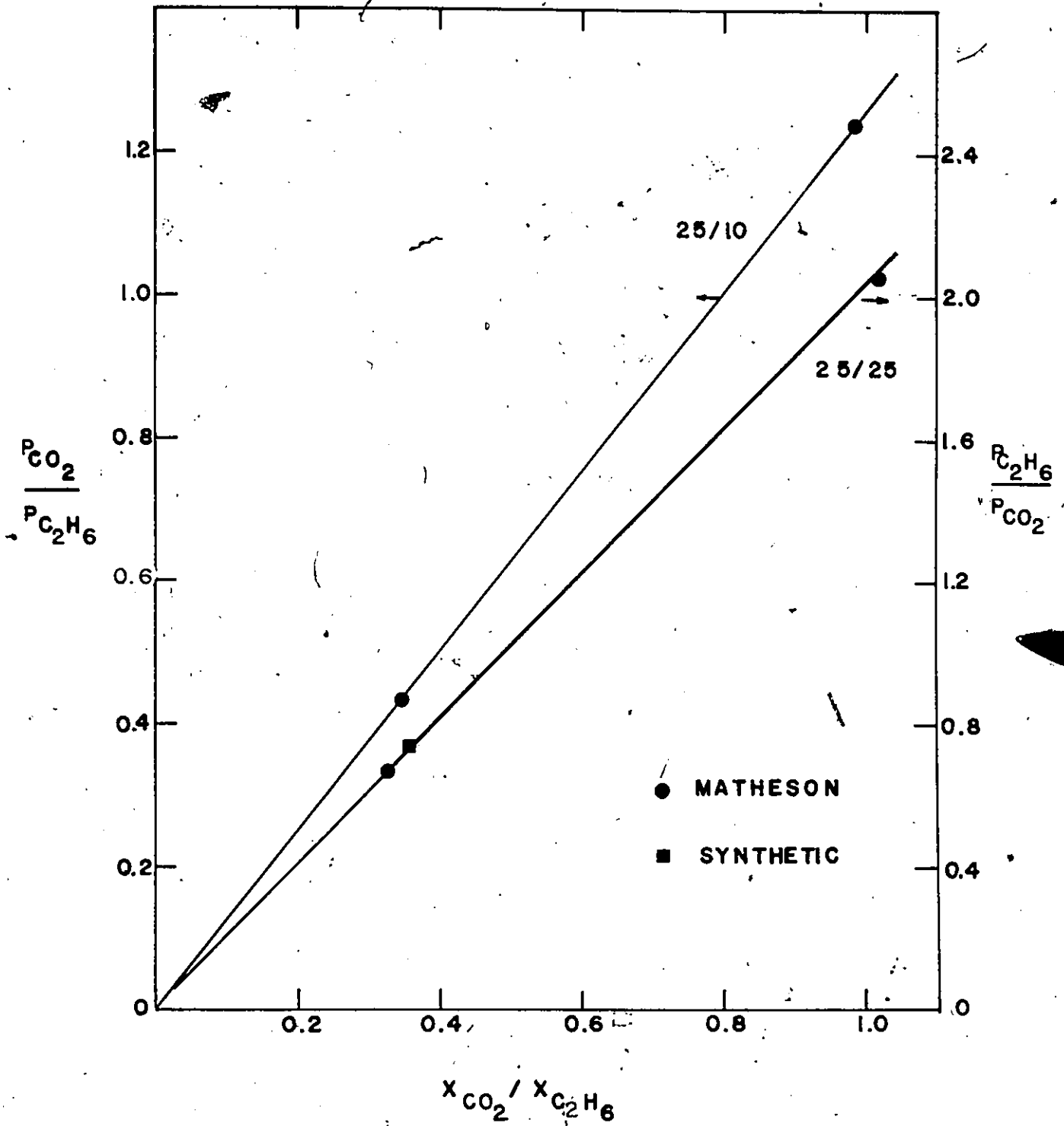


Figure III.13. Gas Partitioner Calibration for the $CO_2-C_2H_6$ Mixture

the reported composition of the standards. The composition of the prepared mixtures were calculated from Dalton's law of partial pressures since, at low pressure, the gas behaves ideally. The mole fraction ratio of the synthetic mixture with the corresponding peak height ratio are compared in Figures III.12 and III.13 with those analysed and reported by the Matheson Company Ltd. Values reported by Matheson were used in all phase equilibrium calculations.

III.C.2.d Temperature Calibration

A mercury-in-glass thermometer having smallest division equal to one tenth of a degree was calibrated in a constant temperature bath at 25.00°C . The temperature of the bath was read by a Beckman Thermometer calibrated by the National Research Council against a platinum-resistance thermometer. The thermometer used in this experiment indicated a reading of 25.3°C . Hence the correction was made on all temperature observations. The temperatures listed in this work have been corrected.

III.C.3 Experimental Procedure

The observations recorded when studying adsorption equilibria for mixtures are the room temperature, the system pressure and the gas phase composition. They must be noted before and after adsorption has taken place.

The system was evacuated to 10^{-4} mmHg pressure while the adsorbent was heated at 140°C for 2 hours. The pressure gauge was set at the zero position. The vacuum could be measured either from the McLeod gauge on the Porta-Vac or on the Precision pressure gauge. Readings of both equipment agreed with one another.

The system was isolated from the vacuum pump and the adsorption cell isolated from the manifold. A gas mixture of known composition was introduced into the manifold through the needle valve until the manifold pressure approached atmospheric. The pressure and temperature were noted and the initial number of moles were calculated with the following equation,

$$N_i = \frac{P_i V_m}{RT_i}$$

The gas was expanded into the adsorption cell by opening the valves isolating it, a constant temperature bath was raised over the cell and the electromagnetic pump was turned on for recirculating the gas until equilibrium was reached. This became evident when the pressure of the system remained constant followed by oscillations of ± 0.001 psi - probably due to room temperature fluctuations. When the pump was turned off a spontaneous decrease in pressure of about 0.001 psi occurred. The equilibrium pressure and room temperature were noted and the number of moles of gas unadsorbed, N_e , was calculated with the

following equation:

$$N_e = \frac{P_e (V_m + V_d)}{RT_e}$$

in which P_e and T_e are respectively the equilibrium pressure and temperature. It follows that the number of moles of gas mixture adsorbed is given by $N_a = N_i - N_e$.

The surface composition of a component can be obtained by performing a material balance and solving for X_1 to get

$$X_1 = \frac{Y_{i,1} N_i - Y_{e,1} N_e}{N_a}$$

and

$$X_2 = 1 - X_1$$

The quantity $Y_{e,1}$ was obtained by isolating a small quantity of gas mixture at equilibrium and analysing it with the gas chromatograph. The mole fraction $Y_{e,1}$ was then obtained by converting the peak height ratio to mole fraction ratio using either Figures III.12 or III.13.

III.C.4 Experimental Results

The systems investigated with the constant volume apparatus were $\text{CO}_2 - \text{C}_3\text{H}_8$ and $\text{C}_2\text{H}_6 - \text{CO}_2$ at (ice-water temperature) pressures near 500 mmHg. The experimental

observations of initial and equilibrium pressures, temperatures and gas phase compositions are listed for the $\text{CO}_2 - \text{C}_3\text{H}_8$ system and for the $\text{C}_2\text{H}_6 - \text{CO}_2$ system in Table III.7. Also noted were the adsorbent weight, the manifold and dead space volumes.

The pressures P_i and P_e were obtained by converting the precision pressure gage readings to millimeters of mercury pressure. The conversion factors have been listed in Table III.1. The temperature is reported in degree Kelvin. The initial gas mixture composition have been obtained from those reported by the Matheson Co. Ltd. and are also listed in Section III.A.1. The equilibrium composition has been determined by chromatographic analysis of the mixture. The peak height ratio with equilibrium pressures are listed for both systems in Table III.6.

The adsorption equilibrium data for both systems are listed in Tables IV.8 and IV.9. Reported are the total pressure in mmHg, gas phase and adsorbent phase molar compositions, and the total number of moles of gas adsorbed per gram of adsorbent.

III.C.5 Reproducibility

An essential condition for obtaining reproducible data, when using a constant volume apparatus for mixture adsorption, is to make sure that the condition of equilibrium was attained.

TABLE III.6

EQUILIBRIUM GAS PHASE COMPOSITION ANALYSIS

Equilibrium Pressure (mmHg)	$C_3H_8 - CO_2$		$CO_2 - C_2H_6$	
	Equilibrium Pressure (mmHg)	$\frac{P_{C_3H_8}}{P_{CO_2}} \left(\frac{10}{10} \right)$	Equilibrium Pressure (mmHg)	$\frac{P_{CO_2}}{P_{C_2H_6}} \left(\frac{25}{10} \right)^*$
32.930		0.2511 ± 0.0011	30.767	1.0047 ± 0.0023
31.169		1.3055 ± 0.097	37.846	0.2671 ± 0.0055
35.386		1.1746 ± 0.0044	34.209	0.8128 ± 0.0041
39.172		0.3086 ± 0.0068	31.260	1.0223 ± 0.0026
38.461		$0.3014 \pm \checkmark$	39.094	0.9237 ± 0.0065
			38.819	$0.9318 \pm -$
			39.140	$0.9185 \pm -$

* $\left(\frac{25}{10}\right)$ is the gas partitioner sensitivity set for maximum resolution at 25% for CO_2 and at 10% for C_2H_6 .

P: peak height in inches.

TABLE III.7
MEASURED MIXTURE ADSORPTION BY THE MANOMETRIC METHOD

System	Vd (litres)	Adsorbent weight (mg)	P _i (mmHg)	T _i (°K)	Y _{i,1}	P _e	T _e	Y _{e,1}
CO ₂ (2)-C ₂ H ₆	0.1187	16.543	758.86	302.96	0.7522	307.67	300.56	0.6685
			770.059	299.16	0.2592	378.46	299.26	0.1756
			758.82	298.46	0.4960	342.09	299.01	0.3932
	0.1199	11.0251	759.06	299.06	0.7522	312.6	299.31	0.6646
			762.49	298.16	0.7522	390.94	298.01	0.6868
			757.39	297.91	0.7522	388.19	297.96	0.6850
C ₃ H ₈ (1)-CO ₂	0.1201	9.372	757.39	297.91	0.7522	391.40	298.51	0.6881
			722.95	297.86	0.4527	329.30	297.86	0.3604
			722.85	297.91	0.2385	365.29	297.86	0.1987
	0.1203	7.799	726.96	297.76	0.2385	345.51	297.86	0.1900
			745.27	299.46	0.7494	353.86	298.61	0.7250
			758.1	297.86	0.4527	384.61	297.96	0.4035
			746.54	295.26	0.2385	403.08	300.56	0.2483
			767.59	298.16	0.4527	391.71	298.56	0.4092
			731.19	297.56	0.7494	311.69	297.71	0.7455

V_m = 0.7489

The $\text{CO}_2 - \text{C}_2\text{H}_6$ system has been used to serve as an illustrative example.

An experimental run was performed on a given weight of silica gel. When the gas phase was in equilibrium with the adsorbed phase, once a constant pressure was observed, the equilibrium pressure and mole fraction of CO_2 were respectively noted as 38.819 mmHg and 0.6850. The system was left in the manifold for 20 hours after which the system pressure and CO_2 mole fraction were found to be respectively, 39.140 mmHg and 0.6881. The per cent deviation of Y_{CO_2} from the average value (0.6866 ± 0.0016) is 0.23%, which is within the tolerance limit of the experimental determination of the peak ratio. As for the slight increase in pressure; it corresponds to a rise in room temperature of about 1°C .

It was possible to reproduce the adsorption equilibrium data. The $\text{C}_3\text{H}_8 - \text{CO}_2$ system is used to illustrate this fact for a given weight of silica gel and on different occasions the equilibrium observations are noted below:

	P_e (cm-Hg)	T_e ($^\circ\text{K}$)	Y_{CO_2}
(1)	39.172	298.56	0.4092
(2)	38.461	297.96	0.4035

It follows that an average value for $Y_{\text{CO}_2} = 0.4064 \pm 0.0019$ (0.70%). This value is within the limits of the experimental

error of peak height ratio measurements.

The sources of error in determining adsorption equilibria with a constant volume apparatus are numerous. They are listed as follows:

1. Calibration of the
 - a) bulb volume
 - b) manifold volume
 - c) dead space volume

2. Calculation of the
 - a) moles adsorbed
 - b) adsorbed phase composition

An attempt has been made to determine what the maximum possible error is and how it will affect the value of the surface composition and the adsorbed moles. The per cent deviations are reported in the following table and are compared with the experimentally observed deviation for the parameters measured.

/

ERROR ANALYSIS

Parameter	Measured Deviation	Estimated Maximum Possible Error
Temperature	$\pm 0.04\%$	$\pm 0.04\%$
Pressure	$\pm 0.07\%$	$\pm 0.001\%$
Volume V_b	$\pm 0.005\%$	$\pm 0.2\%$
V_m	$\pm 0.15\%$	$\pm 0.73\%$
V_d	$\pm 0.45\%$	$\pm 1.28\%$
Moles adsorbed	$\pm 1.0\%$	$\pm 3.1\%$
Mole fraction adsorbed	1.1% (at 50% x)	$\pm 5.4\%$ (at 80% x)

CHAPTER IV

CORRELATION AND PREDICTION OF GAS-SOLID EQUILIBRIA

This chapter is subdivided into three main topics: the correlation of the experimentally determined adsorption isotherms, the prediction of pure component isotherms and finally, the prediction of mixed adsorption equilibria.

Presented in the first division are the uses made of the Brunauer - Emmett - Teller (BET) equation. In our work, it was not only used for the calculation of the specific surface area of the adsorbent but also it was employed to represent the measured adsorption isotherms in view of facilitating computer programming. Also, some of our measured isotherms are compared with the existing literature.

Discussed in the second part are the results of the testing of various simple equations of state, most of them having in common the same parameters namely, α and β . The prediction of pure component isotherms using the ideal values of the parameters is compared with the prediction of the pure isotherms when the values of α and β are calculated by two different methods employing measured isothermal data with special attention given to the analog of the Redlich and Kwong equation of state (18). One method consists in calculating a single set of values for α and β for a given isotherm covering the entire pressure range investigated (33). Our proposed method involves the application

of an already existing approach employed in vapor-liquid equilibria (27). Consequently a set of values for α and β are easily determined for a pure component isotherm at a given pressure. For completion, other correlations considered are summarized briefly.

The last topic deals with the prediction of phase equilibria of mixtures, in particular, of a binary mixture. In the first place, the results of the calculation of phase equilibria for the measured binary mixtures using an exact thermodynamic relationship approach (3) are compared with those measured with the constant volume apparatus described earlier. The next steps deals with the prediction of phase equilibria using the ideal solution theory (19, 20) and involves the working and testing of an equation of state. Considerable efforts were made on the prediction of phase equilibria with an equation of state, in particular, the original equation of Redlich and Kwong (18) which constitutes our proposed method for predicting phase equilibria in mixed adsorption. The mixing rules used in vapor-liquid equilibria were extended to gas-solid equilibria. The important parameter of the equation involves the quantity C_{ij} . The supporting data required to predict and compare phase equilibria so as to yield a best value for C_{ij} are presented. The results of the prediction of gas-solid equilibria are presented in the last section with a proposed method for the prediction of phase equilibria at higher pressures. A practical application for the calculation of measurable properties such as P , v and X

concludes the discussion on the prediction of gas-solid equilibria.

IV.A Experimentally Determined Adsorption Isotherms

IV.A.1 Specific Surface of the Adsorbent

In the calculation of the specific surface area of the silica gel, the standard BET equation was used. It was necessary to employ the n-layers BET equation in the form of Equation I.7 because the data did not give a satisfactory fit when correlated with the infinite form of the BET equation or the Langmuir equation. It was advantageous to determine the best possible straight line passing through the points by the method of least squares because the curvature of Equation I.7 is not very sensitive to n. The amount of nitrogen adsorbed at 77.4°K was then calculated using Equation I.4 and compared with the original data of the isotherm. This approach has been used originally by Joyner (23) and more recently by Wenzel (24) in their determination of the specific surface area.

The average value of the surface area obtained with the Cahn electrobalance is $722.9 \pm 3.3 \text{ m}^2/\text{gm}$ while that obtained from the McBain-Bakr apparatus is $695.4 \pm 5.4 \text{ m}^2/\text{gm}$. They differ only by 4%. The computer program is listed in Appendix II. Values of specific surface area of silica gel calculated with the data obtained from different apparatus are reported in

Table IV.1 of Appendix I.

IV.A.2 Empirical Representation of the Adsorption Isotherms

The n-layers BET Equation I.1 (22) was also found useful in the correlation of the adsorption isotherms measured at all temperatures for the entire pressure range covered. A total of 45 isotherms were fitted using this equation. The overall average of the per cent deviation between the calculated and the experimental values of the amount adsorbed was estimated as 0.54% while the range of the per cent deviation spanned from 0.1% to 1%.

This empirical correlation further provided an analytical tool for the calculation of the spreading pressure defined by Equation I.14.

The analytical expression of Equation I.1 quantified the reproducibility of the adsorption isotherm. For example, the adsorption of CO_2 at 298.2°K , which was repeated twice on different occasions using the same sample of silica gel, was fitted using Equation I.1. The per cent deviation was calculated as 0.32% and 0.21%. The CO_2 adsorption data plotted in Figure III.7 of Section III.B.6 agree very well with the calculated curve. The difficulty to produce the same data points under exactly the same experimental conditions has been mentioned in this earlier section and supports the need for an analytical expression to represent the experimental data.

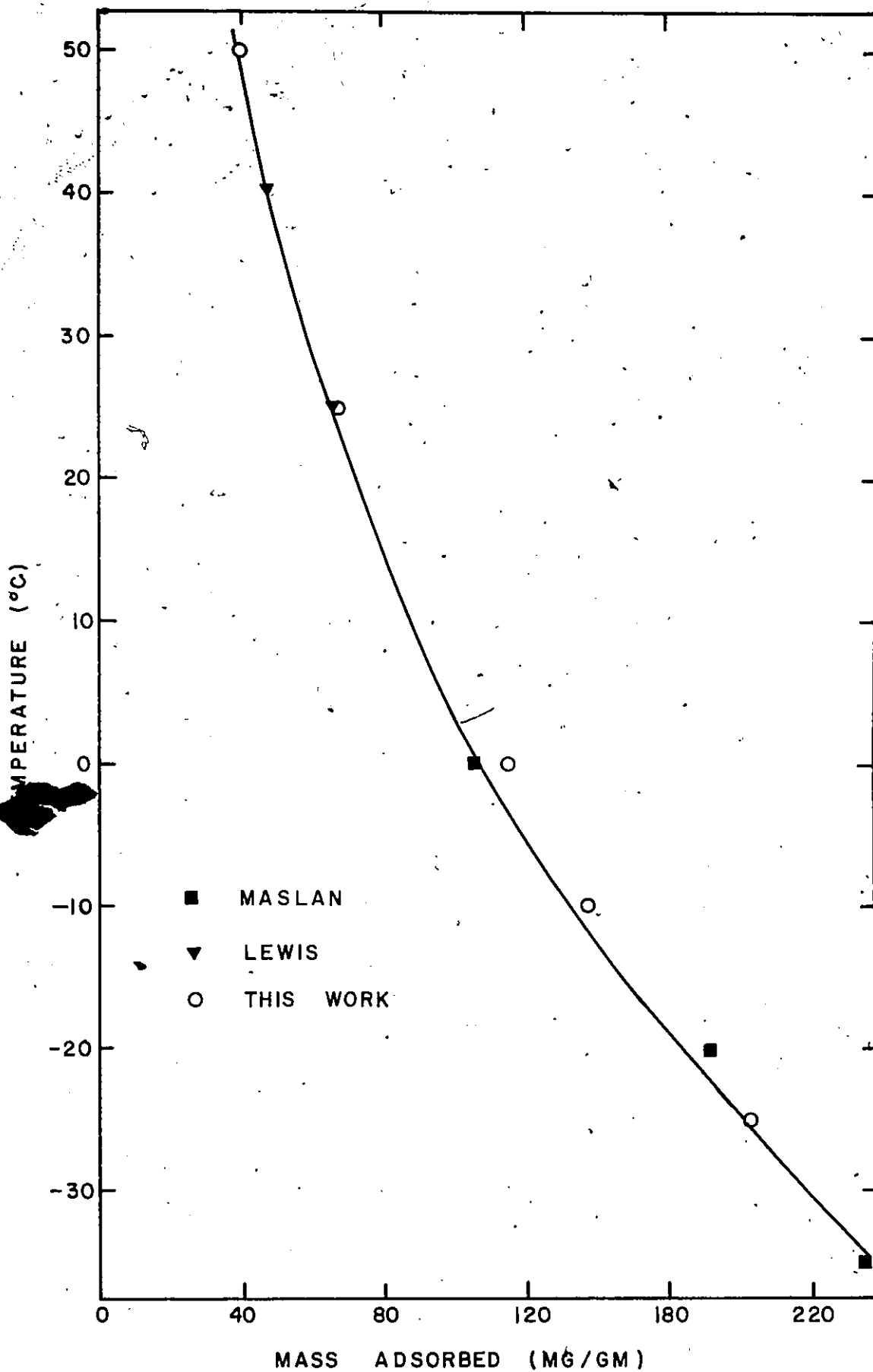


Figure IV.1' Adsorption of C_3H_8 at 750 mmHg.

IV.A.3 Data Comparison with the Literature

IV.A.3.a Adsorption Isotherms

The properties of silica gel vary according to the method of the manufacturer's preparation and the steps involved in the reactivation of the surface. It is difficult to compare point for point obtained by different workers, unless both have used the same adsorbent and have prepared its surface regeneration with identical procedures. For example, Maslan (9) and Lewis (10) have tested the same kind of adsorbent over a different range of temperature. Our observations for the system C_3H_8 - silica gel agree well with theirs as seen on Figure IV.1 for different temperatures. However, with CO_2 , entirely different curves are obtained. Although the surface areas may have similar values, the porosity is likely to be different in both silica gel samples. Therefore, the agreement shown in Figure IV.1 is purely by chance.

IV.A.3.b Heat of Adsorption

The adsorption of gases on surfaces of solids is accompanied by the evolution of heat; the amount of heat varies with the fraction of the surface covered by the adsorbed gas. The isosteric heat of adsorption, Q_{st} , may be obtained from calorimetric methods or from adsorption isotherms. In the latter

method, Q_{st} is usually determined using Equation I.9 from isosteres and as plotted in Figure IV.2 for CO_2 on silica gel.

Equation I.9 is used when the isosteres are linear. The linearity of the isosteres also provides a useful check as to the internal consistency of the isotherms (4). This property was found true for all systems investigated in this work.

The isosteric heat of adsorption determined from Figure IV.2 with Equation I.9 are listed in the following table for different isosteres.

n (millimoles/gm)	Q_{st} (Kcal/mole)
0.2	6.555
0.4	6.656
0.6	6.559
0.8	6.619
1.0	6.579

The results of the calculations suggest that Q_{st} is independent of the amount of gas adsorbed because an average value of $Q_{st} = 6.59 \pm 0.03$ Kcal/mole was obtained. The deviation from the average, being $\pm 0.52\%$, lies within the experimental measurements of the adsorption isotherms. Hence, no definite trend in Q_{st} exists with the coverage. This lends to the belief that

the repulsive forces of the adsorbed molecules are uniform or the adsorption sites are uniformly distributed (51).

The linearity of the isosteres of Figure IV.2 indicates that Q_{st} is independent of temperature. However, the calorimetric heats of adsorption for CO_2 on silica gel (52) reveal the isosteric heat of adsorption to be temperature dependent as seen in Figure IV.3

For similar reasons stated earlier concerning the silica gel surface, these values cannot be compared; however, they are useful for comparing the order of magnitude of Q_{st} with those reported in the literature. Furthermore, isosteric heats measured by calorimetry are more precise than those measured from adsorption isotherms (5).

Equation I.10 provides the means for calculating the differential entropy of adsorption, ΔS . The results are plotted in Figure IV.4 and are compared with those calculated using the data reported in Mantell (52). The decrease in entropy with increasing temperature is further indication that the capacity of adsorption is lowered at higher temperatures.

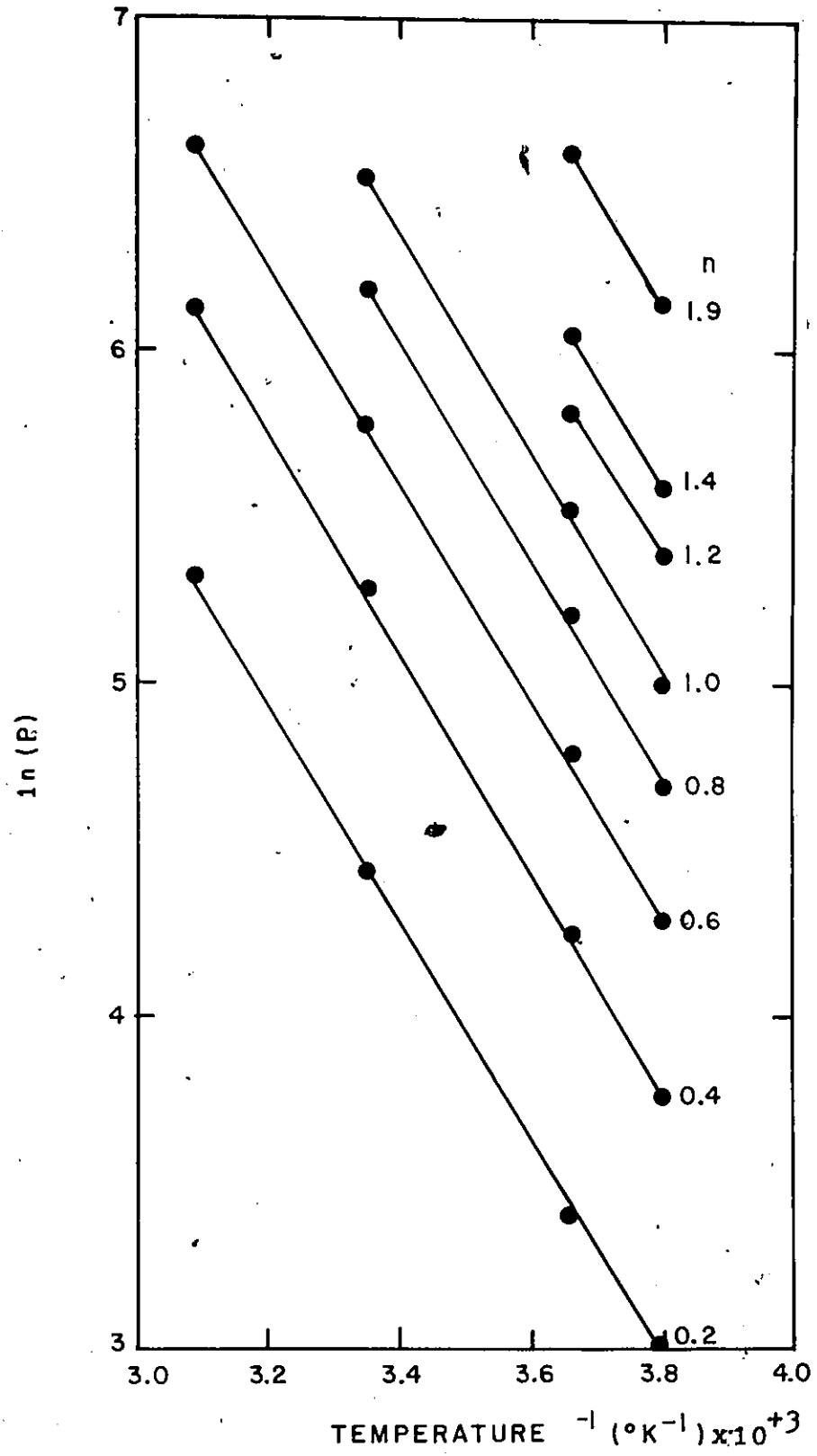


Figure IV.2 Adsorption Isotherms for CO_2

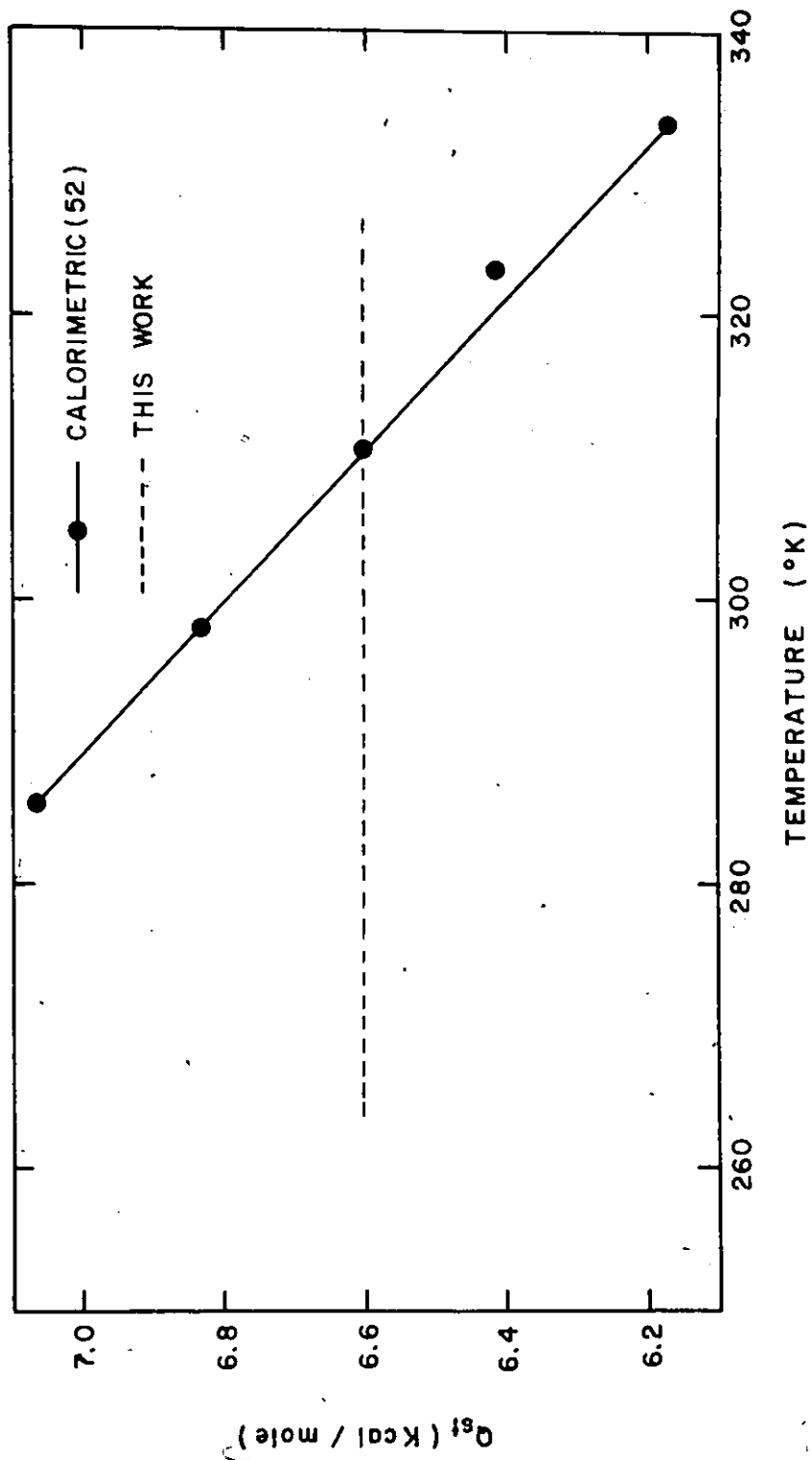


Figure IV.3 Isosteric Heat of Adsorption for CO_2



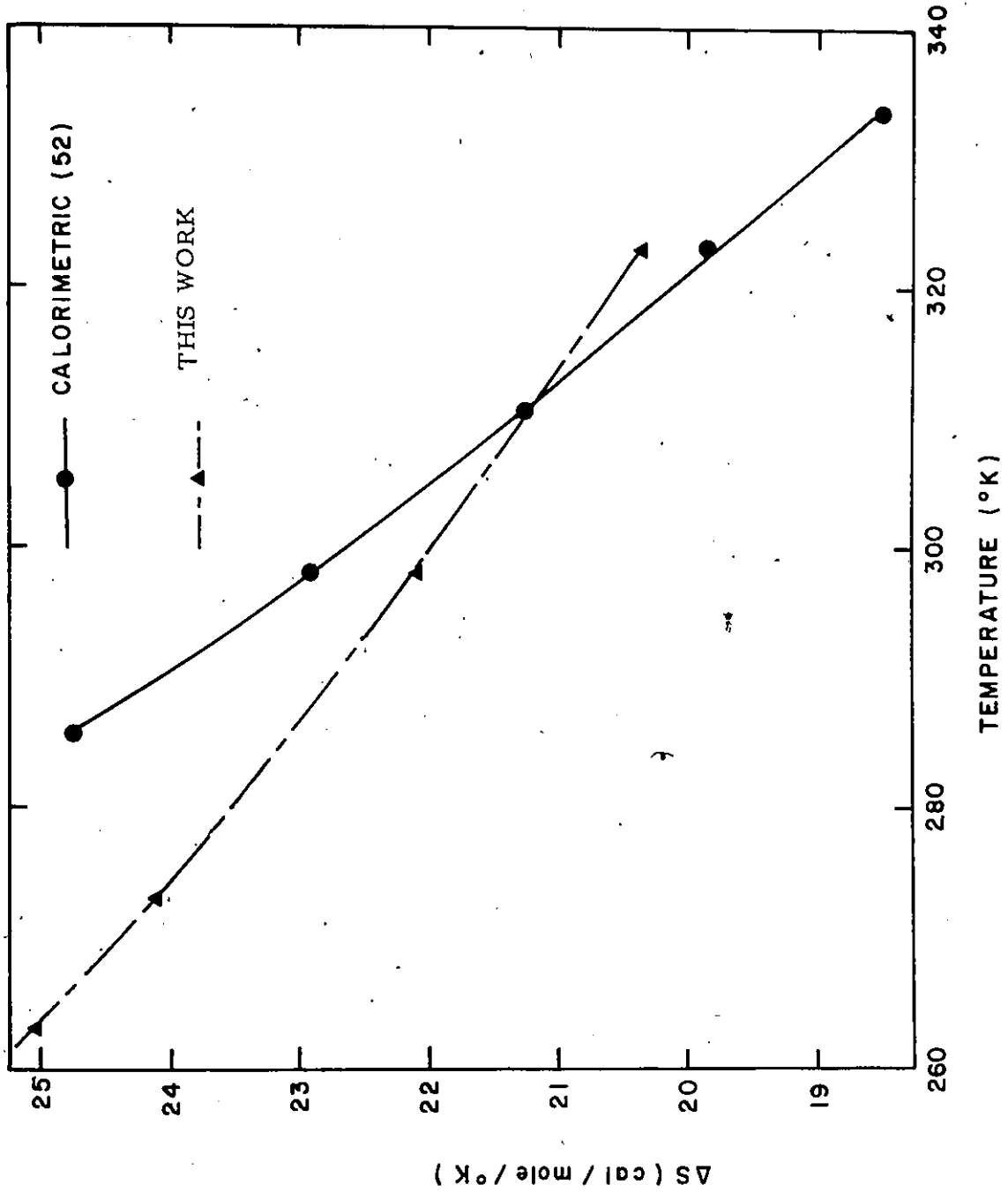


Figure IV.4 Entropy of Adsorption for CO₂



IV.A.4 Spreading Pressure Calculation

The n-layers BET Equation I.1 together with the spreading pressure Equation II.14 were employed in the calculation of the spreading pressure for both the pure component and mixed isotherms.

The usual (53, 54) method to calculate the spreading pressure is to obtain an analytical expression for the amount adsorbed as a function of the total pressure. Various functions were tested. In the final analysis, the n-layers BET equation was found the most appropriate to represent the entire range of pressure covered.

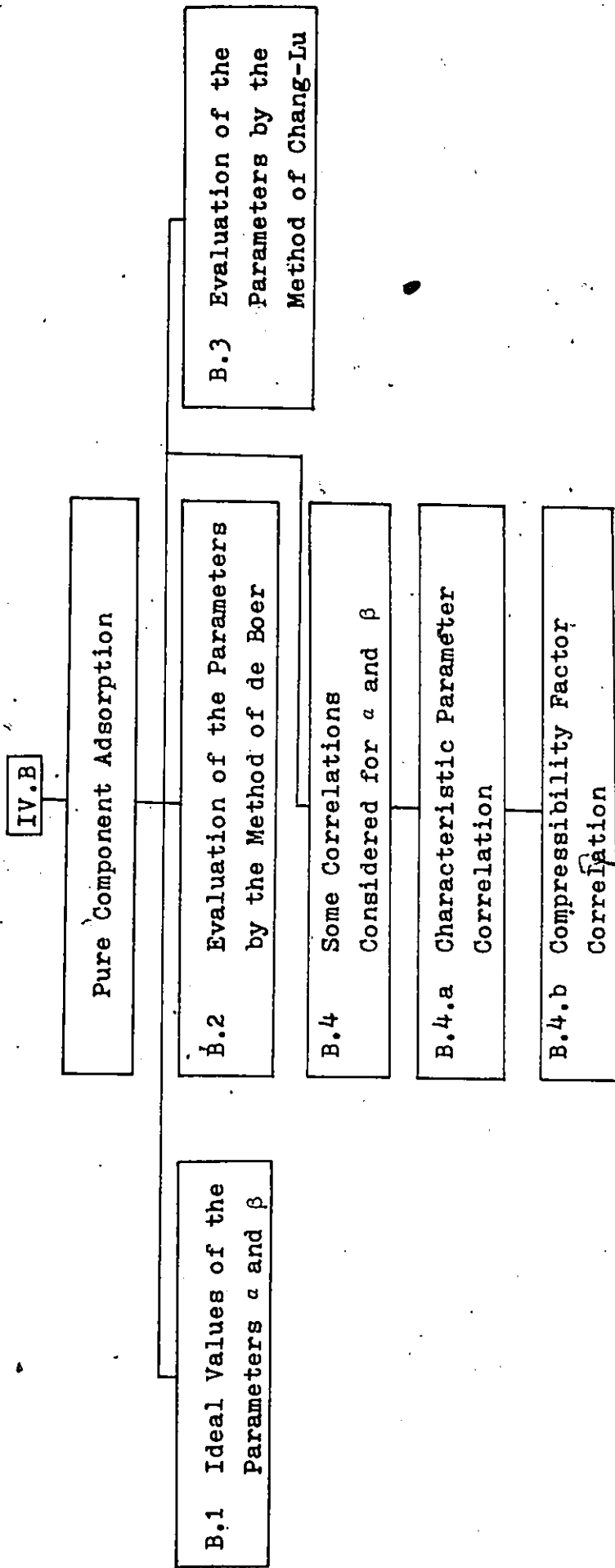
The integration of Equation II.14 was carried out by Simpson-Newton 3/8 Rule (56) at regular intervals of pressure obtained from Equation I.1.

Values of $\frac{\pi A}{RT}$ are listed in Tables IV.2 at regular intervals of pressure with corresponding amount adsorbed for each system at every temperature. Values of $\frac{\pi A}{RT}$ for mixtures are also listed in Tables IV.6. The computer program is listed in Appendix IV. Tables IV.2 and IV.6 are reported in Appendix I.

IV.B Pure Component Adsorption

The values of the calculated spreading pressure will depend largely on the values of the characteristic parameters α and β . The methods employed in the calculation of α and β are

The topics discussed in Section IV.B are illustrated in the following block diagram:



discussed in the following sections. Ideal values of α and β were first employed in testing various equations of state. The values α and β of the Redlich-Kwong equation analog were calculated using de Boer's method (33), and by extending the method of Chang-Lu (27) proposed in vapor-liquid equilibria to adsorption equilibria.

Calculated spreading pressures are compared with those measured by the gravimetric method. The results of the predictions of the spreading pressure using the models described by Equations I.14, I.15, I.16 and I.32 are summarized in Table IV.3. Listed for all systems at each temperature investigated are the average per cent deviation in the spreading pressure defined by

$$\% \Delta \pi = \frac{1}{n} \sum \left[\frac{\left(\frac{\pi A}{RT} \right)_{\text{experimental}} - \left(\frac{\pi A}{RT} \right)_{\text{calculated}}}{\left(\frac{\pi A}{RT} \right)_{\text{calculated}}} \right] \times 100$$

IV.B.1 Ideal Values of the Parameters α and β

Equations of states used to characterize the π - σ equilibrium data are numerous. Each model has its own restraints as to the range of applicability. It is not the purpose of this work to test all the equations found in the literature describing the equilibrium between the adsorbate and the gas phase. Only those equations of state mentioned earlier were tested. The results are summarized in Table IV.3 in terms of the per cent deviation in spreading pressure for all systems at all temper-

TABLE IV.3
A COMPARISON OF PREDICTED SPREADING PRESSURES
USING DIFFERENT EQUATIONS OF STATE

	Temperature (°K)	% $\Delta\pi$ **				
		Ideal	Volmer	Hill de-Boer	RK(Ideal)/	RK(DB)//
		Eq.I.14	Eq.I.15	Eq.I.16	Eq.I.31	Eq.I.31
CO ₂	263.2	31.75	12.05	40.49	46.84	3.07
	273.2	26.46	11.29	33.97	39.07	2.37
	298.2	15.54	7.27	19.86	22.71	1.52
	323.2	8.27	3.81	10.42	11.87	0.31
C ₃ H ₈	263.2	37.36	26.79	42.32	64.52	3.08
	273.2	34.62	12.31	47.01	61.27	4.05
	298.2	26.52	6.36	38.1	45.8	3.27
	323.2	18.79	7.65	26.06	30.62	2.27
C ₂ H ₆	263.2	20.0	4.96	28.79	34.80	3.41
	273.2	18.35	7.56	24.95	29.39	1.31
	298.2	13.98	7.89	17.45	19.86	0.41
C ₂ H ₄	263.2	39.5	20.79	45.48	50.56	2.10
	273.2	28.54	23.13	34.66	38.55	0.63
	298.2	24.10	14.62	27.79	30.08	1.84

* Observed values of π are listed in Tables IV.2 in Appendix I.

** Defined in Section IV.B.

/ Ideal values of α and β have been used.

// Values of α and β have been determined with de Boer's method.

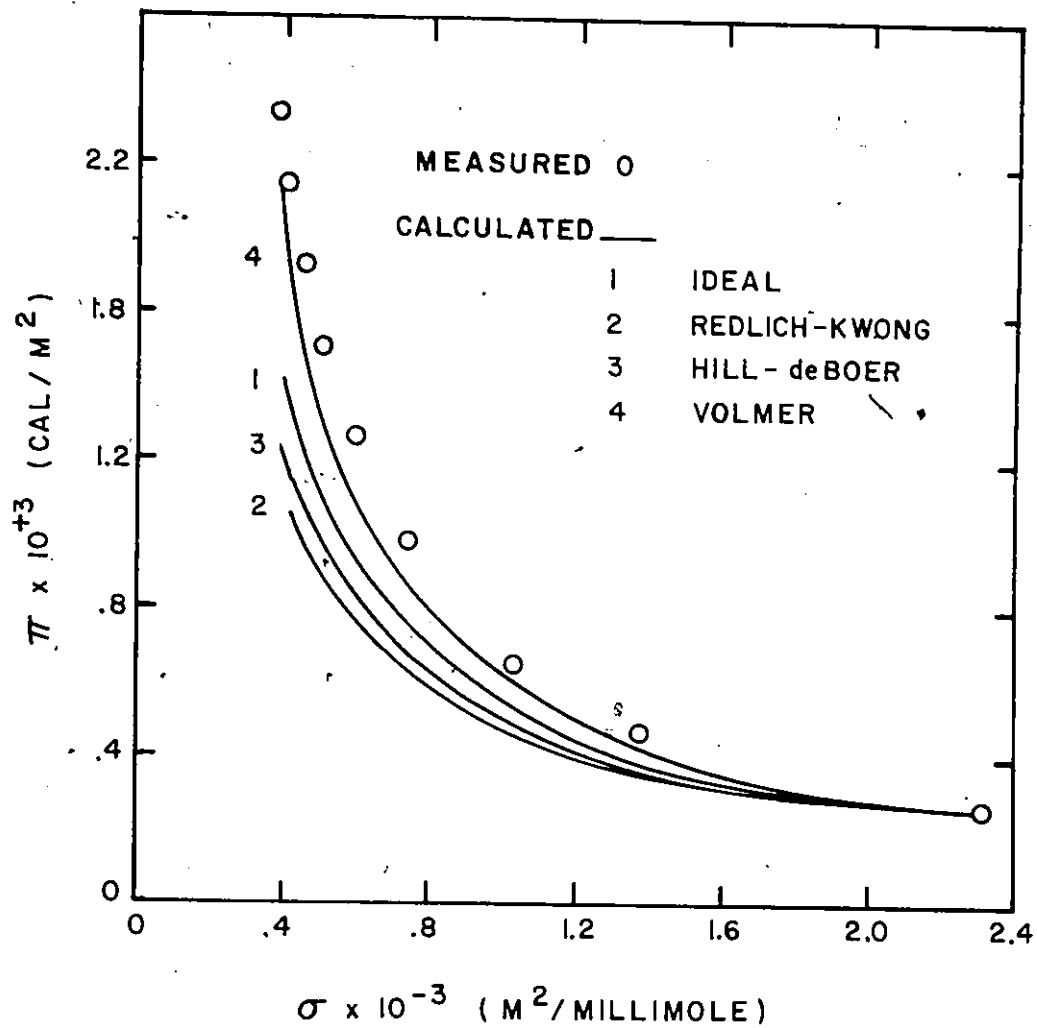


Figure IV.5 Prediction of π for CO_2 at 273.2°K using Different Equations of State - Ideal Values of α and β .

atures.

As a first approximation, Volmer's Equation, I.15, gives best results as seen in Figure IV.5, for the system CO_2 at 273.2°K . However, the model does not take into account the correction terms describing the molecular interaction in the adsorbed phase.

The constants α and β employed in Equations I.16 and I.31 are those defined by Equations I.17 and I.18.

IV.B.2 Evaluation of the Parameters by the Method of de Boer

The representation of π - σ or π - P data is greatly improved when the operative constants are obtained by the method of de Boer (33) as described in II.C.4.a. The computer program is listed in Appendix V.

It is important to observe that the equation of Redlich and Kwong, (Equation I.32) exhibits a minimum sum of squared deviation in pressure when this procedure of optimizing is followed. This characteristic is clearly depicted in Figure IV.6 for the system C_3H_8 at 263.2°K .

An interesting trend in the characteristic constants α , β and K , listed in Table IV.4, is observed with the temperature. Also noted was the sum of square of the deviation in pressure increased with decreasing temperature. In general, this trend is observed as well in all the other systems investigated in this work.

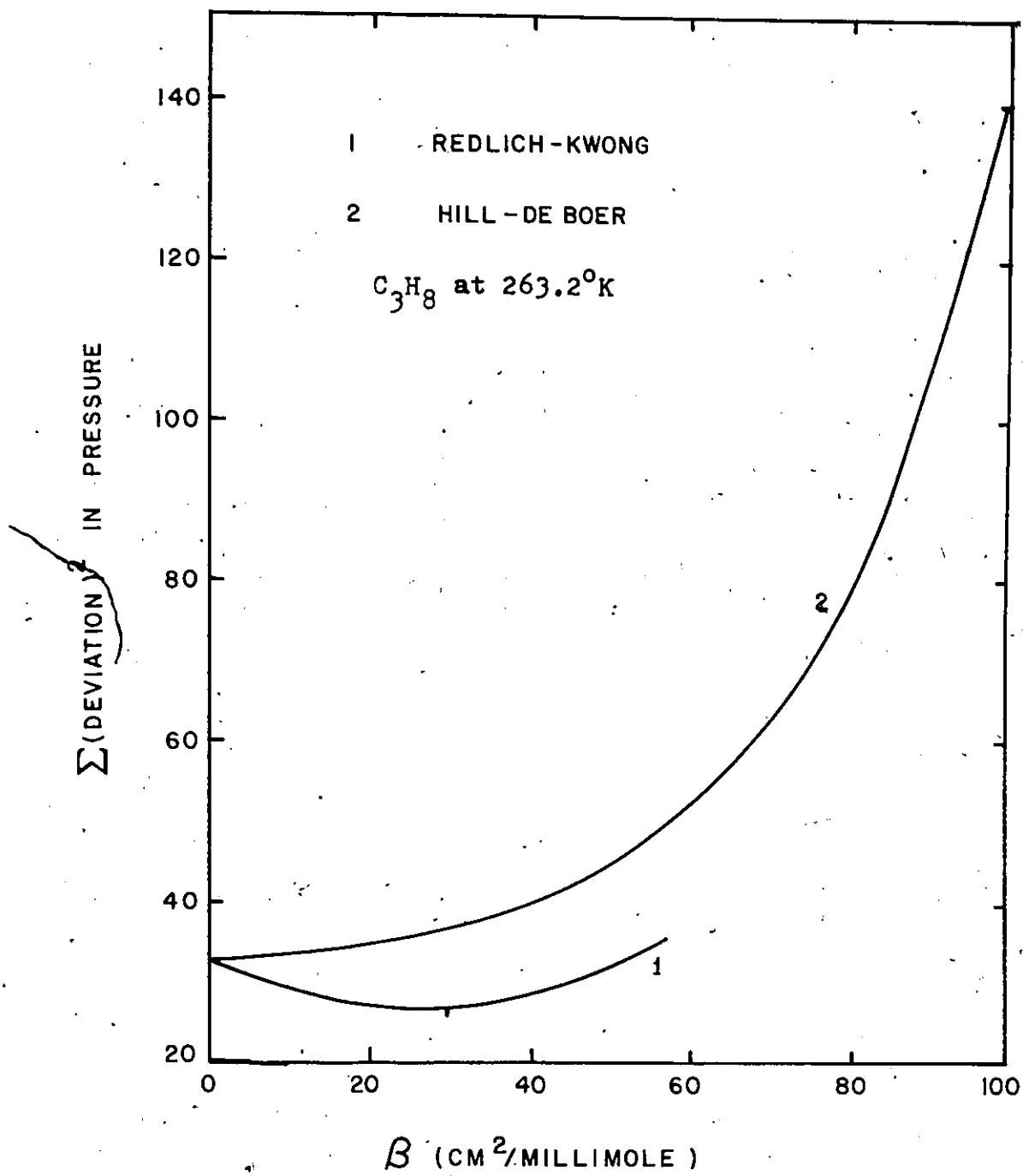


Figure IV.6 Selection of β by de Boer's Method

TABLE IV.4

PARAMETERS OF THE ANALOG OF THE REDLICH-KWONG EQUATION OF STATE
OBTAINED BY THE METHOD OF DE BOER

Component	Parameters	263.2°K	273.2°K	298.2°K	323.2°K
C ₂ H ₆	β	70.0	50.0	70.0	
	α	-1594.6	-1771.1	-2593.0	
	K'	334.27	529.8	753.39	
C ₂ H ₄	β	50.0	20.0	60.0	
	α	-2536.4	-2363.4	-2853.4	
	K'	93.653	526.90	350.48	
CO ₂	β	30.0	30.0	40.0	50.0
	α	-1468.8	-1568.0	-1706.0	-1744.7
	K'	213.26	345.86	702.74	1334.9
C ₃ H ₈	β	30.0	30.0	40.0	50.0
	α	-1429.0	-1628.5	-2088.0	-2648.7
	K'	118.42	178.61	338.14	618.8

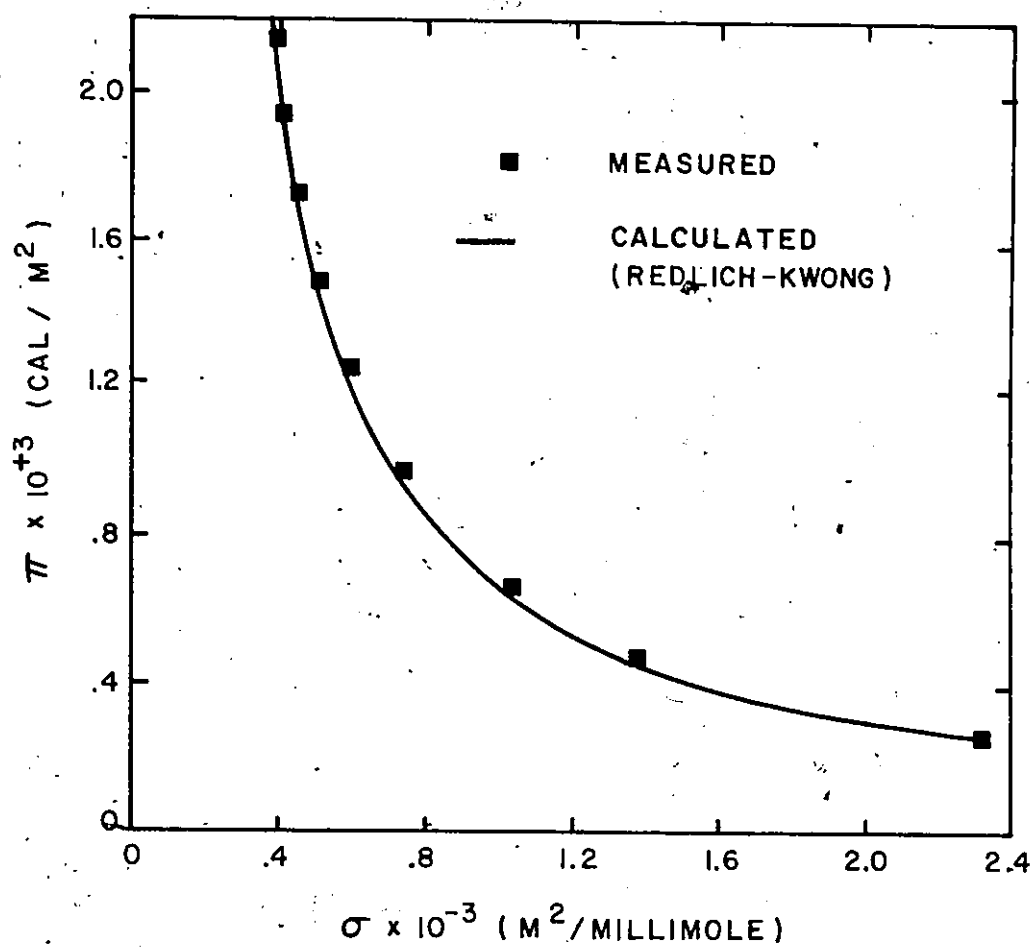


Figure IV.7 Prediction of π for CO₂ at 273.2°K -
Method of de Boer Applied to the
Redlich-Kwong Analog

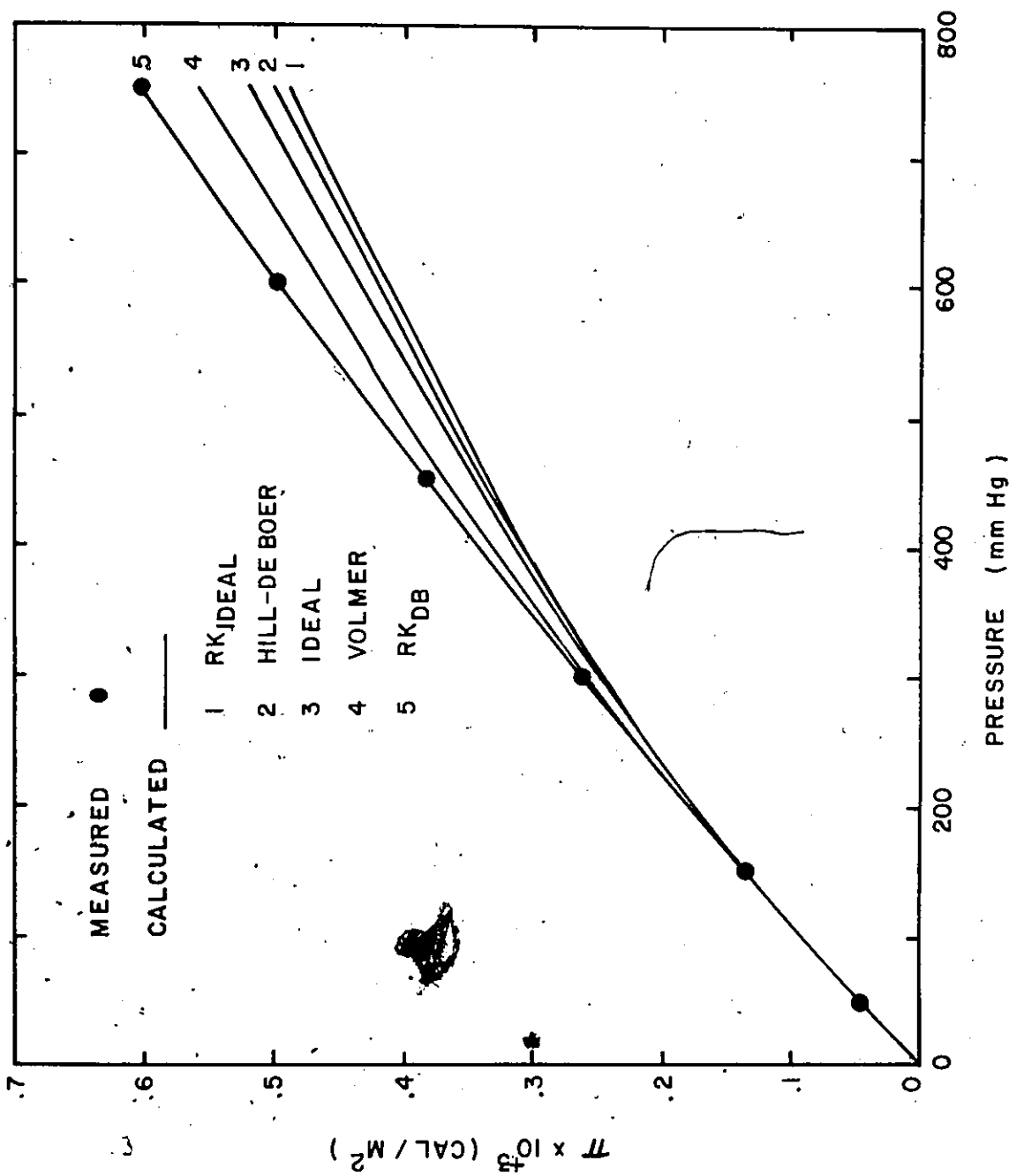


Figure IV.8 Prediction of π for CO_2 at 323.2°K Using Different Equations of State

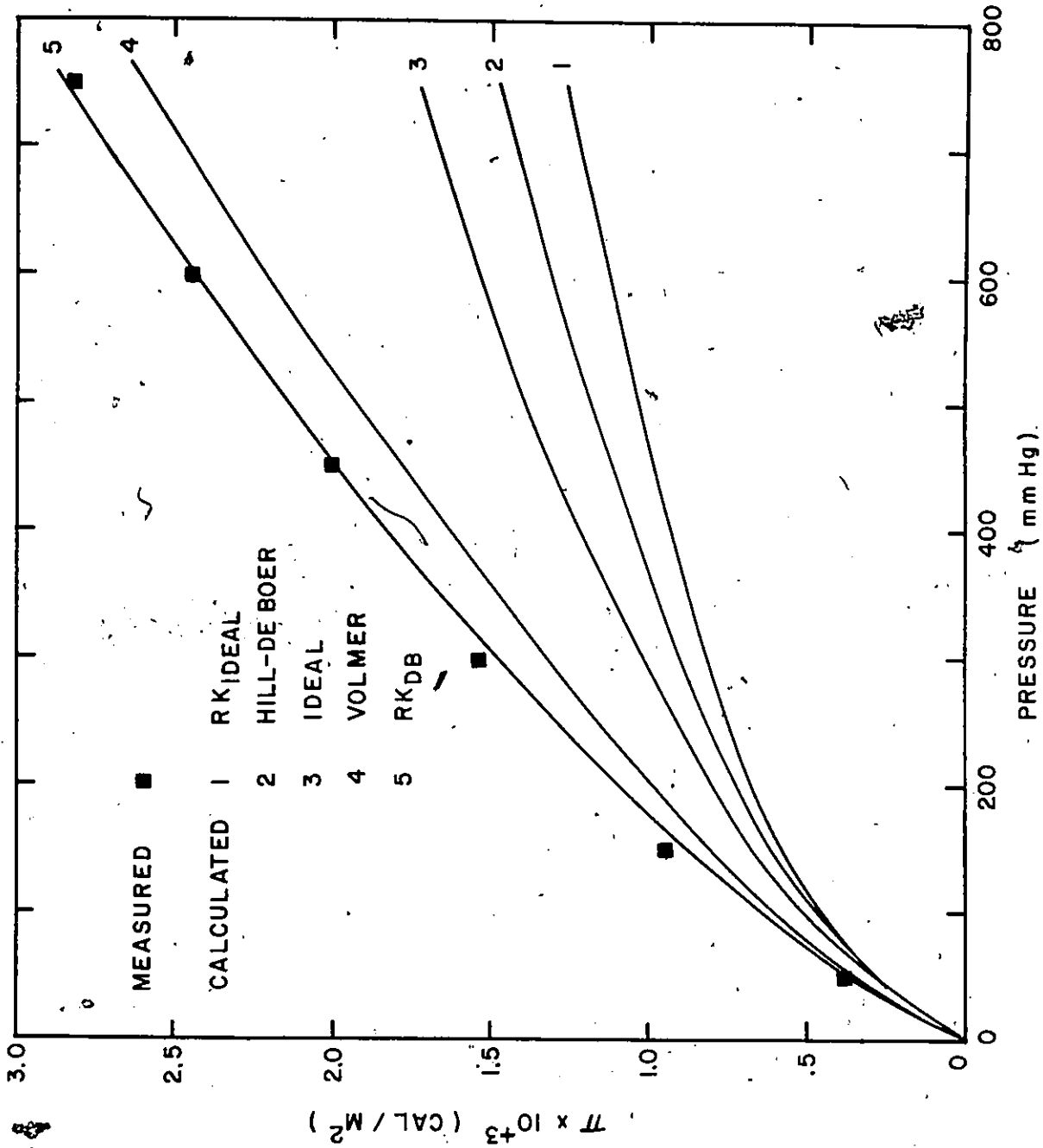


Figure IV.9 Prediction of π for CO₂ at 263.20K Using Different Equations of State

UNIVERSITY OF ILLINOIS

For all models tested in all systems, the value of the per cent deviation is reduced at higher temperatures. This is explained by the fact that less gas is adsorbed and consequently, there is less interaction between the molecules adsorbed on the surface.

For the CO_2 - silica gel system the π predictions at 273.2°K are compared in Figure IV.7. For the same system at 323.2°K and 263.2°K , the π -P curves are plotted in Figures IV.8 and IV.9. These curves were selected to emphasize the effect of the temperature on the prediction of gas-solid equilibria. At lower concentrations, the π prediction is better for most systems, however; the deviation is accentuated at elevated pressures due to interaction effects. The best representation of the data is achieved through the use of the Redlich and Kwong equation - RK(DB) - when the characteristic constants α and β were determined by the method of de Boer.

For all models tested, except for RK(DB), the deviation is largest for the heavily adsorbed components. Nevertheless, the prediction of phase equilibria for all data points is greatly ameliorated when the optimized values of α and β are used together with the Redlich-Kwong Equation I.32, and furthermore, it is slightly better than the Hill-de Boer Equation I.16.

IV.B.3 Evaluation of the Parameters by the Method of Chang-Lu

Our approach consists in representing the characteristic

constants α and β of the Redlich and Kwong equation of state as a function of temperature and pressure.

The values of α and β are readily obtained when Equation II.73 is employed. It has the form of $F(h) = 0$ in which the root h is solved by Newton's method. Once the value of h is known for a set of experimental conditions, the calculation of α and β is readily made using Equations II.60 through II.63.

The results of the calculation of α and β are listed in Tables IV.5 of Appendix I for each system and temperature. The computer program is presented in Appendix VI.

A summary of the behavior of α and β are summarized graphically for typical systems. At a given temperature, the pressure effects on α and β are seen in Figure IV.10 for the system CO_2 at 273.2°K . The temperature dependence of α for CO_2 and C_3H_8 at 750 mmHg are plotted in Figure IV.11. A similar plot for β is presented in Figure IV.12.

The plot of Figures IV.13 and IV.14 for different isotherms, representing the relation between $\frac{\pi A}{RT}$ with α and β respectively, seems to form a single curve for the adsorption of C_2H_6 . However, the temperature can be considered a parameter in the system CO_2 as illustrated in Figures IV.15 and IV.16. This observation indicates that the parameters for C_2H_6 are less sensitive to temperature changes than are those for CO_2 . For the same temperature range, the maximum change in β_{CO_2} is twice that of $\beta_{\text{C}_2\text{H}_6}$.

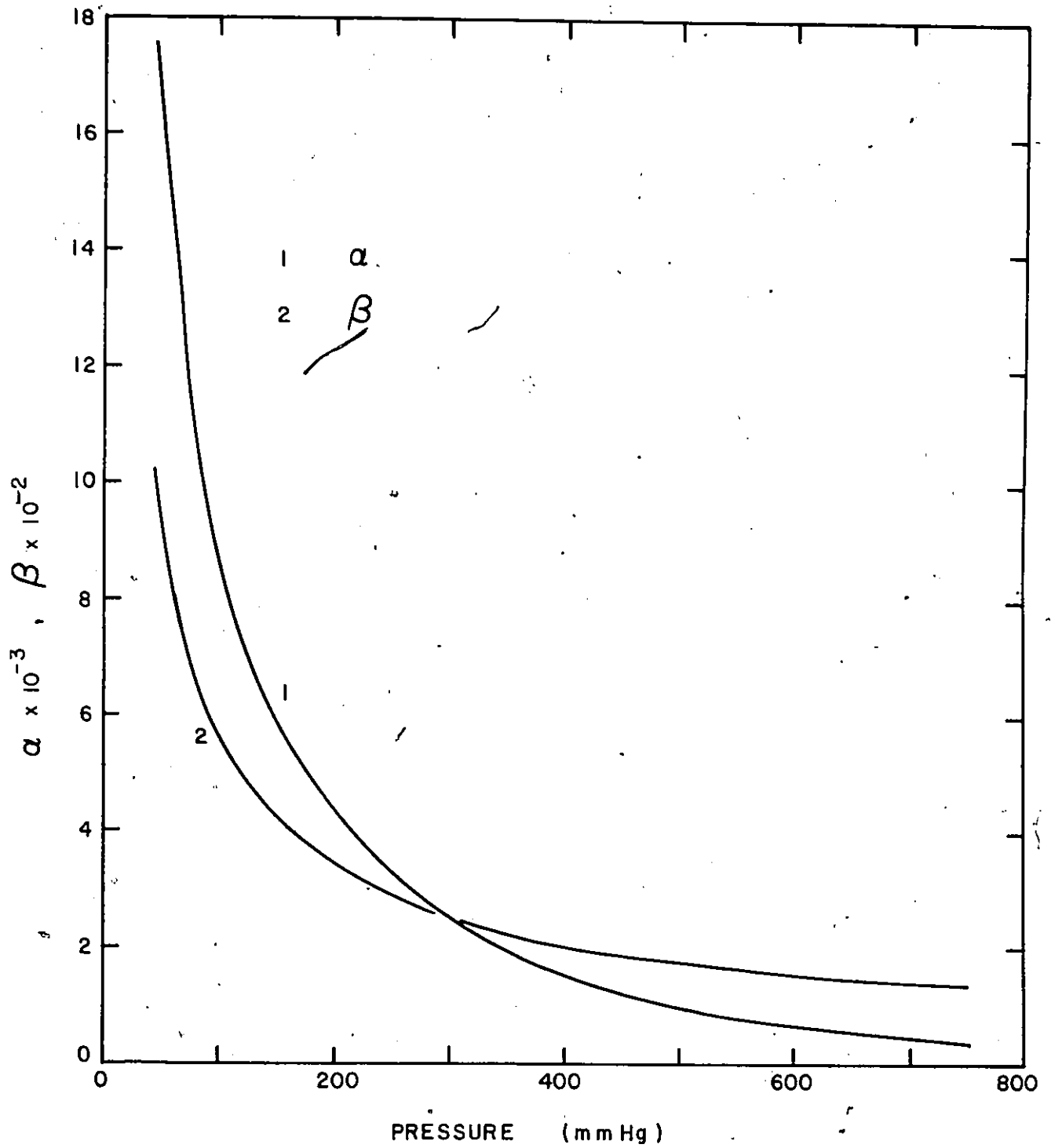


Figure IV.10 Pressure Dependent α and β of the Redlich-Kwong Equation Analog at 273.2°K for CO_2 -- Method of Chang-Lu.

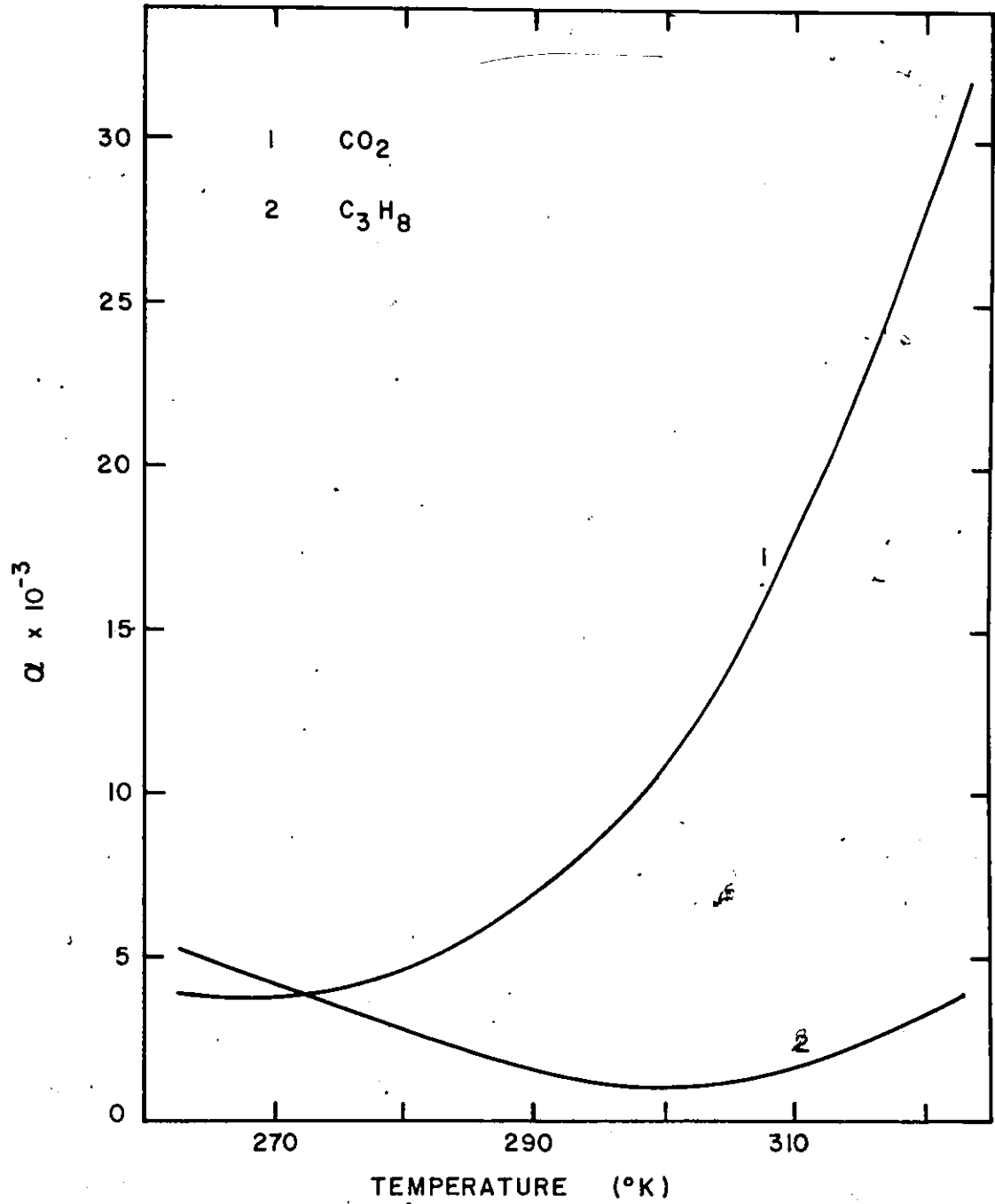


Figure IV.11 Temperature Dependent α at 750 mmHg
- Method of Chang-Lu

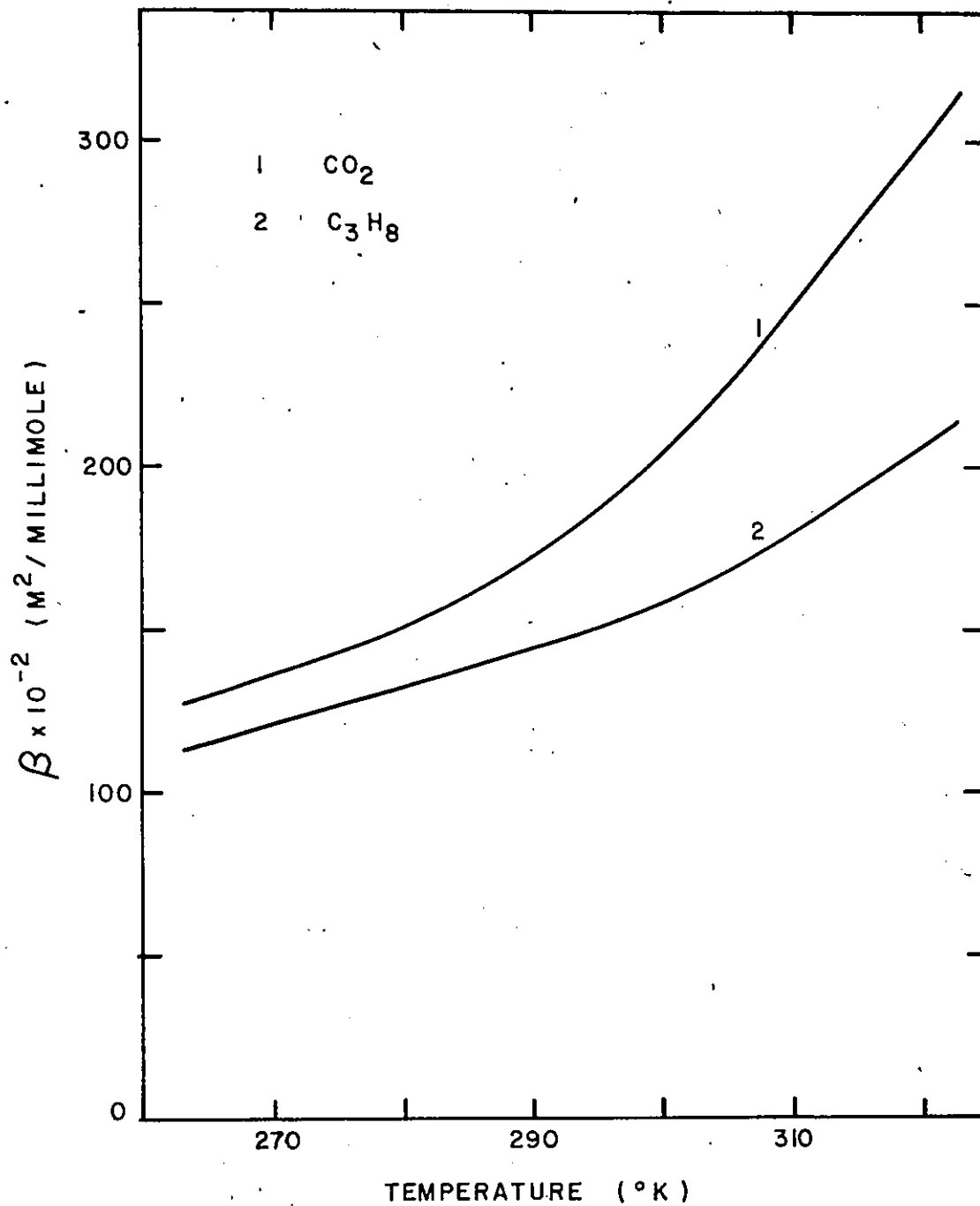


Figure IV.12 Temperature Dependent β at 750 mmHg - Method of Chang-Lu

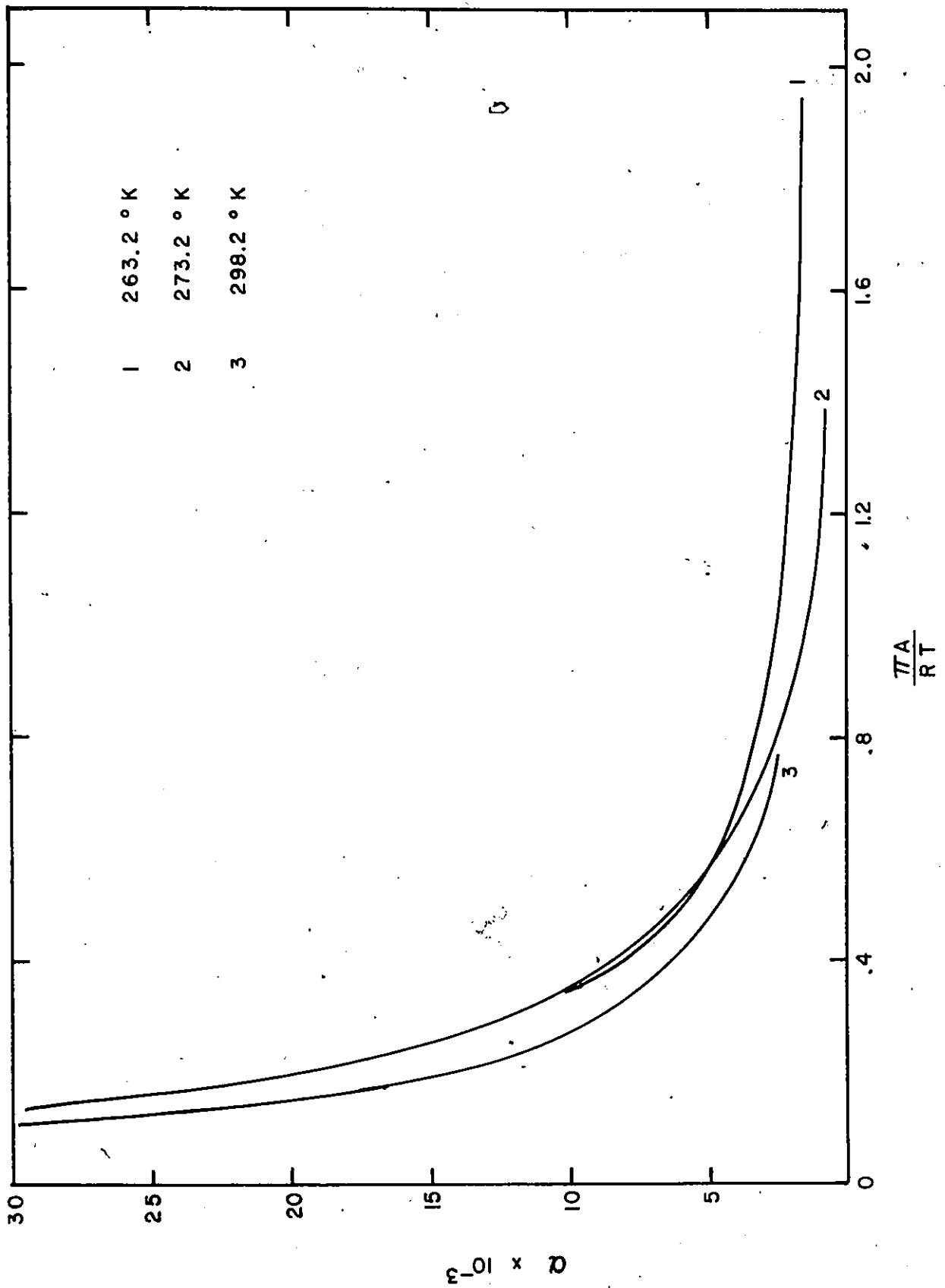


Figure IV.13 Temperature Effect on π -dependent α for C_2H_6 .

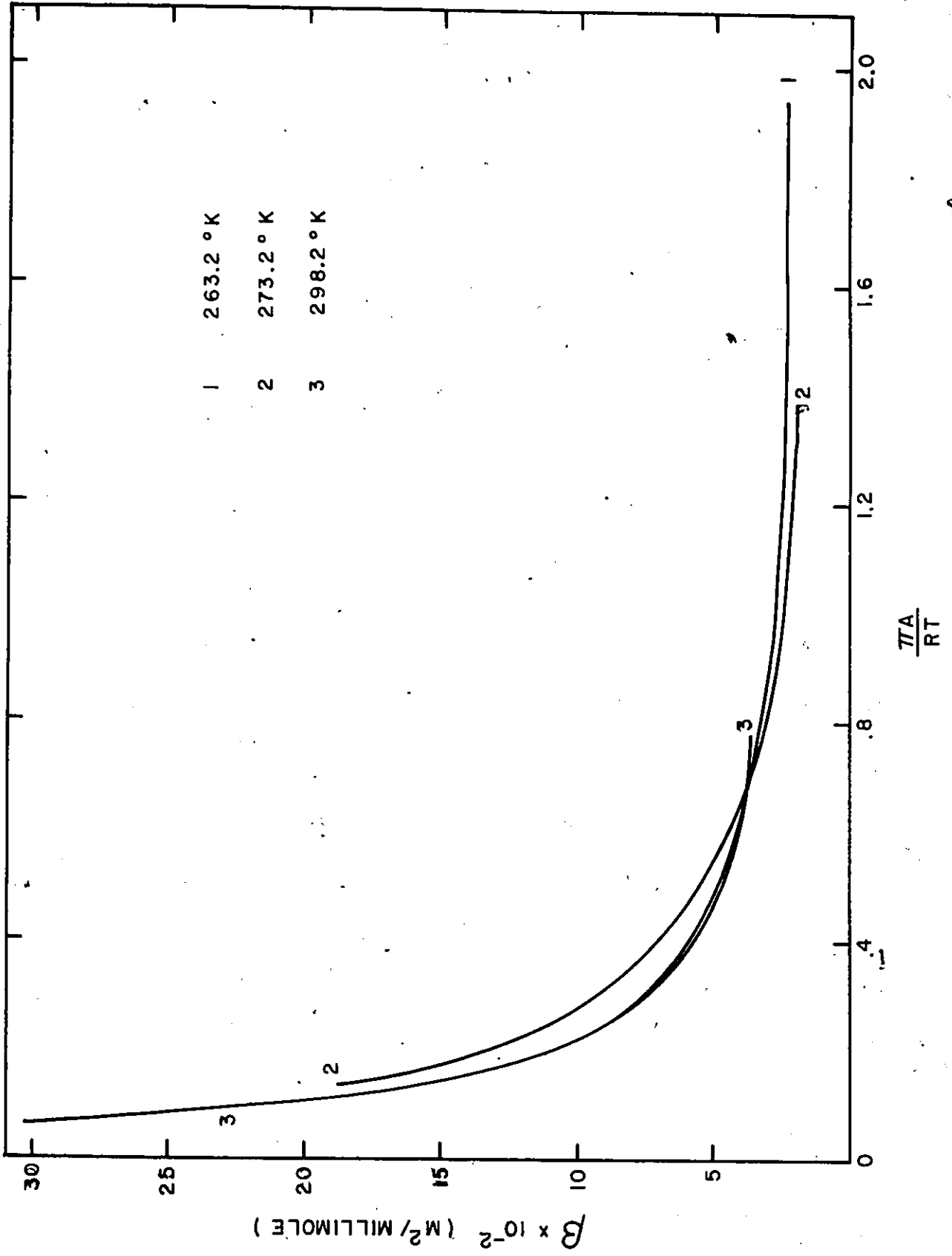
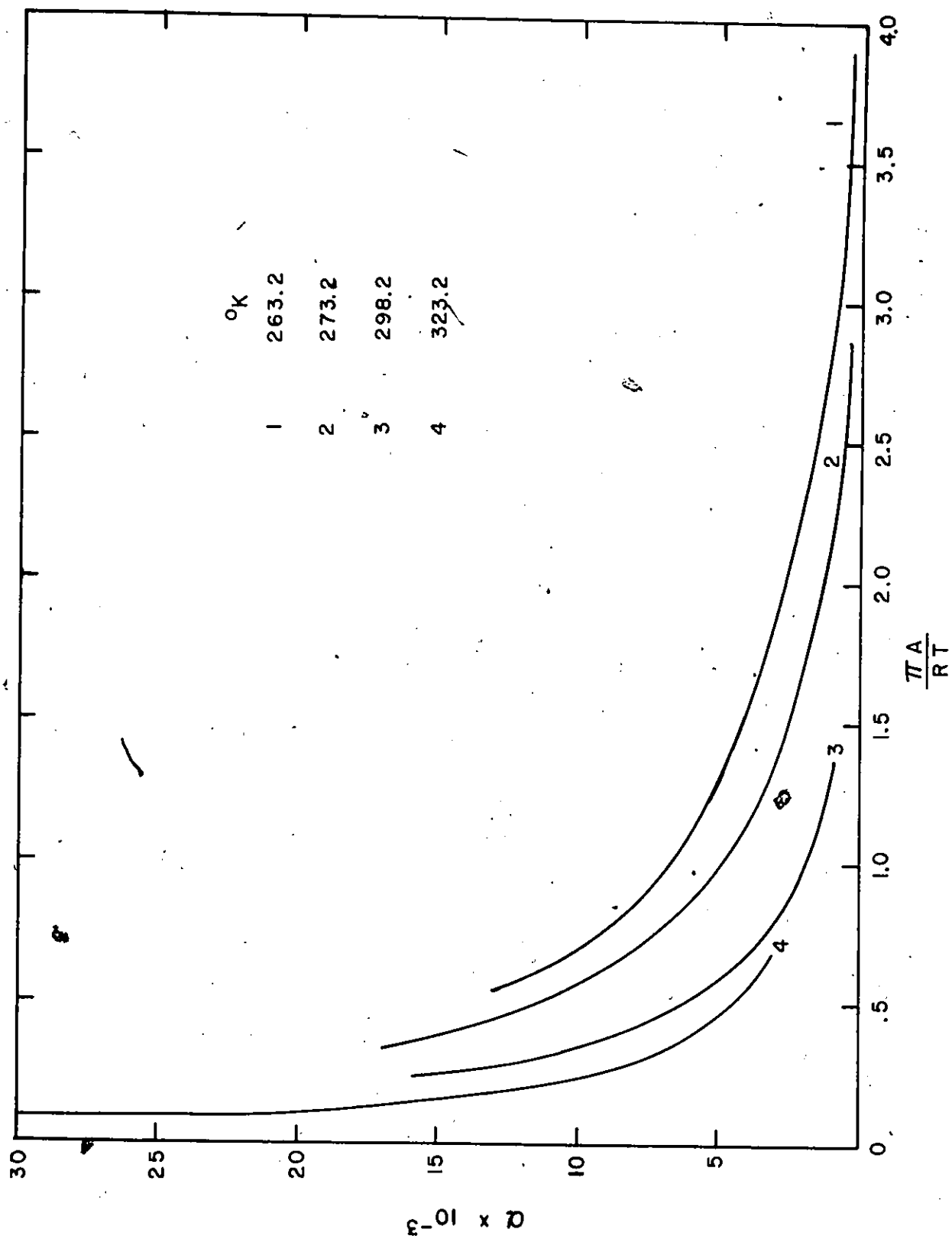


Figure IV.14 Temperature Effect on n -dependent β for C_2H_6

Figure IV.15 Temperature Effect on n -dependent α for CO_2

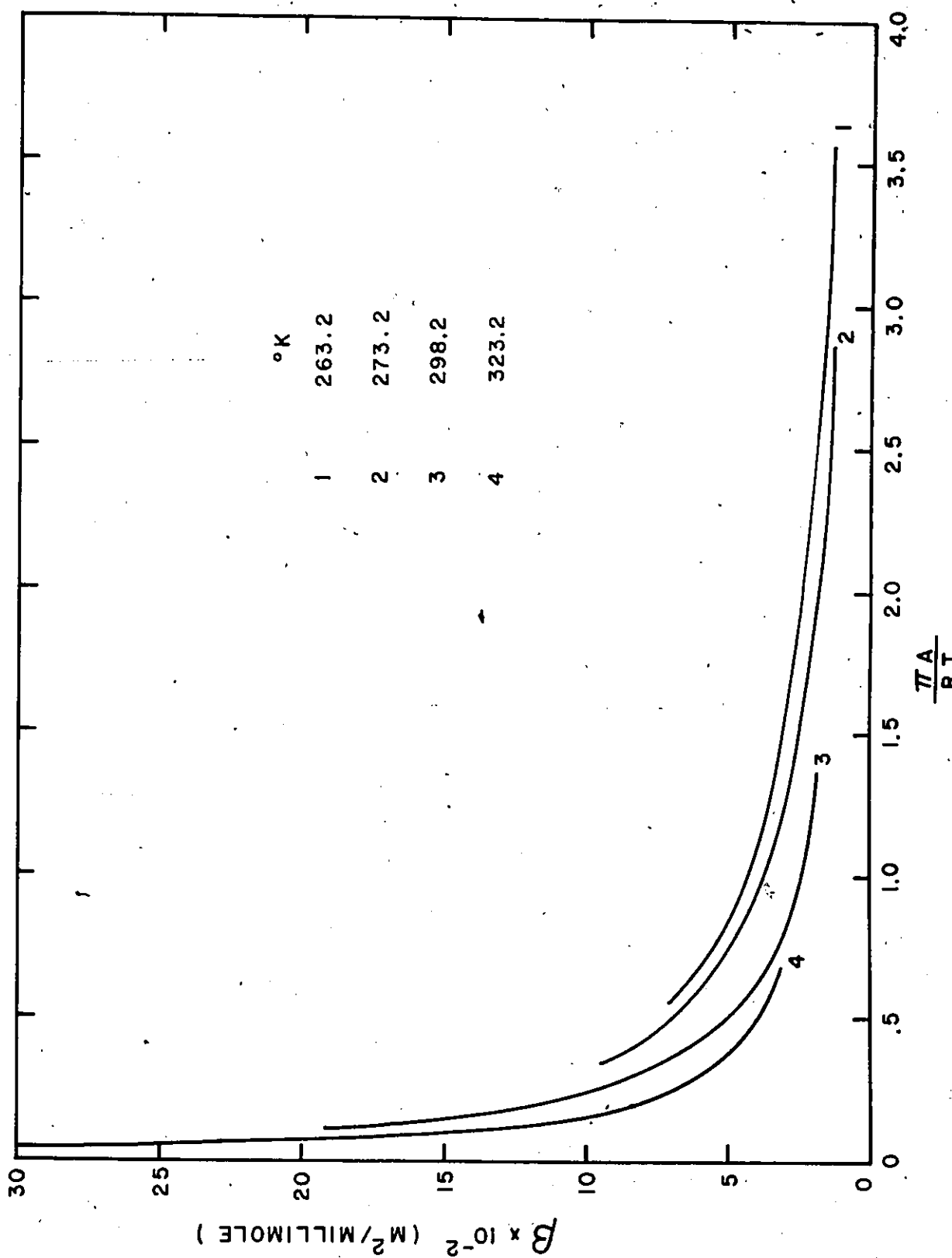


Figure IV.16 Temperature Effect on π -dependent β for CO₂

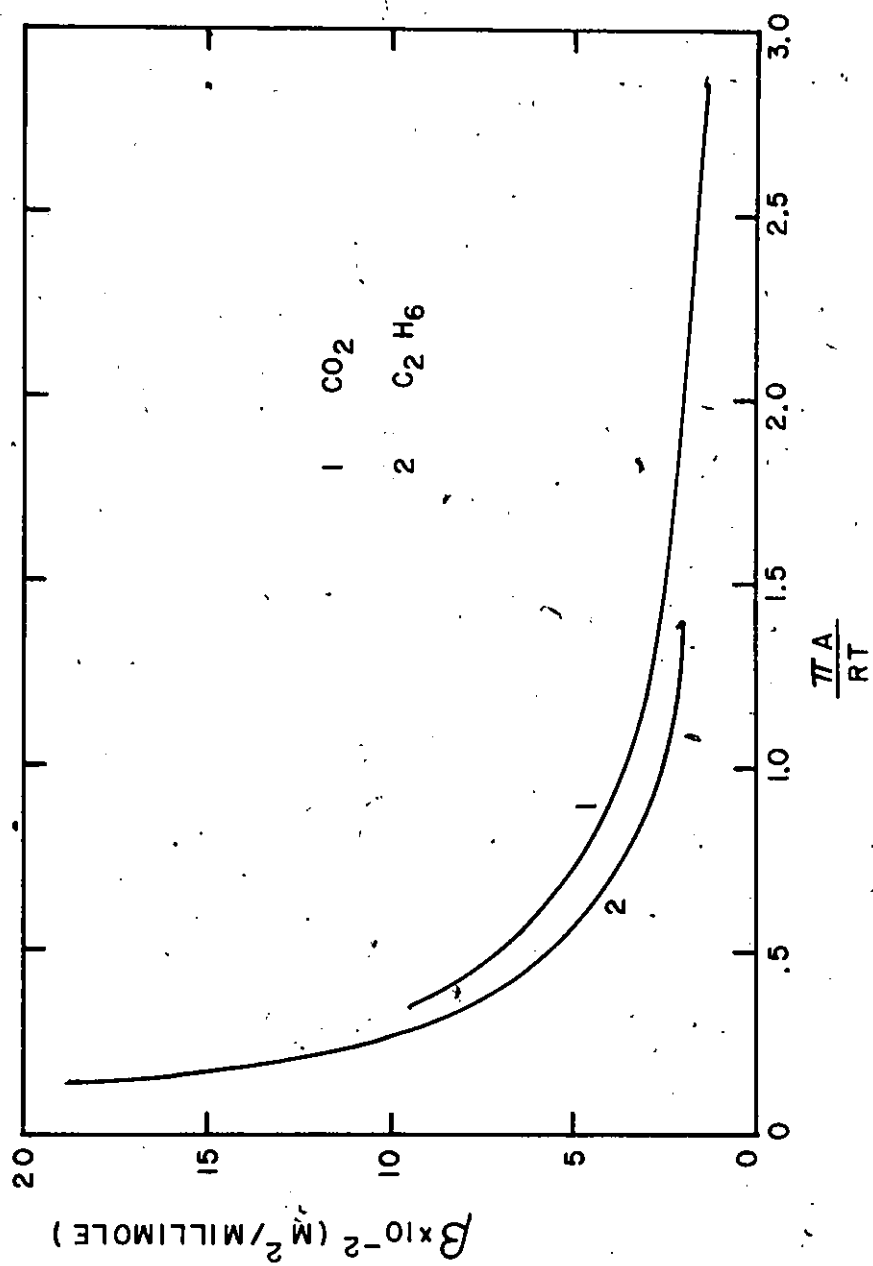


Figure IV.17 π -dependent β for CO_2 and C_2H_6 at 273.2°K

The comparison between the values of β for CO_2 and C_2H_6 at 273.2°K is shown in Figure IV.17.

For each system, the values of α and β approach a lower limit as $\frac{\pi A}{RT}$ is increased regardless of the temperature. The tapering of the curves occur faster when the temperature is lowest. This lower limiting value could be an indication of saturation. This behaviour could be further investigated by measuring adsorption isotherms at higher pressures over a larger temperature range.

IV.B.4 Some Correlations Considered for α and β

IV.B.4.a Characteristic Parameter Correlation

Attempts were made to correlate the characteristic parameters obtained from the method described in Section IV.B.3. The first method consisted in representing the parameters by a simple analytical relation for $\alpha = F(T, P)$ and $\beta = F(T, P)$. However, as observed from the nature of the curves in the previous section, this relation could have temperature and pressure dependent parameters for each system. In fact, it was impossible to represent the entire pressure range by a single relation and when used with Equation II.52, this relation hindered greatly the prediction of the adsorbed phase properties.

When the characteristic parameters Ω_a and Ω_b , or α

and β , are related to the acentric factor, difficulties in the correlation are encountered. The nature of the curves are illustrated in Figures IV.18 and IV.19 for a reduced pressure of 0.014 with the reduced temperature being the parameter.

The reduced pressure dependence of Ω_b at a given reduced temperature is summarized in Figure IV.20. A similar trend is also noted for Ω_a . Different curves are obtained for different components. The effect of using reduced quantities smoothes the trend of the curves as opposed to those of Figure IV.10. The experimental temperature and pressure range investigated limit the use of reduced quantities in the correlation.

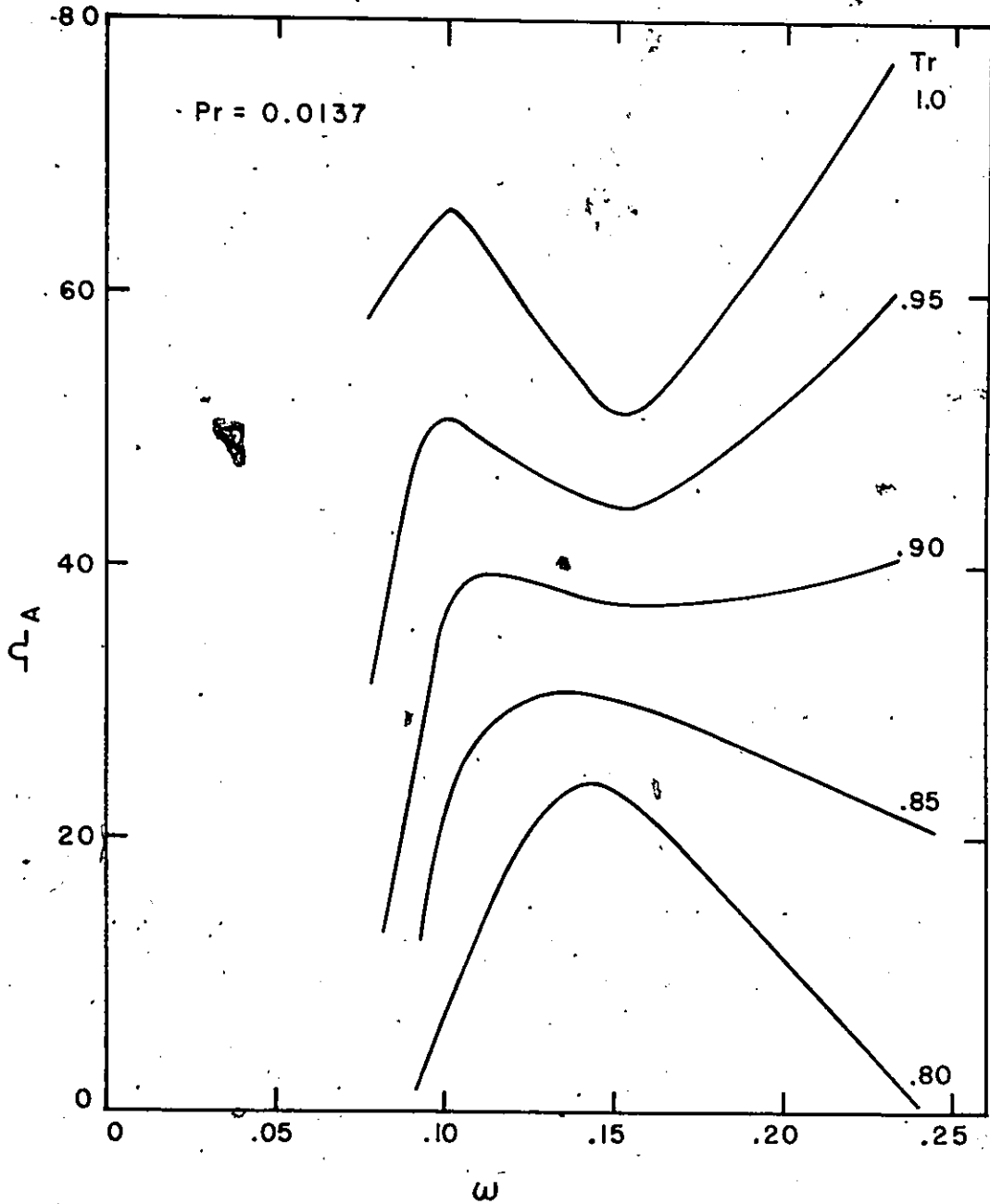


Figure IV.18 Reduced Temperature Effect on Ω_a with ω

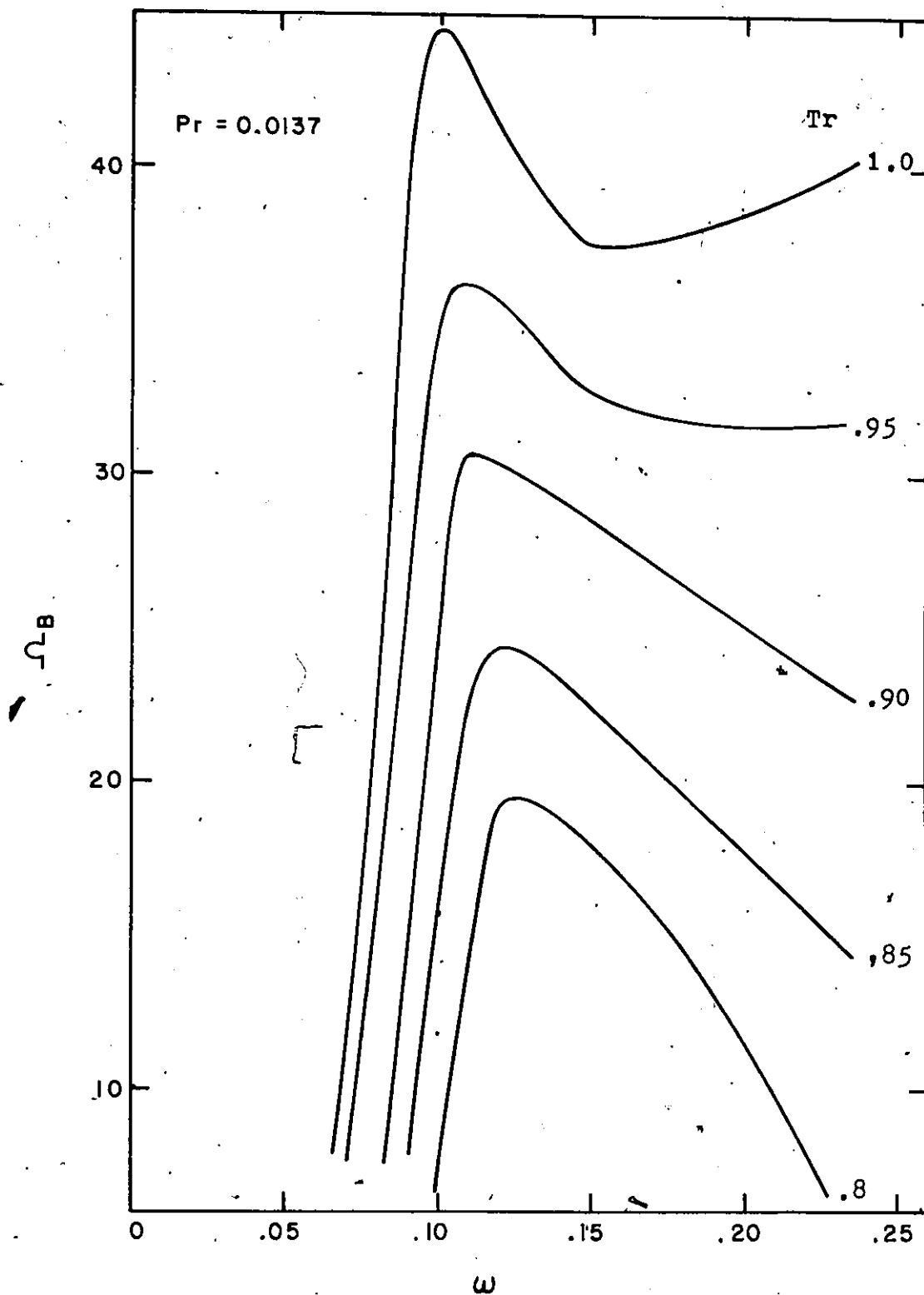


Figure IV.19 Reduced Temperature Effect on Ω_b with ω

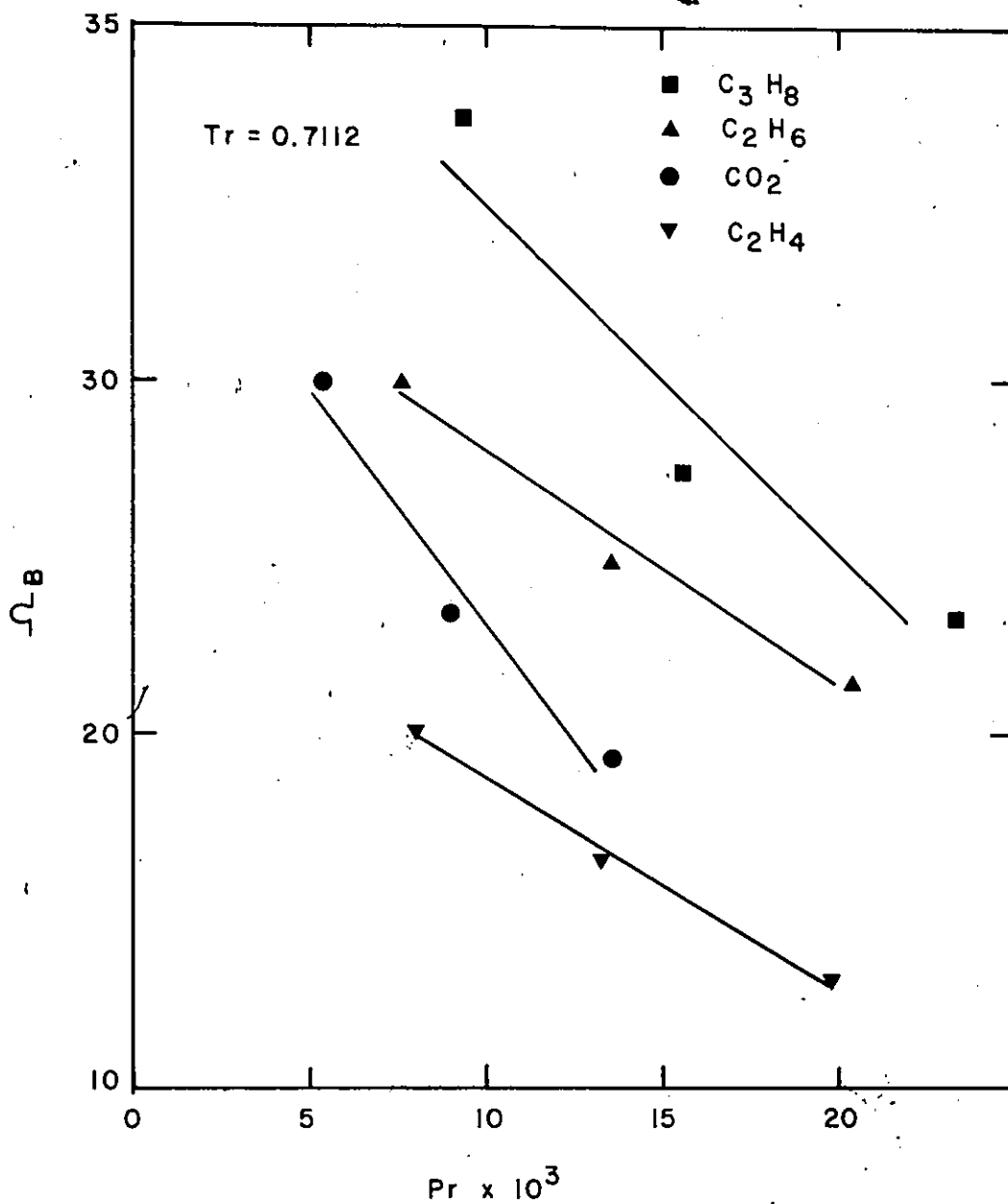


Figure IV.20 Reduced Temperature Dependence of Ω_b for Different Adsorbates

IV.B.4.b Compressibility Factor Correlation

The analog of Pitzer's correlation (21) of the compressibility factor, Z , in vapor-liquid equilibria was tested. This correlation was extended to adsorption phase equilibria. It consists in representing the Z -values as a function of the variables T_r , P_r and ω ;

$$\frac{\pi \sigma}{RT} = Z(T_r, P_r, \omega)$$

The compressibility factors of the adsorbed phase were computed from the experimental data consisting of the spreading pressure and the molar area of the adsorbed phase at a given temperature. The Z -values are listed in Tables IV.5 (Appendix I).

The relationship between the compressibility factor and the acentric factor for the adsorbed components investigated in this work is shown in Figure IV.21. The compressibility factor is positive and greater than one. Furthermore, it increases with decreasing temperature.

The relationship between T , P and Z was examined. The following behavior was observed in all systems; the adsorbed phase Z -values increase with reducing temperature and with increasing pressure. This is illustrated in Figure IV.22 in which the compressibility factor for C_3H_8 is plotted against the total gas phase pressure for different temperatures, and in

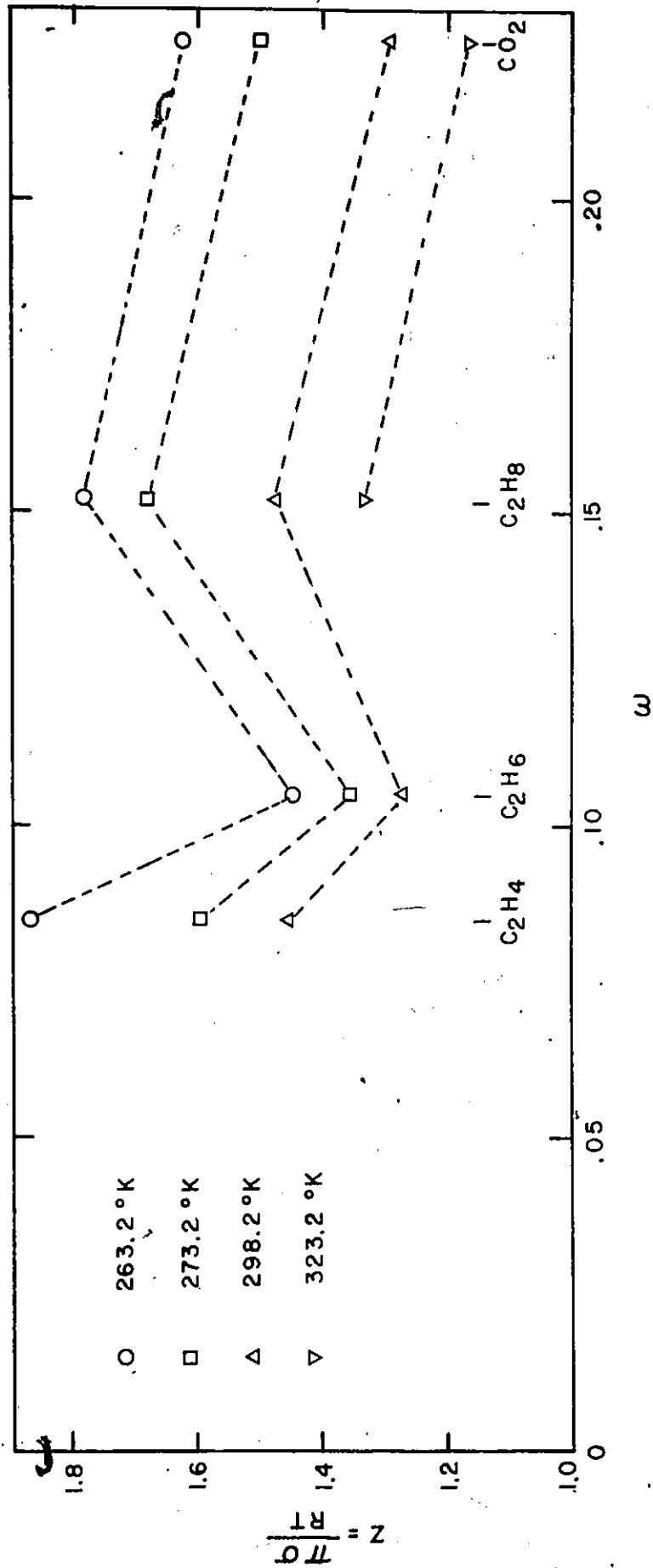


Figure IV.21 Adsorbed Phase Compressibility Factors, Z , and Acentric Factors, ω , for Different Adsorbates at 750 mmHg.



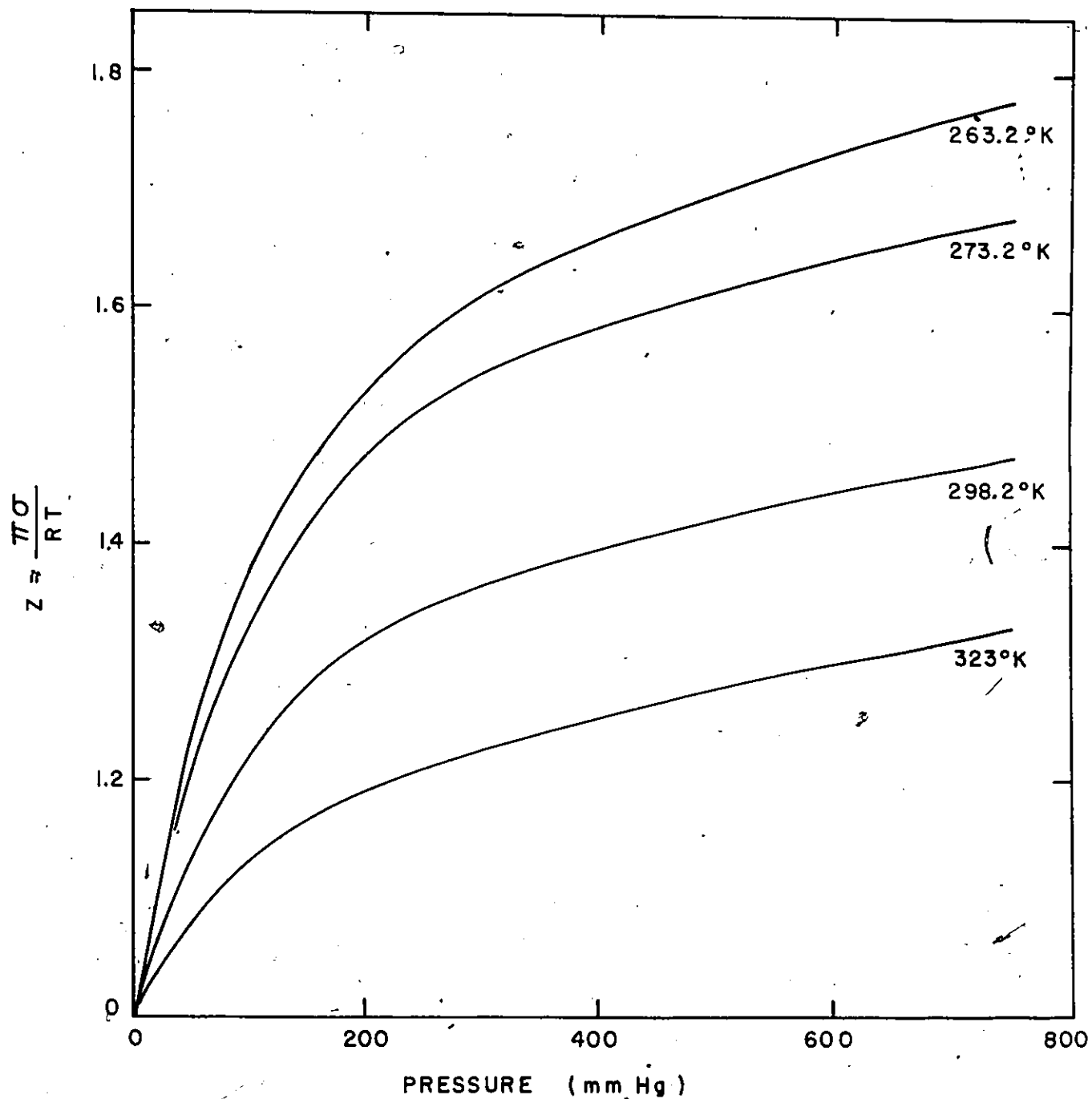


Figure IV.22 Temperature Effect on the Pressure Dependent Z for C_3H_8 .

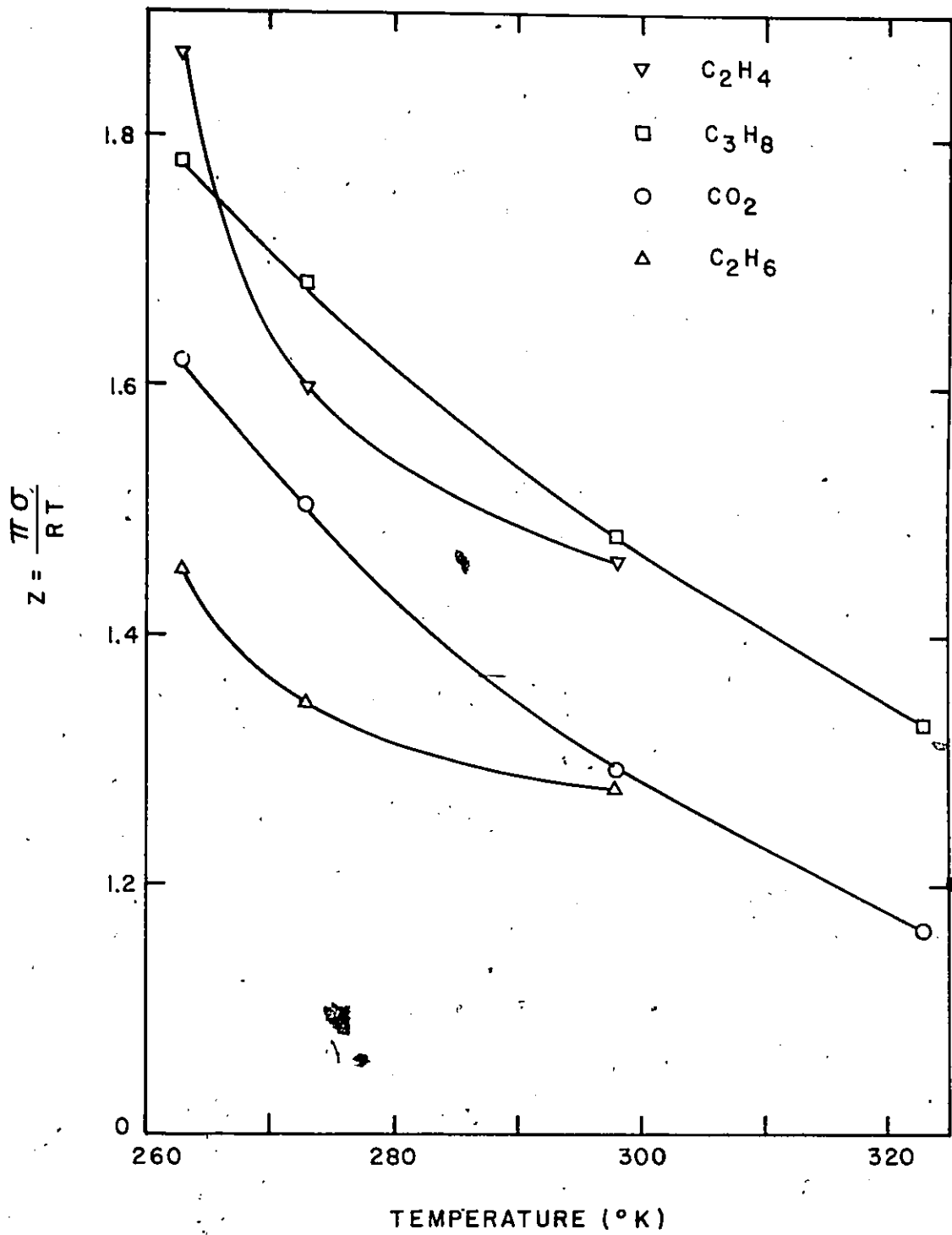


Figure IV.23 Temperature Dependent Z for Different Adsorbates at 750 mmHg

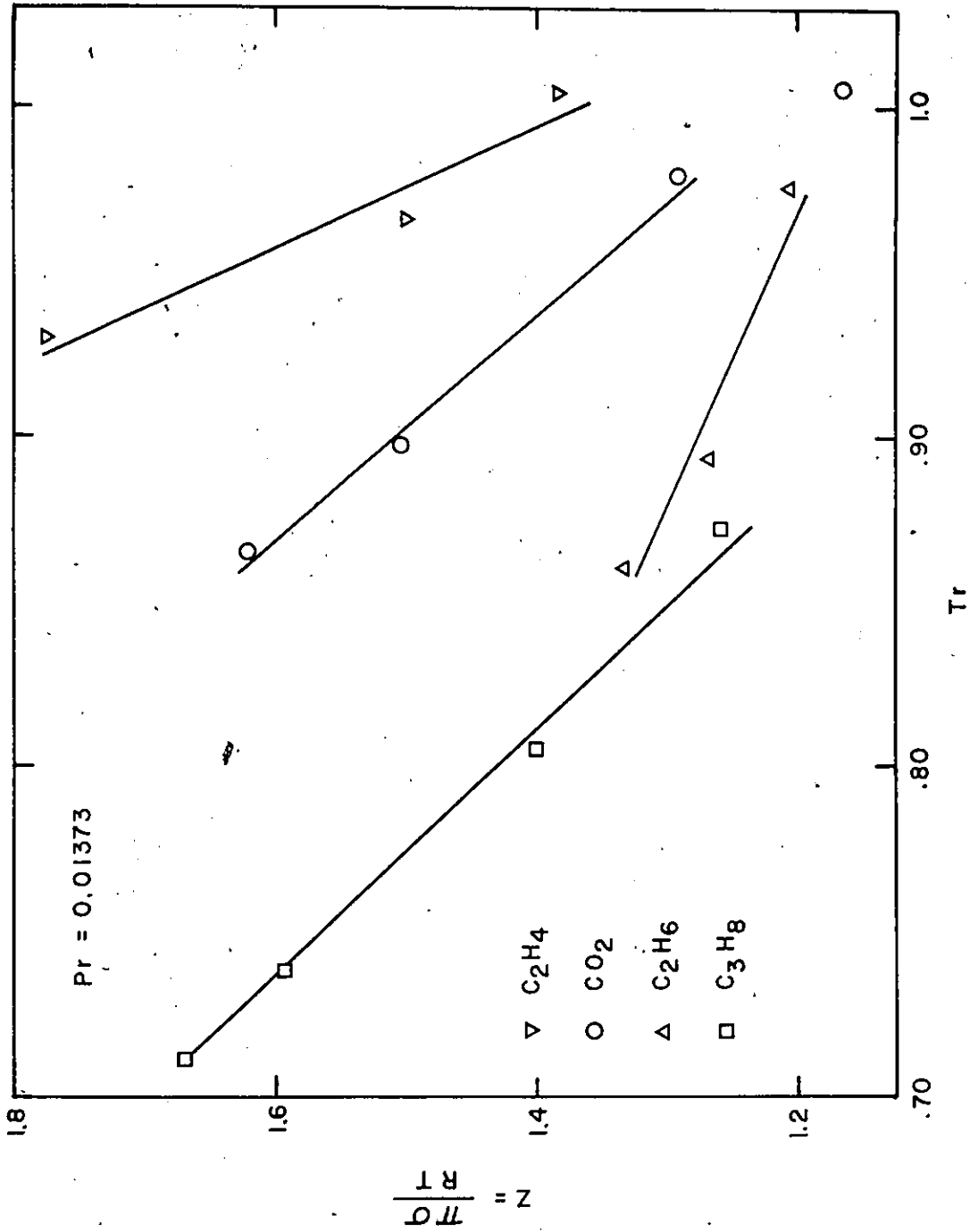


Figure IV.24 Reduced Temperature Dependent Z for Different Adsorbates



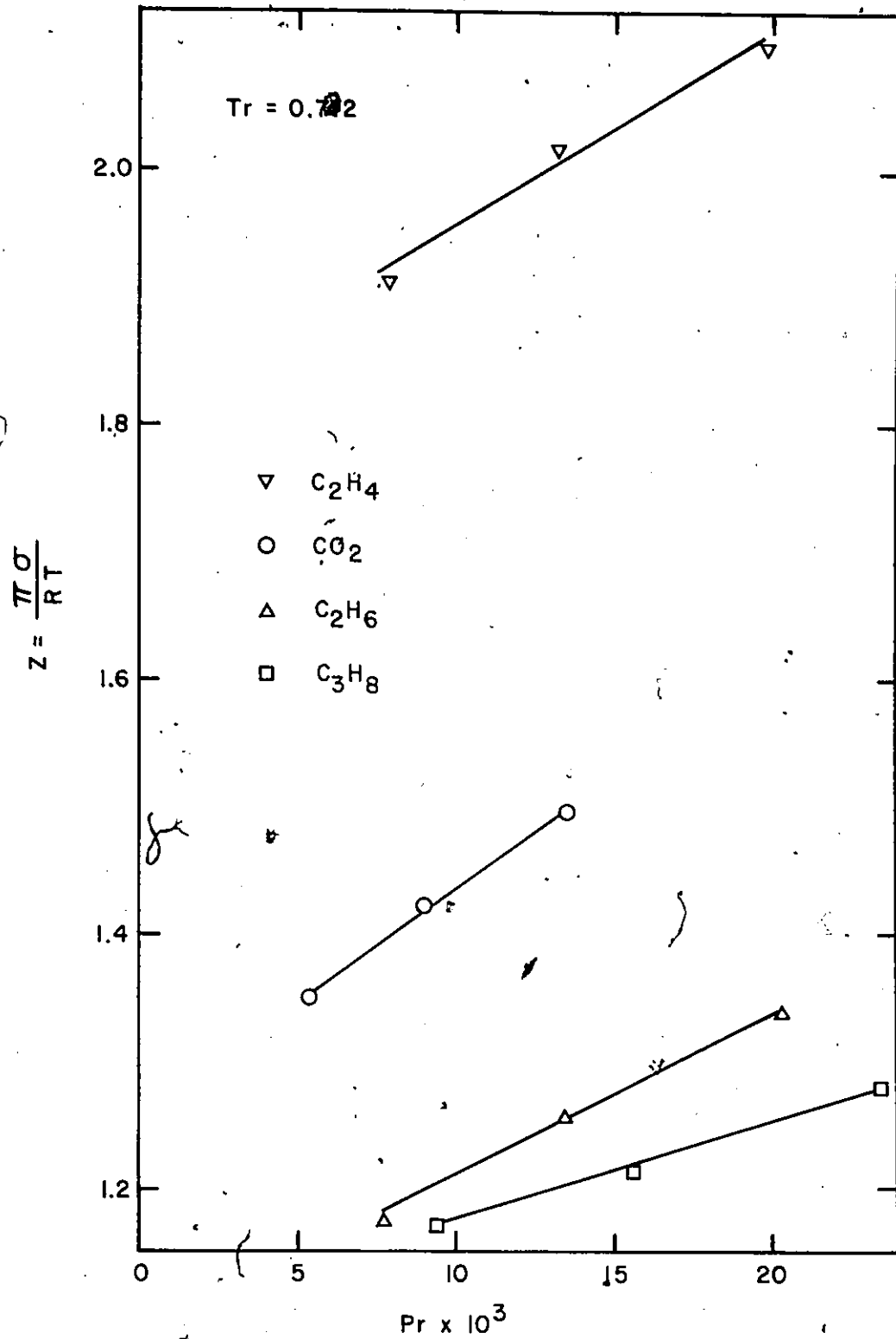


Figure IV.25 Reduced Pressure Dependent Z for Different Adsorbates

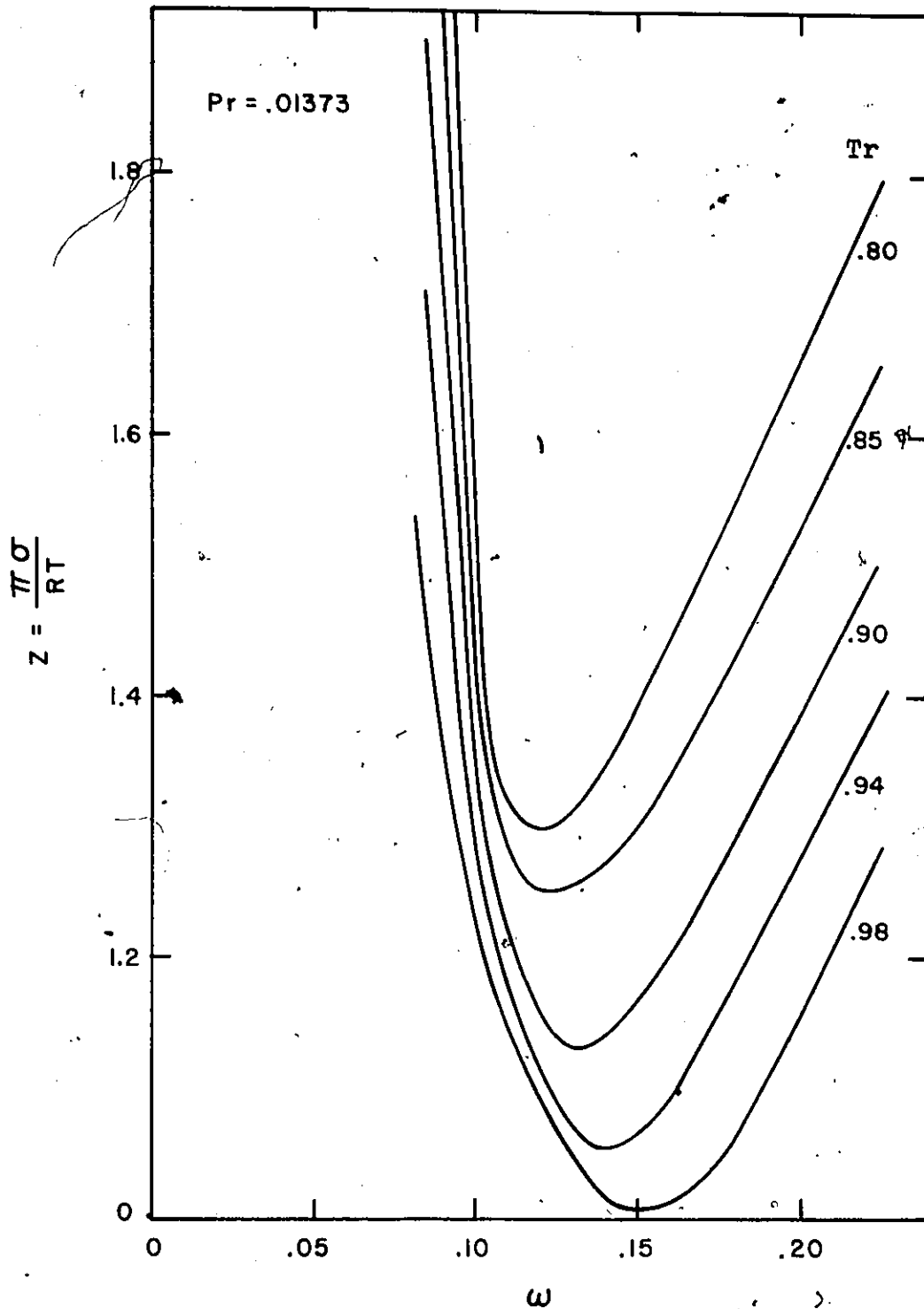


Figure IV.26 Reduced Temperature Effect on Z with ω

Figure IV.23 in which Z is a function of the temperature at 750 mmHg for different components.

In Pitzer's correlation of Z versus T_r , at a given P_r , a single curve is obtained for gas and liquid phases. For the adsorbed phase, the complexities of the relation $Z(T_r, P_r, \omega)$ are illustrated in Figures IV.24, -25 and -26. The compressibility factor and the acentric factor, with temperature as the parameter, involve a complex function as seen in Figure IV.26 in which a series of curves is reproduced for a reduced pressure of 0.014.

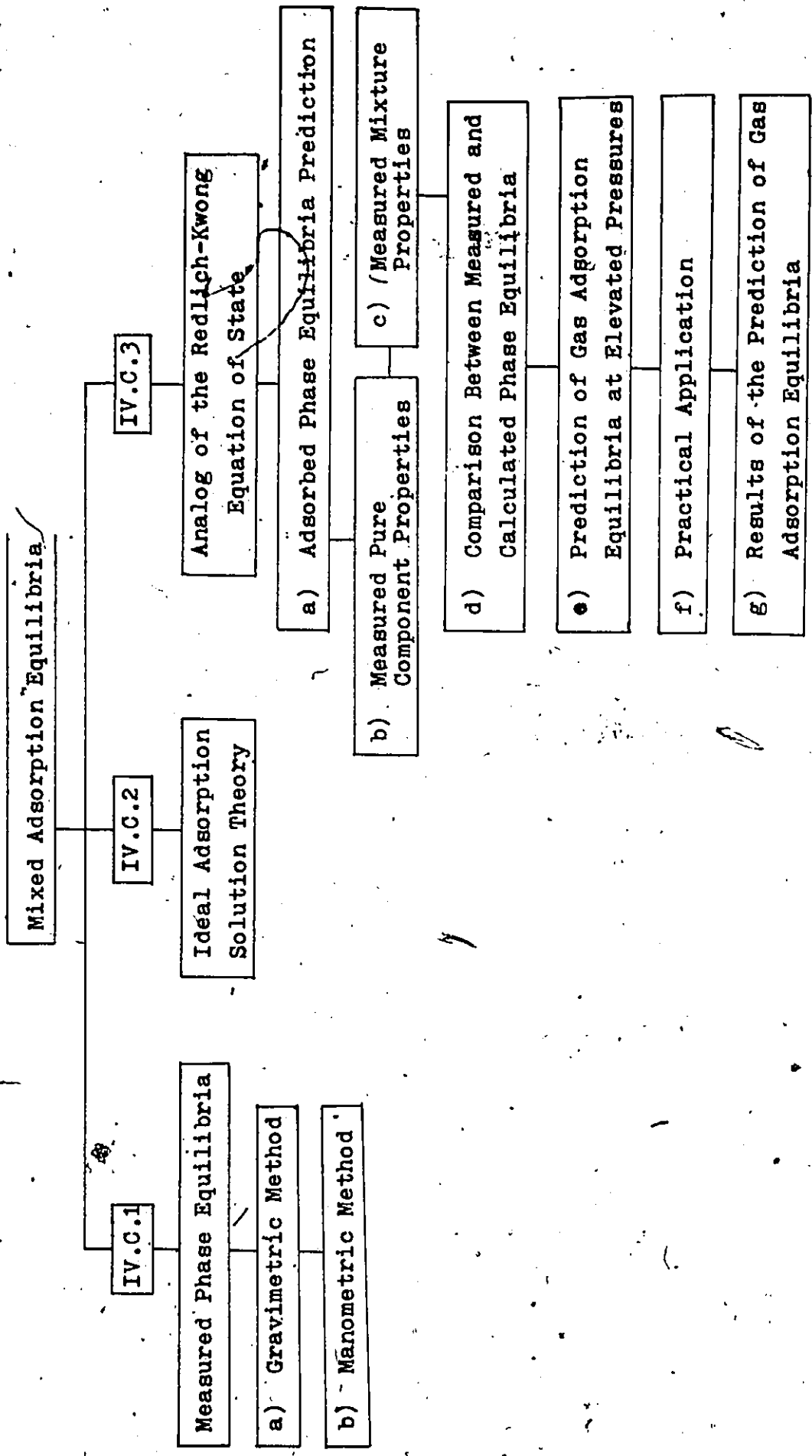
These correlations were abandoned because the values of α and β can be obtained directly and precisely from the experimental data with the analog of the Redlich-Kwong equation of state.

IV.C Mixed Adsorption Equilibria

IV.C.1.a Measured Phase Equilibria with the Gravimetric Method

The calculation of the adsorbed phase molar composition can be performed with the exact thermodynamic relationship, Equation I.11, which represents the adsorbed phase in equilibrium with the gas phase. The calculation involves an iteration scheme described in Appendix IV. The imposition of certain constraints on the relationship leads to expressions useful for the calculation of the spreading pressure term $\frac{\pi A}{RT}$ with Equation II.14, and the adsorbed phase molar composition with Equation II.16.

SUBDIVISIONS OF SECTION IV.C



The results of the calculation for all systems investigated at all temperatures are listed in Tables IV.6 (Appendix I.6). They are presented for each system temperature, at regular pressure intervals with corresponding moles adsorbed, surface pressure terms $\frac{VA}{RT}$, and the adsorbed molar composition. The pressure and temperature effects on the adsorbed phase composition for the binary systems investigated is next summarized in terms of the component mostly adsorbed; that is, the heaviest component in a binary mixture.

The molar composition of an adsorbed species has the general tendency to decrease with increasing gas phase pressure by an amount approximately equal to 0.04 mole fraction. This is observed in most systems investigated at all temperatures and is more pronounced for systems containing CO_2 .

The temperature effects on the composition of the adsorbed phase at 750 mmHg are listed in Table IV.7 for different gas phase molar compositions. At this pressure and for a range of temperature of 60°K, the average change in the adsorbed mole fraction in all systems is roughly 0.03 for any gas phase molar composition. The effect of the gas phase composition on the temperature dependent adsorbed phase composition are illustrated in Figure IV.27. For a given pressure and temperature, the composition characteristics presented in Table IV.7 are illustrated in Figure IV.28 for the indicated systems. It is interesting to note that the presence of CO_2 or C_2H_4 with C_2H_6 gives similar mixed adsorption equilibria on a composition

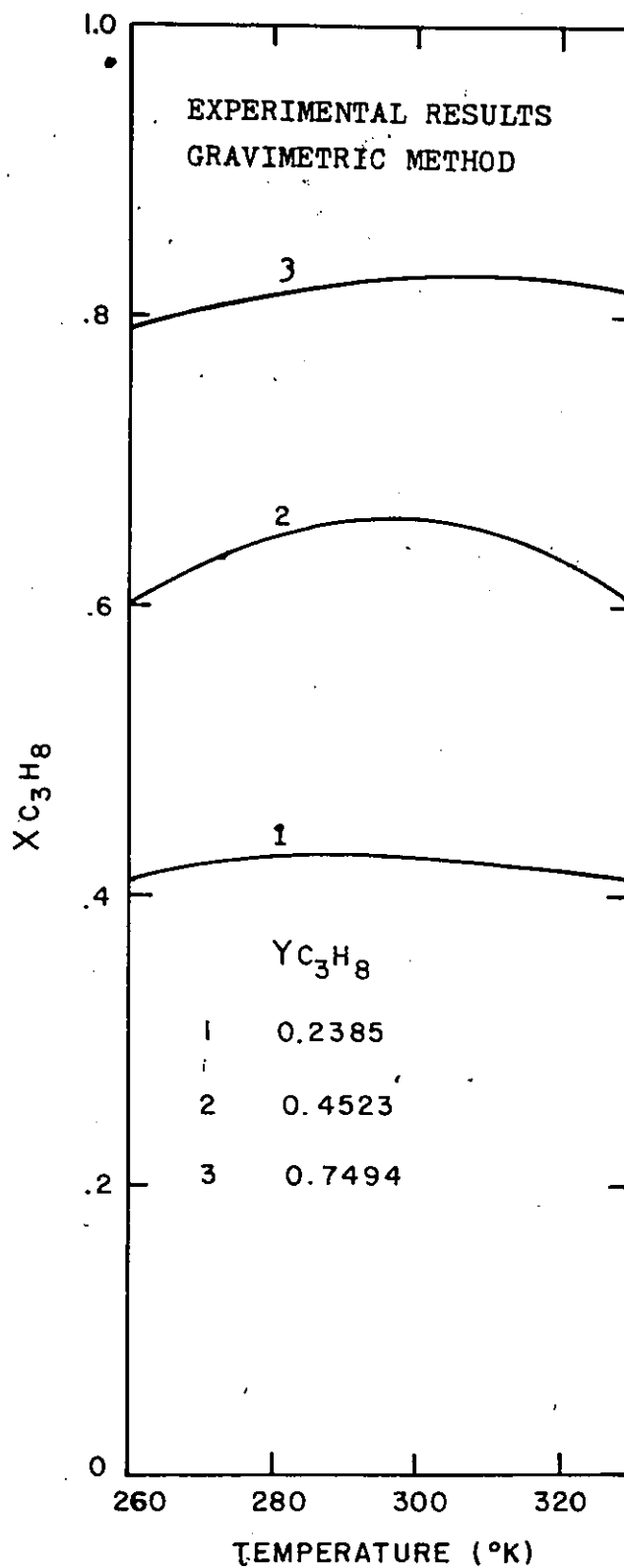


Figure IV.27 Effect of Y on the Temperature Dependent X for the System $C_3H_8 - CO_2$ at 750 mmHg

TABLE IV.7

ADSORBED PHASE COMPOSITIONS at 750mmHg

Mole Fraction of Component 1 - K_1

System	Y_1	$T^{\circ}K$			
		263.2	273.2	298.2	323.2
$CO_2 - C_3H_8(1)$.2385	.4148	.4261	.4237	.4149
	.4527	.6077	.6361	.6643	.6297
	.7494	.7973	.8065	.8259	.8252
$C_2H_6 - C_2H_4(1)$.2635	.5118	.4583	.4684	
	.5042	.6812	.7373	.6872	
	.7547	.8623	.8907	.8693	
$C_2H_6 - CO_2(1)$.2592	.4996	.5133	.4398	
	.4960	.6697	.7943	.7035	
	.7522	.8704	.9003	.8594	

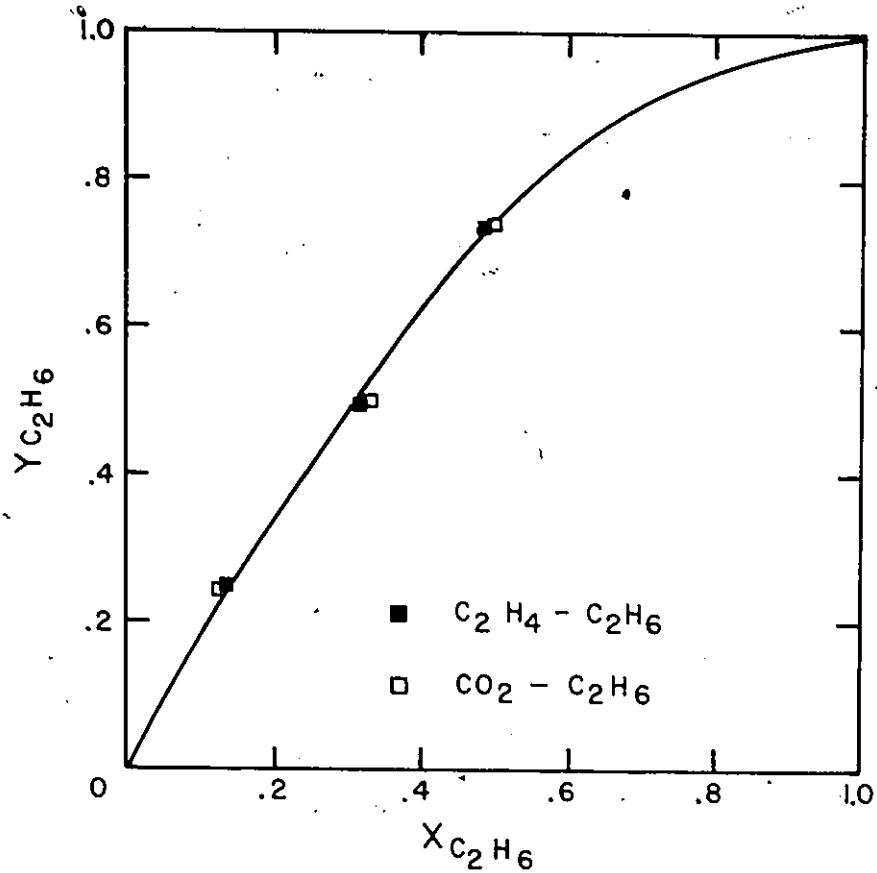


Figure IV.28a Composition Diagram for $CO_2 - C_2H_6$ and $C_2H_4 - C_2H_6$ at $263.2^\circ K$ and 750 mmHg - Gravimetric Method

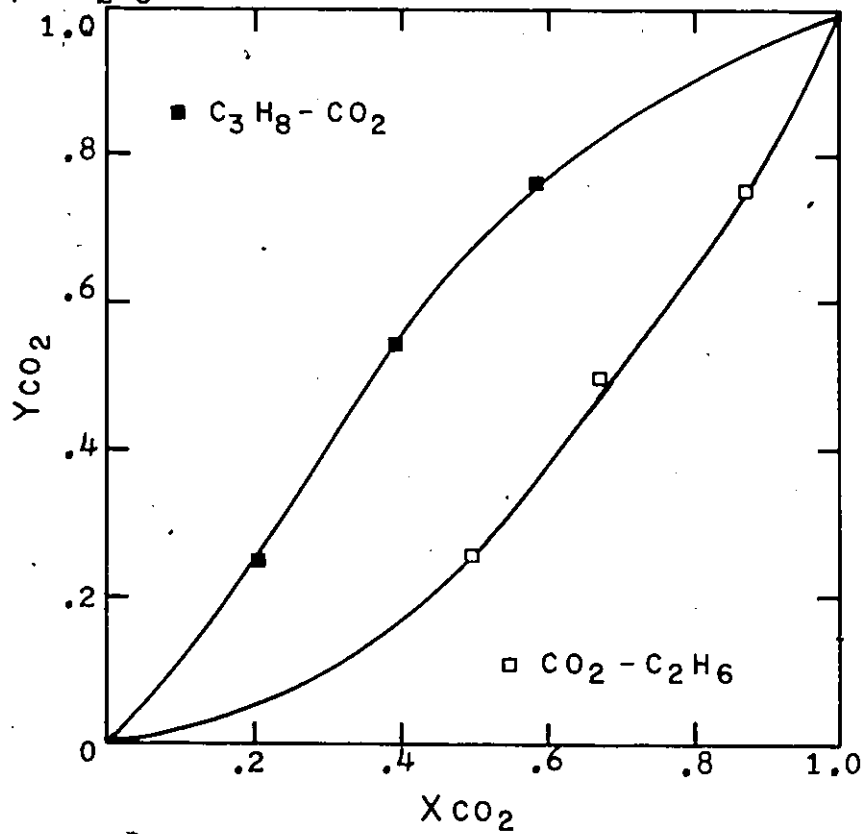


Figure IV.28b Composition Diagram for $CO_2 - C_2H_6$ and $C_3H_8 - CO_2$ at $263.2^\circ K$ and 750 mmHg - Gravimetric Method

diagram of Figure IV.28a. However, the adsorption of CO_2 in the presence of C_2H_6 is greatly favored over CO_2 with C_3H_8 . This is depicted in Figure IV.28b.

IV.C.1.b Measured Phase Equilibria with the Manometric Method

An independent experimental approach provided a verification of the method for calculating the surface composition described in IV.C.1.a. It was not necessary to experiment with all systems at the different temperatures investigated. Systems exhibiting the largest deviation in the prediction of the pure component pressures were investigated at 273.2°K which is midway in the temperature range investigated.

In this particular investigation, the experimental conditions were chosen so as to cover the entire range of gas phase composition. In this way, the data measured gravimetrically can be compared with those measured using the manometric method. Measured phase equilibria for the system $\text{CO}_2 - \text{C}_2\text{H}_6$ at 273.2°K and $\text{C}_3\text{H}_8 - \text{CO}_2$ at 273.2°K are respectively reported in Tables IV.8 and I.V9.

Phase equilibria for the system $\text{CO}_2 - \text{C}_2\text{H}_6$ are illustrated in Figure IV.29 for the experimental run 1.2 and in Figure IV.30 for the average experimental conditions of runs 1.5, 1.6 and 1.7. The comparison between the two methods used for measuring phase equilibrium data indicate that the average

deviation in both phases is 0.03 mole fraction while the average deviation in moles adsorbed is roughly 2%.

Similarly, phase equilibrium data for the system $C_3H_8 - CO_2$ at $273.2^\circ K$ are compared in Figure IV.31 for the experimental run 2.1 and in Figure IV.32 for run 2.3. In the latter case, the equilibrium point is plotted in Figure IV.33 to show its position in relation to the gas phase molar composition effect on the temperature dependent moles adsorbed. The same point is brought on a composition diagram of Figure IV.34. The comparison between the calculated and measured phase equilibria indicate an average deviation of 0.02 mole fraction and a deviation of less than 1% in the number of moles adsorbed.

In effect, phase equilibria calculated with the exact thermodynamic relationship are shown to be quite reliable and to serve as a basis for the comparison of predicted phase equilibria when an adsorbent is in equilibrium with a mixture of gases. These predicted quantities can be obtained from adsorption theories or equations of state.

TABLE IV.8

MEASURED PHASE EQUILIBRIA FOR THE SYSTEM

CO₂ (1) - C₂H₆ AT 273.0°K
 - MANOMETRIC METHOD -

Run	System Pressure P (mmHg)	Gas Phase Composition Y (mole fraction)	Adsorbed Phase Composition X (mole fraction)	Amount Adsorbed n (millimoles/gram)
1.1	307.67	0.6685	0.8275	0.9574
1.2	378.46	0.1756	0.3696	0.8050
1.3	342.09	0.3932	0.6080	0.8834
1.4	312.6	0.6646	0.8320	0.9641
1.5	390.94	0.6868	0.8482	1.1316
1.6	388.19	0.6850	0.8506	1.1266
1.7	391.40	0.6881	0.8476	1.1160

The average deviation between properties measured by the manometric and gravimetric method

are $\Delta Q = Q_{\text{manometric}} - Q_{\text{gravimetric}}$ 1) $\Delta Y = +.031$ 3) $\Delta n_Y = -.0157$
 2) $\Delta X = -.029$ 4) $\Delta n_X = +.0214$

TABLE IV.9

MEASURED PHASE EQUILIBRIA FOR THE SYSTEM

C₃H₈(1) - CO₂ AT 273.0°K

- MANOMETRIC METHOD -

Run	System Pressure P (mmHg)	Gas Phase Composition Y (mole fraction)	Adsorbed Phase Composition X (mole fraction)	Moles Adsorbed n (millimoles/gram)
2.1	329.30	0.3604	0.5562	1.4667
2.2	311.69	0.7455	0.7532	1.5721
2.3	353.86	0.7250	0.7796	1.7086
2.4	391.71	0.4092	0.5157	1.6139
2.5	384.61	0.4035	0.5232	1.6067

The average deviation between the calculated and the measured properties are

$$\Delta Q = Q_{\text{manometric}} - Q_{\text{gravimetric}}$$

- 1) $\Delta Y = +.028$
- 2) $\Delta X = -.008$
- 3) $\Delta n_y = -.014$
- 4) $\Delta n_x = +.011$

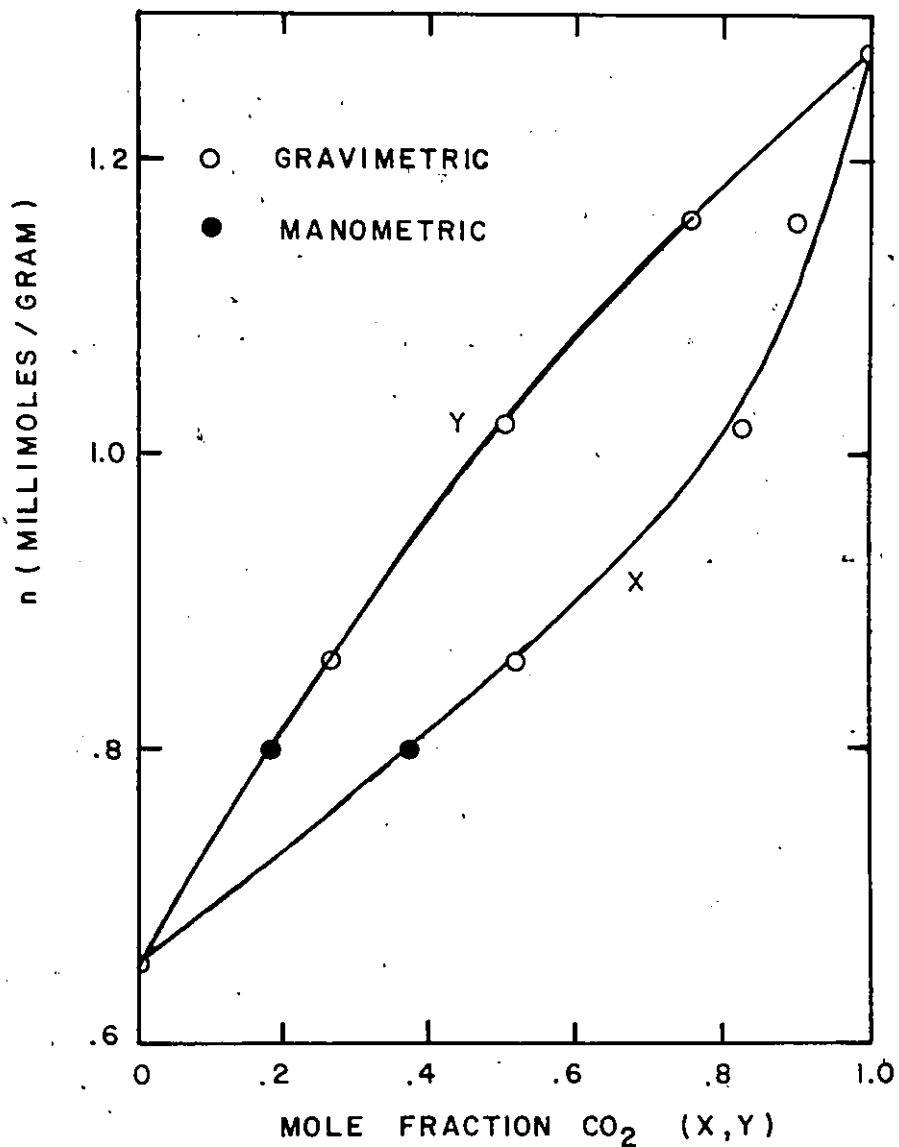


Figure IV.29 Comparison Between Two Methods of Measuring Phase Equilibria for $\text{CO}_2 - \text{C}_2\text{H}_6$ at 273.2°K and 342.1 mmHg

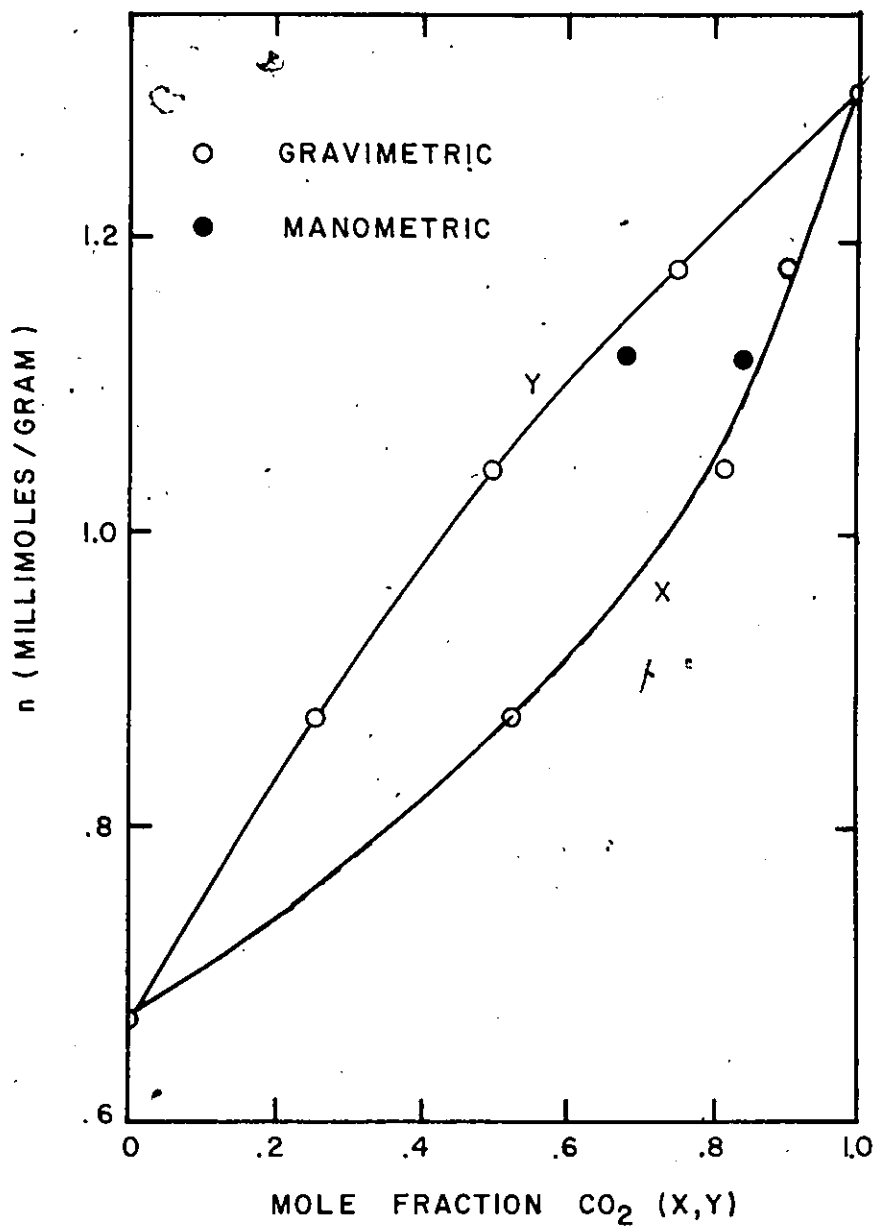


Figure IV.30 Comparison Between Two Methods of Measuring Phase Equilibria for CO₂ - C₂H₆ at 273.2°K and 390.18 mmHg

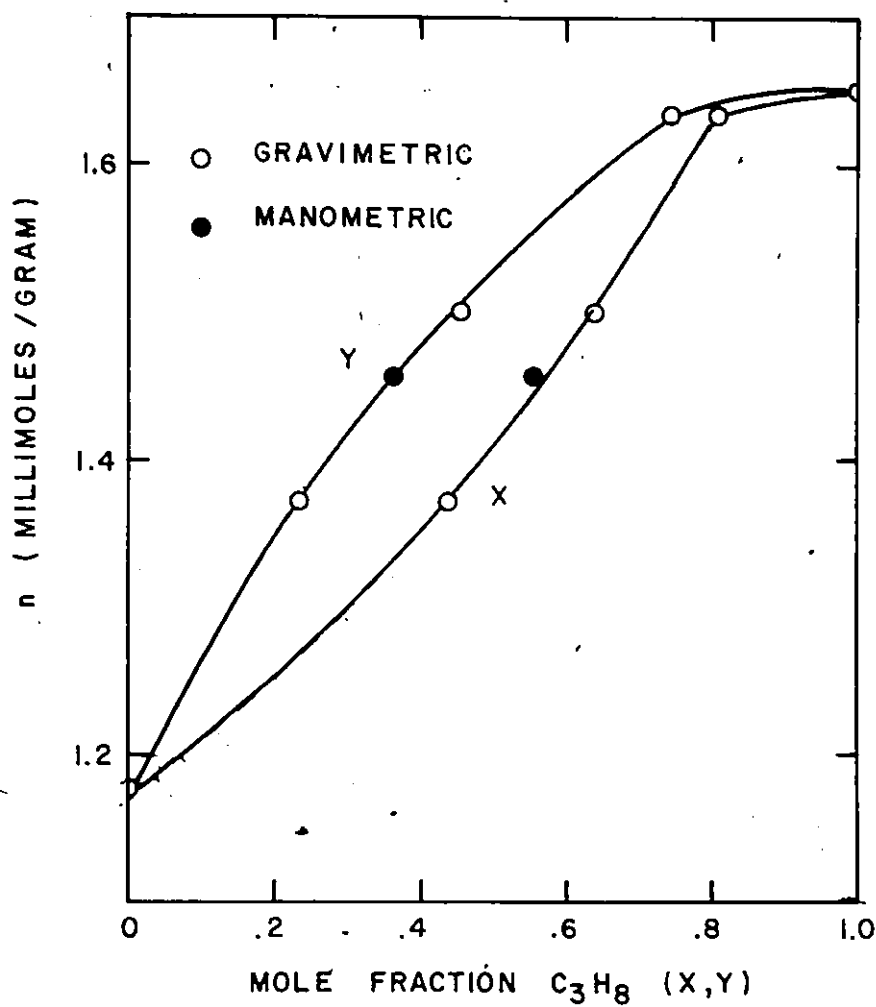


Figure IV.31 Comparison Between Two Methods for Measuring Phase Equilibria for C₃H₈ - CO₂ at 273.2°K and 329.3 mmHg

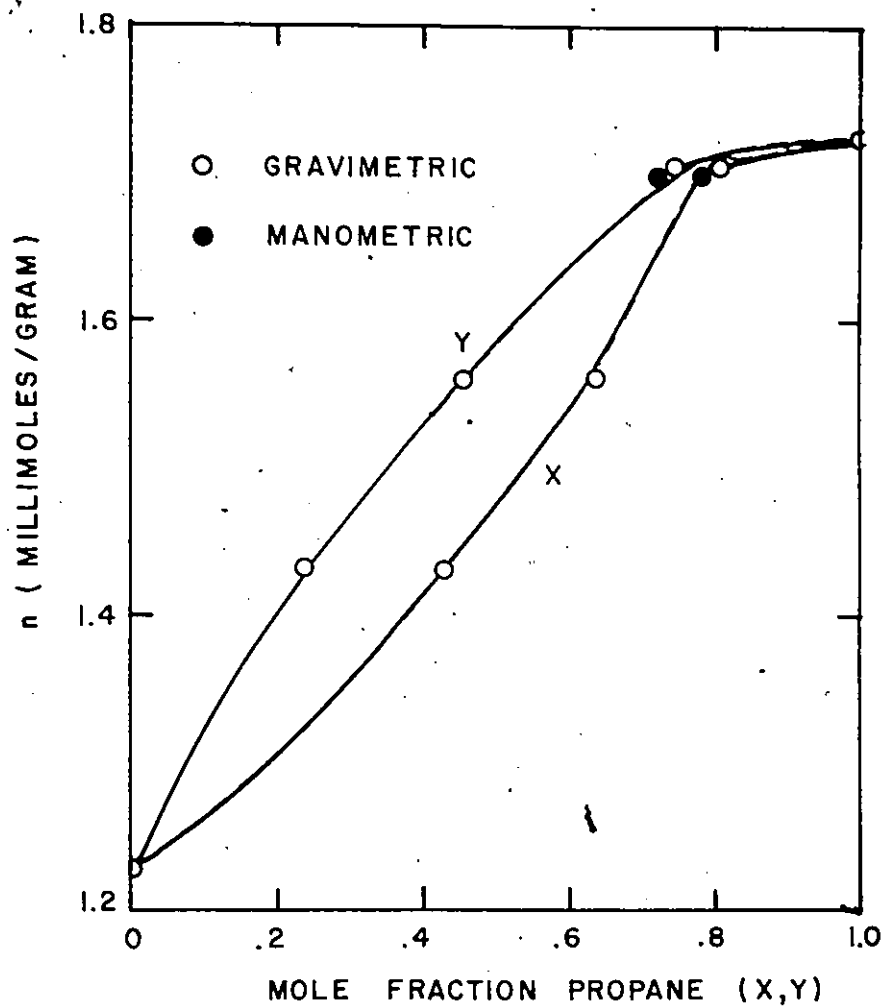


Figure IV.32 Comparison Between Two Methods for Measuring Phase Equilibria for $\text{CO}_2 - \text{C}_3\text{H}_8$ at 273.2°K and 353.86 mmHg .

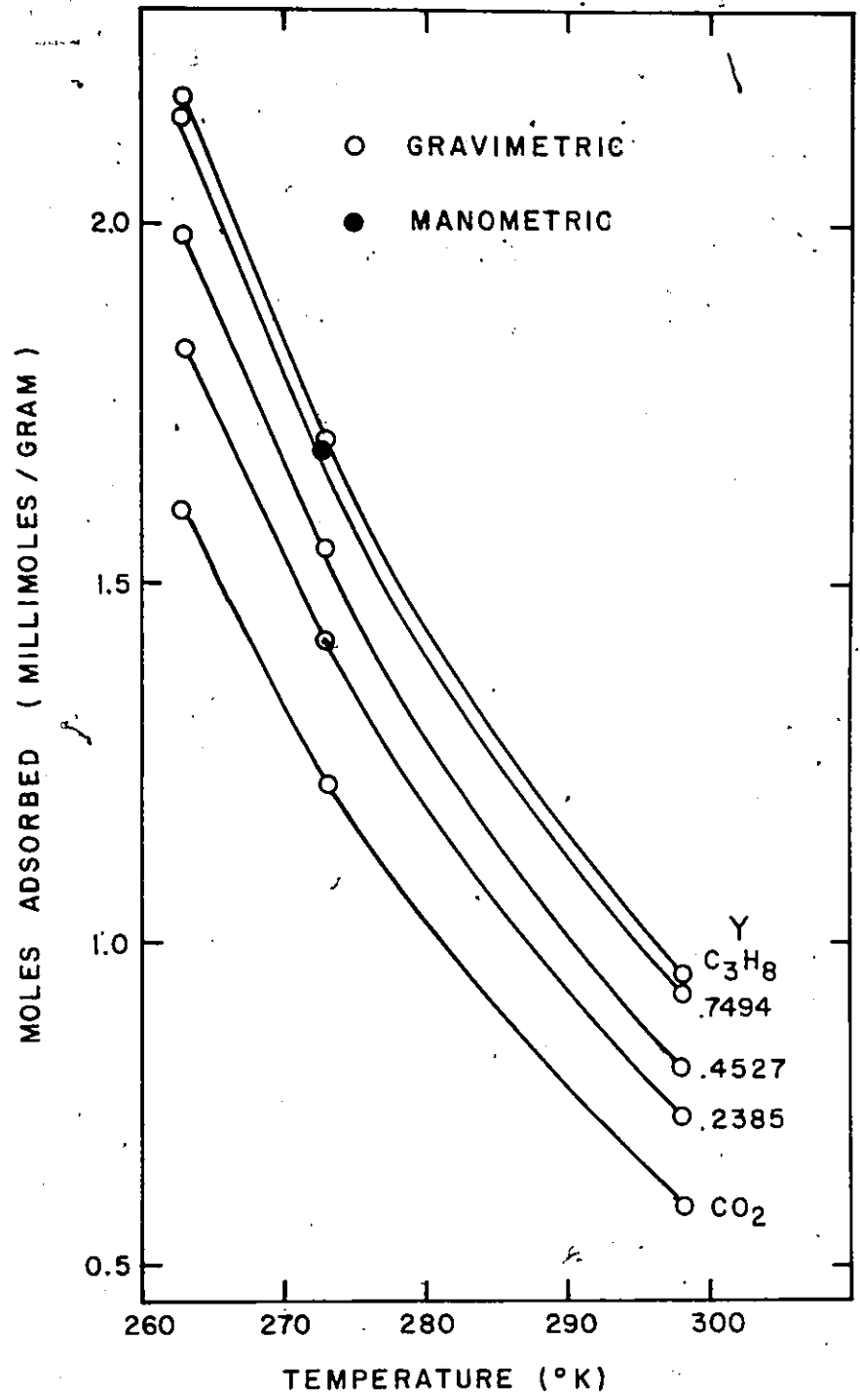


Figure IV.33 Effect of Y on the Temperature Dependent Moles Adsorbed for C₃H₈ - CO₂ at 273.2°K and 350 mmHg

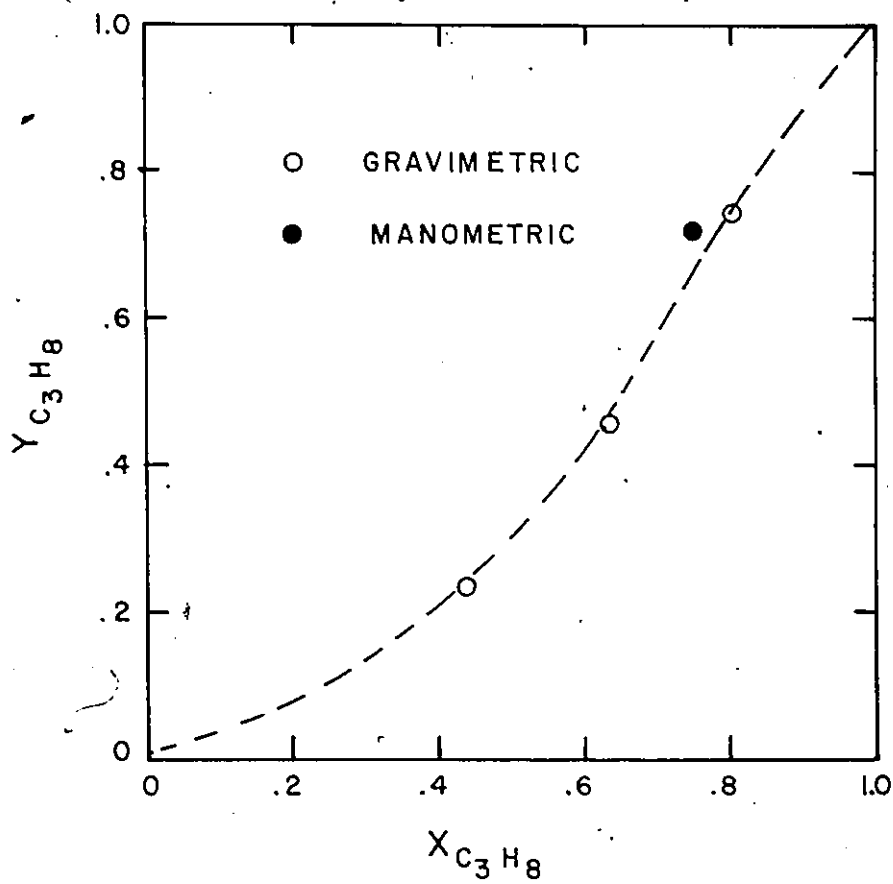


Figure IV.34 Comparison Between Two Methods for Measuring Molar Compositions (X-Y) for $C_3H_8 - CO_2$ at $273.2^\circ K$ and 350 mmHg

IV.C.2 Ideal Adsorption Solution Theory

The ideal solution theory (19, 20) for the prediction of the adsorbed phase composition, X , was tested. The results are summarized for all systems in the following table:

<u>Ideal Solution Theory</u>		
<u>Average Absolute Deviation in X-Y for all Temperatures</u>		
<u>System</u>	<u>Adsorbed Phase</u>	<u>Gas Phase</u>
$C_2H_4 - C_2H_6$	0.029	0.011
$CO_2 - C_2H_6$	0.041	0.022
$C_3H_8 - CO_2$	0.086	0.127

In Figure IV.35, the deviation in X is plotted against the temperature for the system $C_3H_8 - CO_2$ at 300 mmHg. For high density adsorption, the deviation from the ideal solution theory is greatest. Also the heavier are the molecules adsorbed, the greater is the deviation. The presence of heavy molecules in the adsorbed state does not favor a good prediction of X as seen in Figure IV.36a for the system $C_3H_8 - CO_2$ at $263.2^\circ K$ and 300 mmHg. The average deviation in the mole fraction X is 0.08 (16%). However, the prediction of the lighter adsorbed component is slightly better as seen in Figure IV.36b. In this case, the average deviation in composition is roughly 0.025 mole fraction (5%).

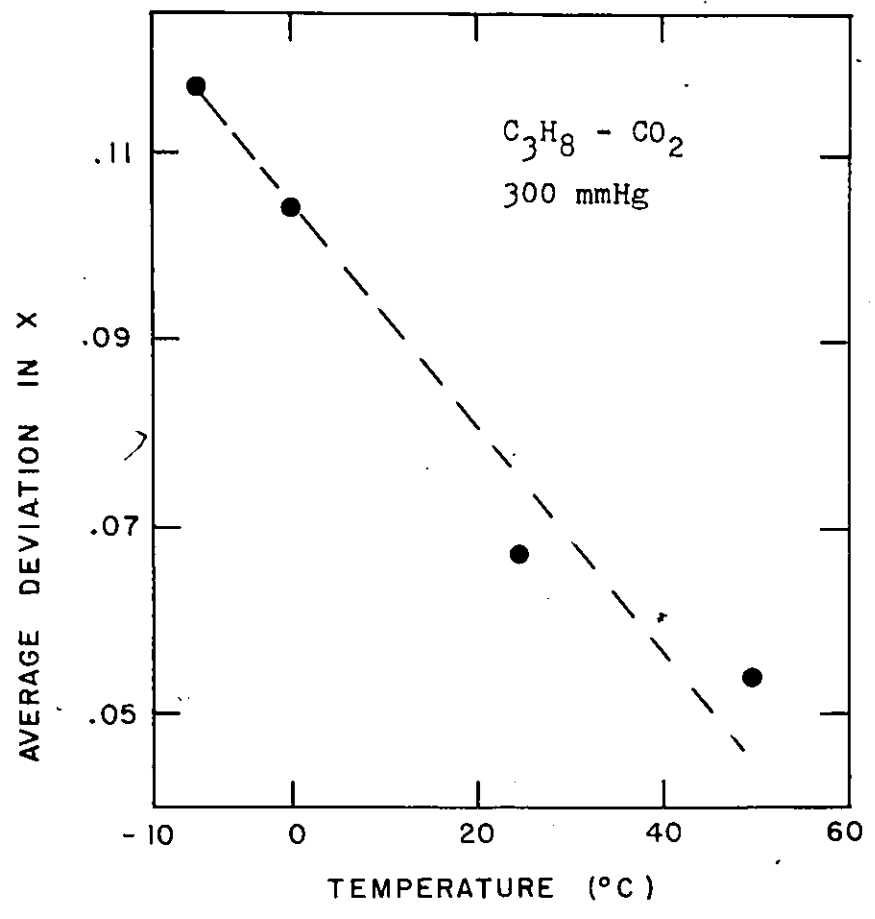


Figure IV.35 Average Deviation in Adsorbed Phase Composition with Temperature

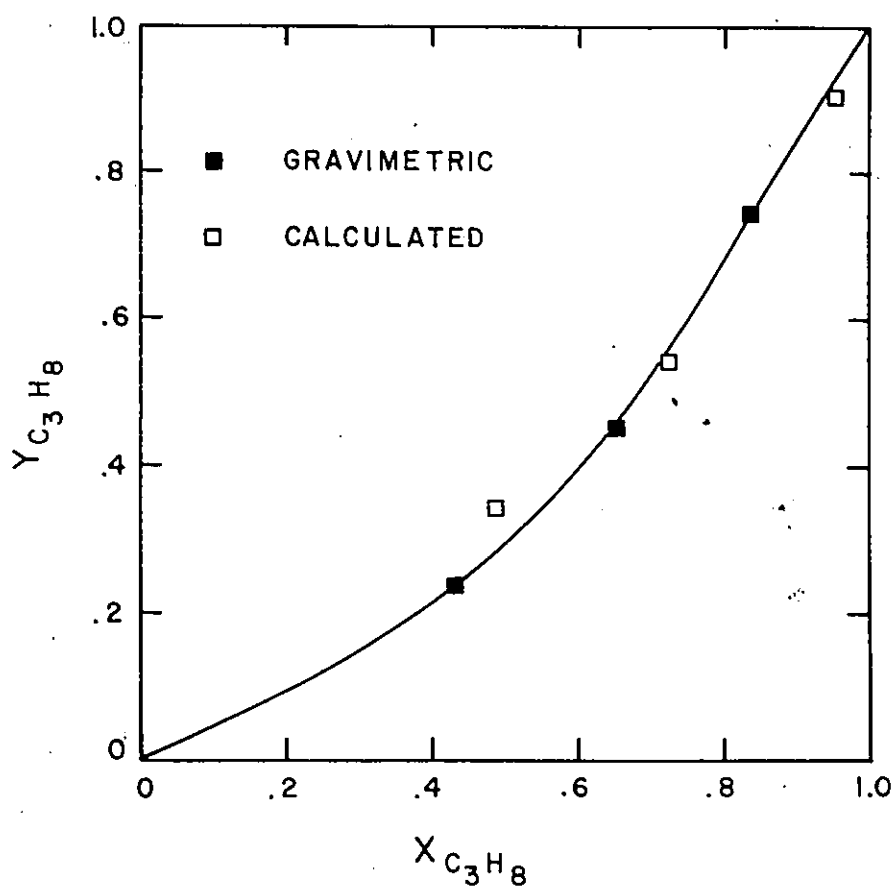


Figure IV.36a Comparison Between Calculated and Measured Composition Diagram for $C_3H_8 - CO_2$ at $263.2^\circ K$ and 300 mmHg - Ideal Adsorption Solution Theory

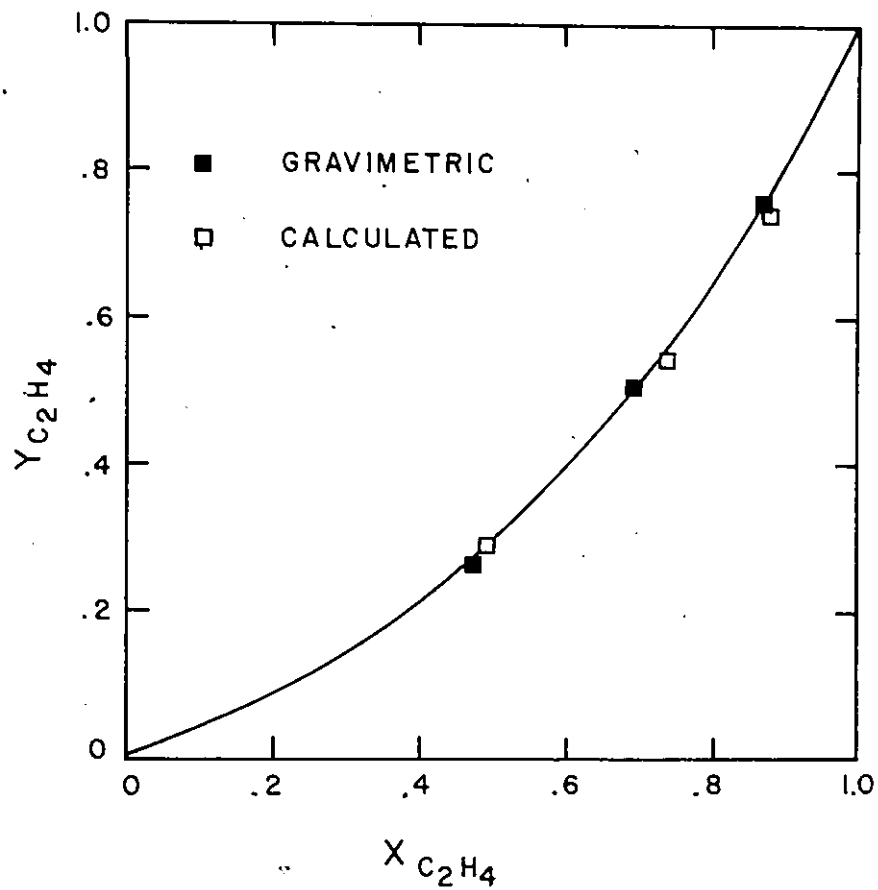


Figure IV.36b Comparison Between Calculated and Measured Composition Diagram for $C_2H_4 - C_2H_6$ at $298.2^\circ K$ and 300 mmHg - Ideal Adsorption Solution Theory

IV.C.3 Analog of the Redlich-Kwong Equation of State

The prediction of a mixed adsorption isotherm is essentially a two-step operation. The pure component isotherms constituting the binary mixture are needed to calculate the characteristic parameters a and β of the analog of the Redlich-Kwong equation (Equation II.60). They are readily obtained when the method described in IV.B.3 is employed. The second operation consists in obtaining, at a given spreading pressure, a set of equilibrium properties, P and n , from the pure constituents making up the binary system. These supporting data together with a set of mixing rules form the basis for the prediction of mixed gas adsorption isotherms.

In the following sections, the words predicted and calculated are used interchangeably. They refer to mixed phase equilibria calculated using the analog of the Redlich-Kwong equation. Similarly, the words measured or calculated refer to phase equilibria in mixtures calculated using the exact thermodynamic relationship which employs data measured with the Cahn Electrobalance Assembly.

IV.C.3.a Adsorbed Phase Equilibria Prediction

The general approach employed in the computation of the prediction of phase equilibria and, the comparison between the calculated and measured quantities are presented in this

section. The calculations are for a binary system and the quantity X represents the molar composition of the heavier component adsorbed. The computer program is presented in Appendix VII.

The calculation of the adsorbed phase molar area, σ , and its composition, X , were executed using Equation II.81. It has the form $F(\sigma, X) = 0$. The application of the method of False Position (57) has proven itself excellent for phase equilibrium calculations (58). In this investigation it has been used to solve for the roots σ and X for a particular equilibrium condition. In the calculation of σ and X , an iterative procedure was employed in which the gas phase pressure is increased until the difference between the calculated and measured spreading pressure term, $\frac{\pi A}{RT}$, was within the desired tolerance. When this condition was satisfied, the quantities P , σ and X were compared with the measured values at the same spreading pressure. The comparison between predicted and measured properties will be presented in Section IV.C.3.d.

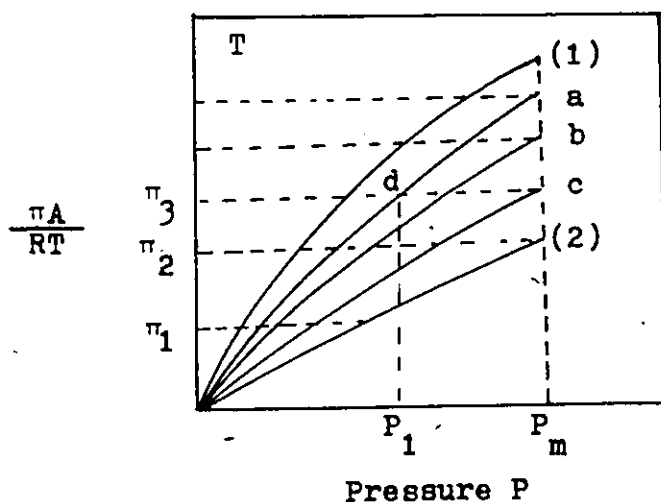
As with all equations of state employed in the prediction of mixed properties (26), the set of mixing rules are sensitive to the model used for representing the quantity a_{ij} . The quantity a_{ij} , defined by Zudkevitch (30), is related to pure component properties, a_i and a_j , with the following relation

$$a_{ij} = \sqrt{a_i a_j} (1 - C_{ij}) \quad \text{II.77}$$

in which C_{ij} is an interaction constant. Many values of C_{ij} are

possible; the simplest value would be to consider $C_{ij} = 0$. However, as will be observed in later sections, this value does not necessarily produce a satisfactory prediction of the equilibrium properties. On the other hand, an optimized value of C_{ij} , $C_{ij,opt}$, may be calculated directly from an experimental isotherm. The optimization of C_{ij} is arrived at by considering the minimum deviation between the measured and the calculated quantities P , σ and X , considered all together, at a given temperature for any spreading pressure and gas phase molar composition.

The prediction of the adsorbed phase properties at different spreading pressures covering the entire range of the adsorption isotherm for a particular binary system is illustrated schematically in the following diagram:



- i: a, b, c = mixture isotherms of constant molar composition in the gas phase.
- ii: d = one equilibrium point, P, σ, X, Y, π, T .
- iii: (1), (2) = pure component isotherms.

The selection of the optimum values of C_{ij} — $C_{ij,opt}$ — was based on the following criteria. If n is the number of properties considered at one equilibrium point ($n = 3$), which

is depicted in the above diagram, then the average absolute per cent deviation between calculated and measured properties, ΔD , is given by the following relation,

$$\Delta D = \frac{1}{n} \sum_{i=1}^n \Delta Q_i$$

The quantity ΔQ_i is defined by the following relation,

$$\Delta Q_i = \frac{Q_{i,\text{calculated}} - Q_{i,\text{measured}}}{Q_{i,\text{measured}}} \times 100$$

In the last equation, Q_i refers to either P , σ or X for a particular system temperature, spreading pressure and gas phase composition. The determination of $C_{ij,\text{opt}}$ was based on the prediction of the adsorbed properties of 9 equilibrium points for each isotherm. The value of $C_{ij,\text{opt}}$ giving minimum deviation in the prediction of phase equilibria was associated to a minimum value in the quantity $\Delta D_{\text{opt}} = \frac{1}{n'} \sum_{i=1}^{n'} (\Delta D)_i$ in which n' is the number of equilibrium points calculated for a given isotherm ($n' = 9$).

Another quantity that was found useful is $C_{ij,\text{avg}}$ which is calculated by averaging the values of $C_{ij,\text{opt}}$ over the temperature range investigated for a given binary system. The values $C_{ij,\text{avg}}$ correspond to a minimum value of the quantity $\Delta D_{\text{avg}} = \frac{1}{n''} \sum_{i=1}^{n''} (\Delta D_{\text{opt}})_i$ in which n'' refers to the number of isotherms studied for each system. The values of $C_{ij,\text{opt}}$ and $C_{ij,\text{avg}}$ will be seen in a later section.

For all systems investigated at all temperatures, a total of 90 equilibrium points were calculated. In fact, each point involves the prediction of 3 quantities, P , σ and X , totalling 270 predicted properties. The quantity $\overline{\Delta Q}_i$ is defined as the average absolute per cent deviation between calculated and measured Q_i based on 90 equilibrium points. The overall deviation is then defined by $\Delta = \frac{1}{3} \sum_{i=1}^3 \overline{\Delta Q}_i$.

IV.C.3.b Measured Pure Component Properties

The supporting equilibrium data needed for the prediction of the adsorbed phase properties, P , σ and X , of a binary mixed adsorbate are: the pure component adsorbate pressures P_1 and P_2 , the amount of pure component n_1 and n_2 adsorbed, and the characteristic parameters for each constituent a_1 , a_2 , β_1 and β_2 . The pure component properties are obtained at a given system temperature and spreading pressure. These quantities are interpolated graphically and the method employed is illustrated schematically in Figure IV.37. The four supporting properties, $\frac{\pi A}{RT}$, n_i , a_i and β_i as a function of P_i are combined on a single plot in Figure IV.38 for C_2H_4 at $273.2^\circ K$. The values of n_i , P_i and a_i , β_i are listed respectively in Tables IV.2 and IV.5. In fact, the interpolation was done on large graph paper. Values of the quantities n , P , a , β for the binary system $C_2H_4 - C_2H_6$ at $298.2^\circ K$ at $\frac{\pi A}{RT} = 0.771$ are listed as follows:

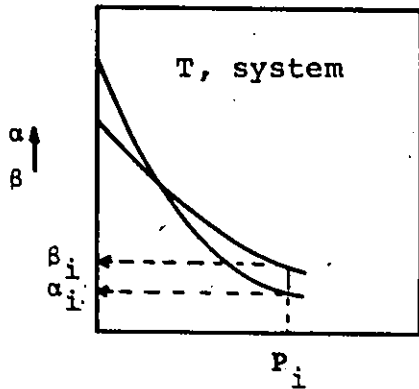


figure b

1. a $\pi A/RT$ is selected
2. P_1 and P_2 are obtained from figure a.

3. at P_1 and P_2 , α_1, β_1 and α_2, β_2 are obtained from figure b.

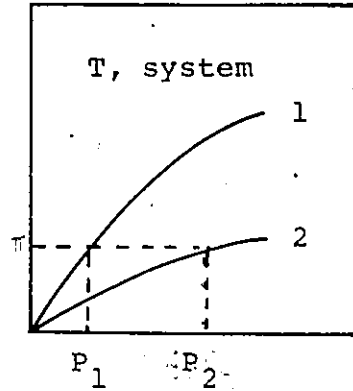


figure a

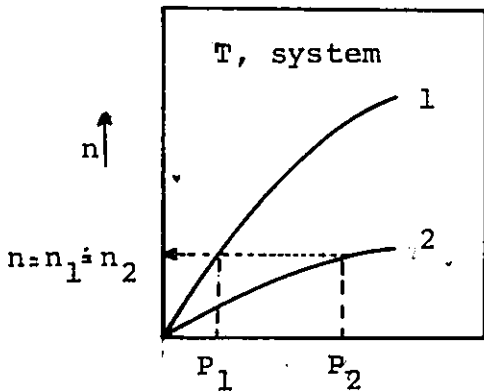


figure c

4. at P_1 and P_2 , n_1 and n_2 are obtained from figure c.

Figure IV.37: SUPPORTING DATA FOR THE PREDICTION OF MIXED EQUILIBRIA USING THE ANALOG OF THE REDLICH-KWONG EQUATION OF STATE.

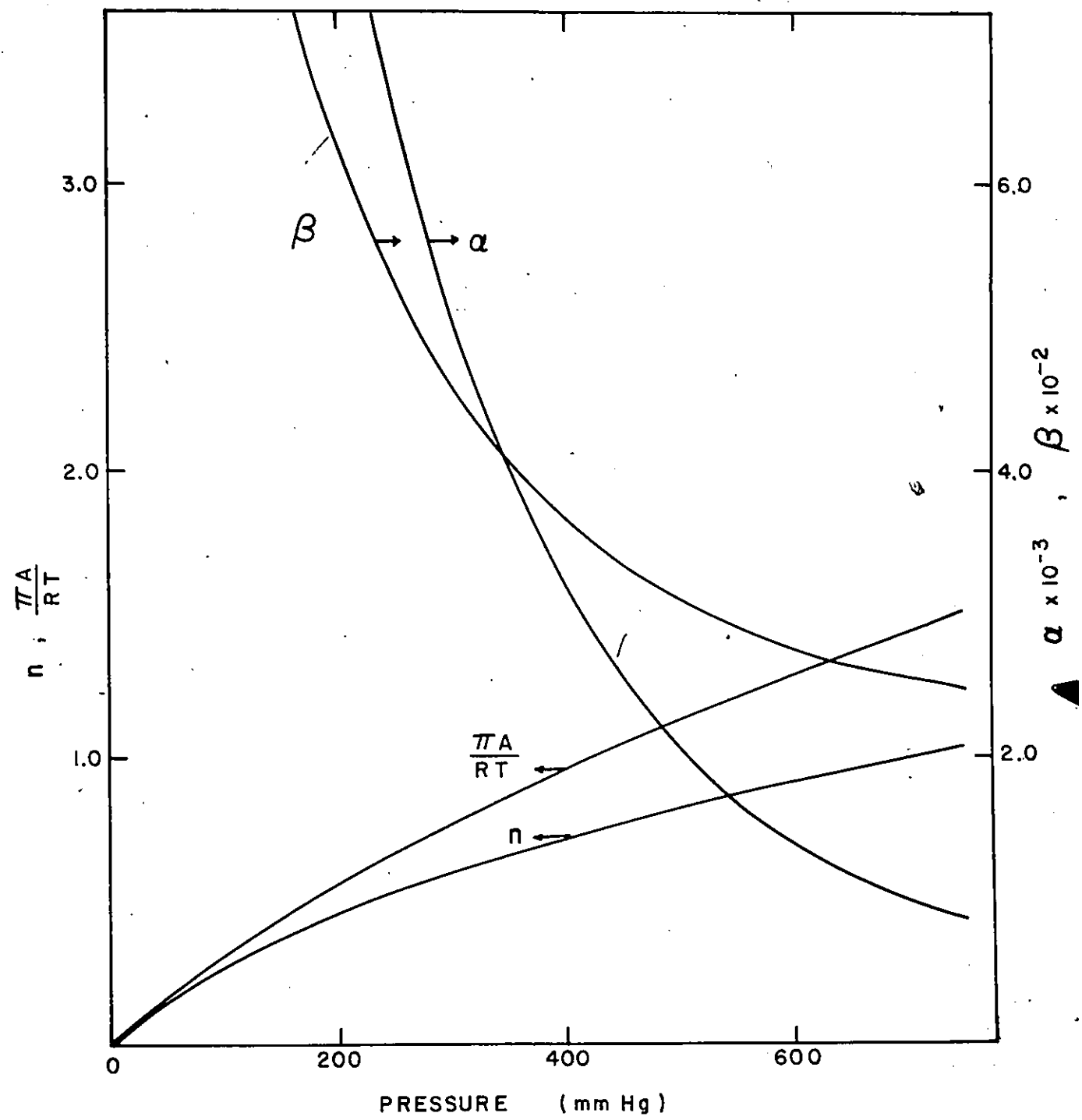


Figure IV.38 Pure Component Supporting Data for C_2H_4 at $298.2^\circ K$ for Phase Equilibrium Predictions

Values of Supporting Data Used in Calculating
Mixture Phase Equilibria

298.2°K	$\frac{\pi A}{RT}$	n	P	σ	β
C ₂ H ₄	.771	.589	300	5090	460
C ₂ H ₆	.771	.604	750	2514	362

(See Figures IV.37 and IV.38)

IV.C.3.c Measured Mixture Properties

The predicted mixed adsorbate equilibria, P , σ and X for a given system temperature, spreading pressure and gas phase composition were compared with properties calculated using the exact thermodynamic relationship. The interpolations at constant $\frac{\pi A}{RT}$ for the pure component pressure and moles adsorbed were performed using Tables IV.2 while the interpolations for the mixtures P_i , n_i , X , were done using Tables IV.6. Listed below are the supporting data for comparison purposes for the system C₂H₄ - C₂H₆ at 298.2°K and $\frac{\pi A}{RT} = 0.771$ for different gas phase compositions. These data were required for each system temperature and different spreading pressures considered earlier.

 Measured Phase Equilibria

$$\frac{\pi A}{RT} = 0.771, \quad T = 298.2^\circ\text{K}$$

		$\text{C}_2\text{H}_4(1) - \text{C}_2\text{H}_6(2)$			
Y_1	0	0.2635	0.5042	0.7547	1.0
n	0.6041	0.6140	0.5947	0.5989	0.5896
P	750	526.5	414.4	363.3	306.4
X_1	0	0.4679	0.6888	0.8738	1.0
		$\bar{n} = 0.6003 \pm 0.0070 \quad (1.1\%)$			

(Data interpolated from Tables IV.2 and IV.6 of Appendix I).

The last two tables serve as illustration. For each system and temperature, three representative spreading pressures were selected, totalling 30 n-P-X sets of tables as shown above.

IV.C.3.d Comparison Between Measured and Calculated Phase Equilibria

For a given system temperature and spreading pressure, the supporting data together with the corresponding measured phase equilibrium data, such as those listed in the last two tables, were compiled and fed into the computer. The computer program is listed in Appendix VII. In this program, arrangements are provided for the insertion of the interaction constant

C_{ij} . Provisions are made so that, C_{ij} may either be considered a constant or may take up any value. In the latter case, C_{ij} is determined by the comparison between measured and calculated phase equilibrium data for each incremental value of C_{ij} . In this way, an averaged value of C_{ij} is readily obtained for each system.

Comparisons were made between the calculated and the measured system pressure, P , the mixed molar area, σ and the adsorbate molar composition, X , at all T and $\frac{\pi A}{RT}$. The average absolute per cent deviation, $\overline{\Delta P}$, $\overline{\Delta \sigma}$, $\overline{\Delta X}$ are compiled in Table IV.10, irrespective of the binary system, temperature, spreading pressure and gas phase molar composition considered.

The results listed in Table IV.10 tell us the prediction for P , σ and X , in all systems at all T and $\frac{\pi A}{RT}$ considered, is better when an averaged value of C_{ij} is used for each system. The overall deviation in the prediction of phase equilibrium properties is 4.8% when $C_{ij} = 0$ compared to 4.2% when the values of C_{ij} are averaged. The averaged value of C_{ij} has been defined for a particular system regardless of the temperature, spreading pressure and gas phase composition. For each binary system, these values are listed in Table IV.11 under $C_{ij,avg}$. Also listed, are the values of $C_{ij,opt}$ calculated for each system temperature. The temperature characteristic is plotted in Figure IV.39 for each system. Erratic trends of C_{ij} were observed with the spreading pressure and gas phase composition; therefore, the values of C_{ij} listed in Table IV.11 are

TABLE IV.10

PHASE EQUILIBRIUM PREDICTION FOR ALL SYSTEMS, TEMPERATURES
AND SPREADING PRESSURES

C_{ij}	Average Absolute Per cent Deviation			$\overline{\Delta X}$	$\Delta = \text{Overall}$	Predictions
	$\overline{\Delta P}$	$\overline{\Delta \sigma}$				
0	6.6	2.6	5.3		4.8	270
$C_{ij, \text{avg}}$	4.3	3.8	4.5		4.2	270
$k_{ij, \text{VLE}}$	6.5	2.6	5.3		4.8	270

$C_{ij, \text{avg}}$: The values of the quantity C_{ij} were determined from measured phase equilibria obtained with the gravimetric method. It is a value independent of the temperature, spreading pressure and gas phase composition.

$k_{ij, \text{VLE}}$: The values of the quantity k_{ij} were taken from vapor-liquid equilibria.

TABLE IV.11
TEMPERATURE DEPENDENT VALUES OF C_{ij} — $C_{ij,opt}$

<u>System</u>	<u>$C_{ij,opt}$</u>			<u>$C_{ij,avg}$</u>
	<u>263.2°K</u>	<u>273.2°K</u>	<u>298.2°K</u>	
$C_3H_8-CO_2$	-1.13	-0.87	-0.80	-0.93
$C_2H_4-C_2H_6$	-0.47	+0.2	-0.33	-0.10
$C_2H_6-CO_2$	-0.47	-0.07	-0.27	-0.27

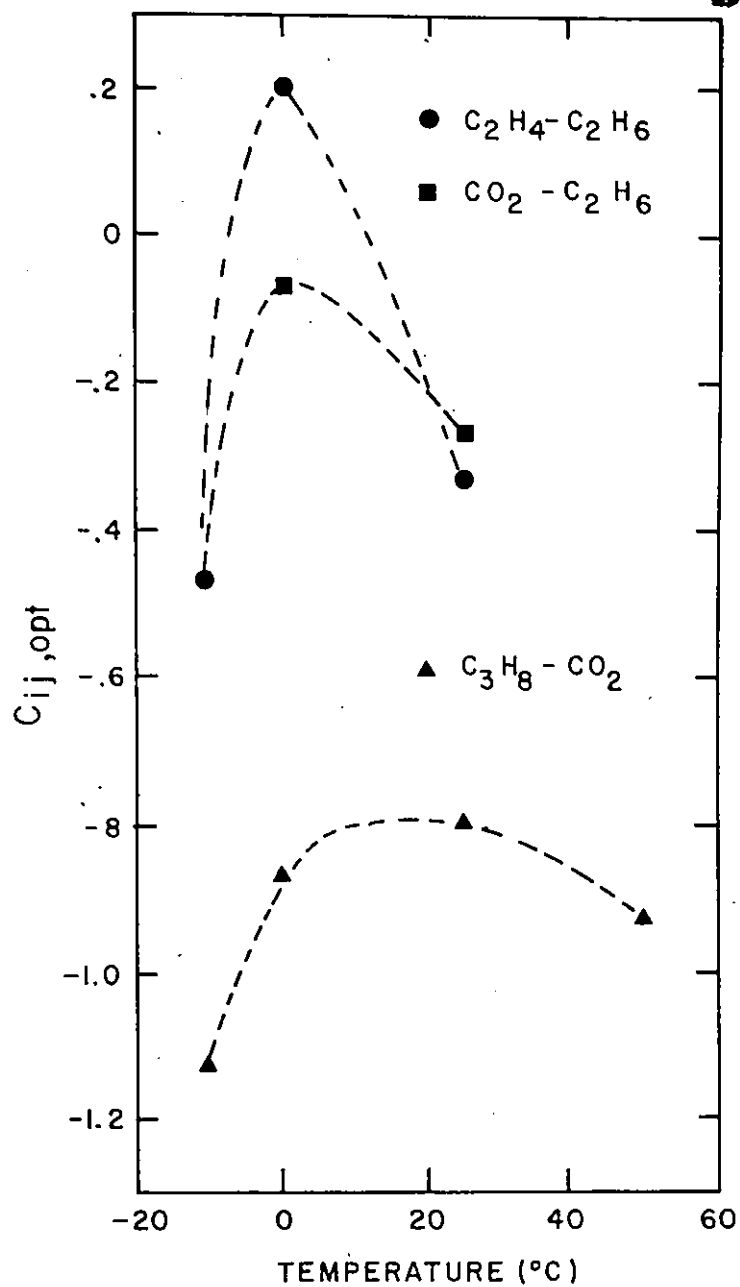


Figure IV.39 Temperature Dependence of C_{ij} for Different Binary Mixtures

TABLE IV.12
 SPREADING PRESSURE AND TEMPERATURE DEPENDENCE OF C_{ij} FOR THE SYSTEM
 $C_3H_8 - CO_2$

Temperature (°K)	C_{ij}			$C_{ij,opt}$
	π_1	π_2	π_3	
263.2	-0.6	-1.4	-1.4	-1.13
273.2	-0.6	-1.2	-0.08	-0.87
298.2	-0.6	-0.6	-1.2	-0.80
323.2	-1.0	-0.8	-1.0	-0.93
$-0.93 = C_{ij, avg}$ (Table IV.11)				



TABLE IV.13
 PER CENT DEVIATION FOR ALL T AND π
 FOR EACH SYSTEM P, σ and X

System	$C_{ij,avg}$	ΔP	$\Delta \sigma$	ΔX	ΔD_{avg}
$CO_2-C_3H_8$	-0.93	5.5	5.2	5.2	5.3
$C_2H_6-CO_2$	-0.27	3.7	2.5	4.8	3.7
$C_2H_6-C_2H_4$	-0.10	3.7	3.6	3.0	3.5
					$\Delta = 4.2$ (Table IV.10)

considered independent of the spreading pressure and of the gas phase composition. Typical values of C_{ij} at different temperatures and spreading pressures for the system $C_3H_8 - CO_2$ are listed in Table IV.12. An examination of this table depicts the uselessness of considering a spreading pressure dependent C_{ij} . The contributions of each system to ΔP , $\Delta\sigma$ and ΔX when $C_{ij,avg}$ is used are compiled in Table IV.13.

Precision in phase equilibrium predictions of mixtures relies on the choice of mixing rules mentioned earlier, in which the most important parameter is the quantity a_{ij} defined in Equation II.75. Evaluation of this quantity may be arrived at by making use of an equation which takes into account parameters in the adsorbed phase a_i and β_i , and the critical properties of the gas phase. This relation was derived earlier as

$$a_{ij} = k(1 - k_{ij})^{1.5} \quad \text{II.78}$$

The mixing rules employed in the above equation were those already employed in vapor-liquid equilibrium calculations. The mixing rules described by Equations I.36 to I.42 are contained in the term k defined earlier by Equation II.78a. The values of the interaction constant k_{ij} , for the binary system investigated in this work, are listed in the following table:

System	$k_{ij,VLE} = k_{ij}$	Source
$C_2H_4 - C_2H_6$	0.0	Chueh and Prausnitz (59)
$CO_2 - C_2H_6$	0.102	Hamam and Lu (60)
$C_3H_8 - CO_2$	0.088	Hsi and Lu (61)

The results of the prediction are summarily reported in Table IV.10 while details of the calculation results are presented in Table IV.14.

The values of the critical constants P_c , V_c and T_c of Equation II.78a for the pure gas employed in this work were taken from Din (62, 63, 64).

The experimental values of C_{ij} listed in Table IV.11 are negative while the values of k_{ij} reported in the literature are positive. The role of a negative value of k_{ij} on the predictions of phase equilibria was studied. Combining Equations II.77 with II.78 yields the following expression

$$k(1 - k_{ij,ads})^{1.5} = \sqrt{a_i a_j} (1 - C_{ij}^*)$$

in which C_{ij}^* is a quantity obtained when negative values of k_{ij} , $k_{ij,ads}$, are used. The average values of C_{ij}^* calculated with the above equation are listed and compared with $C_{ij,avg}$ in the

TABLE IV.14
 COMPARISON BETWEEN CALCULATED AND MEASURED PHASE EQUILIBRIA WHEN VAPOR-LIQUID
 INTERACTION CONSTANT IS EXTENDED TO GAS-SOLID EQUILIBRIA

Temp. °K	π	Average Absolute Per cent Deviation*, ΔD								
		C ₂ H ₆ - CO ₂		C ₂ H ₄ - C ₂ H ₆		C ₃ H ₈ - CO ₂				
		ΔP	Δσ	ΔX	ΔP	Δσ	ΔX	ΔP	Δσ	ΔX
263.2	π ₁	5.08	0.88	5.84	6.07	6.73	5.70	16.26	1.12	10.21
	π ₂	5.61	1.67	5.45	3.27	1.42	3.85	11.94	1.54	8.57
	π ₃	6.91	4.06	6.14	4.75	3.48	4.09	10.94	0.30	7.61
273.2	π ₁	4.64	4.96	4.48	1.59	7.22	4.50	17.06	1.03	8.62
	π ₂	4.14	3.48	5.65	5.89	4.43	3.29	12.43	0.70	8.19
	π ₃	3.14	3.10	3.90	4.58	3.55	2.51	9.05	0.85	7.84
298.2	π ₁	6.63	2.26	8.58	2.73	2.56	2.13	7.49	2.41	7.84
	π ₂	5.32	2.41	3.98	2.51	1.33	1.91	12.08	2.30	7.26
	π ₃	4.07	3.06	3.32	3.35	2.70	2.32	7.64	1.95	6.78
323.2	π ₁	*The average absolute per cent deviation, ΔD, is based on the prediction of Q at three different gas phase compositions.								
	π ₂									
	π ₃									
Average **		5.06	2.88	5.26	3.86	3.72	3.37	10.69	1.28	7.10

** Can be compared with values reported in Table IV.13

following table,

	$\text{CO}_2 - \text{C}_2\text{H}_6$	$\text{C}_2\text{H}_4 - \text{C}_2\text{H}_6$	$\text{C}_3\text{H}_8 - \text{CO}_2$
$k_{ij, \text{VLE}} = k_{ij}$	+0.102	0.0	+0.088
$k_{ij, \text{ads}}$	-0.102	0.0	-0.088
C_{ij}^*	-0.334	-0.145	-0.214
$C_{ij, \text{avg}}$	-0.270	-0.10	-0.93

The prediction results are improved slightly when negative interaction constants are considered, as apposed to positive ones. However, when $k_{ij, \text{ads}}$ are used, the overall deviation, Δ , approaches that of the prediction results which are obtained with $C_{ij, \text{avg}}$. Although C_{ij}^* value for the system $\text{C}_3\text{H}_8 - \text{CO}_2$ is lower than $C_{ij, \text{avg}}$, the calculation results are better than those obtained using $C_{ij} = 0$. Phase equilibrium predictions using $k_{ij, \text{ads}}$ are compared with those calculated with $k_{ij, \text{VLE}}$ and $C_{ij} = 0$ in the following table:

 Per cent Average Absolute Deviation

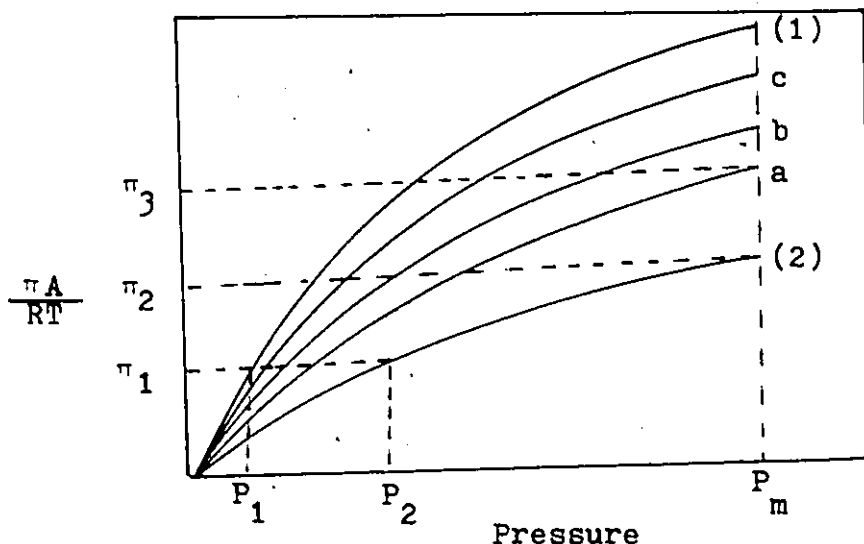
	<u>CO₂ - C₂H₆</u>			<u>C₂H₄ - C₂H₆</u>			<u>C₃H₈ - CO₂</u>		
	<u>ΔP</u>	<u>Δσ</u>	<u>ΔX</u>	<u>ΔP</u>	<u>Δσ</u>	<u>ΔX</u>	<u>ΔP</u>	<u>Δσ</u>	<u>X</u>
$k_{ij,VLE}$	5.06	2.88	5.26	3.86	3.72	3.37	10.69	1.28	7.10
$k_{ij,ads}$	4.13	2.49	5.02	3.86	3.72	3.37	7.86	1.77	6.05
$C_{ij} = 0$	5.20	2.60	5.10	4.64	3.58	3.52	10.09	1.53	7.19

The calculation of $C_{ij,avg}$ requires considerable experimental data on gas mixture adsorption, however, the use of an interaction constant, k_{ij} in determining a_{ij} , is promising since it relies only on physical critical properties of the gas phase (Equation II.78) and on parameters, a_i and β_i , easily obtained from pure component adsorption isotherms constituting a binary mixture.

The system C₂H₄ - C₂H₆ at 298.2°K has been used to illustrate graphically the results of the prediction of phase equilibria when the analog of the Redlich-Kwong equation of state is used. Remarks made apply equally well to all other systems. The parameter investigated was the quantity C_{ij} . Three different values were used: $C_{ij} = 0$, a temperature dependent C_{ij} , $C_{ij,opt}$ and an averaged value of C_{ij} independent of temperature,

$C_{ij,avg}$. The computed results are reported in Tables IV.15 and IV.16 when $C_{ij} = 0$ is used in the mixing rules.

Phase equilibrium prediction was tested at three different levels of the spreading pressure, namely: at π_1 , π_2 and π_3 . The π -P plot is illustrated in the following figure.



The results of the comparison between the calculated and the measured phase equilibria for different values of C_{ij} are reported in Table IV.17 and are plotted in Figure IV.40 when $\frac{\pi A}{RT} = 0.25$ corresponding to a value of π_1 . Similarly, the results are listed and plotted respectively in Table IV.18 and Figure IV.41 for $\frac{\pi A}{RT} = 0.771$ (level π_2). The overall deviation of the predicted quantities is lower where $k_{ij,VLE}$ is used when compared with the results where $C_{ij} = 0$.

TABLES IV.15 AND IV.16.

The system $C_2H_4 - C_2H_6$ has been used to illustrate the prediction of phase equilibria when the analog of the Redlich-Kwong equation of state is employed. The prediction and comparison results are listed in Table IV.15 while the calculated phase equilibria at regular intervals of gas phase compositions are reported in Table IV.16.

The computation was performed at the following conditions:

$$T = 298.2^{\circ}K$$

$$\pi = 0.632 \text{ millical/m}^2 \text{ or at}$$

$$\frac{\pi A}{RT} = 0.771 \text{ millimole/gm.}$$

The symbols employed are defined in the order as they appear in Tables IV.16 and IV.17 for the system $C_2H_4(1) - C_2H_6(2)$.

PI1	calculated π_1
PI2	calculated π_2
P1	interpolated P_1
P2	interpolated P_2
SIG1	interpolated $\sigma_1 = \frac{A}{n_1}$
SIG1	interpolated $\sigma_2 = \frac{A}{n_2}$
K1	graphical K_1 (limiting slope)
K2	graphical K_2

ALFA1	interpolated α_1
BETA1	interpolated β_1
ALFA2	interpolated α_2
BETA2	interpolated β_2
I	isotherm of constant gas composition Y_1
P	calculated Pressure.
Y1	experimental molar composition in gas phase, Y_1
X1	calculated molar composition adsorbed, X_1
SIGMA	calculated mixture molar area, σ
PIMIX	calculated mixture spreading pressure, π
CIJ	$C_{ij,avg}$
ALFA12	$\alpha_{12} = \sqrt{\alpha_1 \alpha_2} (1 - C_{ij})$
SIGAV	calculated average value of σ
PIAV	calculated average value of π

Considering the fact that the predictions were effected for 3 systems, 10 isotherms, 3 different values of spreading pressure, and 4 different values of C_{ij} , the results reported here represent 1/120 of the total number of tables such as listed in Tables IV.15 and IV.16. The results have been compressed into tabular form and are presented in Sections IV.C.3.d and IV.C.3.e.

TABLE IV.15
COMPARISON BETWEEN CALCULATED AND MEASURED
EQUILIBRIUM DATA

ETHANE - ETHYLENE - SILICA GEL AT 25.0 DEG. CENTIGRADE

TEMPERATURE=298.16

SPREADING PRESSURE=0.000632

CALCULATED SPREADING PRESSURE

PI1=0.000630

PI2=0.000632

PURE ADSORBATE PRESSURE

P1= 30.00

P2= 75.00

PURE MOLAR AREA

SIG1=1227.33

SIG2=1196.66

LIMITING SLOPE

K1= 0.03024

K2= 0.01271

ALFA1 5090.0000

BETA1 460.0000

ALFA2 2513.7998

BETA2 361.7000

I	P	Y1	X1	SIGMA	PIMIX
1	54.0	0.26	0.4710	1213.99	0.000629
2	42.9	0.50	0.7191	1221.01	0.000629
3	35.3	0.75	0.8863	1225.86	0.000628

CIJ= 0.0

ALFA12= 3577.0437

SIGAV=1220.29

PIAV= 0.000629

Y1	DP	DN	DX
0.2635	2.50	3.02	0.78
0.5042	3.40	0.45	4.22
0.7547	2.92	1.53	1.41
AVG. DEV.	2.94	1.67	2.14

CIJ= 0.0

ALFA12= 3577.0437

SIGAV=1220.29

PIAV= 0.000629

TABLE IV.16

- PREDICTION OF PHASE EQUILIBRIUM DATA

ETHANE - ETHYLENE - SILICA GEL AT 25.0 DEG. CENTIGRADE

TEMPERATURE=298.16

SPREADING PRESSURE=0.000632

CALCULATED SPREADING PRESSURE P11=0.000630 P12=0.000632

PURE ADSORBATE PRESSURE P1= 30.00 P2= 75.00

PURE MOLAR AREA SIG1=1227.33 SIG2=1196.66

LIMITING SLOPE K1= 0.03024 K2= 0.01271

ALFA1 5090.0000

BETA1 460.0000

ALFA2 2513.7998

BETA2 361.7000

I	P	Y1	X1	SIGMA	PIMIX
1	65.3	0.10	0.2153	1207.34	0.000628
2	61.4	0.15	0.3043	1209.55	0.000629
3	54.8	0.25	0.4538	1213.38	0.000629
4	49.4	0.35	0.5742	1217.13	0.000629
5	45.0	0.45	0.6728	1219.53	0.000629
6	41.3	0.55	0.7550	1221.70	0.000629
7	38.2	0.65	0.8244	1222.84	0.000629
8	35.5	0.75	0.8837	1224.35	0.000630
9	33.1	0.85	0.9349	1226.86	0.000629
10	32.1	0.90	0.9580	1227.16	0.000629

CIJ= 0.0

ALFA12= 3577.0437

SIGAV=1218.96

PIAV= 0.000629

TABLE IV.17

COMPARISON BETWEEN CALCULATED AND MEASURED PHASE EQUILIBRIA

$$C_2H_4(1) - C_2H_6 \text{ at } 298.2^\circ K \text{ and } \frac{PA}{RT} = 0.250 \quad (= \pi_1)$$

Case	C_{ij}	% Deviation			Overall
		ΔP	$\Delta \alpha$	ΔX	
1)	0.0	2.96	2.48	2.22	2.55
2)	-0.10	2.71	2.69	2.07	2.50
3)	-0.33	1.15	5.79	1.53	2.82
4)	$k_{ij, VLE}$	2.73	2.56	2.13	2.47

Values of α_i and β_i are evaluated at T and π_1 , (see Figure IV.42).

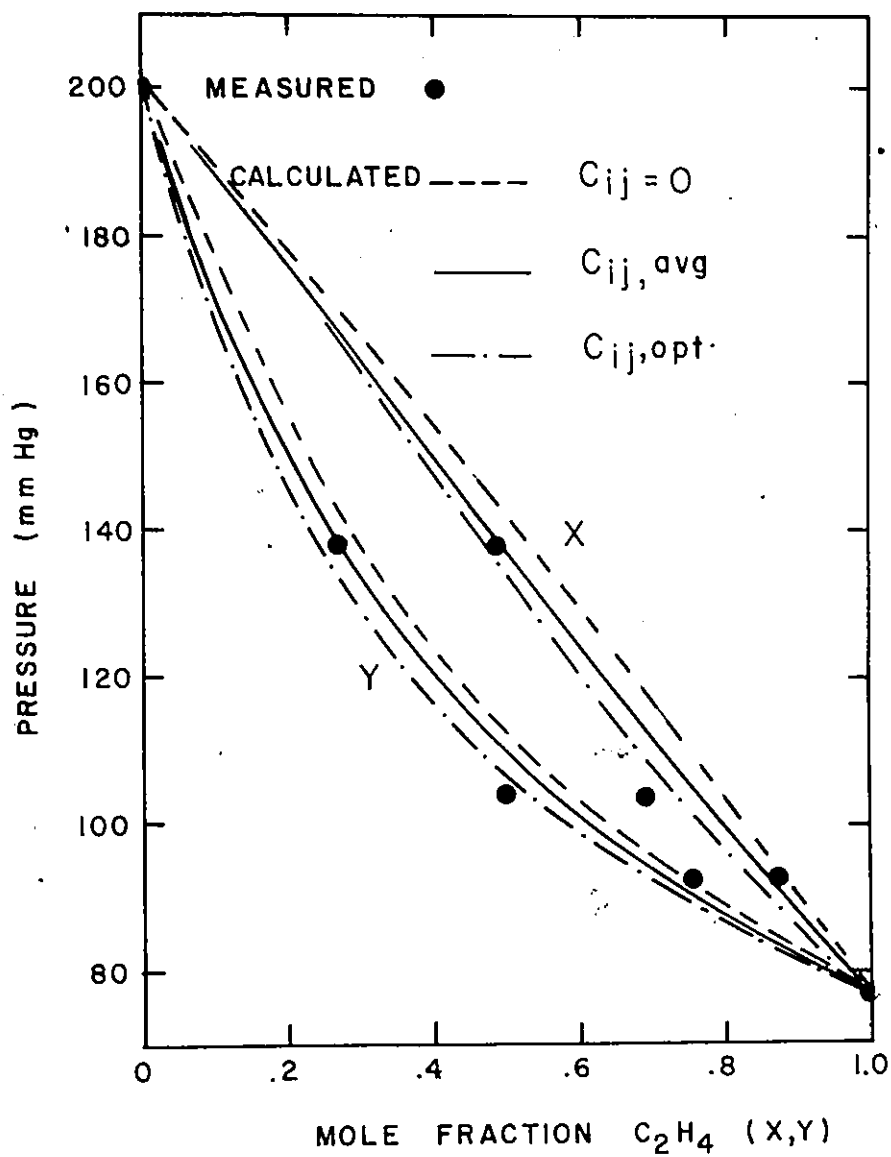


Figure IV.40 Comparison Between Calculated and Measured Phase Equilibria for C₂H₄ - C₂H₆ at 298.2°K and $\frac{\pi A}{RT} = 0.250$ - Our Proposed Method

TABLE IV.18

COMPARISON BETWEEN CALCULATED AND MEASURED PHASE EQUILIBRIUM DATA

$$C_2H_4(1) - C_2H_6 \text{ at } 298.2^\circ K \text{ and } \frac{\pi_A}{RT} = 0.771 \quad (= \pi_2)$$

Case	$C_{i,j}$	% Deviation			<u>Overall</u>
		$\frac{\Delta P}{P}$	$\frac{\Delta \sigma}{\sigma}$	$\frac{\Delta X}{X}$	
1)	0.0	2.64	1.37	1.95	1.99
2)	-0.10	2.31	1.25	1.84	1.80
3)	-0.33	2.16	1.01	1.16	1.44
4)	$k_{i,j, VLE}$	2.51	1.33	1.91	1.91

Values of α_i and β_i are evaluated at π and π_2 (see Figure IV.42)

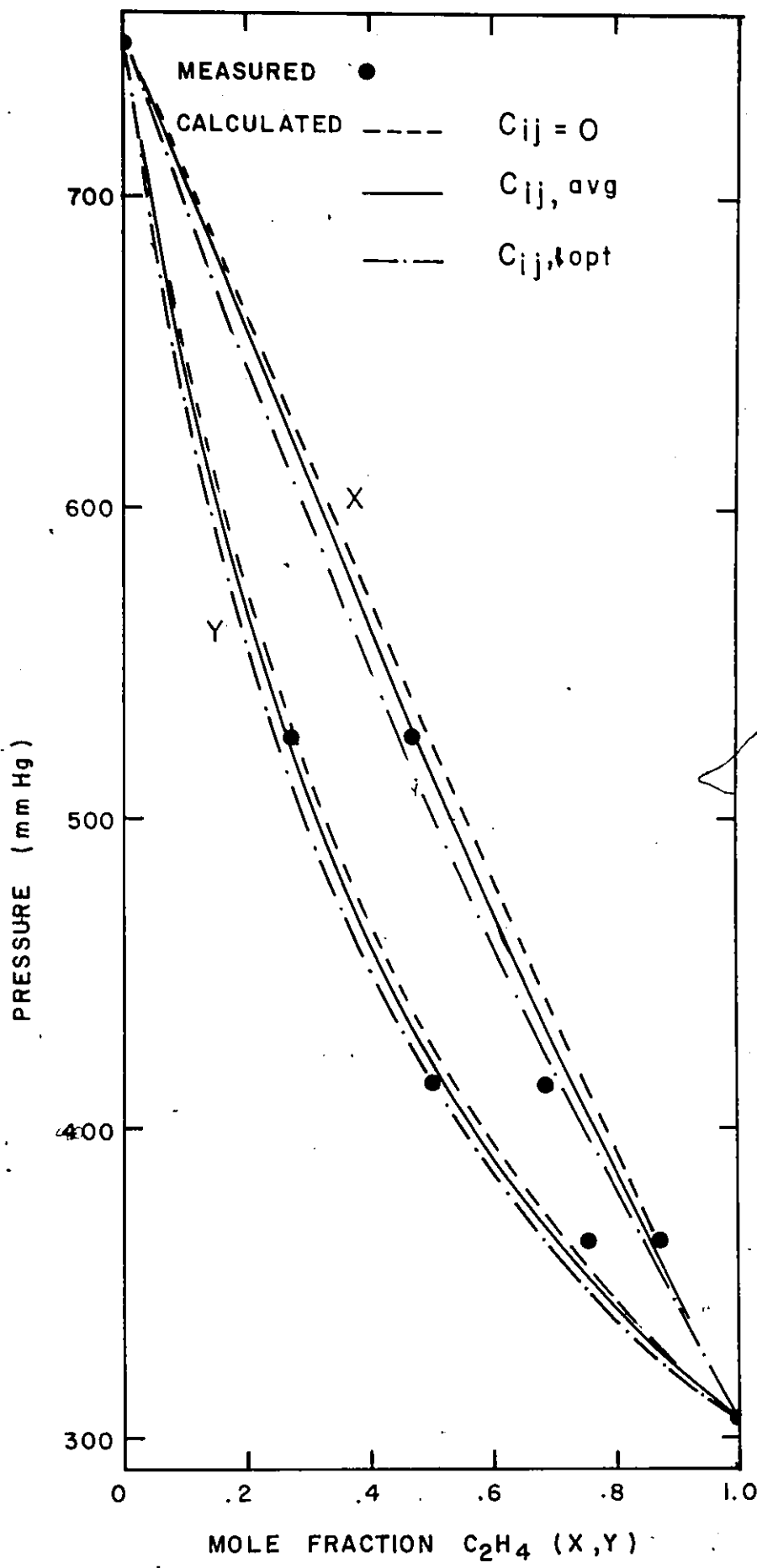


Figure IV.41 Comparison Between Calculated and Measured Phase Equilibria for $C_2H_4 - C_2H_6$ at $298.2^\circ K$ and $\frac{\Delta A}{RT} = 0.771$ - Our Proposed Method

IV.C.3.e Prediction of Gas Adsorption at Elevated Pressures

The π -P plot reveals that, for $\pi > \pi_2$, values of a_2 and β_2 are not obtained directly because the adsorption isotherms were measured up to a pressure of 750 mmHg. The values of $a_2(\pi_3)$ and $\beta_2(\pi_3)$ were estimated by two different methods as depicted in Figure IV.42. The first consisted in taking an extrapolated value of a_2 and β_2 at π_3 from a plot of $\ln a$ or $\ln \beta$ versus $\frac{RT}{\pi A}$. The second approach was to employ values of $a_2(\pi_2)_1$ and $\beta_2(\pi_2)_1$. For example, results for $C_3H_8 - CO_2$ at different temperatures are reported in the following table when $C_{ij,avg}$ were used:

Per cent Deviation Between Measured and Calculated Properties

Temperature (°K)	Values of a_i and β_i used in the Redlich-Kwong Equation are given by $a_i(\pi_j)_k$ defined in Figure IV.42					
	$a_2(\pi_3)_e, \beta_2(\pi_3)_e,$ $a_1(\pi_3), \beta_1(\pi_3).$			$a_2(\pi_2)_1, \beta_2(\pi_2)_1,$ $a_1(\pi_3), \beta_2(\pi_3).$		
	Δp	$\Delta \sigma$	ΔX	ΔP	$\Delta \sigma$	ΔX
263.2	1.57	2.93	5.35	0.94	2.66	3.28
273.2	1.98	4.99	9.12	1.24	1.91	5.33
298.2	2.34	2.86	5.32	3.42	3.01	5.34
323.2	2.15	4.57	2.43	2.05	3.71	1.92

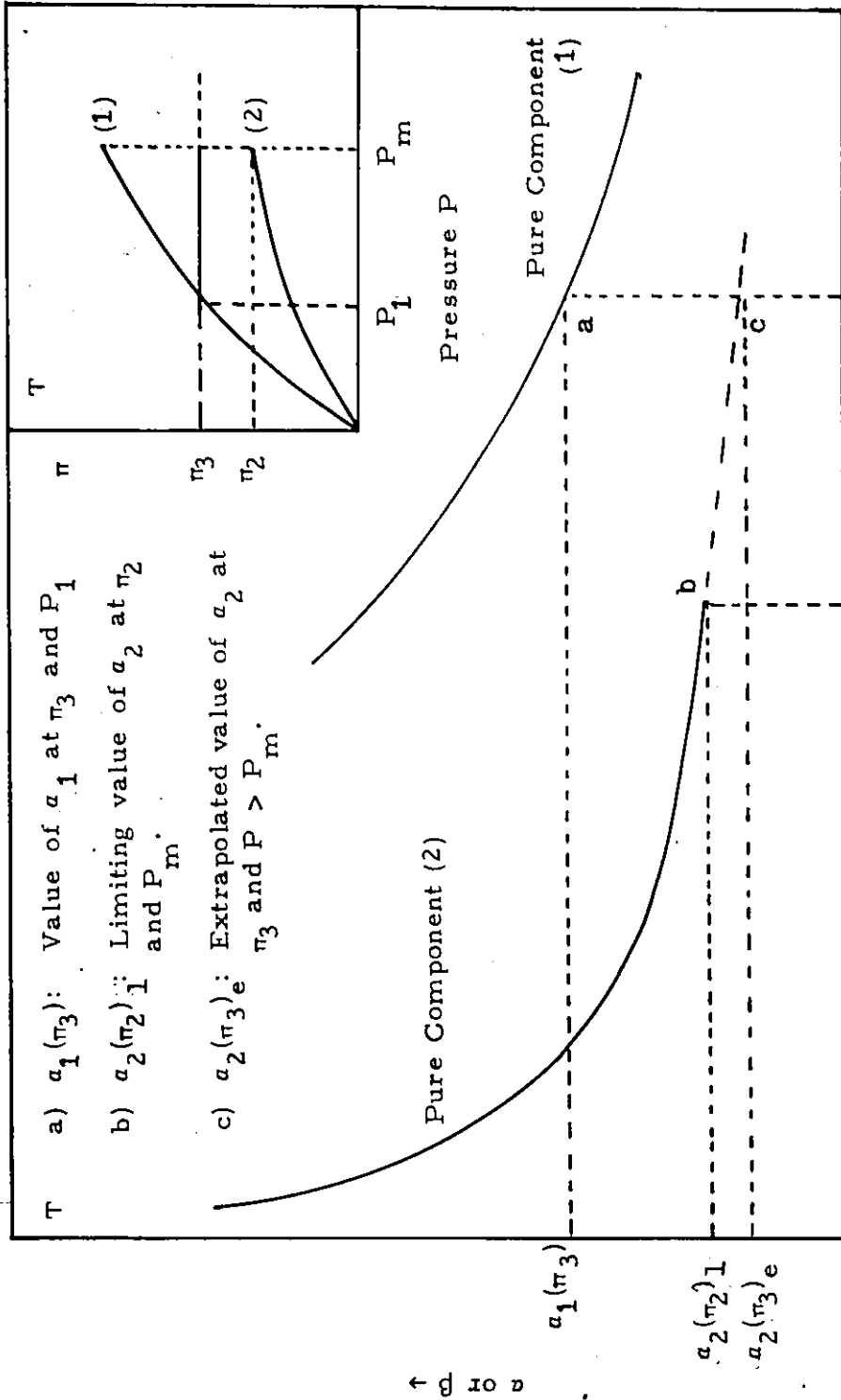


Figure IV.42 Proposed Methods for the Evaluation of α and β at Elevated Pressures

Similar observations were made for the other systems. It was concluded that the prediction of phase equilibria is made easier when the values of α_2 and β_2 were calculated at values of π_2 where the pressure is 750 mmHg for cases where $\pi > \pi_2$. Prediction results for $C_2H_4 - C_2H_6$ at $298.2^\circ K$ are reported in Table IV.19 and are plotted in Figure IV.43.

It has been stated earlier that α_i and β_i values approach a limiting value as the pressure or spreading pressure becomes higher. The second method just mentioned for the evaluation of $\alpha_2(\pi_2)_1$ and $\beta_2(\pi_2)_1$ has been extended to both components covering values of $\pi_1 \leq \pi \leq \pi_3$. That is, the prediction of phase equilibria at each temperature, was based on the calculated values of α_i and β_i when the pressure is 750 mmHg. The results of the comparison are reported in the following table for $C_2H_4 - C_2H_6$ at $298.2^\circ K$ for the case where $C_{ij} = 0$.

Value of π	ΔP	$\Delta \sigma$	ΔX	Overall
π_1	14.96	6.97	2.90	8.26
π_2	3.53	3.10	1.81	1.81
π_3	3.51	1.49	1.97	2.32

An examination of the values presented in the above table reveals

TABLE IV.19

COMPARISON BETWEEN CALCULATED AND MEASURED PHASE EQUILIBRIA
 FOR THE SYSTEM $C_2H_4(1) - C_2H_6$, at $298.2^\circ K$ and $\frac{P_A}{RT} = 1.014 (= \pi_3)$

Case	$\frac{C_{1,j}}{k_{i,j,VLE}}$	% Deviation			Overall
		$\frac{\Delta P}{\Delta \sigma}$	$\frac{\Delta \sigma}{\Delta X}$	$\frac{\Delta X}{\Delta \sigma}$	
1)	0.0	3.21	2.62	2.26	2.70
2)	-0.1	2.65	2.31	2.01	2.32
3)	-0.33	2.06	1.53	1.42	1.67
4)	$k_{i,j,VLE}$	3.35	2.70	2.32	2.79

Values of α_1 and β_1 are evaluated at π_3 and those of α_2 and β_2 are evaluated at π_2 which is the limiting value of π at T.

(See Figure IV.42)

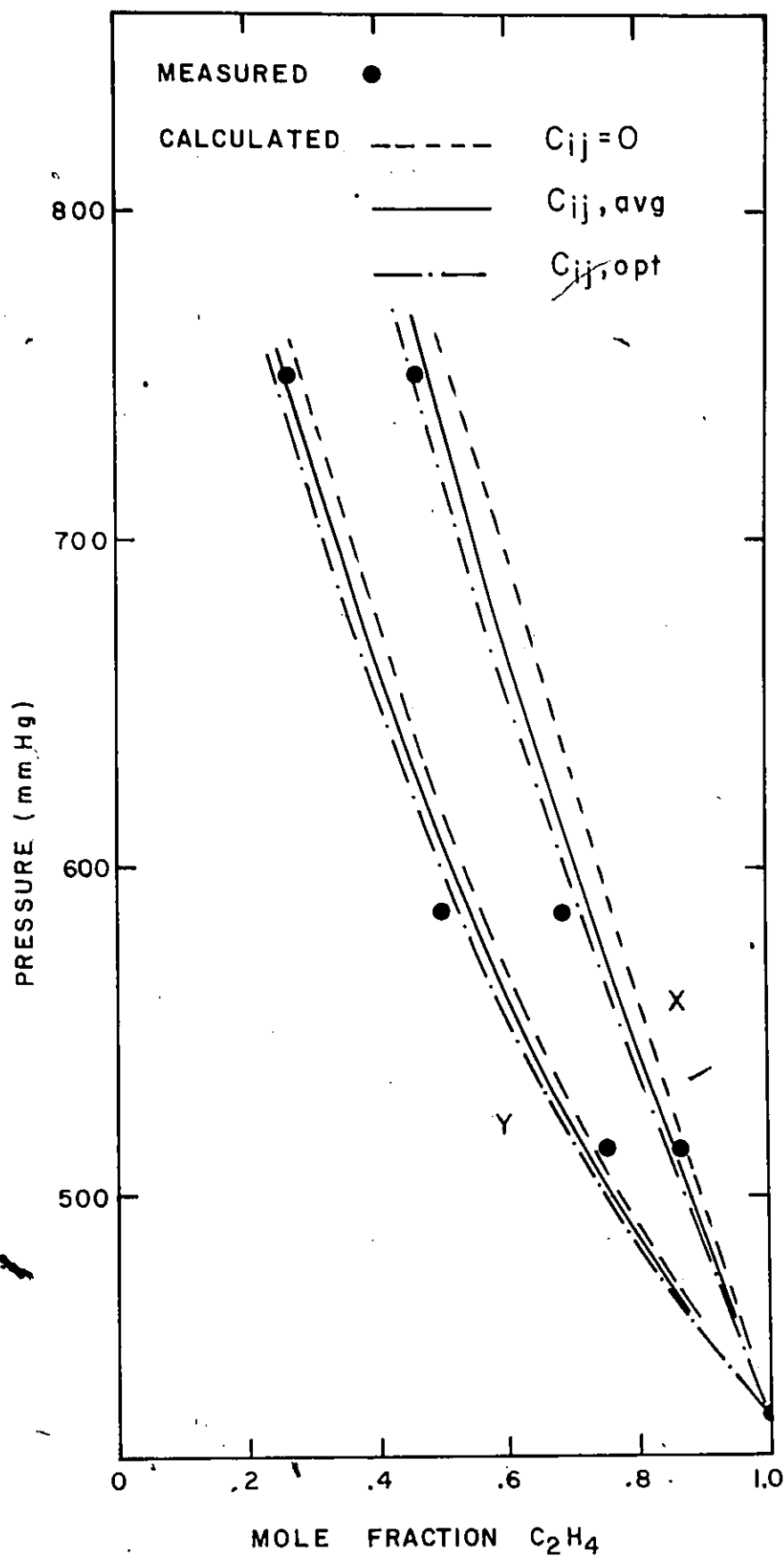


Figure IV.43 Comparison Between Calculated and Measured Phase Equilibria for $C_2H_4 - C_2H_6$ at $298.2^\circ K$ and $\frac{\pi A}{RT} = 1.101$ - Our Proposed Method

that the prediction becomes better the greater are the values of π .

It can be concluded that at higher pressures, the task of predicting phase equilibria in mixtures is facilitated since the only data required are the α_i and β_i of each component evaluated at one single spreading pressure, namely, where it becomes a constant at higher pressure for a given isotherm, as shown in Figures IV.13 and IV.14.

IV.C.3.f Practical Application

In the previous sections, phase equilibria predictions were carried out at constant temperature and spreading pressure. These conditions were met because the fugacity equations in Chapter II were derived at constant T and π . The P-X-Y phase diagrams of Figures IV.40, IV.41 and IV.43 are typical illustrations of constant temperature and spreading pressure conditions. These plots are not very attractive from a practical point of view because the spreading pressure is a variable that does not have industrial physical meaning with respect to process control. However, a phase diagram depicting the relation between measurable variables, such as gas pressure, temperature, moles adsorbed and compositions in the gas and adsorbed phase, is easily understood. Representative results at 298.2°K for the binary system $C_2H_4 - C_2H_6$ are given in Figures IV.44 and IV.45 respectively at gas pressures of 300 mmHg and 750 mmHg.

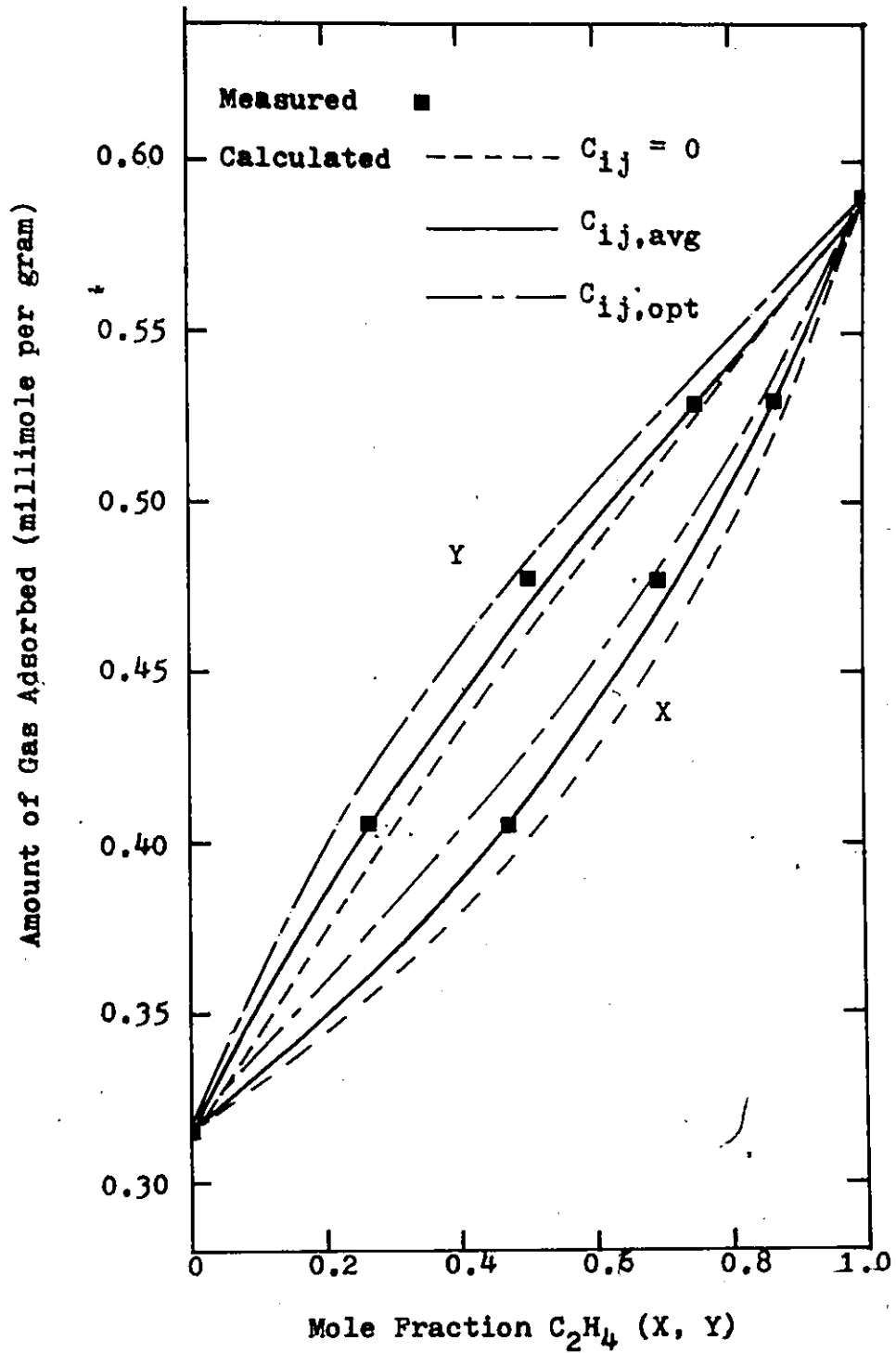


Figure IV.44 Comparison Between Calculated and Measured Phase Equilibria for $C_2H_4 - C_2H_6$ at $298.2^\circ K$ and 300 mmHg Our Proposed Method

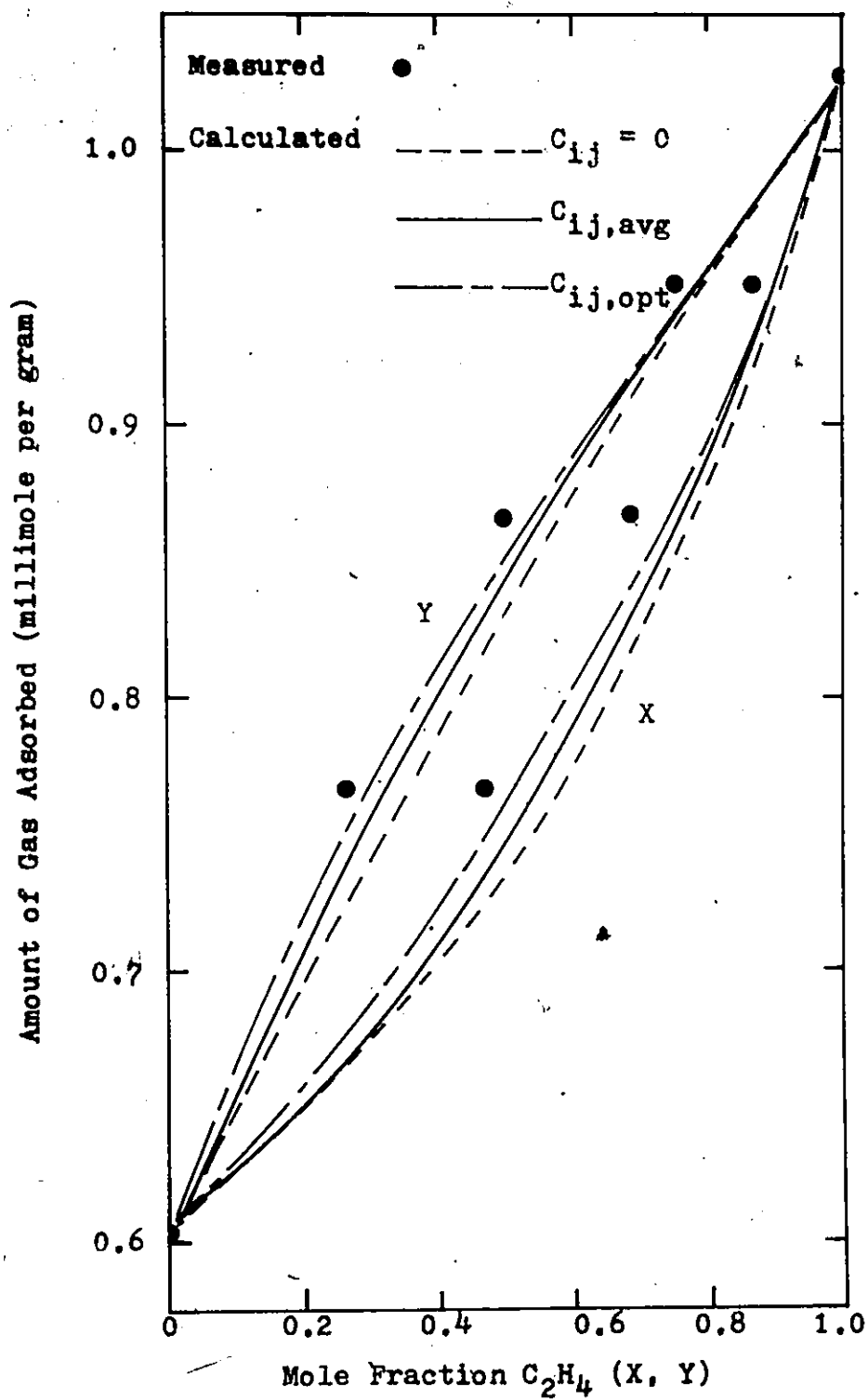


Figure IV.45 Comparison Between Calculated and Measured Phase Equilibria for $C_2H_4 - C_2H_6$ at $298.2^\circ K$ and 750 mmHg Our Proposed Method

TABLE IV.20
 COMPARISON BETWEEN CALCULATED AND MEASURED PHASE EQUILIBRIA
 AT 298.2°K FOR THE BINARY SYSTEM $C_2H_4 - C_2H_6$

Case	C_{ij}	Average Absolute Per cent Deviation							
		300 mmHg			750 mmHg				
		ΔP	$\Delta\sigma$	ΔX	Overall	ΔP	$\Delta\sigma$	ΔX	Overall
1)	0	3.00	0.96	1.92	1.96	2.58	2.86	2.42	2.62
2)	$C_{ij, avg}$	2.29	0.78	1.56	1.54	2.13	2.56	2.21	2.30
3)	$C_{ij, opt}$	2.47	1.61	0.97	1.68	1.47	1.91	1.73	1.70
4)	$K_{ij, VLE}$	2.29	0.81	1.58	1.56	2.74	3.78	2.72	3.08
5)	$C_{ij, opt}$	5.00	6.48	1.76	4.41	2.23	0.84	1.68	1.58
6)	$K_{ij, VLE}$	5.79	5.80	2.19	4.59	3.03	1.26	2.16	2.15

Results of the comparison between calculated and measured phase equilibria when different values of C_{ij} and $k_{ij,VLE}$ are used with the analog of Redlich-Kwong equation are reported in Table IV.20.

The average absolute per cent deviations in P , σ and τ have similar values at both pressures for Cases 1) to 4). In the case where the pressure is 300 mmHg, the values of α_i and β_i are evaluated at T and π considered. However, at $P = 750$ mmHg, the values of α_1 and β_1 are taken at T and π considered while those of α_2 and β_2 are taken at T and π_1 .

Binary mixture adsorption calculations, as in Cases 5) and 6), were obtained using values of α_i and β_i of each component taken at π_1 and T . This approach was used at $P = 300$ mmHg and $P = 750$ mmHg. Better results are obtained at the higher pressure, and they are comparable to those obtained as in Cases 1) to 4) at both pressures considered.

IV.C.3.g Results of the Prediction of Gas-Adsorption Equilibria

Gas-solid equilibria have been predicted using two general approaches and are summarized as follows. The first consisted in using the ideal adsorption solution theory (19), the second, consisted in using an equation of state, namely, the analog of the Redlich-Kwong equation (18). The predicted equilibrium quantities were compared with those calculated using the exact thermodynamic approach (3) which were identified as

measured quantities. The results are listed in Table IV.21 in terms of the average deviation in the adsorbed phase properties, namely; the molar composition, X and the molar area, σ .

Phase equilibria measured by the manometric method were compared with those calculated using the exact thermodynamic relationship.

To summarize this Section, phase equilibria in mixtures were predicted using an interaction constant C_{ij} (Equation II.77) determined from experimental mixture adsorption isotherms. In this way an optimized value of C_{ij} was calculated for each binary system temperature. No particular trend in C_{ij} was observed with gas phase composition and spreading pressure, although, a characteristic and uniform trend with temperature was observed. An average value of C_{ij} was calculated for a given binary system from the optimized values of C_{ij} . The prediction of the adsorbed phase properties is only slightly better when an optimum value of C_{ij} is employed.

A more elegant method for predicting phase equilibria was to extend to the adsorbed phase, mixing rules employed in vapor-liquid equilibrium calculations. The values of α_i and β_i calculated from the pure components constituting the binary mixture and the critical properties together with an interaction constant, k_{ij} , were employed to calculate the value of the quantity α_{ij} defined by Equation II.78. Prediction of phase equilibria using either $C_{ij} = 0$ or k_{ij} yield comparable results. However, negative values of k_{ij} improve the calculations of the

adsorbed phase properties.

Our proposed method for calculating the quantities α_i and β_i from isothermal data of a pure gas adsorbed was tested covering pressures from 300 to 750 mmHg. There are indications that phase equilibria in mixture adsorption could be simplified at elevated pressure by using a single set of values for α_i and β_i for each component constituting a binary mixture. This is due to the fact that α_i and β_i approach a limiting value at elevated spreading pressure or gas phase pressure. Therefore the task of predicting phase equilibria could be substantially reduced at higher pressures.

TABLE IV.21

RESULTS OF PREDICTION METHODS IN GAS-SOLID EQUILIBRIA

Overall Deviation	Manometric Method	Calculated		
		Ideal Adsorption Solution Theory	Analog of Redlich-Kwong Equation RK($C_{ij,avg}$)	Redlich-Kwong Equation RK($k_{ij,VLE}$)
$\overline{\Delta X}$	0.019	0.052	0.030	0.038
$\overline{\Delta \sigma}$	1%	19.1%	3.8%	2.8%

1) RK($C_{ij,avg}$) and RK($C_{ij}=0$) are respectively, phase equilibrium predictions using the analog of the Redlich-Kwong equation of state (Equation II.81) with mixing rules (Equations II.74, II.75, II.77) in which $C_{ij} = C_{ij,avg}$ and $C_{ij} = 0$.

2) RK($k_{ij,VLE}$) is same as 1.) except mixing rules are defined by Equations II.74, II.75 and II.78.

CHAPTER V

SUMMARY AND CONCLUSIONS

Scope:

Gas adsorption isotherms have been obtained in such a way as to satisfy an exact thermodynamic relationship which has been used to obtain an estimate of the properties of a mixed adsorbed phase. An equation of state satisfying the Gibb's adsorption isotherm was developed from pure gaseous component adsorption isotherms. Mixed gas adsorption isotherms were predicted using the equation of state together with appropriate mixing rules and were compared with the data calculated from the exact thermodynamic relationship.

Objectives:

The first objective of this investigation was to set-up an apparatus capable of measuring gravimetrically accurate and reproducible adsorption equilibrium isotherms of some pure components and their binary mixtures. These measured data were then employed in conjunction with an exact thermodynamic relationship for the calculation of the mixed adsorbate properties.

Measured adsorption phase equilibria for selected binary mixtures obtained from an independent experimental approach

have revealed that the calculation of the adsorbed phase properties lie within the experimental error.

The second objective set forth was the proposal of a new predictive method for gas adsorption phase equilibria. This proposed method is based on an extension of the Redlich-Kwong equation of state to represent the equilibrium between the gaseous and adsorbed phase. Mixing rules similar to those employed in vapor-liquid equilibrium calculations were adopted, and were tested with success with the analog of the Redlich-Kwong equation of state.

Conclusions:

It can be stated that the adsorption isotherms measured on silica gel with a Cahn electrobalance assembly are internally consistent, and where applicable, are comparable with existing literature. The adsorbate properties are calculated from a thermodynamic definition with no reference to any model. The values predicted from the analog of the Redlich-Kwong equation of state are in agreement with the values calculated with the thermodynamic relationship, thus demonstrating the equation to be quantitatively in agreement with the thermodynamics of the data.

The exact thermodynamic relation employed in the calculation of the adsorbed phase properties is the Gibb's adsorption isotherm given by Equation II.11.

$$-\frac{\sigma}{RT} d\pi + d\ln P + \sum(x_i d\ln y_i) = 0 \quad \text{II.11}$$

The calculations of π and x_i , hence σ , are possible when certain restrictions on II.11 are made. These restrictions are translated into the design of an apparatus capable of meeting those requirements. Therefore, when the temperature and gas phase composition are held constant, the expression resulting from Equation II.11 provides an equation yielding the spreading pressure:

$$\frac{\pi A}{RT} = \left[\int_0^P \frac{n}{P} dp \right]_{T, y_i} \quad \text{II.14}$$

A constant pressure operation at a given temperature yields an expression for the calculation of the molar composition, x_i , in particular for a binary system;

$$x_1 = y_1 + \left[\frac{y_1(1-y_1)}{n} \right] \left[\frac{\partial (\frac{\pi A}{RT})}{\partial y_1} \right]_{T, P} \quad \text{II.16}$$

Convergence of x_i within a few iterations is possible when an appropriate initial value of x_i is chosen.

The equation of state tested for the prediction of gas-solid equilibria was the analog of the Redlich-Kwong equation used in its original form,

$$Z = \frac{1}{1-h} - \frac{A^2}{B} \left(\frac{h}{1+h} \right) \quad \text{II.60}$$

in which

$$h = \frac{BRT}{\sigma} \quad \text{II.61}$$

and

$$A^2 = \frac{\alpha}{R^2 T^{2.5}} \quad \text{II.62}$$

$$B = \frac{\beta}{RT} \quad \text{II.63}$$

The characteristic parameters, α and β were evaluated using Equation II.73 which is a mathematical statement of the equilibrium existing between the gas phase and the adsorbed phase properties:

$$\ln(KP\sigma) + 1 - Z + \ln(1-h) + \left[\frac{(1-Z(1-h))(1+h)}{(1-h)h} \right] \ln(1+h) = 0 \quad \text{II.73}$$

in which

$$Z(P,T) = \left[\frac{1}{n(P)} \int_0^P \frac{n}{P} dP \right]_T \quad \text{II.65}$$

and

$$K = \frac{1}{A} \left(\frac{n}{P} \right)^* \quad \text{II.37}$$

Equation II.73 demonstrates the temperature and pressure dependence of α and β . Thus, for each equilibrium point

on an isotherm of a pure component, there exists an easily computed set of values for α and β .

Equation II.73, which has the form $F(h) = 0$, can be solved for h using the method of Newton.

The prediction of mixed adsorption equilibria can be done with the following equation:

$$-\ln \left[\frac{K_i y_i P}{x_i} \right] + \ln(\sigma - \beta) - \frac{\beta_i}{\sigma - \beta} + \frac{2 \sum_j (x_j a_{ij})}{RT^{1.5} \beta} \ln \left(\frac{\sigma + \beta}{\sigma} \right) - \frac{\alpha \beta_i}{RT^{1.5} \beta^2} \left[\ln \left(\frac{\sigma + \beta}{\sigma} \right) - \frac{\beta}{\sigma + \beta} \right] = 0$$

II.81

Equation II.81 is an equilibrium expression which relates the properties of the gas phase mixture to those of the adsorbed phase mixture. It has the mathematical form, $F(x_i, \sigma) = 0$, in which the mixture quantities x_i and σ are readily obtained when the method of False-Position is employed.

The mixing rules employed with Equation II.81 were

$$\beta = \sum x_i \beta_i \quad \text{II.74}$$

and

$$\alpha = \sum_i \sum_j x_i x_j a_{ij} \quad \text{II.75}$$

where

$$a_{ij} = \sqrt{a_i a_j} (1 - C_{ij}) \quad \text{II.77}$$

The quantity C_{ij} was obtained by comparing the predicted properties, P , σ and x_1 with those calculated from the exact thermodynamic relationship for each isotherm. The interaction constants C_{ij} were found to be independent of the temperature, spreading pressure and gas phase composition.

Equation II.78 was also employed to calculate a_{ij} ,

$$a_{ij} = k(1 - k_{ij})^{1.5} \quad \text{II.78}$$

In the above equation, gas phase critical properties, P_c , V_c , T_c and acentric factor ω are considered, together with adsorbed phase quantities, a_i and a_j , obtained from the pure component isotherms constituting a binary mixture. In Equation II.78, the values of k_{ij} , used in vapor-liquid equilibrium studies, were extended with success to the adsorbed phase. They are recommended in the absence of experimental mixture adsorption data necessary to calculate C_{ij} . The negative of the interaction constant yielded slightly better results however they are usually not considered in vapor-liquid equilibrium studies.

Significance:

A Cahn electrobalance assembly was set-up to meet the mathematical restrictions imposed on the Gibb's adsorption equation. In this way, the adsorbed phase properties are calculated with no reference to any model. The calculated values serve as

a basis for testing equations of state or theories. The tremendous amount of data collected in this investigation needed to calculate mixed adsorption equilibria have led specially to the testing of the analog of the Redlich-Kwong equation.

Recommendations:

For future work, it is recommended to extend the predictive method, based on the analog of the Redlich-Kwong equation of state, to the adsorption of gas mixtures on adsorbents other than silica gel. Investigations could be directed to the elaboration of possible relationship between the specific surface area and the quantity k_{ij} of II.77. Further work could cover a larger gas pressure and temperature range to ascertain that k_{ij} is really a constant.

The determination of adsorption isotherms at higher pressures could establish a lower limiting value of the characteristic parameters a and β . At higher coverage, a single value of a and β could be employed in the prediction of mixed gas adsorption isotherms. There are reasons to believe that carrying out this investigation to higher pressure would indicate a pressure independent value of a and β irrespective of the temperature.

BIBLIOGRAPHY

- 1) Carter, J.W., British Chemical Engineering, 9, 232 (1964).
- 2) Kidnay, A.J. and Hiza, M.J., Cryogenics, 10 (8), 271 (1970).
- 3) Van Ness, H.C., Ind. Eng. Chem. Fundamentals, 8, 464 (1969).
- 4) Young, D.M. and Crowell, A.D., "Physical Adsorption of Gases", Butterworths, London, England (1962).
- 5) Ross, S and Oliver, J.P., "On Physical Adsorption", John Wiley and Sons, Inc. New York, (1964).
- 6) Flood, E.A., "The Solid-Gas Interface", Volume 1, Marcel Bekker, Inc., New York, (1967).
- 7) Flood, E.A., "The Solid-Gas Interface", Volume 2, Marcel Bekker, Inc., New York, (1967).
- 8) de Boer, J.H., The Dynamical Character of Adsorption Oxford Press (1953).
- 9) Maslan, F. and Abert, E.R. J. Chem. and Engineering Data, 17, 286, (1972).

- 10) Lewis, W.K., Gilliland, E.R., Chertow, B. and Hoffman, W.H., J. Amer. Chem. Soc., 72, 1153 (1950).
- 11) Lewis, W.K., Gilliland, E.R., Chertow, B. and Milliken, W., J. Amer. Chem. Soc., 72, 1157 (1950).
- 12) Lewis, W.K., Gilliland, E.R., Chertow, B. and Bareis, D., J. Amer. Chem. Soc., 72, 1160 (1950).
- 13) Lewis, W.K., Gilliland, E.R., Chertow, B. and Cadogan, Ind. Eng. Chem., 42, 1326 (1950).
- 14) Lewis, W.K., Gilliland, E.R., Chertow, B. and Cadogan, Ind. Eng. Chem., 42, 1319 (1950).
- 15) Brunauer, "The Adsorption of Gases and Vapors", Princeton Univ. Press., Princeton, New Jersey, 1945.
- 16) Jelinek, R.V., Ph. D. Thesis, Columbia Univ. (1953).
- 17) Hsi, C., Ph. D. Thesis, Univ. of Ottawa, Canada (1965).
- 18) Redlich, O. and Kwong, J.N.S., Chem. Rev., 44, 233 (1949).
- 19) Myers, A.L., Ind. Eng. Chem., 60, 45 (1968).

- 20) Kidnay, A.J. and Myers, A.L. AICHE Journal, 12, 981 (1966).
- 21) Pitzer, K.S., Lippmann, D.A., Ceul, R.F., Huggins, C.M. and Petersen, D.E. J. Amer. Chem. Soc., 77, 3433 (1955).
- 22) Brunauer, S., Emmett, P.H. and Teller, E., J. Amer. Chem. Soc., 60, 309 (1938).
- 23) Joyner, L.G., Weinberger, E.B. and Montgomery, C.W., J. Amer. Chem. Soc., 67, 2182 (1945).
- 24) Danner, R.P. and Wenzel, L.A., AICHE Journal, 15, 515 (1969).
- 25) Volmer, M., Z. Physikal Chem. 115, 253 (1925).
- 26) Prausnitz, J.M., "Molecular Thermodynamics of Fluid-phase Equilibria", Prentice-Hall Inc., Englewood Cliffs, New Jersey (1969).
- 27) Chang, S.-D. and Lu, B.C.Y., Can. J. Chem. Eng., 48, 261 (1970).
- 28) Chueh, P.L. and Prausnitz, J.M., AICHE Journal, 13, 1099 (1967).

- 29) van Ness, H.C., "Classical Thermodynamics of Non-Electrolyte Solutions", MacMillan Company, New York, (1964).
- 30) Zudkevitch, D. and Joffe, J., I. Chem. E. SYMPOSIUM SERIES, No. 32, (1969) Instn. Chem. Engr., London.
- 31) Denbigh, K., "The Principles of Chemical Equilibrium", Cambridge, Univ. Press. (1964).
- 32) Yon, C.M. and Turnock, P.H., AIChE Adsorption Technology, Symposium Series, No. 117, 67 (19).
- 33) de Boer, J.H. and Kruyer, S. Trans. Faraday Soc., 54, 540 (1958).
- 34) Bartell, F.E. and Almy, E.G., J. Phys. Chem., 36, 475 (1932).
- 35) Malanchuk, M. and Stuart, E.B., Ind. Engng. Chem., 50, 1207 (1958).
- 36) Lu, B.C.-Y. and Lama, R.F., Trans. Farad Soc., 63, 727 (1967).
- 37) Lama, R.F., PhD Thesis, Univ. of Ottawa, Ottawa, Canada (1965).

- 38) Bastick, J., Bull Soc. Chem. France, 437 (1953).
- 39) Flood, E.A., "The Solid-Gas Interface", Volume 1, p. 77, Marcel Bekker, Inc., New York, (1967).
- 40) Flood, E.A. "The Solid-Gas Interface", p. 413, Marcel Bekker, Inc., New York, (1967).
- 41) McBain, J.W. and Bakr, A.M., J. Amer. Chem. Soc., 48, 690 (1926).
- 42) Rhodin, T.N., Jr., J. Amer. Chem. Soc., 72, 4343 (1950).
- 43) Williams, C.J., "A new lease on life for Gravimetric Adsorption", Amer. Laboratory, p. 40, Jan. (1969).
- 44) Cahn, L. and Schultz H.R., in "Vacuum Microbalance Technique", Vol. 2, Plenum Pres., Inc., New York, p. 7 (1962).
- 45) Cahn, L. and Schultz, H.R., in "Vacuum Microbalance Technique", Vol. 3, Plenum Pres., Inc., New York, p. 29 (1963).
- 46) "Cahn Electrobalance Operating Manual", (N.B.S. Circular 47)
- 47) Evans, B. and White, T.E., in: "Vacuum Microbalance Techniques", Volume 6, Plenum Sciences, Inc., New York, p. 157 (1967).

- 48) Tripp, W.C., West, R.W. and Graham, H.C., in "Vacuum Microbalance Techniques", Volume 6, Plenum Sciences, Inc. New York, p. 107, (1967).
- 49) Barrer R.M. and Robins, A.B., Trans. Faraday Soc., ~~42~~, 733 (1951).
- 50) Little, R.C., Carpenter, F.G. and Deitz, V.R., J. Chem. Phys., 37, 1896 (1962).
- 51) Moore, W.J. "Physical Chemistry", Prentice-Hall, Inc., Englewood Cliffs, New Jersey, 3rd ed., p. 310 (1960).
- 52) Mantell, C.L., "Adsorption", McGraw-Hill, New York, 2nd Ed., p. 605 (1951).
- 53) Hill, T.L., Emmett, P.H. and Joyner, L.G., J. Amer. Chem. Soc., 73, 5102 (1951).
- 54) Jura, G. and Harkins, W.D., J. Amer. Chem. Soc., 66, 1356 (1944).
- 55) Chang, S.-D., PhD Thesis, Univ. of Ottawa, Ottawa, Canada (1968).
- 56) I.B.M. Application Program System 360, Scientific Subroutine Package, Vernon III, I.B.M. Corporation.

- 57) Sokolnikoff, I.S., "Mathematics of Physics and Modern Engineering", 2nd edition, McGraw-Hill, p. 653 (1967).
- 58) Lu, B.C.-Y., Yu, P. and Sugie, A.H., Chemical Engineering Science, 29, 321 (1974).
- 59) Chueh, P.L., and Prausnitz, J.M., Ind. Eng. Chem. Fundamentals, 6, 492 (1967).
- 60) Hamam, S.E.M. and Lu, B.C.-Y., Can. J. Chem. Eng., 52, 283 (1974).
- 61) Hsi, C. and Lu, B.C.-Y., Can. J. Chem. Eng., 50, 144 (1972).
- 62) Din., F., "Thermodynamic Functions of Gases", Volume 1, first edition, London, Butterworths (1962), p. 121.
- 63) Din., F., "Thermodynamic Functions of Gases", Volume 2, first edition, London, Butterworths (1962), pp. 107, 130.
- 64) Din., F., "Thermodynamic Functions of Gases", Volume 3, first edition, London, Butterworths (1962), p.193.

APPENDICES

The tables of experimental measurements and calculation results are reported in Appendix I. The computer programs used in the correlation and prediction of phase equilibria are presented in Appendices II to VII.

The tables reported in Appendix I are the following:

<u>APPENDIX</u>	<u>TITLE</u>	<u>TABLE</u>	<u>PAGE</u>
I.1	Specific Surface Area of Silica Gel.	IV.1	240
I.2	Measured Adsorption Isotherms.	III.3	242
I.3	Corrected Adsorption Isotherms.	III.4	253
I.4	Pure Component Adsorption Isotherms and Spreading Pressures.	IV.2	264
I.5	Parameters of the Analog of the Redlich-Kwong Equation of State and Compressibilities of the Adsorbed Phase.	IV.5	276
I.6	Measured Values of the Adsorbed Phase Properties in Mixtures.	IV.6	292

The computer programs, written in FORTRAN IV, employed in this investigation are presented in the following order:

	<u>PAGE</u>
Appendix II: Specific Surface Area Calculation using the BET Equation.	304
Appendix III: Correlation of the Adsorption Data using the BET Equation.	311
Appendix IV: Calculation of Phase Equilibria using an Exact Thermodynamic Relationship.	314
Appendix V: Calculation of the Characteristic Parameters of the Analog of the Redlich-Kwong Equation using de Boer's Method.	336
Appendix VI: Calculation of the Characteristic Parameters of the Analog of the Redlich-Kwong Equation by Extending the Method of Chang-Lu Proposed in V.L.E. Calculations.	340
Appendix VII: Prediction of Phase Equilibria in Mixtures using the Analog of the Redlich-Kwong Equation whose Coefficients have been calculated by the Method employed in V.L.E. Calculations Proposed by Chang and Lu.	345

APPENDIX I.1

SPECIFIC SURFACE AREA OF SILICA GEL

The specific surface area of silica gel was calculated using Equation I.1. The experimental values obtained with the McBain spring balance are the following:

TABLE IV.1a

Specific Surface Area* (m ² /gram)	Average Absolute Per cent Deviation** (%)
688.2	0.20
703.5	0.12
694.4	0.38

$$* A = 0.3481 \times V_m \text{ (m}^2\text{/gram) (37)}$$

$$** \frac{1}{n} \sum_{i=1}^n \frac{(\text{Experimental mass} - \text{Calculated Mass})}{\text{Calculated mass}} \times 100$$

The specific surface area of silica gel calculated using Equation I.1 with data obtained with the Cahn Electrobalance Assembly are listed as follows:

TABLE IV.1b

Specific Surface Area* (m ² /gram)	Average Absolute Per cent Deviation** (%)
725.5	0.001
729.3	0.36
727.3	0.16
709.6	0.0001

The computer program is found in Appendix II.

APPENDIX I.2

TABLES III.3

MEASURED ADSORPTION ISOTHERMS

Measured adsorption equilibrium data of pure and mixture isotherms using the Cahn Electrobalance Assembly.

<u>TABLE</u>	<u>SYSTEM</u>	<u>TEMPERATURE</u> °K
III.3.1	Carbon dioxide (1) - Ethane (2)	263.2
III.3.2	Carbon dioxide (1) - Ethane (2)	273.2
III.3.3	Carbon dioxide (1) - Ethane (2)	298.2
III.3.4	Ethylene (1) - Ethane (2)	263.2
III.3.5	Ethylene (1) - Ethane (2)	273.2
III.3.6	Ethylene (1) - Ethane (2)	298.2
III.3.7	Propane (1) - Carbon dioxide (2)	263.2
III.3.8	Propane (1) - Carbon dioxide (2)	273.2
III.3.9	Propane (1) - Carbon dioxide (2)	298.2
III.3.10	Propane (1) - Carbon dioxide (2)	323.2

TABLE III.3.1

EXPERIMENTAL ADSORPTION DATA
MILLIGRAMS ADSORBED PER GRAM ADSORBENT ~ M
TOTAL PRESSURE IN CMHG ~ P

ETHANE - CARBON DIOXIDE - SILICA GEL AT -10.0 DEG. CENTIGRADE GRAVELLE

GAS PHASE COMPOSITION - PER CENT HEAVY COMPONENT

0.0 0.2592 0.4960 0.7522 1.0000

P	M	P	M	P	M	P	M		
3.819	5.279	3.090	9.625	3.046	11.820	3.716	15.853	2.810	15.340
13.664	16.466	11.419	23.014	11.365	27.932	11.566	33.352	11.386	38.265
24.562	23.151	23.999	36.363	24.169	44.084	24.154	51.928	24.489	60.307
41.361	31.286	39.203	48.243	40.967	59.393	40.461	69.309	40.755	79.782
59.987	38.617	59.196	60.279	58.342	72.487	59.266	85.241	59.368	96.162
73.727	43.419	73.772	67.630	74.212	82.268	73.346	95.411	73.989	108.446

TABLE III.3.2

EXPERIMENTAL ADSORPTION DATA
MILLIGRAMS ADSORBED PER GRAM ADSORBENT - M
TOTAL PRESSURE IN CM-HG - P

ETHANE - CARBON DIOXIDE - SILICA GEL AT 0,0 DEG, CENTIGRADE GRAVELLE

GAS PHASE COMPOSITION - PER CENT HEAVY COMPONENT

0.0		0.2592		0.4960		0.7522		1.0000	
P	M	P	M	P	M	P	M	P	M
2.850	3.550	3.230	5.387	2.798	7.229	2.888	9.317	3.550	11.610
11.210	9.170	10.810	13.790	10.680	19.560	10.610	22.980	10.930	26.080
23.480	15.230	23.380	24.220	27.990	34.530	23.620	38.790	23.770	43.630
38.620	21.240	39.200	34.280	35.440	44.920	38.820	51.800	37.900	57.860
61.660	28.870	64.290	46.280	59.530	56.700	59.750	66.380	57.750	73.730
75.450	32.640	75.230	50.800	73.910	63.740	74.840	74.870	75.670	85.530

TABLE III.3.4

EXPERIMENTAL ADSORPTION DATA
 MILLIGRAMS ADSORBED PER GRAM ADSORBENT * M
 TOTAL PRESSURE IN CM-HG * P

ETHANE * ETHYLENE * SILICA GEL AT -10.0 DEG. CENTIGRADE GRAVELLE

GAS PHASE COMPOSITION * PER CENT HEAVY COMPONENT

0.0		0.2635		0.5042		0.7547		1.0000	
P	M	P	M	P	M	P	M	P	M
3.819	5.279	2.885	8.526	3.085	10.090	3.156	11.210	2.914	11.894
13.664	16.466	11.627	18.699	11.134	20.845	11.243	22.713	11.716	25.120
24.562	23.151	24.101	28.107	24.205	31.366	24.682	33.883	24.370	35.899
41.361	31.286	40.258	36.946	40.510	40.476	40.819	43.074	40.813	45.344
59.987	38.617	59.992	45.296	60.128	48.978	59.382	50.913	59.864	53.280
73.727	43.419	60.901	45.512	75.398	54.817	74.376	56.048	75.049	58.179

TABLE III.3.5

EXPERIMENTAL ADSORPTION DATA
MILLIGRAMS ADSORBED PER GRAM ADSORBENT - M.
TOTAL PRESSURE IN CMHG - P

ETHANE - ETHYLENE - SILICA GEL AT 0.0 DEG. CENTIGRADE GRAVELLE
GAS PHASE COMPOSITION - PER CENT HEAVY COMPONENT
0.0 0.2635 0.5042 0.7547 1.0000

P	M	P	M	P	M	P	M
2,895	9,159	2,895	4,483	2,895	5,461	2,895	6,971
11,120	15,428	11,120	11,124	11,120	13,418	11,120	16,716
23,470	21,265	23,470	18,608	23,470	21,562	23,470	25,673
38,000	26,238	38,000	25,342	38,000	28,619	38,000	33,263
52,530	29,973	52,530	30,726	52,530	34,342	52,530	39,072
64,830	32,300	64,830	34,684	64,830	38,490	64,830	43,213
73,100	33,107	73,100	37,141	73,100	41,079	73,100	45,687
76,000		76,000	37,985	76,000	41,886	76,000	46,512

TABLE III.3.6

EXPERIMENTAL ADSORPTION DATA
 MILLIGRAMS ADSORBED PER GRAM ADSORBENT = M
 TOTAL PRESSURE IN CM-HG = P.

ETHANE - ETHYLENE - SILICA GEL AT 25.0 DEG. CENTIGRADE GRAVELLE

GAS PHASE COMPOSITION - PER CENT HEAVY COMPONENT

0.0 0.2635 0.5042 0.7547 1.0000

P	M	R	M	P	M	P	M	P	M
3.029	3.528	3.046	4.037	3.093	4.393	3.105	4.934	3.102	5.213
11.615	6.624	11.935	6.251	11.387	9.140	11.843	10.122	11.960	11.093
24.094	10.230	24.496	12.582	24.371	14.043	24.443	15.615	25.314	17.200
23.516	10.367	41.377	17.364	40.740	19.181	40.890	21.186	40.948	22.696
40.705	14.169	59.606	21.695	59.283	23.967	60.158	26.306	59.582	27.949
59.559	18.069	74.986	24.968	63.636	25.006	75.200	29.876	74.975	31.555

TABLE III.8

EXPERIMENTAL ADSORPTION DATA
 MILLIGRAMS ADSORBED PER GRAM ADSORBENT ~ M
 TOTAL PRESSURE IN CM-HG - P

CARBON DIOXIDE - PROPANE - SILICA GEL AT 0.0 DEG CENTIGRADE GRAVELLE

GAS PHASE COMPOSITION - PER CENT HEAVY COMPONENT

0.0		0.2385		0.4527		0.7494		1.0000	
P	M	P	M	P	M	P	M	P	M
2.893	9.735	2.893	12.963	2.893	15.097	2.893	16.701	2.893	17.749
11.130	26.146	11.130	32.500	11.130	36.545	11.130	39.415	11.130	40.618
23.460	42.947	23.460	51.202	23.460	56.396	23.460	61.108	23.460	62.772
38.000	57.986	38.000	67.192	38.000	73.388	38.000	79.814	38.000	81.744
52.540	70.132	52.540	79.783	52.540	87.092	52.540	94.567	52.540	96.501
64.870	78.959	64.870	88.772	64.870	96.618	64.870	105.070	64.870	107.004
73.110	84.373	73.110	94.176	73.110	102.505	73.110	111.453	73.110	113.271
76.000	85.801	76.000	96.293	76.000	104.455	76.000	113.439	76.000	115.831

TABLE III.3.9

EXPERIMENTAL ADSORPTION DATA
 MILLIGRAMS ADSORBED PER GRAM ADSORBENT - M
 TOTAL PRESSURE IN CMHG - P

 CARBON DIOXIDE - PROPANE - SILICA GEL AT 25.0 DEG CENTIGRADE GRAVELLE
 GAS PHASE COMPOSITION - PER CENT HEAVY COMPONENT
 0.0 0.2585 0.4527 0.7494 1.0000

P	M	P	M	P	M	P	M		
3.131	5.831	2.759	6.539	2.697	7.203	2.493	8.522	2.923	9.205
11.988	14.135	11.124	16.653	11.341	18.782	11.453	21.815	11.891	22.746
24.989	23.774	24.282	28.357	24.440	31.167	24.732	35.482	24.433	35.876
40.224	33.001	41.103	39.766	40.649	42.942	40.660	47.872	40.800	49.104
59.321	42.719	59.558	49.977	59.830	54.228	59.509	59.968	59.460	61.351
74.870	49.727	75.265	57.734	75.358	62.117	75.906	68.981	74.948	70.163

TABLE III.3.10

EXPERIMENTAL ADSORPTION DATA
 MILLIGRAMS ADSORBED PER GRAM ADSORBENT - M
 TOTAL PRESSURE IN CM-HG - P

CARBON DIOXIDE - PROPANE - SILICA GEL AT 50.0 DEG CENTIGRADE GRAVELLE

GAS PHASE COMPOSITION - PER CENT HEAVY COMPONENT

P	M	P	M	P	M	P	M
0.0	0.2385	0.4527	0.7494	1.0000			
9.993	7.092	9.983	7.713	10.008	9.031	9.983	10.563
30.000	15.028	29.994	17.390	30.009	19.514	30.007	22.206
49.972	21.609	50.003	25.107	50.000	27.759	49.972	31.159
70.000	27.424	69.978	31.678	89.970	34.905	70.013	39.680
						69.997	41.226

APPENDIX I.3

TABLES III.4

CORRECTED ADSORPTION ISOTHERMS

The measured adsorption equilibrium data of pure and mixture isotherms using the Cahn Electrobalance Assembly are listed in the following tables.

The thermomolecular effect and the buoyancy corrections have been included in the tabulated values of the mass of gas adsorbed per gram of adsorbent.

<u>TABLE</u>	<u>SYSTEM</u>	<u>TEMPERATURE</u> °K
III.4.1	Carbon dioxide (1) - Ethane (2)	263.2
III.4.2	Carbon dioxide (1) - Ethane (2)	273.2
III.4.3	Carbon dioxide (1) - Ethane (2)	298.2
III.4.4	Ethylene (1) - Ethane (2)	263.2
III.4.5	Ethylene (1) - Ethane (2)	273.2
III.4.6	Ethylene (1) - Ethane (2)	298.2
III.4.7	Propane (1) - Carbon dioxide (2)	263.2
III.4.8	Propane (1) - Carbon dioxide (2)	273.2
III.4.9	Propane (1) - Carbon dioxide (2)	298.2
III.4.10	Propane (1) - Carbon dioxide (2)	323.2

TABLE III.4.1

EXPERIMENTAL ADSORPTION DATA
 MILLIGRAMS ADSORBED PER GRAM ADSORBENT - M
 TOTAL PRESSURE IN MM-HG - P

ETHANE - CARBON DIOXIDE - SILICA GEL AT -10.0 DEG. CENTIGRADE GRAVELLE

GAS PHASE COMPOSITION - PER CENT HEAVY COMPONENT

0.0 0.2592 0.4960 0.7522 1.0000

P	C	M	P	M	P	M	P	M
38.19	4.271	30.90	7.358	30.46	9.370	37.16	13.350	28.10 13.179
136.64	13.916	114.19	20.675	113.65	25.398	115.66	30.761	113.86 36.004
245.62	20.533	239.99	33.930	241.69	41.442	241.54	49.219	244.89 57.920
413.61	28.568	392.03	45.706	409.67	56.624	404.61	66.464	407.55 77.256
599.87	35.793	591.96	57.613	583.42	69.592	592.66	82.250	593.68 93.488
737.27	40.518	737.72	64.874	742.12	79.264	733.46	92.314	739.89 105.658

TABLE III.4.2

EXPERIMENTAL ADSORPTION DATA
MILLIGRAMS ADSORBED PER GRAM ADSORBENT - M
TOTAL PRESSURE IN MM-HG - P

ETHANE - CARBON DIOXIDE - SILICA GEL AT 0.0 DEG. CENTIGRADE GRAVELLE

GAS PHASE COMPOSITION - PER CENT HEAVY COMPONENT

0.0 0.2592 0.4960 0.7522 1.0000

P	M	P	M	P	M	P	M		
28.50	2.836	32.30	4.479	27.98	6.318	28.80	8.460	35.50	10.759
112.10	9.075	108.10	13.497	106.80	19.007	106.10	22.485	109.30	25.585
234.80	15.295	233.80	24.077	279.90	36.419	236.20	38.631	237.70	43.468
386.20	21.457	392.00	34.277	354.40	43.357	388.20	52.053	379.00	58.032
610.60	29.297	642.90	46.467	595.30	57.193	597.50	66.914	577.50	74.214
754.50	33.245	752.30	51.169	739.10	64.429	748.40	75.593	756.70	86.239



TABLE III.4.3

EXPERIMENTAL ADSORPTION DATA
MILLIGRAMS ADSORBED PER GRAM ADSORBENT - M
TOTAL PRESSURE IN MM-HG - P

ETHANE - CARBON DIOXIDE - SILICA GEL AT 25.0 DEG. CENTIGRADE GRAVELLE

GAS PHASE COMPOSITION - PER CENT HEAVY COMPONENT

0.0 0.2592 0.4960 0.7522 1.0000

P	M	P	M	P	M	P	M		
30.29	1.222	33.70	1.925	28.13	2.260	37.20	3.840	31.32	3.452
116.15	4.283	119.82	6.591	111.77	7.942	119.46	10.459	115.05	11.366
240.94	7.840	244.86	11.888	249.09	15.345	240.18	18.275	249.93	21.370
407.05	11.715	403.53	17.682	408.25	22.465	404.95	27.031	402.11	30.545
595.59	15.545	588.67	23.329	589.82	29.302	596.11	35.463	593.17	40.191
747.03	18.310	745.77	27.597	745.75	34.389	755.24	41.618	747.94	47.033

TABLE III.4.4

EXPERIMENTAL ADSORPTION DATA
MILLIGRAMS ADSORBED PER GRAM ADSORBENT - M
TOTAL PRESSURE IN MM-HG - P

ETHANE ETHYLENE - SILICA GEL AT -10.0 DEG. CENTIGRADE GRAVELLE

GAS PHASE COMPOSITION - PER CENT HEAVY COMPONENT

0.6 0.2635 0.5042 0.7547 1.0000

P	M	P	M	P	M	P	M		
38.19	4.271	28.85	6.401	30.85	7.922	31.56	9.157	29.14	9.781
136.64	13.916	116.27	16.510	111.34	18.613	112.43	20.594	117.16	22.933
245.62	20.533	241.01	25.837	242.05	29.046	246.82	31.672	243.70	33.622
413.61	28.568	402.58	34.578	405.10	38.054	408.19	40.761	408.13	42.959
599.87	35.793	599.92	42.814	601.38	46.439	593.82	48.487	598.64	50.777
737.27	40.518	609.01	43.025	753.98	52.188	743.76	53.534	750.49	55.585

TABLE III.4.6

EXPERIMENTAL ADSORPTION DATA
 MILLIGRAMS ADSORBED PER GRAM ADSORBENT - M
 TOTAL PRESSURE IN MM-HG - P

ETHANE - ETHYLENE - SILICA GEL AT 25.0 DEG. CENTIGRADE GRAVELLE

GAS PHASE COMPOSITION - PER CENT HEAVY COMPONENT

0.0 0.2635 0.5042 0.7547 1.0000

P	M	P	M	P	M	P	M		
30.29	1.222	30.46	1.730	30.93	2.239	31.05	2.464	31.02	2.901
116.15	4.283	119.35	5.903	113.87	6.947	118.43	7.607	119.60	8.734
240.94	7.840	244.96	10.181	243.71	11.793	244.43	13.040	253.14	14.783
235.16	7.978	413.77	14.895	407.40	16.861	408.96	18.536	409.48	20.198
407.05	11.715	596.06	19.153	592.83	21.571	601.58	23.572	595.82	25.367
595.59	15.545	749.86	22.366	636.36	22.592	752.00	27.077	749.75	28.906

TABLE III.4.8

EXPERIMENTAL ADSORPTION DATA
 MILLIGRAMS ADSORBED PER GRAM ADSORBENT - M
 TOTAL PRESSURE IN MM-HG - P

 CARBON DIOXIDE - PROPANE - SILICA GEL AT 0.0 DEG CENTIGRADE GRAVELLE

 0.0 0.2385 0.4527 0.7494 1.0000

VAS PHASE COMPOSITION - PER CENT, HEAVY COMPONENT

P	M	P	M	P	M	P	M	P	M
28.93	8.691	28.93	11.897	28.93	13.730	28.93	15.824	28.93	16.020
111.30	25.044	111.30	31.376	111.30	35.116	111.30	38.491	111.30	38.827
234.60	41.764	234.60	50.003	234.60	54.890	234.60	60.124	234.60	60.908
380.00	56.714	380.00	65.909	380.00	71.800	380.00	78.764	380.00	79.807
525.40	68.773	525.40	78.421	525.40	85.426	525.40	93.456	525.40	94.497
648.70	77.528	648.70	87.344	648.70	94.889	648.70	103.908	648.70	104.948
731.10	82.894	731.10	92.705	731.10	100.735	731.10	110.257	731.10	111.180
760.00	84.306	760.00	94.806	760.00	102.671	760.00	112.232	760.00	113.728

TABLE III.4.9

EXPERIMENTAL ADSORPTION DATA
 MILLIGRAMS ADSORBED PER GRAM ADSORBENT - M
 TOTAL PRESSURE IN MM-HG - P

CARBON DIOXIDE - PROPANE - SILICA GEL AT 25.0 DEG CENTIGRADE GRAVELLE

GAS PHASE COMPOSITION - PER CENT HEAVY COMPONENT

0.0 0.2385 0.4527 0.7494 1.0000

P	M	P	M	P	M	P	M		
31.31	3.453	27.59	4.221	26.97	4.945	24.93	6.282	29.23	7.045
119.88	11.696	111.24	14.278	113.41	16.468	114.53	19.522	118.91	20.538
249.89	21.252	242.82	25.902	244.40	28.780	247.32	33.122	244.33	33.614
402.24	30.387	411.03	37.217	406.49	40.473	406.60	45.442	408.00	46.780
593.21	39.993	595.58	47.330	598.30	51.667	595.09	57.460	594.60	58.963
748.70	46.913	752.65	55.006	753.58	59.484	759.06	66.409	749.48	67.724

TABLE III.4.10

EXPERIMENTAL ADSORPTION DATA
 MILLIGRAMS ADSORBED PER GRAM ADSORBENT - M
 TOTAL PRESSURE IN MM-HG - P

CARBON DIOXIDE - PROPANE - SILICA GEL AT 50.0 DEG CENTIGRADE GRAVELLE

GAS PHASE COMPOSITION - PER CENT HEAVY COMPONENT

0.0		0.2385		0.4527		0.7494		1.0000	
P	M	P	M	P	M	P	M	P	M
99.93	4.486	99.83	6.059	100.08	7.104	99.83	8.364	99.93	8.936
300.00	12.321	299.94	15.652	300.09	17.509	300.07	19.939	300.09	21.107
499.72	18.804	500.03	23.284	500.00	25.681	499.72	28.830	499.65	30.362
700.00	24.523	699.78	29.779	699.70	32.756	700.13	37.290	699.97	38.186

APPENDIX I.4

TABLES IV.2

PURE COMPONENT ADSORPTION ISOTHERMS AND
SPREADING PRESSURES

The calculated isothermal amount of gas adsorbed (millimoles/gram) with the corresponding spreading pressure ($\frac{\pi A}{RT}$; millimoles/gram) for each component constituting the binary mixtures investigated in this work are listed in the following tables at regular intervals of system pressure (mmHg). The correlation of the measured adsorption isotherms was made using the BET Equation while the spreading pressures were calculated using Equation II.14.

<u>TABLE</u>	<u>SYSTEM</u>	<u>TEMPERATURE</u> °K
IV.2.1	Carbon dioxide (1) - Ethane (2)	263.2
IV.2.2	Carbon dioxide (1) - Ethane (2)	273.2
IV.2.3	Carbon dioxide (1) - Ethane (2)	298.2
IV.2.4	Ethylene (1) - Ethane (2)	263.2
IV.2.5	Ethylene (1) - Ethane (2)	273.2
IV.2.6	Ethylene (1) - Ethane (2)	298.2
IV.2.7	Propane (1) - Carbon dioxide (2)	263.2
IV.2.8	Propane (1) - Carbon dioxide (2)	273.2
IV.2.9	Propane (1) - Carbon dioxide (2)	298.2
IV.2.10	Propane (1) - Carbon dioxide (2)	323.2

The symbols and units employed in Tables IV.2 are defined as follows:

- P gas pressure, mmHg.
- N1, N2 amount of pure gas adsorbed, millimoles/gram.
- PI1, PI2 spreading pressure of pure gas adsorbed defined by
Equation II.14, millimoles/gram.
- 1 pure gas 1
- 2 pure gas 2

The computer program is listed in Appendix IV.

TABLE IV.2.1

ETHANE - CARBON DIOXIDE - SILICA GEL AT -10.0 DEG. CENTIGRADE GRAVELLE

P	N2	PI2	N1	PI1
50.0	0.1832	0.1905	0.4700	0.5491
100.0	0.3407	0.3672	0.7581	0.9692
150.0	0.4774	0.5318	0.9749	1.3191
200.0	0.5973	0.6859	1.1568	1.6251
250.0	0.7033	0.8308	1.3181	1.9009
300.0	0.7976	0.9676	1.4653	2.1544
350.0	0.8821	1.0970	1.6015	2.3906
400.0	0.9582	1.2198	1.7284	2.6129
450.0	1.0272	1.3367	1.8469	2.8234
500.0	1.0899	1.4482	1.9575	3.0238
550.0	1.1473	1.5549	2.0607	3.2153
600.0	1.1999	1.6570	2.1569	3.3989
650.0	1.2483	1.7549	2.2466	3.5752
700.0	1.2930	1.8491	2.3302	3.7448
750.0	1.3345	1.9397	2.4080	3.9084

TABLE IV.2.2

THANE - CARBON DIOXIDE - SILICA GEL AT 0.0 DEG. CENTIGRADE GRAVELLE

P	N2	PI2	N1	PI1
50.0	0.1293	0.1379	0.3098	0.3465
100.0	0.2338	0.2606	0.5257	0.6310
150.0	0.3247	0.3730	0.6982	0.8778
200.0	0.4071	0.4778	0.8471	1.0595
250.0	0.4837	0.5770	0.9809	1.3031
300.0	0.5554	0.6716	1.1038	1.4929
350.0	0.6230	0.7623	1.2180	1.6718
400.0	0.6866	0.8497	1.3244	1.8414
450.0	0.7463	0.9341	1.4238	2.0032
500.0	0.8023	1.0156	1.5165	2.1581
550.0	0.8547	1.0946	1.6030	2.3068
600.0	0.9035	1.1711	1.6836	2.4498
650.0	0.9490	1.2452	1.7586	2.5875
700.0	0.9913	1.3171	1.8283	2.7205
750.0	1.0306	1.3869	1.8932	2.8489

TABLE IV.2.3

THANE - CARBON DIOXIDE - SILICA GEL AT 25.0 DEG. CENTIGRADE GRAVELLE

P'	N2	P12	N1	PI1
50.0	0.0655	0.0685	0.1217	0.1284
100.0	0.1230	0.1319	0.2263	0.2456
150.0	0.1753	0.1918	0.3203	0.3554
200.0	0.2237	0.2489	0.4063	0.4596
250.0	0.2687	0.3038	0.4858	0.5589
300.0	0.3110	0.3565	0.5598	0.6541
350.0	0.3508	0.4075	0.6292	0.7457
400.0	0.3884	0.4568	0.6944	0.8341
450.0	0.4241	0.5047	0.7560	0.9195
500.0	0.4581	0.5512	0.8144	1.0022
550.0	0.4905	0.5964	0.8698	1.0825
600.0	0.5215	0.6404	0.9226	1.1605
650.0	0.5511	0.6834	0.9730	1.2365
700.0	0.5795	0.7253	1.0211	1.3104
750.0	0.6067	0.7662	1.0672	1.3825

TABLE IV.2.4

THANE - ETHYLENE - SILICA GEL AT -10.0 DEG. CENTIGRADE GRAVELLE

P	N2	PI2	N1	PI1
50.0	0.1632	0.1905	0.5082	0.6340
100.0	0.3407	0.3672	0.7658	1.0722
150.0	0.4774	0.5318	0.9444	1.4182
200.0	0.5973	0.6859	1.0875	1.7101
250.0	0.7033	0.8308	1.2105	1.9663
300.0	0.7976	0.9676	1.3200	2.1969
350.0	0.8821	1.0970	1.4194	2.4080
400.0	0.9582	1.2198	1.5104	2.6036
450.0	1.0272	1.3367	1.5943	2.7865
500.0	1.0899	1.4482	1.6718	2.9587
550.0	1.1473	1.5549	1.7436	3.1216
600.0	1.1999	1.6570	1.8102	3.2764
650.0	1.2483	1.7549	1.8720	3.4240
700.0	1.2930	1.8491	1.9284	3.5652
750.0	1.3345	1.9397	1.9828	3.7006

TABLE IV.2.5

THANE - ETHYLENE - SILICA GEL AT 0.0 DEG. CENTIGRADE GRAVELLE

P	N2	P12	N1	P11
50.0	0.1293	0.1379	0.2803	0.3134
100.0	0.2338	0.2606	0.4748	0.5705
150.0	0.3247	0.3730	0.6276	0.7930
200.0	0.4071	0.4778	0.7561	0.9916
250.0	0.4837	0.5770	0.8683	1.1726
300.0	0.5554	0.6716	0.9685	1.3399
350.0	0.6230	0.7623	1.0591	1.4961
400.0	0.6866	0.8497	1.1415	1.6430
450.0	0.7463	0.9341	1.2169	1.7819
500.0	0.8023	1.0156	1.2861	1.9138
550.0	0.8547	1.0946	1.3498	2.0394
600.0	0.9035	1.1711	1.4084	2.1594
650.0	0.9490	1.2452	1.4626	2.2743
700.0	0.9913	1.3171	1.5126	2.3846
750.0	1.0306	1.3869	1.5589	2.4905

TABLE IV.2.6

THANE - ETHYLENE - SILICA GEL AT 25.0 DEG. CENTIGRADE GRAVELLE

P	N2	PI2	N 1	PI1
50.0	0.0655	0.0678	0.1559	0.1716
100.0	0.1239	0.1315	0.2701	0.3163
150.0	0.1773	0.1920	0.3638	0.4441
200.0	0.2265	0.2498	0.4457	0.5602
250.0	0.2722	0.3053	0.5198	0.6677
300.0	0.3148	0.3588	0.5883	0.7686
350.0	0.3547	0.4103	0.6519	0.8641
400.0	0.3922	0.4602	0.7113	0.9551
450.0	0.4275	0.5084	0.7668	1.0421
500.0	0.4609	0.5552	0.8186	1.1256
550.0	0.4925	0.6007	0.8669	1.2059
600.0	0.5225	0.6448	0.9118	1.2833
650.0	0.5510	0.6878	0.9536	1.3580
700.0	0.5782	0.7297	0.9925	1.4301
750.0	0.6041	0.7705	1.0287	1.4998

TABLE IV.2.7

ARBON DIOXIDE - PROPANE - SILICA GEL AT -10.0 DEG CENTIGRADE GRAVELLE

P	N2	PI2	N1	PI1
50.0	0.4700	0.5491	0.7405	0.9096
100.0	0.7581	0.9692	1.1333	1.5534
150.0	0.9749	1.3191	1.4121	2.0680
200.0	1.1568	1.6251	1.6393	2.5063
250.0	1.3181	1.9009	1.8374	2.8938
300.0	1.4653	2.1544	2.0162	3.2449
350.0	1.6015	2.3906	2.1802	3.5682
400.0	1.7284	2.6129	2.3319	3.8694
450.0	1.8469	2.8234	2.4728	4.1524
500.0	1.9575	3.0238	2.6038	4.4200
550.0	2.0607	3.2153	2.7258	4.6741
600.0	2.1569	3.3989	2.8393	4.9164
650.0	2.2466	3.5752	2.9450	5.1482
700.0	2.3302	3.7448	3.0434	5.3705
750.0	2.4080	3.9084	3.1351	5.5841

TABLE IV.2.8

ARBON DIOXIDE - PROPANE - SILICA GEL AT 0.0 DEG CENTIGRADE GRAVELLE

P	N2	PI2	N1	PI1
50.0	0.3119	0.3496	0.5450	0.6569
100.0	0.5282	0.6357	0.8508	1.1356
150.0	0.7007	0.8835	1.0738	1.5245
200.0	0.8495	1.1059	1.2592	1.8595
250.0	0.9835	1.3101	1.4237	2.1584
300.0	1.1068	1.5004	1.5745	2.4315
350.0	1.2215	1.6797	1.7147	2.6849
400.0	1.3287	1.8499	1.8459	2.9226
450.0	1.4288	2.0123	1.9689	3.1472
500.0	1.5224	2.1677	2.0842	3.3608
550.0	1.6098	2.3170	2.1922	3.5646
600.0	1.6913	2.4606	2.2932	3.7599
650.0	1.7672	2.5990	2.3876	3.9474
700.0	1.8378	2.7326	2.4757	4.1278
750.0	1.9035	2.8617	2.5579	4.3016

TABLE IV.2.9

ARBON DIOXIDE - PROPANE - SILICA GEL AT 25.0 DEG CENTIGRADE GRAVELLE

P	N2	P12	N1	P11
50.0	0.1214	0.1285	0.2482	0.2812
100.0	0.2253	0.2452	0.4154	0.5073
150.0	0.3185	0.3545	0.5477	0.7016
200.0	0.4039	0.4580	0.6626	0.8752
250.0	0.4828	0.5568	0.7674	1.0344
300.0	0.5564	0.6514	0.8653	1.1831
350.0	0.6255	0.7425	0.9579	1.3235
400.0	0.6905	0.8303	1.0457	1.4572
450.0	0.7521	0.9153	1.1288	1.5852
500.0	0.8105	0.9976	1.2074	1.7083
550.0	0.8661	1.0776	1.2815	1.8269
600.0	0.9191	1.1553	1.3511	1.9414
650.0	0.9698	1.2309	1.4163	2.0522
700.0	1.0183	1.3047	1.4772	2.1594
750.0	1.0648	1.3766	1.5341	2.2633

TABLE IV.2.10

ARBON DIOXIDE - PROPANE - SILICA GEL AT 50.0 DEG CENTIGRADE GRAVELLE

P	N2	PI2	N1	PI1
50.0	0.0523	0.0530	0.1135	0.1223
100.0	0.1020	0.1046	0.2027	0.2293
150.0	0.1494	0.1550	0.2793	0.3263
200.0	0.1947	0.2043	0.3488	0.4162
250.0	0.2380	0.2524	0.4137	0.5011
300.0	0.2794	0.2995	0.4752	0.5820
350.0	0.3191	0.3455	0.5339	0.6597
400.0	0.3571	0.3907	0.5897	0.7347
450.0	0.3936	0.4348	0.6427	0.8072
500.0	0.4288	0.4781	0.6929	0.8776
550.0	0.4625	0.5206	0.7402	0.9459
600.0	0.4950	0.5622	0.7846	1.0122
650.0	0.5263	0.6031	0.8262	1.0767
700.0	0.5565	0.6432	0.8650	1.1393
750.0	0.5856	0.6826	0.9012	1.2002

APPENDIX I.5

TABLES IV.5

PARAMETERS OF THE ANALOG OF THE REDLICH-KWONG
EQUATION OF STATE AND COMPRESSIBILITIES OF THE ADSORBED PHASE

The amount of gas adsorbed (N : millimoles/gram), the spreading pressure ($\frac{\pi A}{RT}$: millimoles/gram), the compressibility factor ($Z = \frac{pV}{RT}$), and the characteristic parameters α (cal.m². °K^{0.5}. millimole⁻²) and β (m²/millimole) are listed in the following tables at regular pressure intervals. The values of α and β were calculated using the method described in Section IV.B.3.

<u>TABLE</u>	<u>SYSTEM</u>	<u>TEMPERATURE</u> °K
IV.5.1	Carbon dioxide	263.2
IV.5.2	Propane	263.2
IV.5.3	Ethane	263.2
IV.5.4	Ethylene	263.2
IV.5.5	Carbon dioxide	273.2
IV.5.6	Propane	273.2
IV.5.7	Ethane	273.2
IV.5.8	Ethylene	273.2
IV.5.9	Carbon dioxide	298.2
IV.5.10	Propane	298.2
IV.5.11	Ethane	298.2

<u>TABLE</u>	<u>SYSTEM</u>	<u>TEMPERATURE</u> °K
IV.5.12	Ethylene	298.2
IV.5.13	Carbon dioxide	323.2
IV.5.14	Propane	323.2

The symbols and units employed in Tables IV.5 are defined as follows:

J	number of iterations required for the convergence of Equation II.73.
N	number of moles of pure gas adsorbed, millimoles/gram.
PI	spreading pressure of pure gas adsorbed defined by Equation II.14.
Z	compressibility factor of pure gas adsorbed defined by Equation II.65.
ALFA	α defined by Equation II.62.
BETA	β defined by Equation II.63.

The computer program is listed in Appendix VI.

TABLE IV.5.1

CARBON DIOXIDE -			SILICA GEL AT -10.0 DEG CENTIGRADE			
I	J	N	PI	Z	ALFA	BETA
1	26	0.4700	0.5491	1.1683	12842.19	703.80
2	25	3.7581	0.9692	1.2785	7156.89	446.63
3	25	0.9749	1.3191	1.3531	5022.35	350.29
4	25	1.1568	1.6251	1.4048	3800.31	294.63
5	26	1.3181	1.9009	1.4422	2973.99	256.37
6	26	1.4653	2.1544	1.4713	2368.19	227.74
7	26	1.6015	2.3906	1.4927	1905.52	205.37
8	26	1.7284	2.6129	1.5117	1543.94	187.46
9	26	1.8469	2.8234	1.5287	1256.28	172.89
10	26	1.9575	3.0238	1.5447	1026.28	160.99
11	26	2.0607	3.2153	1.5603	841.06	151.23
12	26	2.1569	3.3989	1.5758	691.72	143.23
13	26	2.2466	3.5752	1.5914	570.10	136.63
14	26	2.3302	3.7448	1.6071	470.82	131.20
15	26	2.4080	3.9084	1.6231	390.86	126.78

LIMITING SLOPE=0.09118

TABLE IV.5.2

PRORANE - SILICA GEL AT -10.0 DEG CENTIGRADE

I	J	N	PI	Z	ALFA	BETA
1	25	0.7405	0.9096	1.2284	9821.84	492.20
2	25	1.1333	1.5534	1.3707	5808.27	330.84
3	25	1.4121	2.0680	1.4645	4251.06	268.89
4	25	1.6393	2.5063	1.5289	3332.01	232.22
5	25	1.8374	2.8938	1.5749	2693.19	206.46
6	25	2.0162	3.2449	1.6094	2214.32	186.83
7	25	2.1802	3.5682	1.6366	1841.39	171.27
8	25	2.3319	3.8694	1.6593	1544.32	158.62
9	25	2.4728	4.1524	1.6792	1304.19	148.20
10	25	2.6138	4.4200	1.6975	1108.49	139.56
11	25	2.7258	4.6741	1.7148	946.98	132.31
12	25	2.8393	4.9164	1.7316	813.55	126.24
13	25	2.9450	5.1482	1.7481	702.65	121.12
14	25	3.0434	5.3705	1.7646	610.22	116.81
15	25	3.1351	5.5841	1.7812	532.72	113.17

LIMITING SLOPE=0.14366

TABLE IV.5.3

ETHANE -		SILICA GEL AT -10.0 DEG. CENTIGRADE				
I	J	N	PI	Z	ALFA	BETA
1	28	0.1832	0.1905	1.0393	15447.76	1125.31
2	28	0.3407	0.3672	1.0778	7860.69	622.75
3	28	0.4774	0.5318	1.1139	5348.57	458.03
4	28	0.5973	0.6859	1.1483	4105.96	377.44
5	28	0.7033	0.8308	1.1813	3374.99	330.62
6	28	0.7976	0.9676	1.2131	2903.66	300.79
7	27	0.8821	1.0970	1.2436	2570.94	280.10
8	27	0.9582	1.2198	1.2730	2327.63	265.22
9	27	1.0272	1.3367	1.3013	2142.93	254.09
10	27	1.0899	1.4482	1.3287	2000.73	245.66
11	27	1.1473	1.5549	1.3553	1888.43	239.07
12	27	1.1999	1.6570	1.3809	1797.00	233.82
13	27	1.2483	1.7549	1.4058	1721.60	229.58
14	26	1.2930	1.8491	1.4301	1661.02	226.19
15	26	1.3345	1.9357	1.4535	1608.43	223.31

LIMITING SLOPE=0.03554

TABLE IV.5.4

- ETHYLENE - SILICA GEL AT -10.0 DEG. CENTIGRADE

I	J	N	PI	Z	ALFA	BETA
1	25	0.5082	0.6340	1.2475	15051.24	735.25
2	25	0.7658	1.0722	1.4001	9067.63	502.67
3	24	0.9444	1.4182	1.5017	6748.75	413.75
4	24	1.0875	1.7101	1.5725	5376.57	361.24
5	24	1.2105	1.9663	1.6244	4422.73	324.51
6	24	1.3200	2.1969	1.6643	3707.94	296.67
7	25	1.4194	2.4980	1.6965	3148.47	274.60
8	25	1.5104	2.6036	1.7238	2701.60	256.72
9	25	1.5943	2.7865	1.7478	2337.83	241.95
10	25	1.6718	2.9587	1.7698	2039.22	229.67
11	25	1.7436	3.1216	1.7903	1790.92	219.34
12	25	1.8102	3.2764	1.8100	1583.31	210.62
13	25	1.8720	3.4240	1.8291	1408.99	203.22
14	25	1.9294	3.5652	1.8478	1262.22	196.95
15	25	1.9828	3.7006	1.8664	1137.92	191.59

LIMITING SLOPE=0.09859

TABLE IV.5.5

CARBON DIOXIDE - SILICA GEL AT 0.0 DEG CENTIGRADE

I	J	N	PI	Z	ALFA	BETA
1	26	0.3119	0.3496	1.1209	16862.82	551.09
2	26	0.5282	0.6357	1.2035	8935.27	571.48
3	26	0.7007	0.8835	1.2609	6036.73	432.08
4	26	0.8495	1.1059	1.3018	4433.65	383.91
5	26	0.9835	1.3101	1.3321	3380.49	301.54
6	26	1.1068	1.5004	1.3556	2628.24	263.28
7	27	1.2215	1.6797	1.3781	2067.31	234.04
8	27	1.3287	1.8499	1.3923	1638.43	211.12
9	27	1.4288	2.0123	1.4084	1307.76	193.04
10	27	1.5224	2.1677	1.4239	1047.31	178.54
11	27	1.6098	2.3170	1.4393	843.40	166.97
12	27	1.6913	2.4606	1.4549	682.40	157.73
13	27	1.7672	2.5990	1.4707	556.01	150.40
14	27	1.8378	2.7326	1.4869	457.66	144.66
15	27	1.9035	2.8617	1.5034	381.15	140.18

LIMITING SLOPE=0.06051

TABLE IV.5.6

PROPANE - SILICA GEL AT 0.0 DEG CENTIGRADE

I	U	N	PI	Z	ALFA	BETA
1	25	0.5450	0.6569	1.2053	13214.82	646.65
2	25	0.8508	1.1356	1.3347	7628.90	425.22
3	25	1.1738	1.5245	1.4197	5475.91	340.27
4	25	1.2592	1.8595	1.4767	4206.50	289.82
5	25	1.4237	2.1584	1.5160	3323.99	254.18
6	25	1.5745	2.4315	1.5443	2664.07	226.92
7	25	1.7147	2.6849	1.5658	2152.47	205.24
8	25	1.8459	2.9226	1.5833	1747.40	187.61
9	26	1.9689	3.1472	1.5985	1422.00	173.09
10	26	2.0842	3.3638	1.6125	1159.47	161.07
11	26	2.1922	3.5646	1.6260	945.31	151.05
12	26	2.2932	3.7599	1.6396	770.98	142.72
13	26	2.3876	3.9474	1.6533	627.95	135.76
14	26	2.4757	4.1278	1.6673	510.68	129.98
15	26	2.5579	4.3016	1.6817	414.11	125.16

LIMITING SLOPE=0.10573

TABLE IV.5.7

ETHANE -		SILICA GEL AT C.O DEG. CENTIGRADE				
I	J	N	PI	Z	ALFA	BETA
1	27	0.1293	0.1379	1.0665	29478.68	1879.46
2	27	0.2338	0.2606	1.1146	14723.25	1046.02
3	27	0.3247	0.3730	1.1488	9497.03	746.88
4	28	0.4071	0.4778	1.1737	6700.82	584.13
5	28	0.4837	0.5770	1.1929	4947.21	479.41
6	28	0.5554	0.6716	1.2092	3758.86	406.72
7	28	0.6230	0.7623	1.2236	2900.83	353.02
8	28	0.6866	0.8497	1.2375	2281.30	313.33
9	28	0.7463	0.9341	1.2516	1829.04	283.82
10	28	0.8023	1.0156	1.2659	1488.29	261.36
11	28	0.8547	1.0946	1.2807	1242.18	244.93
12	28	0.9035	1.1711	1.2962	1065.48	233.11
13	28	0.9490	1.2452	1.3121	936.97	224.56
14	28	0.9913	1.3171	1.3287	850.32	218.80
15	28	1.0306	1.3869	1.3457	795.29	215.15

LIMITING SLOPE=0.02508

TABLE IV.5.8

ETHYLENE - SILICA GEL AT 10.0 DEG. CENTIGRADE

I	J	N	PI	Z	ALFA	BETA
1	26	0.2803	0.3134	1.1181	18516.86	1050.13
2	26	0.4748	0.5705	1.2016	9846.88	632.62
3	26	0.6276	0.7930	1.2635	6761.02	483.85
4	26	0.7561	0.9916	1.3115	5095.63	403.23
5	26	0.8683	1.1726	1.3505	4031.24	351.32
6	26	0.9685	1.3399	1.3835	3285.41	314.62
7	26	1.0591	1.4961	1.4126	2735.93	287.35
8	26	1.1415	1.6430	1.4393	2320.07	266.54
9	26	1.2169	1.7819	1.4643	1996.61	250.25
10	26	1.2861	1.9138	1.4881	1741.45	237.35
11	26	1.3498	2.0394	1.5109	1536.39	226.97
12	26	1.4084	2.1594	1.5332	1372.72	218.68
13	26	1.4626	2.2743	1.5550	1238.94	211.91
14	26	1.5126	2.3846	1.5765	1131.82	206.50
15	26	1.5589	2.4905	1.5976	1043.29	202.07

LIMITING SLOPE=0.05438

TABLE IV.5.9

CARBON DIOXIDE -			SILICA GEL AT 25.0 DEG CENTIGRADE			
I	J	N	PI	Z	ALFA	BETA
1	28	0.1214	0.1285	1.0585	33885.57	1918.87
2	28	0.2253	0.2452	1.0883	15815.57	1003.89
3	28	0.3185	0.3545	1.1130	10015.44	696.86
4	28	0.4039	0.4580	1.1339	7113.72	540.27
5	28	0.4828	0.5568	1.1533	5414.71	446.94
6	28	0.5564	0.6514	1.1707	4275.44	383.69
7	31	0.6655	0.7425	1.1157	727.08	159.99
8	28	0.6905	0.8303	1.2025	2877.04	304.71
9	28	0.7521	0.9153	1.2170	2417.67	278.36
10	28	0.8105	0.9976	1.2303	2052.09	257.28
11	28	0.8661	1.0776	1.2442	1760.80	240.31
12	28	0.9191	1.1553	1.2570	1518.29	226.14
13	28	0.9698	1.2309	1.2692	1312.86	214.11
14	28	1.0183	1.3047	1.2818	1144.97	204.17
15	28	1.0648	1.3766	1.2928	998.37	195.50

LIMITING SLOPE=0.02355

TABLE IV.5.10

PROPANE - SILICA GEL AT 25.0 DEG CENTIGRADE

I	J	N	PI	Z	ALFA	BETA
1	26	0.2482	0.2812	1.1330	25525.08	1233.61
2	26	0.4154	0.5073	1.2212	13635.73	749.55
3	26	0.5477	0.7016	1.2810	9246.65	569.67
4	26	0.6626	0.8752	1.3209	6747.84	465.64
5	26	0.7674	1.0344	1.3479	5067.27	393.92
6	26	0.8653	1.1831	1.3673	3852.21	340.37
7	27	0.9579	1.3235	1.3817	2928.43	298.27
8	27	1.0457	1.4572	1.3935	2215.04	264.58
9	27	1.1288	1.5852	1.4043	1658.85	237.40
10	27	1.2074	1.7083	1.4149	1222.16	215.32
11	27	1.2815	1.8269	1.4256	877.08	197.37
12	28	1.3511	1.9414	1.4369	605.85	182.90
13	28	1.4163	2.0522	1.4490	395.68	171.43
14	28	1.4772	2.1594	1.4618	233.15	162.42
15	28	1.5341	2.2633	1.4753	109.05	155.46

LIMITING SLOPE=0.04815

TABLE IV.5.11

ETHANE - SILICA GEL AT 25.0 DEG. CENTIGRADE

I	J	N	PI	Z	ALFA	BETA
1	28	0.0655	0.0673	1.0351	49364.75	3028.61
2	28	0.1239	0.1315	1.0613	24108.45	1601.31
3	28	0.1773	0.1920	1.0829	15542.60	1113.32
4	29	0.2265	0.2498	1.1029	11300.71	870.17
5	28	0.2722	0.3053	1.1216	8794.84	725.51
6	29	0.3148	0.3588	1.1398	7184.25	631.86
7	28	0.3547	0.4103	1.1568	6007.93	563.84
8	28	0.3922	0.4602	1.1734	5168.45	514.89
9	28	0.4275	0.5084	1.1892	4504.34	476.53
10	28	0.4619	0.5552	1.2046	3987.50	446.56
11	28	0.4925	0.6007	1.2197	3583.93	423.09
12	28	0.5225	0.6448	1.2341	3233.15	402.98
13	28	0.5510	0.6878	1.2483	2954.80	386.94
14	28	0.5782	0.7297	1.2620	2717.38	373.27
15	28	0.6041	0.7705	1.2755	2513.76	361.67

LIMITING SLOPE=0.01271

TABLE IV.5.12

ETHYLENE - SILICA GEL AT 25.0 DEG. CENTIGRADE

I	J	N	PI	Z	ALFA	BETA
1	27	0.1559	0.1716	1.1007	34726.15	1790.21
2	27	0.2701	0.3163	1.1710	17998.96	1047.90
3	27	0.3638	0.4441	1.2207	11575.98	778.43
4	27	0.4457	0.5602	1.2569	8694.70	629.56
5	27	0.5193	0.6677	1.2846	6580.38	531.79
6	27	0.5883	0.7686	1.3065	5088.48	461.19
7	27	0.6519	0.8641	1.3255	3999.71	408.48
8	27	0.7113	0.9551	1.3428	3179.62	367.26
9	27	0.7668	1.0421	1.3590	2546.37	336.02
10	27	0.8186	1.1256	1.3750	2062.42	311.09
11	27	0.8669	1.2059	1.3910	1685.82	291.51
12	27	0.9118	1.2833	1.4074	1398.44	276.42
13	27	0.9536	1.3580	1.4241	1177.04	264.72
14	27	0.9925	1.4301	1.4409	1004.80	255.62
15	27	1.0287	1.4958	1.4580	872.68	248.66

LIMITING SLOPE=0.03024

TABLE IV.5.13

CARBON DIOXIDE -			SILICA GEL AT 50.0 DEG CENTIGRADE			
Iv	J	N	PI	Z	ALFA	BETA
1	30	0.0523	0.0530	1.0134	50059.45	2954.65
2	30	0.1020	0.1046	1.0255	24539.52	1517.87
3	29	0.1494	0.1550	1.0375	16216.71	1047.12
4	30	0.1947	0.2043	1.0493	12131.30	815.35
5	29	0.2380	0.2524	1.0605	9596.02	672.66
6	29	0.2794	0.2995	1.0719	7578.56	581.72
7	29	0.3191	0.3455	1.0827	6770.82	514.36
8	29	0.3571	0.3907	1.0941	5959.98	468.60
9	29	0.3936	0.4348	1.1047	5265.57	430.23
10	29	0.4288	0.4781	1.1150	4719.93	399.94
11	29	0.4625	0.5206	1.1256	4310.63	377.20
12	29	0.4950	0.5622	1.1358	3946.26	357.25
13	29	0.5263	0.6031	1.1459	3656.56	341.31
14	29	0.5565	0.6432	1.1558	3400.35	327.37
15	29	0.5856	0.6826	1.1656	3187.06	315.79

LIMITING SLOPE=0.01015

TABLE IV.5.14

PROPANE - SILICA GEL AT 50.0 DEG CENTIGRADE

I	J	N	PI	Z	ALFA	BETA
1	27	0.1135	0.1223	1.0775	46758.91	2252.98
2	27	0.2027	0.2293	1.1312	23481.53	1268.42
3	27	0.2793	0.3263	1.1683	15158.54	911.40
4	27	0.3488	0.4162	1.1932	10595.44	711.64
5	28	0.4137	0.5011	1.2113	7701.33	580.78
6	28	0.4752	0.5820	1.2247	5674.00	486.12
7	28	0.5339	0.6597	1.2356	4188.30	414.26
8	28	0.5897	0.7347	1.2459	3097.49	359.61
9	28	0.6427	0.8072	1.2560	2271.20	316.99
10	29	0.6929	0.8776	1.2666	1659.66	284.45
11	29	0.7402	0.9459	1.2779	1204.99	259.75
12	29	0.7846	1.0122	1.2901	873.05	241.45
13	29	0.8262	1.0767	1.3032	643.07	228.60
14	29	0.8650	1.1393	1.3171	485.69	219.85
15	29	0.9012	1.2002	1.3318	388.60	214.45

LIMITING SLCPE=0.02202

APPENDIX I.6

TABLES IV.6

MEASURED VALUES OF THE ADSORBED PHASE
 PROPERTIES IN MIXTURES

The calculated adsorbed phase properties constituted of the molar composition (X), the mixture molar area (N : millimoles/gram) and the mixture spreading pressure ($\frac{\pi A}{RT}$: millimoles/gram) for each constant gas phase molar composition isotherm are listed in the following tables, at regular interval of system pressure (mmHg). Phase equilibrium calculations have been done using the exact thermodynamic relationship.

<u>TABLE</u>	<u>SYSTEM</u>	<u>TEMPERATURE</u> °K
IV.6.1	Carbon dioxide (1) - Ethane (2)	263.2
IV.6.2	Carbon dioxide (1) - Ethane (2)	273.2
IV.6.3	Carbon dioxide (1) - Ethane (2)	298.2
IV.6.4	Ethylene (1) - Ethane (2)	263.2
IV.6.5	Ethylene (1) - Ethane (2)	273.2
IV.6.6	Ethylene (1) - Ethane (2)	298.2
IV.6.7	Propane (1) - Carbon dioxide (2)	263.2
IV.6.8	Propane (1) - Carbon dioxide (2)	273.2
IV.6.9	Propane (1) - Carbon dioxide (2)	298.2
IV.6.10	Propane (1) - Carbon dioxide (2)	323.2

The symbols and units employed in Tables IV.6 are defined as follows:

- P gas pressure, mmHg.
- X mole fraction of component 1 adsorbed defined by Equation II.16.
- N amount of gas mixture adsorbed defined by Equations II.12 and II.13, millimoles/gr.
- PI spreading pressure of mixture defined by Equation II.14.

Values of the mole fractions in the gas mixture are those for the heavier component adsorbed; component 1.

The computer program is listed in Appendix IV.

TABLE IV.6.1

THANE - CARBON DIOXIDE - SILICA GEL AT -10.0 DEG. CENTIGRADE GRAVELLE

P	0.4960				0.7522				
	X	N	PI	X	N	PI	X	N	PI
50.0	0.5089	0.2960	0.3328	0.6508	0.3576	0.4099	0.8698	0.4003	0.4575
100.0	0.5077	0.5026	0.6061	0.6567	0.5915	0.7348	0.8721	0.6594	0.8188
150.0	0.5048	0.6675	0.8433	0.6601	0.7731	1.0111	0.8732	0.8592	1.1251
200.0	0.5016	0.8092	1.0560	0.6619	0.9281	1.2559	0.8734	1.0288	1.3960
250.0	0.4987	0.9356	1.2509	0.6628	1.0672	1.4789	0.8731	1.1801	1.6421
300.0	0.4964	1.0508	1.4322	0.6632	1.1950	1.6854	0.8726	1.3187	1.8697
350.0	0.4947	1.1568	1.6025	0.6636	1.3140	1.8791	0.8720	1.4472	2.0828
400.0	0.4937	1.2546	1.7636	0.6639	1.4252	2.0623	0.8715	1.5669	2.2839
450.0	0.4933	1.3451	1.9167	0.6643	1.5291	2.2366	0.8710	1.6786	2.4750
500.0	0.4935	1.4288	2.0629	0.6649	1.6263	2.4031	0.8706	1.7829	2.6573
550.0	0.4941	1.5062	2.2029	0.6656	1.7170	2.5628	0.8703	1.8802	2.8318
600.0	0.4950	1.5778	2.3372	0.6664	1.8015	2.7162	0.8702	1.9708	2.9993
650.0	0.4963	1.6439	2.4664	0.6674	1.8801	2.8639	0.8702	2.0552	3.1604
700.0	0.4978	1.7050	2.5907	0.6685	1.9531	3.0064	0.8703	2.1336	3.3156
750.0	0.4996	1.7614	2.7106	0.6697	2.0210	3.1440	0.8704	2.2065	3.4653

TABLE IV.6.2

THANE - CARBON DIOXIDE - SILICA GEL AT 0.0 DEG. CENTIGRADE GRAVELLE

P	0.4960				0.7522				
	X	N	PI	X	N	PI	X	N	PI
50.0	0.5798	0.1589	0.1664	0.9157	0.2245	0.2428	0.9049	0.2929	0.3308
100.0	0.5599	0.2988	0.3208	0.8949	0.3918	0.4510	0.9079	0.4894	0.5974
150.0	0.5461	0.4238	0.4657	0.8759	0.5308	0.6366	0.9081	0.6440	0.8263
200.0	0.5365	0.5366	0.6028	0.8593	0.6532	0.8063	0.9071	0.7767	1.0305
250.0	0.5296	0.6389	0.7330	0.8453	0.7644	0.9642	0.9057	0.8962	1.2171
300.0	0.5245	0.7322	0.8571	0.8337	0.8670	1.1127	0.9041	1.0062	1.3907
350.0	0.5209	0.8177	0.9758	0.8242	0.9621	1.2534	0.9028	1.1086	1.5538
400.0	0.5182	0.8964	1.0896	0.8166	1.0506	1.3875	0.9016	1.2042	1.7083
450.0	0.5163	0.9690	1.1989	0.8105	1.1329	1.5159	0.9007	1.2937	1.8555
500.0	0.5150	1.0363	1.3040	0.8057	1.2094	1.6390	0.9001	1.3773	1.9963
550.0	0.5141	1.0989	1.4054	0.8019	1.2803	1.7574	0.8998	1.4554	2.1314
600.0	0.5135	1.1572	1.5033	0.7991	1.3461	1.8714	0.8996	1.5281	2.2613
650.0	0.5132	1.2117	1.5979	0.7969	1.4071	1.9813	0.8997	1.5958	2.3864
700.0	0.5132	1.2627	1.6895	0.7954	1.4636	2.0875	0.8999	1.6587	2.5072
750.0	0.5133	1.3106	1.7783	0.7943	1.5159	2.1900	0.9003	1.7173	2.6238

TABLE IV.6.3

THANE - CARBON DIOXIDE - SILICA GEL AT 25.0 DEG. CENTIGRADE GRAVELLE

GAS MOLE FRACTION:
0.2592

0.4960

0.7522

P	X	N	PI	X	N	PI	X	N	PI
50.0	0.4620	0.0785	0.0814	0.7745	0.0945	0.1006	0.8476	0.1194	0.1279
100.0	0.4533	0.1496	0.1581	0.7595	0.1762	0.1921	0.8516	0.2147	0.2408
150.0	0.4468	0.2154	0.2314	0.7460	0.2505	0.2779	0.8543	0.2974	0.3439
200.0	0.4422	0.2767	0.3017	0.7353	0.3191	0.3594	0.8560	0.3730	0.4400
250.0	0.4392	0.3341	0.3695	0.7271	0.3831	0.4374	0.8569	0.4441	0.5311
300.0	0.4373	0.3881	0.4350	0.7210	0.4431	0.5124	0.8573	0.5117	0.6181
350.0	0.4363	0.4390	0.4985	0.7165	0.4997	0.5847	0.8575	0.5763	0.7020
400.0	0.4359	0.4871	0.5601	0.7132	0.5532	0.6548	0.8575	0.6380	0.7831
450.0	0.4359	0.5327	0.6199	0.7108	0.6041	0.7227	0.8576	0.6967	0.8617
500.0	0.4362	0.5760	0.6782	0.7090	0.6525	0.7888	0.8577	0.7523	0.9380
550.0	0.4368	0.6172	0.7349	0.7076	0.6987	0.8531	0.8578	0.8047	1.0122
600.0	0.4375	0.6565	0.7902	0.7064	0.7430	0.9159	0.8581	0.8539	1.0844
650.0	0.4382	0.6940	0.8443	0.7054	0.7855	0.9771	0.8584	0.9000	1.1547
700.0	0.4390	0.7299	0.8970	0.7044	0.8264	1.0369	0.8589	0.9430	1.2230
750.0	0.4398	0.7643	0.9486	0.7035	0.8658	1.0955	0.8594	0.9830	1.2895

TABLE IV.6.4

THANE - ETHYLENE - SILICA GEL AT -10.0 DEG. CENTIGRADE GRAVELLE

GAS MOLE FRACTION: 0.2635		0.5042		0.7547					
P	X	N	PI	X	N	PI	X	N	PI
50.0	0.5618	0.3349	0.4022	0.6685	0.3932	0.4772	0.8614	0.4488	0.5499
100.0	0.5668	0.5292	0.6993	0.6805	0.6124	0.8230	0.8666	0.6903	0.9418
150.0	0.5645	0.6729	0.9425	0.6877	0.7716	1.1030	0.8696	0.8620	1.2558
200.0	0.5590	0.7933	1.1530	0.6917	0.9034	1.3436	0.8712	1.0013	1.5235
250.0	0.5523	0.9008	1.3417	0.6934	1.0198	1.5580	0.8717	1.1221	1.7602
300.0	0.5455	0.9999	1.5147	0.6937	1.1261	1.7534	0.8716	1.2305	1.9746
350.0	0.5391	1.0926	1.6758	0.6931	1.2245	1.9344	0.8710	1.3293	2.1717
400.0	0.5333	1.1797	1.8274	0.6919	1.3163	2.1040	0.8701	1.4203	2.3553
450.0	0.5283	1.2618	1.9711	0.6904	1.4020	2.2640	0.8690	1.5044	2.5275
500.0	0.5240	1.3389	2.1081	0.6888	1.4823	2.4159	0.8678	1.5823	2.6901
550.0	0.5204	1.4114	2.2392	0.6871	1.5572	2.5608	0.8667	1.6547	2.8445
600.0	0.5175	1.4794	2.3650	0.6855	1.6273	2.6994	0.8655	1.7218	2.9915
650.0	0.5151	1.5430	2.4860	0.6840	1.6926	2.8324	0.8644	1.7842	3.1320
700.0	0.5132	1.6025	2.6027	0.6825	1.7535	2.9602	0.8633	1.8423	3.2666
750.0	0.5118	1.6581	2.7153	0.6812	1.8104	3.0834	0.8623	1.8962	3.3958

TABLE IV.6.5

THANE - ETHYLENE - SILICA GEL AT 0.0 DEG. CENTIGRADE GRAVELLE

GAS MOLE FRACTION:
0.2635

0.5042 0.7547

P	X	N	PI	X	N	PI	X	N	PI
50.0	0.4649	0.1452	0.1487	0.7938	0.1980	0.2129	0.9380	0.2347	0.2554
100.0	0.4605	0.2757	0.2901	0.7841	0.3539	0.3997	0.9302	0.4124	0.4751
150.0	0.4579	0.3930	0.4245	0.7750	0.4854	0.5687	0.9231	0.5585	0.6708
200.0	0.4564	0.4986	0.5523	0.7670	0.6008	0.7244	0.9171	0.6842	0.8490
250.0	0.4555	0.5942	0.6740	0.7603	0.7046	0.8698	0.9119	0.7954	1.0139
300.0	0.4551	0.6809	0.7901	0.7547	0.7988	1.0067	0.9075	0.8952	1.1678
350.0	0.4550	0.7599	0.9011	0.7502	0.8846	1.1364	0.9039	0.9856	1.3127
400.0	0.4551	0.8322	1.0074	0.7467	0.9636	1.2597	0.9009	1.0679	1.4498
450.0	0.4554	0.8985	1.1093	0.7439	1.0362	1.3775	0.8984	1.1432	1.5800
500.0	0.4557	0.9595	1.2072	0.7417	1.1030	1.4902	0.8964	1.2121	1.7040
550.0	0.4561	1.0159	1.3013	0.7401	1.1646	1.5982	0.8947	1.2755	1.8226
600.0	0.4566	1.0681	1.3920	0.7389	1.2215	1.7020	0.8934	1.3338	1.9361
650.0	0.4572	1.1165	1.4794	0.7381	1.2739	1.8019	0.8923	1.3874	2.0450
700.0	0.4577	1.1616	1.5638	0.7376	1.3224	1.8981	0.8914	1.4370	2.1497
750.0	0.4583	1.2037	1.6454	0.7373	1.3673	1.9909	0.8907	1.4828	2.2504

TABLE IV.6.6

THANE - ETHYLENE - SILICA GEL AT 25.0 DEG. CENTIGRADE GRAVELLE

GAS MOLE FRACTION:
0.2635

0.5042

0.7547

P	X	N	PI	X	N	PI	X	N	PI
50.0	0.4907	0.0932	0.0994	0.6854	0.1191	0.1295	0.8779	0.1323	0.1437
100.0	0.4884	0.1690	0.1879	0.6898	0.2104	0.2412	0.8788	0.2336	0.2678
150.0	0.4850	0.2352	0.2692	0.6919	0.2873	0.3414	0.8787	0.3189	0.3791
200.0	0.4814	0.2956	0.3452	0.6924	0.3558	0.4336	0.8780	0.3947	0.4814
250.0	0.4779	0.3521	0.4173	0.6921	0.4189	0.5198	0.8769	0.4641	0.5770
300.0	0.4749	0.4055	0.4863	0.6913	0.4777	0.6015	0.8757	0.5287	0.6674
350.0	0.4725	0.4560	0.5526	0.6903	0.5330	0.6793	0.8744	0.5892	0.7535
400.0	0.4705	0.5039	0.6166	0.6893	0.5850	0.7539	0.8733	0.6459	0.8359
450.0	0.4691	0.5492	0.6786	0.6884	0.6339	0.8256	0.8722	0.6991	0.9151
500.0	0.4682	0.5919	0.7388	0.6877	0.6798	0.8948	0.8713	0.7488	0.9913
550.0	0.4676	0.6319	0.7971	0.6872	0.7228	0.9617	0.8706	0.7953	1.0649
600.0	0.4674	0.6694	0.8537	0.6869	0.7629	1.0263	0.8700	0.8386	1.1360
650.0	0.4675	0.7044	0.9087	0.6868	0.8004	1.0889	0.8697	0.8790	1.2047
700.0	0.4679	0.7370	0.9621	0.6869	0.8352	1.1495	0.8694	0.9166	1.2713
750.0	0.4684	0.7673	1.0140	0.6872	0.8677	1.2082	0.8693	0.9515	1.3357

TABLE IV.6.7

ARBON DIOXIDE - PROPANE - SILICA GEL AT -10.0 DEG CENTIGRADE GRAVELLE

GAS MOLE FRACTION:
0.2385

0.4527

0.7494

P	X	N	PI	X	N	PI	X	N	PI
50.0	0.4140	0.6041	0.7334	0.5655	0.6763	0.8343	0.7770	0.7223	0.8842
100.0	0.4201	0.9353	1.2619	0.5770	1.0312	1.4211	0.7817	1.1093	1.5133
150.0	0.4226	1.1730	1.6880	0.5842	1.2828	1.8889	0.7850	1.3853	2.0176
200.0	0.4231	1.3677	2.0529	0.5891	1.4885	2.2869	0.7875	1.6110	2.4479
250.0	0.4226	1.5379	2.3767	0.5925	1.6688	2.6388	0.7893	1.8086	2.8290
300.0	0.4215	1.6916	2.6709	0.5949	1.8322	2.9577	0.7907	1.9874	3.1749
350.0	0.4203	1.8328	2.9425	0.5968	1.9829	3.2517	0.7918	2.1519	3.4938
400.0	0.4191	1.9635	3.1959	0.5984	2.1228	3.5258	0.7927	2.3044	3.7913
450.0	0.4180	2.0848	3.4343	0.5998	2.2531	3.7835	0.7935	2.4463	4.0711
500.0	0.4171	2.1978	3.6600	0.6011	2.3747	4.0274	0.7943	2.5784	4.3359
550.0	0.4163	2.3029	3.8746	0.6024	2.4880	4.2593	0.7949	2.7016	4.5876
600.0	0.4157	2.4007	4.0794	0.6037	2.5938	4.4806	0.7956	2.8163	4.8279
650.0	0.4152	2.4918	4.2754	0.6050	2.6924	4.6925	0.7962	2.9232	5.0579
700.0	0.4149	2.5766	4.4634	0.6063	2.7842	4.8958	0.7967	3.0227	5.2786
750.0	0.4148	2.6555	4.6442	0.6077	2.8699	5.0913	0.7973	3.1155	5.4907

TABLE IV.6.8

ARBON DIOXIDE - PROPANE - SILICA GEL AT 0.0 DEG CENTIGRADE GRAVELLE

GAS MOLE FRACTION:
0.2385

0.4527

0.7494

P	X	N	PI	X	N	PI	X	N	PI
50.0	0.4464	0.4147	0.4828	0.6405	0.4727	0.5589	0.8040	0.5383	0.6483
100.0	0.4481	0.6710	0.8541	0.6431	0.7524	0.9784	0.8053	0.8408	1.1213
150.0	0.4473	0.8644	1.1642	0.6433	0.9598	1.3243	0.8058	1.0616	1.5057
200.0	0.4452	1.0266	1.4356	0.6424	1.1326	1.6247	0.8058	1.2452	1.8369
250.0	0.4426	1.1702	1.6804	0.6410	1.2853	1.8941	0.8057	1.4081	2.1325
300.0	0.4398	1.3011	1.9055	0.6395	1.4245	2.1409	0.8055	1.5574	2.4026
350.0	0.4371	1.4219	2.1153	0.6382	1.5531	2.3703	0.8054	1.6963	2.6533
400.0	0.4347	1.5343	2.3126	0.6370	1.6728	2.5856	0.8053	1.8262	2.8884
450.0	0.4326	1.6389	2.4994	0.6361	1.7845	2.7892	0.8052	1.9480	3.1107
500.0	0.4308	1.7365	2.6772	0.6355	1.8887	2.9827	0.8053	2.0622	3.3220
550.0	0.4293	1.8275	2.8471	0.6352	1.9859	3.1674	0.8054	2.1692	3.5237
600.0	0.4281	1.9123	3.0098	0.6351	2.0766	3.3442	0.8056	2.2692	3.7169
650.0	0.4272	1.9912	3.1661	0.6353	2.1612	3.5139	0.8059	2.3626	3.9024
700.0	0.4266	2.0647	3.3165	0.6356	2.2399	3.6771	0.8062	2.4499	4.0809
750.0	0.4261	2.1331	3.4614	0.6361	2.3133	3.8343	0.8065	2.5313	4.2530

TABLE IV.6.9

ARBON DIOXIDE - PROPANE - SILICA GEL AT 25.0 DEG CENTIGRADE GRAVELLE

P	GAS MOLE FRACTION: 0.2385				0.4527				0.7494			
	X	N	PI	X	N	PI	X	N	PI	X	N	PI
50.0	0.4886	0.1633	0.1756	0.7836	0.1924	0.2106	0.8425	0.2509	0.2883			
100.0	0.4774	0.2922	0.3297	0.7618	0.3360	0.3899	0.8428	0.4130	0.5149			
150.0	0.4671	0.4026	0.4695	0.7434	0.4553	0.5493	0.8416	0.5392	0.7070			
200.0	0.4582	0.5018	0.5991	0.7278	0.5609	0.6950	0.8398	0.6482	0.8774			
250.0	0.4506	0.5933	0.7210	0.7146	0.6575	0.8307	0.8376	0.7480	1.0329			
300.0	0.4443	0.6788	0.8369	0.7035	0.7475	0.9586	0.8354	0.8417	1.1776			
350.0	0.4392	0.7590	0.9476	0.6943	0.8320	1.0803	0.8334	0.9308	1.3141			
400.0	0.4351	0.8343	1.0539	0.6868	0.9114	1.1966	0.8316	1.0157	1.4440			
450.0	0.4319	0.9050	1.1563	0.6807	0.9860	1.3083	0.8300	1.0966	1.5683			
500.0	0.4294	0.9712	1.2551	0.6758	1.0560	1.4159	0.8288	1.1734	1.6879			
550.0	0.4274	1.0331	1.3506	0.6720	1.1216	1.5196	0.8278	1.2461	1.8032			
600.0	0.4260	1.0908	1.4430	0.6691	1.1828	1.6199	0.8270	1.3146	1.9146			
650.0	0.4249	1.1445	1.5325	0.6669	1.2399	1.7168	0.8265	1.3790	2.0224			
700.0	0.4242	1.1944	1.6191	0.6653	1.2931	1.8107	0.8261	1.4393	2.1269			
750.0	0.4237	1.2409	1.7032	0.6643	1.3426	1.9016	0.8259	1.4957	2.2282			

TABLE IV.6.10

ARBON DIOXIDE - PROPANE - SILICA GEL AT 50.0 DEG CENTIGRADE GRAVELLE

GAS MOLE FRACTION:
0.2385

0.4527

0.7494

P	X	N	PI	X	N	PI	X	N	PI
50.0	0.4809	0.0727	0.0756	0.7080	0.0886	0.0944	0.8368	0.1083	0.1178
100.0	0.4648	0.1378	0.1463	0.6926	0.1611	0.1787	0.8380	0.1908	0.2192
150.0	0.4521	0.1576	0.2136	0.6782	0.2250	0.2563	0.8378	0.2610	0.3101
200.0	0.4424	0.2534	0.2782	0.6656	0.2841	0.3292	0.8367	0.3250	0.3941
250.0	0.4351	0.3057	0.3404	0.6553	0.3400	0.3987	0.8353	0.3856	0.4732
300.0	0.4296	0.3552	0.4006	0.6470	0.3936	0.4654	0.8338	0.4442	0.5487
350.0	0.4256	0.4020	0.4589	0.6407	0.4452	0.5300	0.8322	0.5012	0.6215
400.0	0.4226	0.4465	0.5155	0.6360	0.4947	0.5927	0.8308	0.5567	0.6921
450.0	0.4204	0.4889	0.5706	0.6328	0.5420	0.6537	0.8295	0.6103	0.7607
500.0	0.4188	0.5295	0.6242	0.6306	0.5870	0.7132	0.8284	0.6620	0.8277
550.0	0.4176	0.5683	0.6765	0.6293	0.6296	0.7712	0.8274	0.7113	0.8932
600.0	0.4167	0.6055	0.7276	0.6287	0.6697	0.8277	0.8266	0.7582	0.9571
650.0	0.4160	0.6413	0.7775	0.6287	0.7073	0.8828	0.8260	0.8025	1.0195
700.0	0.4154	0.6757	0.8263	0.6290	0.7425	0.9365	0.8255	0.8441	1.0806
750.0	0.4149	0.7088	0.8741	0.6297	0.7753	0.9889	0.8252	0.8831	1.1401

APPENDIX II

SPECIFIC SURFACE AREA CALCULATION USING THE BET EQUATION

This program was used to calculate the specific surface area of the silica gel employed in this work.

The input data are read as follows:

- 1) Title
- 2) Liquid nitrogen saturation pressure at 77.4°K (P0) and the weight of the adsorbent (WT).
- 3) Pressure in the system (X) and total mass of N_2 adsorbed (Y).

The specific surface areas are reported in Table IV.1 of Appendix I.

CC01 DIMENSION Y(50), X(50), YAXIS(50), XAXIS(50), ER(50), YCALC(50), AN(20)
CC02 DIMENSION THETA(50), PHINX(50), ASLOPE(20), BINTER(20), STD(20), V(50).
CC03 DIMENSION STORE(20), TITLE(20), ERROR(20)

C
C
C READ IN DEPENDENT AND INDEPENDENT VARIABLES
C
C

CCC4 28 READ(1,22,END=30) (TITLE(I), I=1,20)
CCC5 22 FORMAT(20A4)
CCC6 WRITE(3,23) (TITLE(I), I=1,20)
CCC7 23 FORMAT(1H1,20A4//)

C
C READ(1,24) PO,AINC
C
C READ(1,24) PC,WT
CCC8
CCC9 24 FORMAT(4F10.0)

CC10 J=0
CC11 1 J=J+1
C READ(1,3) Y(J), X(J), L
CC12 READ(1,3) X(J), Y(J), L
CC13 IF(L.EQ.1) GC TO 2
C Y(J)=Y(J)/WT

CC14 X(J)=X(J)/PC
CC15 GC TO 1
CC16 2 J=J-1
CC17 AF=J
CC18 3 FCRMAT(2F10.0, I1)

C
C
C SET VALUES OF LAYERS
C
C

CC19 27 IF(PC.EG.1.0) GO TO 31
CC20 PC=PO-AINC

C
C
C IF(PO) 28,28,31
CC19 31 WRITE(3,13)
CC20 13 FCRMAT(1F0, TRIAL NO., 10X, N', 7X, ERROR', 5X, VM', 8X, C'//)

CC21 NFN=10
CC22 NPREC=0
CC23 AK=1.
C FAC=1.

CC24 AN(1)=1.0
CC25
CC26 4 NPREC=NPREC+1
CC27 CC 5 K=2,NFN

5 AN(K)=AN(K-1)+AK

N-LAYERS B.E.T. EQU. PARAMETERS VM AND C

DC 9 K=1,NFN

SUM1=0.

SUM2=0.

SUM3=0.

SUM4=0.

DO 6 I=1,J

PREPARE X- AND Y-AXIS

XX=X(I)

IF(XX-0.6) 25,25,26

25 PHINX(I)=XX*(1.-XX**AN(K))-AN(K)*XX**AN(K)*(1.-XX)
1/((1.-XX)*(1.-XX))

THETA(I)=XX*(1.-XX**AN(K))/(1.-XX)

YAXIS(I)=PHINX(I)/Y(I)

XAXIS(I)=THETA(I)

LEAST-SQUARES METHOD

SUM1=SUM1+YAXIS(I)

SUM2=SUM2+XAXIS(I)*XAXIS(I)

SUM3=SUM3+XAXIS(I)*YAXIS(I)

SUM4=SUM4+XAXIS(I)

CONTINUE

DC=AP*SUM2-SUM4*SUM4

ASLOPE(K)=(AP*SUM3-SUM4*SUM1)/DD

RINTER(K)=(SUM1*SUM2-SUM3*SUM4)/DD

CALCULATE THE DEPENDENT VARIABLES

CC 7 I=1,J

CC49 7 YCALC(I)=ASLCPE(K)*XAXIS(I)+BINTER(K)

C

C

EVALUATE STANDARD DEVIATION

C

C

C

CC50 S=0.

CC51 S1=0.

CC52 S2=0.

CC53 E=0.

CC54 DC 8 I=1,J

CC55 DEL=YCALC(I)-YAXIS(I)

CC56 S=S+DEL*DEL/YCALC(I)

CC57 S2=S2+ABS(DEL)

CC58 ER(I)=DEL*10C./YAXIS(I)

CC59 E=F+ABS(ER(I))

CC60 8 S1=S1+CFL*DEL

CC61 ERROR(K)=E/AP

CC62 CEV=S2/AP

CC63 STD(K)=SQRT(S1/((AP-2.))

CC64 9 CCNTINUE

C

C

C

C

C

SELECT SMALLEST STD

CC65 K=2

CC66 KK=K

CC67 AJ=STD(1)

CC68 33 DO 35 I=KK,NFN

CC69 IF(AJ-STD(I)) 34,34,36

CC70 K=K+1

CC71 35 CCNTINUE

CC72 GC TO 37

CC73 36 AJ=STD(K)

CC74 KK=K

CC75 GO TO 33

CC76 NTEST=1

CC77 IF(KK.EQ.2) GO TO 55

CC78 K=KK

CC79 GC TO 12

CC80 55 IF(STD(1).GT.STD(2)) GO TO 64

CC81 K=1

FCRTRAN IV G LEVEL 19

CC82 GC TO 12

CC83 64 K=2

CC84 12 CCNTINUE

CC85 VM=1./ASLOPE(K)

CC86 C=1./((VM*BINTER(K)))

CC87 WRITE(3,14) NPREC1,AN(K),ERROR(K),VM,C

CC88 14 FCRMAT(IH0,3X,I2,7X,4F10.4)

C

C

SELECT NEW INTERVAL FOR N

C

C

CC89 AN(I)=AN(K)-1.*FAC

CC90 IF(AN(I).EQ.C.000) GO TO 18

CC91 NFN=20

CC92 GC TO 19

CC93 18 NFN=20

CC94 AN(I)=.1

CC95 19 FAC=FAC/10.

CC96 AK=AK/10.

CC97 STORE(NPREC1)=STD(K)

CC98 IF(NPREC1.EQ.1) GO TO 4

CC99 DENO =(STORE(NPREC1))+STORE(NPREC1-1))/200.

CC100 CCMP=ABS(STORE(NPREC1-1)-STORE(NPREC1))/DENO

C101 IF(COMP-0.01) 10,10,20

C102 20 IF(NPREC1.LT.20) GO TO 4

C

C

RECALCULATE THE AMOUNT ADSORBED AND COMPARE

C

C

C103 10 S=0.

C104 S1=0.

C105 S2=0.

C106 E=0.

C107 DO 11 I=1,J

C108 XX=X(I)

C109 PHINX(I)=XX*(1.-XX**AN(K))-AN(K)*XX**AN(K)*(1.-XX))

1/((1.-XX)*(1.-XX))

THETA(I)=XX*(1.-XX**AN(K))/(1.-XX)

V(I)=VM*C*PHINX(I)/(1.+C*THETA(I))

C110 DEL=V(I)-Y(I)

C111 S=S+DEL*DEL/V(I)

C112


```

0150 S=0.
0151 S1=0.0
0152 S2=0.0
0153 E=C.0
0154 DC 40 I=1,J
0155 V(I) =(VM*C*X(I))/(1.-X(I))+X(I)*(1.-X(I))*(C-1.)
0156 CEL=V(I) -Y(I)
0157 S=S+DEL*DEL/V(I)
0158 S2=S2+ABS(DEL)
0159 PR(I)=CEL*100./Y(I)
0160 E=E+ABS(ER(I))
0161 40 S1=S1+DEL*DEL
0162 AVER=E/AP
0163 DEV=S2/AP
0164 SD =SQRT(S1/(AP-2.))
0165 WRITE(3,21)
0166 WRITE(3,15) (I,X(I),Y(I),V(I),ER(I),I=1,J)
0167 WRITE(3,16) AVER,DEV,SD,S
0168 WRITE(3,17) VM,C
0169 WRITE(3,50) AREA
0170 50 FORMAT(1H0,'THE SURFACE AREA IN SQUARE METERS PER GRAM OF ADSORBEN
IT IS',F10.2)
C IF(PO.EQ.1.0) GO TO 28
CC TO 28
0171 C
0172 30 RETURN
0173 END

```

APPENDIX III

CORRELATION OF THE ADSORPTION DATA USING THE BET EQUATION

Adsorption isotherms were measured at irregular pressure intervals. To facilitate computer programming, the n-layers BET equation was found appropriate to represent the isotherms of both pure or mixtures of gases adsorbed. Therefore, the mass of gas adsorbed at equally spaced intervals of pressures were obtained and used in the computer programs described in Appendices IV to VI.

The input data are read in the following order:

- 1) Corrections due to thermomolecular effects for each isotherm (5) of a binary mixture (TMF(I)).
- 2) Corrections due to buoyancy effects for each pure constituent of a binary mixture (CORL, CORH).
- 3) Molecular weights of each component (AM1, AM2).
- 4) Weight of the adsorbent and composition in the gas phase measured for each isotherm (WT, YM(J)).
- 5) Pressure and mass of each experimental point (X(I), Y(I)).

This program uses the subroutine BET listed in Appendix IV.

The solid lines of Figures III.3 were drawn based on results of this correlation.

```

C      TO COMPUTE THE BET REPRESENTATION OF THE ADSORPTION ISOTHERMS
1      DIMENSION X(20),Y(20),YY(20,5),TITLE(20),YM(5),YI(20,5)
2      DIMENSION E(5),TMF(5)
3      DO 13 K=1,10
4      READ(5,10)      (TITLE(I),I=1,20)
5      PO=80.
6      READ(5,26) (TMF(I),I=1,5)
7      READ(5,4) CORL,CORH
8      READ(5,4) AM1,AM2.
9      DO 3 J=1,5
10     READ (5,4)      WT,YM(J)
11     WT1=WT
12     WT=WT+TMF(J)/1000.
13     WT2=WT
14     CORAV=YM (J)*CORH+(1.-YM (J))*CORL
15     I=0
16     1 I=I+1.
17     READ(5,4) X(I),Y(I),N
18     XI(I,J)=X(I)
19     C=CORAV*X(I)/76.
20     X(I)=X(I)/PO
21     Y(I)=Y(I)*WT1
22     Y(I)=Y(I)-TMF(J)-C
23     Y(I)=Y(I)/WT2
24     YI(I,J)=Y(I)
25     IF(N-1) 1,2,2
26     2,N=I-1
27     NR=0
28     CALL BET(Y,X,N,C1,VM,C,A,PO,NR,C4)
29     AN=-5.0
30     DO 5 I=1,16
31     AN=AN+5.0
32     X(I)=AN
33     XX=X(I)/PO
34     PH=XX*((1.-XX**C1)-C1*XX**C1*(1.-XX))/((1.-XX)*(1.-XX))
35     TH=XX*(1.-XX**C1)/(1.-XX)
36     5 YY(I,J)=VM*C*PH/(1.+C*TH)
37     E(J)=A
38     3 CONTINUE
39     WRITE(6,16)
40     WRITE(6,21)
41     WRITE(6,12) (TITLE(I),I=1,20)
42     WRITE(6,20)
43     WRITE(6,19)(YM(J),J=1,5)
44     WRITE(6,21)
45     WRITE(6,22)
46     DO 24 I=1,N
47     DO 24 J=1,5

```

```
24 XI(I,J)=XI(I,J)*10.
DO 17 I=1,N
WRITE(6,18) (XI(I,J),YI(I,J),J=1,5)
17 CONTINUE
WRITE(6,21)
WRITE(6,14)
WRITE(6,11) (TITLE(I),I=1,20)
WRITE(6,15)(YM(J),J=1,5)
DO 25 I=1,16
25 X(I)=X(I)*10.
DO 8 I=1,16
8 WRITE(6,6) X(I),(YY(I,J),J=1,5)
WRITE(6,23) (E(J),J=1,5)
13 CONTINUE
RETURN
4 FORMAT(2F10.0,I1)
7 FORMAT(6F10.3)
10 FORMAT(20A4)
16 FORMAT(1H1,/////////,
1 33X,'EXPERIMENTAL ADSORPTION DATA',/,26X,'MILLIGRAMS AD
1SORBED PER GRAM ADSORBENT - M',/,33X,'TOTAL PRESSURE IN MM-HG - P'
2)
7 20 FORMAT(1H0,21X,'GAS PHASE COMPOSITION - PER CENT HEAVY COMPONENT')
3 19 FORMAT(1H0,5X,5(F8.4,10X))
9 21 FORMAT(1H0,2X,'*****')
6 1 *****')
1 22 FORMAT(1H0,5X,5('P',7X,'M',9X))
1 18 FORMAT(1H0,5(F8.2,F8.3,2X))
2 14 FORMAT(1H1,17X,'SMOOTHED INTERPOLATED DATA',/,11X,'MILLIGRAMS ADSO
2 1RBED PER GRAM ADSORBENT - M')
3 12 FORMAT(1H0,11X,20A4)
4 11 FORMAT(1H0,20A4)
5 15 FORMAT(1H0,2X,'TOTAL',18X,'GAS PHASE COMPOSITION',/,1X,'PRESSURE',
5 116X,'PER CENT HEAVY COMPONENT',/,2X,'(MM-HG)',1X,5F10.4,/,,'*****
6 2*****')
6 6 FORMAT(1H0,F5.1,6X,5F10.3)
7 23 FORMAT(1H0,'AVERAGE PERCENT DEVIATION IN M',/,10X,5F10.3)
8 26 FORMAT(5F10.0)
9 END
```

APPENDIX IV

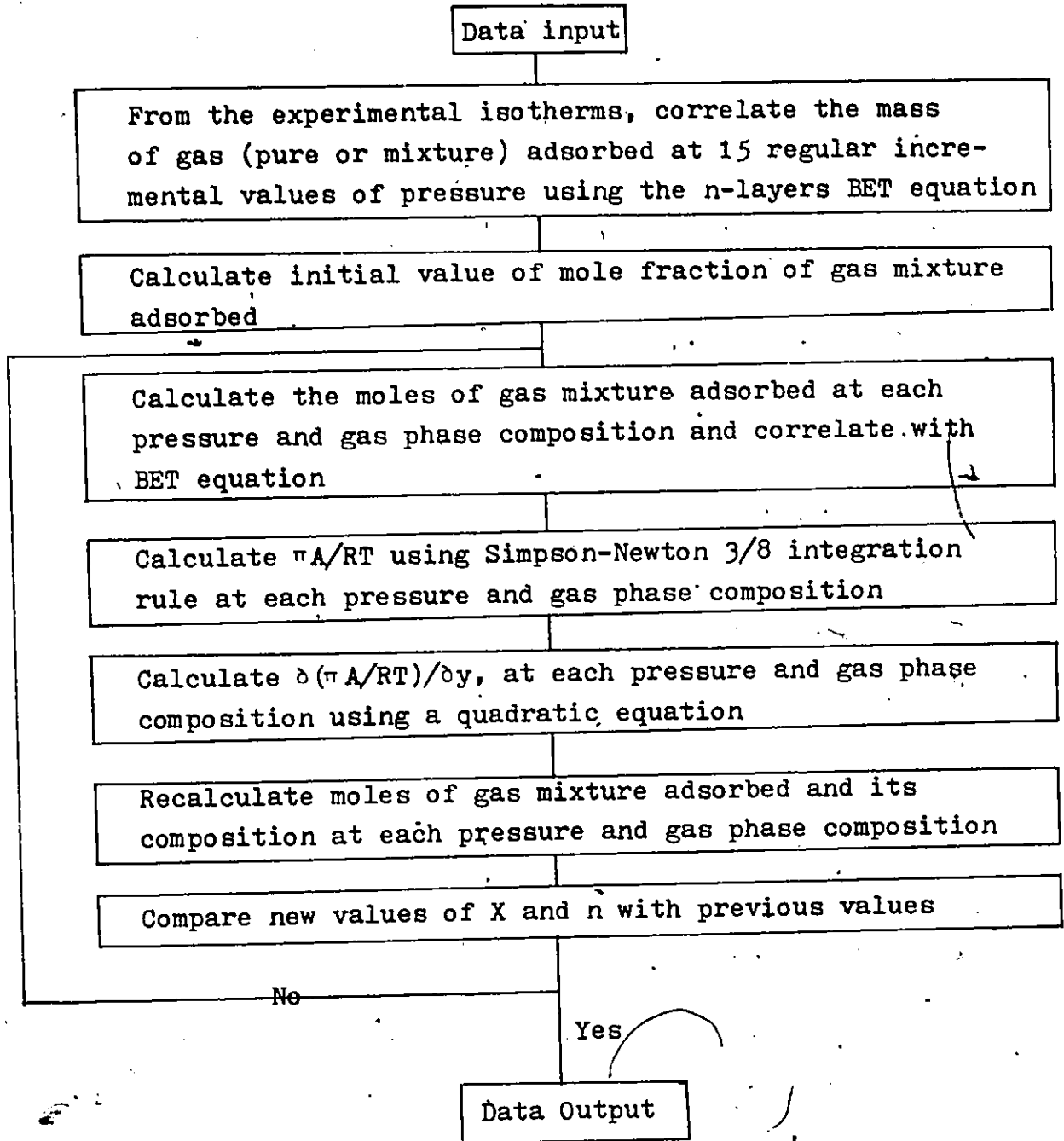
CALCULATION OF PHASE EQUILIBRIA USING AN EXACT
THERMODYNAMIC RELATIONSHIP

This program was used to determine the experimental moles of a binary gas mixture adsorbed and its molar composition using the exact thermodynamic relationship, derived in Section II.A.

The input data are read in the following order:

- 1) Title
- 2) Coefficient n' of the BET equation
- 3) Thermomolecular effects
- 4) Buoyancy effects of each pure component
- 5) Molecular weights of each pure component
- 6) Mass of adsorbent and molar composition in the gas phase
- 7) Mass of gas adsorbed (experimental) and pressure

The iteration scheme followed to determine the experimental values of a mixture of gas adsorbed and its composition is illustrated below:



DATA INPUT

ETHANE - ETHYLENE - SILICA GEL AT 0.0 DEG. CENTIGRADE

3.36	1.07	2.94	2.85	2.89
0.19	0.212	0.212	0.212	0.212

0.022	0.0365
30.068	28.052
0.15785	0.0
2.85	3.55
11.21	9.17
23.48	15.23
38.62	21.24
61.66	28.87
75.45	32.64

1

0.106662	0.2635
2.895	4.483
11.12	11.124
23.47	18.608
38.00	25.342
52.53	30.726
64.83	34.684
73.10	37.141
76.00	37.985

1

0.106574	0.5042
2.895	5.461
11.12	13.418
23.47	21.562
38.00	28.619
52.53	34.342
64.83	38.490
73.10	41.079
76.00	41.886

1

0.106574	0.7547
2.895	6.099
11.12	15.126
23.47	23.646
38.00	31.358
52.53	37.232
64.83	41.286
73.10	43.894
76.00	44.758

1

0.106726	1.0
2.895	6.971
11.12	16.716
23.47	25.673
38.00	33.263
52.53	39.072
64.83	43.213
73.10	45.687
76.00	46.512

1

The output data are listed in Tables IV.2 and IV.6 of Appendix I.

```

FORTRAN IV G LEVEL 21
DATE = 1968
MAIN
C DENIS GRAVELLE,CHEMICAL ENGINEERING
C ADSORPTION ANALYSIS BY THE METHOD OF VAN NESS
C DIMENSION YE(20,5),AM(5),AP(20),VMF(5),SLOPE(5),XTR(5),
1ADMO(20,5),POL(20,5),TITLE(20),Y(20),SPRED(20,5),X(20,10),SPOMF(20,5)
2,S),FIR(20,5),CALMAS(20,5),XX(20),ADM(5),ZX(20),XE(20,5),AN(20)
C DIMENSION Z(20),POLI(20,5),YY(20,5),CN(10),TMF(5)
1 READ(1,20,END=19) (TITLE(I),I=1,20)
20 FORMAT(20A4)
22 WRITE(3,22) (TITLE(I),I=1,20)
22 FORMAT(1H1,20A4)
22 FORMAT(1,21) (CN(J),J=1,5)
22 READ(1,21) (TMF(J),J=1,5)
22 READ(1,21) CORL,CORH
22 READ(1,21) ADM(J),VMF(J)
22 PO=80.
22 NEO=15
22 NM=3
22 NC=5
22 AM(NC)=AM(2)
C C C GENERATE EQUIDISTANT INDEPENDENT VARIABLES CM-HG
C ARG=0.0
C Z(1)=5.0
C DO 10 I=2,NEQ
10 Z(I)=Z(I-1)+5.0
C DO 100 J=1,5
200 READ(1,21) ADM(J),VMF(J)
C C C READ THE INDEPENDENT AND DEPENDENT VARIABLES
C C
23 FORMAT(1X,10F10.4)
24 FORMAT(1X,3I5)
24 CORAV=VMF(J)*CORH+(1.-VMF(J))*CORL
24 WRITE(3,103) CORL,CORH,CORAV
103 FORMAT(1H0,3CORL=,F10.4,3X,CORH=,F10.4,3X,CORAV=,F10.4)
2026 WT1=ADM(J)
2027 WT2=WT1+TMF(J)/1000.
2028 READ IN VALUES X, Y
C I=0
3 I=I+1
3 READ(1,25) XE(I,J),YE(I,J),N
3 C=CORAV*XE(I,J)/76.
3 YE(I,J)=(YE(I,J)*WT1-TMF(J)-C)/WT2.
4 IF(N-1) 3,4,4
4 N=I-1
4 AN(J)=N
C C SMOOTHED M=F(P,Y)
C C
2037 DO 2 I=1,N
2038 ZX(I)=XE(I,J)/PO
2039 Y(I)=YE(I,J)
2040 NR=1
2041 C2=CN(J)
2042 CALL BET(Y,ZX,N,C1,VM,C,AVER,PO,NR,C2)
2043 CN(J)=C1
C C

```

C CALCULATE THE DEPENDENT VARIABLES

```

0044 DD 101 K=1,NEQ
0045 ARG=Z(K)
0046 CALL EVBET(ARG,RES,C1,VM,C,PO)
0047 YY(K,J)FRES
101 WRITE(3,102) J,(YY(K,J),K,I,NEQ)

```

```

100 CONTINUE
102 FORMAT(1H0,12,5X,15F8.3)
25 FORMAT(6F10.0,11)
LIMITING SLOPE FOR PURE COMPONENT ISOTHERM

```

```

NJUMP=NM+1
DO 5 J=1,NC,NJUMP
N=AN(J)
DO 6 I=1,N

```

```

ZX(I)=XE(I,J)/PO
ADMO(I,J)=YE(I,J)/AM(J)
Y(I)=ADMO(I,J)
C2=CN(J)
NR=1
CALL BET(Y,ZX,N,C1,VM,C,AVER,PO,NR,C2)
SLOPE(J)=VM*CVPO

```

5 INITIAL VALUE FOR MOLE FRACTION ADSORBED

```

NSTOP=NC-1
DO 7 J=2,NSTOP
N=AN(J)
XTR(J)=(VMF(J)*SLOPE(NC))/(VMF(J)*SLOPE(NC)+(1.0-VMF(J))*SLOPE(1))
DO 7 I=1,NEQ

```

```

7 FIR(I,J)=XTR(J)
WRITE(3,23) (XTR(I),I=2,NSTOP)

```

C ADSORBED MOLE OF MIXTURE ON SURFACE

```

DO 8 J=2,NSTOP
N=AN(J)
DO 9 I=1,N
ZX(I)=XE(I,J)/PO
ADMO(I,J)=YE(I,J)/(AM(2)*XTR(J)+AM(1))*(1.0-XTR(J))
WRITE(3,24) J
WRITE(3,23) (XE(I,J),ADMO(I,J),I=1,N)

```

```

8 CONTINUE

```

C ITERATION LOOP FOR NTRIAL GREATER THAN 1

```

NTRIAL=0
41 NTRIAL=NTRIAL+1

```

C CALCULATE CONSTANTS FOR THE NC CURVES OF MIXTURE AND SPREADING PRESSURE FROM BET EQUATION USING SIMPSON-NEWTON-3/8 INTEGRATION RULE

```

DO 50 J=1,NC
IF(NTRIAL-1) 54,54,55

```

```

54 N=AN(J)
55 DO 51 I=1,N

```

```

IF(NTRIAL-1) 56,56,57
56 ZX(I)=XE(I,J)/PO
GO TO 51

```

```

57 ZX(I)=Z(I)/PO

```

```

0089      51 Y(I) =ADMO(I,J)
0090      C2=CN(J)
0091      NR=1
0092      CALL BET(Y,ZX,N,C1,VM,C,AVER,PO,NB,C2)
0093      SLOPE(J)=VM*C/PO
0094      DO 50 I=1,NEQ
0095      ARGZ(I)
0096      CALL PIAORT(ARG,RES,C1,VM,C,PO)
0097      SPRED(I,J)=RES
0098      CALL EVBET(ARG,RES,C1,VM,C,PO)
0099      ADMO(I,J)=RES
0100      50 CONTINUE
0101      DO 53 J=1,NC
0102      WRITE(3,24) J
0103      C
0104      NN=N-1
0105      ND=2
0106      ND=3
0107      NCO=ND+1
0108      DO 38 I=1,NEQ
0109      DO 33 J=1,NC
0110      X(J,I)=VMF(J)
0111      33 Y(J)=SPRED(I,J)
0112      WRITE(3,24) I
0113      CALL FIT(X,Y,NC,ND,AP,0,1,0)
0114      ARG=1,1
0115      DO 43 K=1,11
0116      ARG=ARG-0,1
0117      CALL PEV(RES,ARG,AP,NCO)
0118      43 CONTINUE
0119      DO 34 K=1,NCO
0120      34 POL(I,K)=AP(K)
0121      38 CONTINUE
0122      DO 35 I=1,NEQ
0123      DO 37 K=1,NCO
0124      37 AP(K)=POL(I,K)
0125      DO 36 J=2,NSTOP
0126      ARG=VMF(J)
0127      CALL DER(RES,ARG,AP,NCO)
0128      SPDMF(I,J)=RES
0129      WRITE(3,24) I
0130      WRITE(3,23) (SPDMF(I,K),K=2,NSTOP)
0131      35 CONTINUE
0132      C
0133      RECALCULATE THE ADSORBED MOLE AND ITS FRACTION
0134      WRITE(3,42) NTRIAL
0135      42 FORMAT('RO', I4, ' ITERATION NUMBER',I3,2X,'FOR THE CALCULATION OF ADSO',
0136      1R8B3, ' MOLE FRACTION',//)
0137      SDX=0,0
0138      DO 40 I=1,NEQ
0139      DO 39 J=2,NSTOP
0140      FIRSX=FIR(I,J)
0141      XTR(J)=VMF(J)+VMF(J)*(1,0-VMF(J))*SPDMF(I,J)/ADMO(I,J)
0142      FIR(I,J)=XTR(J)
0143      FIRSTN=ADMO(I,J)
0144      ADMO(I,J)=Y(I,J)/(XTR(J)*AM(2)+(1,0-XTR(J))*AM(1))
0145      DELX=(XTR(J)-FIRSX)/XTR(J)*100
0146      DELN=(ADMO(I,J)-FIRSTN)/ADMO(I,J)*100

```

```

0144 WRITE(3,24) I
0145 SDX=SDX+ABS(DELX)
0146 WRITE(3,23) FIRSTX,XTR(J),DELX,FIRSTN,ADMO(I,J),DELN
0147 39 CONTINUE
0148 N=NEG(SDX/(AN(2)+AN(3)+AN(4)))
0149 N=NEG

C
0150 IF THE SUM OF THE ABSOLUTE VALUE OF PERCENT DEVIATION IS LESS THAN
0151 0.005 END THE ITERATION
0152 IF(NTRIAL-2) 47,47,48
0153 47 IF(SDX-0.05) 48,48,41
0154 21 FORMAT(8F10.0)
0155 48 WRITE(3,44)
0156 44 FORMAT(IH1)
0157 70 FORMAT(IH1,////(TITLE(I),I=1,20)
0158 WRITE(2,49) (TITLE(I),I=1,20)
0159 49 FORMAT(20A4)
0160 64. FORMAT(IH0,6X,'P',9X,'N1',8X,'PI1',7X,'N2',8X,'PI2',7X,'K1',8X,'K2',
0161 1)
0162 DO 45 I=1,NEQ
0163 Z(I)=Z(I)*10.
0164 WRITE(3,46) Z(I),ADMO(I,I),SPRED(I,I),ADMO(I,NC),SPRED(I,NC)
0165 WRITE(2,96) Z(I),ADMO(I,I),SPRED(I,I),ADMO(I,NC),SPRED(I,NC)
0166 45 CONTINUE
0167 DO 72 J=1,NC,NJUMP
0168 WRITE(3,71) J,SLOPE(J)
0169 72 WRITE(1H0,' LIMITING SLOPE',I1,F8.4)
0170 71 FORMAT(1H0,' F10.1,4F10.4,2F10.6)
0171 46 WRITE(3,44)
0172 (TITLE(I),I=1,20)
0173 WRITE(2,49) (TITLE(I),I=1,20)
0174 WRITE(3,66) (VMF(I),I=2,NSTOP)
0175 66 FORMAT(1H0,' GAS MOLE FRACTION: ',/ ,14X,F6.4,18X,F6.4,18X,F6.4)
0176 65 WRITE(3,65) P',3(6X,'X',7X,'N',7X,'PI')
0177 DO 62 I=1,NEQ
0178 WRITE(2,93) Z(I), (FIR(I,J),ADMO(I,J),SPRED(I,J),J=2,NSTOP)
0179 (FIR(I,J),ADMO(I,J),SPRED(I,J),J=2,NSTOP)
0180 62 WRITE(3,63) Z(I), (FIR(I,J),ADMO(I,J),SPRED(I,J),J=2,NSTOP)
0181 67 FORMAT(10F10.4)
0182 56 FORMAT(7F10.6)
0183 93 FORMAT(10F8.4)
0184 61 WRITE(2,61) J
0185 J=1
0186 61 FORMAT(50X,I1)
0187 60 FORMAT(5F10.4)
0188 GO TO 1
0189 RETURN
0190 END

```

0001 SUBROUTINE BET(Y,X,J,C1,C2,C3,AVER,PO,NR,C4)
DENIS GRAVELLE,CHEMICAL ENGINEERING
TO SOLVE THE CONSTANTS OF THE BET EQUATION

12/5/71
DIMENSION Y(20),X(20),YAXIS(20),XAXIS(20),ER(20),YCALC(20),AN(80)
DIMENSION THETA(20),PHINX(20),ASLOPE(80),BINTER(80),STD(80),V(20)
DIMENSION STORE(20),TITLE(20),ERROR(80),XC(20,5),CN(10)

CC SET VALUES OF LAYERS
CC
CC

31 WRITE(3,13)
AP=J

AK=1.0
AN(1)=AK
FAC=AK

4 NPREC1=NPREC1+1
IF(NPREC1-1) 41,41,42

41 NFN=5
GO TO 43

42 NFN=21
43 IF(NR-1) 76,77,77
77 NFN=1

AN(1)=C4
GO TO 80

76 DO 5 K=2,NFN
5 AN(K)=AN(K-1)+AK

CC N-LAYERS B.E.T. EQU. PARAMETERS VM AND C
CC
CC

80 DO 9 K=1,NFN
SUM1=0.
SUM2=0.
SUM3=0.
SUM4=0.
DO 6 I=1,J

CC PREPARE X- AND Y-AXIS
CC
CC

XX=X(I)
IF(XX=0.6) 25,25,26
25 PHINX(I)=XX*(1.-XX**AN(K))-AN(K)*XX**AN(K)*(1.-XX)
1/((1.-XX)*(1.-XX))
THETA(I)=XX*(1.-XX**AN(K))/(1.-XX)
YAXIS(I)=PHINX(I)/Y(I)
XAXIS(I)=THETA(I)

CC LEAST-SQUARES METHOD
CC
CC

SUM1=SUM1+YAXIS(I)

```

SUM2=SUM2+XAXIS(I)*XAXIS(I)
SUM3=SUM3+XAXIS(I)*YAXIS(I)
SUM4=SUM4+XAXIS(I)
6 CONTINUE
DD=AP*SUM2-SUM4*SUM4
ASLOPE(K)=(AP*SUM3-SUM4*SUM1)/DD
BINTER(K)=(SUM1*SUM2-SUM3*SUM4)/DD

```

CC CALCULATE THE DEPENDENT VARIABLES

```

DO 7 I=1,J
7 YCALC(I)=ASLOPE(K)*XAXIS(I)+BINTER(K)

```

CC EVALUATE STANDARD DEVIATION

```

S=0.
S1=0.
S2=0.
E=0.
DO 8 I=1,J
DEL=YAXIS(I)-YCALC(I)
S=S+DEL*DEL/YCALC(I)
S2=S2+ABS(DEL)
ER(I)=DEL*100./YCALC(I)
E=E+ABS(ER(I))
8 S1=S1+DEL*DEL
ERROR(K)=E/AP
DEV=S2/AP
STD(K)=S1
IF(K-1) 9,9,12
12 IF(STD(K-1)-STD(K)) 10,9,9
9 CONTINUE
IF(NR-1) 78,74,74

```

CC SELECT SMALLEST STD

```

78 K=2
KK=K
AJ=ERROR(1)
33 DO 35 I=KK,NFN
IF(AJ-ERROR(I)) 34,34,36
34 K=K+1
35 CONTINUE
GO TO 37
36 AJ=ERROR(K)
KK=K
GO TO 33
37 NTEST=1
IF(KK.EQ.2) GO TO 55
K=KK
GO TO 12
55 IF(ERROR(1).GT.ERROR(2)) GO TO 64

```

```

0034
0035
0036
0037
0038
0039
0040
0041
0042
0043
0044
0045
0046
0047
0048
0049
0050
0051
0052
0053
0054
0055
0056
0057
0058
0059
0060
0061
0062
0063
0064
0065
0066
0067
0068
0069
0070
0071
0072
0073
0074

```

```

0075 K=1
0076 GO TO 12
0077 K=2
0078 CN(NPREC1)=AN(K)
0079 CN(NPREC1)=AN(K)
0080 STORE(NPREC1)=ERROR(K)
0081 IF(NPREC1) 86,86,84
0082 IF(STORE(NPREC1)-STORE(NPREC1-1)) 86,86,85
0083 IF(K-1) 82,82,87
0084 AN(I)=CN(NPREC1)
0085 GO TO 86
0086 AN(I)=CN(NPREC1-1)
0087 NR=1
0088 NFN=1
0089 GO TO 80

```

SELECT NEW INTERVAL FOR N

```

0090 K=1
0091 IF(K-1) 70,70,71
0092 IF(NPREC1-2) 81,81,74
0093 AN(I)=AN(I)/10.
0094 FAC=AN(I)
0095 AK=FAC
0096 GO TO 74
0097 K=NFN
0098 IF(K-NFN) 72,73,73
0099 AN(I)=AN(NFN)-AK
0100 GO TO 74

```

```

0101 I<K<NFN
0102 AN(I)=AN(K)-FAC
0103 FAC=FAC/10.
0104 AK=FAC
0105 VM=1./ASLOPE(K)
0106 C=1./((VM*BINTER(K))
0107 WRITE(3,14) K,AN(K),ERROR(K),VM,C
0108 IF(NR-1) 79,75,75
0109 IF(NPREC1-2) 4,4,75
0110 75 CONTINUE

```

RECALCULATE THE AMOUNT ADSORBED AND CCMPARE

```

0111 S=0.0
0112 SI=0.
0113 S2=0.
0114 E=0.
0115 DO 11 I=1,J
0116 XX=X(I)
0117 PHINX(I)=XX*((1.-XX**AN(K))-AN(K)*XX**AN(K))*(1.-XX)
0118 1/((1.-XX)*(1.-XX))
0119 THETA(I)=XX*(1.-XX**AN(K))/(1.-XX)
0120 V(I)=VM*CPHINX(I)/(1.+C*THETA(I))
0121 DEL=Y(I)-V(I)
0122 S=S+DEL*DEL/V(I)
0123 S2=S2+ABS(DEL)
0124
0125
0126
0127
0128
0129
0130
0131
0132
0133
0134
0135
0136
0137
0138
0139

```

```

0120 ER(I)=DEL*100./V(I)
0121 S1=S1+DEL*DEL
0122 E=E+ABS(ER(I))
0123 AVER=E/AP
0124 DEV=S2/AP
0125 SD=SQRT(S1/(AP-3.))
0126 WRITE(3,21)
0127 WRITE(3,15) (I,X(I),Y(I),V(I),ER(I),I=1,J)
0128 WRITE(3,16) AVER,DEV,SD,S
0129 WRITE(3,17) VM,C,PO,AN(K)
C AREA=3481.*VM/WT
C WRITE(3,50) AREA
C1=AN(K)
C2=VM
C3=C
KW=1
IF(KW.EQ.1) GO TO 30

```

INFINITE FORM OF THE B-E-T EQUATION (N=>4)

```

0135 IF(AN(K)-4.) 28,32,32
0136 WRITE(3,39)
0137 FORMAT(1H0.,N>4, THE INFINITE FORM OF THE B-E-T EQU. IS USED'//)
0138 SUM1=0.0
0139 SUM2=0.0
0140 SUM3=0.0
0141 SUM4=0.0
0142 DO 38 I=1,J
0143 YV=X(I)/(Y(I)*(1.-X(I)))
0144 XX=X(I)
0145 SUM1=SUM1+YY
0146 SUM2=SUM2+XX*XX
0147 SUM3=SUM3+XX*YY
0148 SUM4=SUM4+XX
0149 DD=AP*SUM2-SUM4*SUM4
0150 AS=(AP*SUM3-SUM4*SUM1)/DD
0151 AI=(SUM1*SUM2-SUM3*SUM4)/DD
0152 C=AS/AI+1.0
0153 VM=1./(AI*C)
0154 AREA=3481.*VM/WT
0155 S=0.
0156 S1=0.0.
0157 S2=0.0
0158 E=0.0
0159 DO 40 I=1,J
0160 V(I) =(VM*C*X(I))/(1.-X(I))+X(I)*(1.-X(I))*(C-1.)
0161 DEL=V(I)
0162 S=S+DEL*DEL/V(I)
0163 S2=S2+ABS(DEL)
0164 ER(I)=DEL*100./Y(I)
0165 E=E+ABS(ER(I))
0166 S1=S1+DEL*DEL
0167 AVER=E7AP
0168 DEV=S2/AP
0169 SD =SQRT(S1/(AP-2.))
0170 WRITE(3,21)

```


0001 SUBROUTINE PIAORT(ARG,RES,AN,VM,C,PO)
 C DENIS GRAVELLE, CHEMICAL ENGINEERING
 C TO OBTAIN THE SPREADING PRESSURE FROM EQUIDISTANT POINTS BY THE
 C SIMPSON-NEWTON-3/8 RULE
 C 12/5/72

DIMENSION X(50),Y(50),Z(50)

0002 ANEQ=20
 0003 ANEQ=NEQ
 0004 X(1)=0.0
 0005 Y(1)=VM*C/PO
 0006 HINC=ARG/(ANEQ-1.0)
 0007 DO 1 I=2,NEQ
 0008 AI=I
 0009 X(I)=(AI-1.0)*HINC
 0010 R=X(I)/PO

0011 PHI=((1.0-R**AN)-AN*R**AN*(1.-R))/(1.-R)**2.0

0012 TETA=R*(1.-R**AN)/(1.-R)
 0013 Y(I)=VM*C/PO/(1.+C*TETA)*PHI

0014 DO 1 CONTINUE
 0015 CALL SURF(HINC,Y,X,NEQ)
 0016 RES=X(NEQ)
 0017 WRITE(3,3) NEQ,HINC,PO,P

C 3 FORMAT(1H0,' NO. OF EQUIDISTANT POINTS:',I3.3X,' HAVING INTERVAL

C 1 OF: ',F10.4,3X,' REF. PRESS.:',F10.2,3X,' PRESS.:',F10.2)

C C WRITE(3,2) Y(NEQ),X(NEQ)

C 2 FORMAT(1H0,' N/P=',F10.4,3X,' SPREADING PRESSURE ',F10.4)

RETURN
 END

0018
 0019

0001 SUBROUTINE SURF(H,Y,Z,NDIM)
 DENIS GRAVELLE, CHEMICAL ENGINEERING 26/4/72
 SURFACE AREA FOR EQUIDISTANT POINTS BY THE SIMPSON-NEWTON 3/8 S RULE
 00000020
 00000040
 00000070

0002 DIMENSION Y(50),Z(50),X(50)
 0003 HT=.333333333333333 #H
 0004 IF(NDIM-5) 7,8,1

0005 NDIM IS GREATER THAN 5. PREPARATIONS OF INTEGRATION LOOP
 0006 SUM1=Y(2)+Y(2)
 0007 SUM1=SUM1+SUM1
 0008 SUM1=HT*(Y(1)+SUM1+Y(3))
 0009 AUX1=Y(4)+Y(4)
 0010 AUX1=AUX1+AUX1
 0011 AUX1=SUM1+HT*(Y(3)+AUX1+Y(5))
 0012 AUX2=HT*(Y(1)+3.875D0*(Y(2)+Y(5))+2.625D0*(Y(3)+Y(4))+Y(6))
 0013 SUM2=Y(5)+Y(5)
 0014 SUM2=SUM2+SUM2
 0015 SUM2=AUX2-HT*(Y(4)+SUM2+Y(6))
 0016 Z(I)=0.
 0017 AUX=Y(3)+Y(3)
 0018 AUX=AUX+AUX
 0019 Z(2)=SUM2-HT*(Y(2)+AUX+Y(4))
 0020 Z(3)=SUM1
 0021 Z(4)=SUM2
 IF(NDIM-6) 5,5,2

0022 INTEGRATION LOOP
 0023 DO 4 I=7,NDIM,2
 0024 SUM1=AUX1
 0025 SUM2=AUX2
 0026 AUX1=Y(I-1)+Y(I-1)
 0027 AUX1=AUX1+AUX1
 0028 AUX1=SUM1+HT*(Y(I-2)+AUX1+Y(I))
 0029 Z(I-2)=SUM1
 0030 IF(I-NDIM)3,6,6
 0031 AUX2=Y(I)+Y(I)
 0032 AUX2=AUX2+AUX2
 0033 AUX2=SUM2+HT*(Y(I-1)+AUX2+Y(I+1))
 0034 Z(I-1)=SUM2
 0035 Z(NDIM-1)=AUX1
 Z(NDIM)=AUX2
 GO TO 13

0036 RETURN
 0037 Z(NDIM-1)=SUM2
 0038 Z(NDIM)=AUX1
 0039 GO TO 13
 RETURN
 END OF INTEGRATION LOOP

0040 IF(NDIM-3) 12,11,8
 0041 NDIM IS EQUAL TO 4 OR 5
 0042 SUM2=1.125 #HT*(Y(1)+Y(2)+Y(3)+Y(4))
 SUM1=Y(2)+Y(2)

```

0043 SUM1=SUM1+SUM1
0044 SUM1=HT*Y(1)+SUM1+Y(3)
0045 Z(1)=0.
0046 AUX1=Y(3)+Y(3)
0047 AUX1=AUX1+AUX1
0048 Z(2)=SUM2-HT*(Y(2)+AUX1+Y(4))
0049 IF(NDIM-5)10,9,9
0050 9 AUX1=Y(4)+Y(4)
0051 AUX1=AUX1+AUX1
0052 Z(5)=SUM1+HT*(Y(3)+AUX1+Y(5))
0053 10 Z(3)=SUM1
0054 Z(4)=SUM2
      C GO TO 13
      C RETURN

```

```

0055 00000690
      C
0056 NDIM IS EQUAL TO 3
0057 SUM1=HT*(1.25 *Y(1)+Y(2)+Y(2)-2.5D0*Y(3))
0058 SUM2=Y(2)+Y(2)
0059 SUM2=SUM2+SUM2
0060 Z(3)=HT*(Y(1)+SUM2+Y(3))
0061 Z(1)=0.
0062 Z(2)=SUM1

```

```

      C CONTINUE
      C 12 DO 14 I=1,NDIM
      C 13 DO 14 I=1,NDIM
      C 14 X(I)=Z(I)
      C RETURN
      C END
0063
0064

```

```

0001 C SUBROUTINE PEV ( RES,ARG,X,IDI MX )
0002 EVALUATE A POLYNOMIAL FOR A GIVEN VALUE OF THE VARIABLE
0003 DIMENSION X(20)
0004 RES=0.0
0005 J=IDI MX
0006 1 IF(J) 3,3,2
0007 2 RES=RES*ARG+X(J)
0008 J=J-1
0009 GO TO 1
0010 3 RETURN
0011 END

```

```

0001 C
0002 SUBROUTINE FIT(XX,Y,NDATA,NDEG,AP,KLI N,KZERO,NWRITE)
0003 YES=1
0004 K=NDATA-1
0005 DIMENSION XX(20,10),XR(20,10),Y(20),AP(20),STORE(20)
0006 IF(KLIN-1) 2,1,2
0007 1 IF(NDEG-K) 3,3,4
0008 3 CALL REG(XX,Y,NDEG,NDATA,AP,PER,KZERO)
0009 GO TO 4
0010 2 IF (NDEG-K) 5,5,4
0011 5 DO 6 J=1,NDEG
0012 AJ=J
0013 DO 6 I=1,NDATA
0014 XR(I,J)=XX(I,1)**AJ
0015 6 CALL REG(XR,Y,NDEG,NDATA,AP,PER,KZERO,NWRITE)
0016 4 WRITE(3,7) PER
0017 7 FORMAT(1X,' AVERAGE PERCENT DEVIATION ',F10.4)
0018 RETURN
0019 END

```



```

0045 GO TO 2051
0046 END OF CORRECTION CALCULATION
0047 B(K,J)=B(K,J)/B(K,K)
0048 J=J-1
0049 GO TO 2051
0050 DO 2013 I=1,NN
0051 IF(I-K) 2066,2013,2066
0052 J=NN
0053 IF(J-K) 2013,2099,2099
0054 B(I,J)=B(I,J) - B(I,K)*B(K,J)
0055 J=J-1
0056 GO TO 2041
0057 CONTINUE
0058 EQUATION IS MADE TO PASS THROUGH ZERO
0059 IF(KZERO-I) 2101,2102,2101

```

```

2101 NN=N+1
2102 NNN=N+2
2103 DO 2100 I=2,NN
2104 B(I,NNN)=B(I-1,NN)
2105 B(I,NNN)=0.0
2106 WRITE(3,2053)
2107 DO 2011 I=1,NN
2108 MM=I-1
2109 WRITE(3,2077) MM,B(I,NNN)
2110 CALCULATION OF DATA BASED ON REGRESSION COEFFICIENTS
2111 IF(NWRITE-1) 2108,2109,2109
2112 WRITE(3,2091)
2113 DO 2064 MMM=1,NDATA
2114 YCALC(MMM)=B(I,NNN)
2115 DO 2064 I=2,NN
2116 IJK=I-1
2117 YCALC(MMM)=YCALC(MMM) + B(I,NNN)*X(MMM,IJK)
2118 SUMYC=0.0
2119 DSQ=0.0
2120 DO 2110 I=1,NDATA
2121 SUMYE=SUMYE + Y(I)*Y(I)
2122 SUMYC=SUMYC + YCALC(I)*YCALC(I)
2123 DELTAY(I)=Y(I) - YCALC(I)
2124 ERROR(I)=DELTAY(I)/YCALC(I)*100.0
2125 DSQ=DSQ + DELTAY(I)*DELTAY(I)
2126 IF(NWRITE-1) 2110,2111,2111
2127 WRITE(3,2080) (X(I,J),J=1,N),Y(I),YCALC(I),DELTAY(I),ERROR(I)
2128 CONTINUE
2129 SYE=(SUMYE=SUMYC)/DATA
2130 SIGMA=SUMYE/DATA
2131 R=1.0-SY/SIGMA
2132 R=SQRT(ABS(R))
2133 IF(NWRITE-1) 2112,2113,2113
2134 WRITE(3,2021) DSQ
2135 WRITE(3,2082) SY
2136 WRITE(3,2083) SIGMA
2137 WRITE(3,2084) R
2138 DO 2106 I=1,NN
2139 AP(I)=B(I,NNN)
2140 AVERAGE PERCENT ERROR

```

```

0097 S=0.0
0098 DD 2107 I=1,NDATA
0099 S=S+ABS(ERROR(I))
0100 PER=S/DATA
0101 DD 2098 I=1,NDATA
0102 ERR(I,1)=ERROR(I)
0103 XPLOT(I,1)=Y(I)
0104 XPLOT(I,2)=Y(I)
0105 YPLOT(I,1)=YCALC(I)
0106 YPLOT(I,2)=XPLOT(I,2)
0107 NPNTS(1)=NDATA
0108 NPNTS(2)=NDATA
0109 WRITE(3,2097,1)
0110 CALL MPLOTS(XPLOT,YPLOT,NPNTS,2,2,81,49,10,6)
0111 WRITE(3,2096)
0112 CALL MPLOTS(XPLOT,ERR,NPNTS,1,2,81,49,10,6)
0113 RETURN
0114 C2003 WRITE(6,2008)
0115 C2003 WRITE(3,2008)
0116 RETURN
0117 C2010 WRITE(6,2012)
0118 C2010 WRITE(3,2012)
0119 RETURN
0120 C2052 WRITE(3,2052)
0121 C2052 WRITE(6,2052)
0122 RETURN
0123 FORMAT(' N IS GREATER THAN 5.//')
0124 FORMAT(' NDATA IS GREATER THAN 250.//')
0125 FORMAT(' ERROR CRITERION --- SUM OF SQUARES OF DELTAY IS',
0126 'E14.7.//')
0127 FORMAT(' THE REGRESSION COEFFICIENTS ARE',//)
0128 FORMAT(' REGRESSION EQUATION IS OF DEGREE',I2,' AND IS BASED ON',
0129 'I4,' DATA POINTS',//)
0130 FORMAT(32X,'A(',I2,') IS',E14.7,//)
0131 FORMAT(1X,8E14.7)
0132 FORMAT(' EVALUATION IMPOSSIBLE DUE TO ZERO DIAGONAL TERMS',//)
0133 FORMAT(' MEAN SQUARE DEVIATION IS',E14.7,//)
0134 FORMAT(' VARIANCE IS',E14.7,//)
0135 FORMAT(' REGRESSION INDEX OF CORRELATION IS',F9.5,//)
0136 FORMAT(' DATA COMPARISON FOLLOWS AS (K(NDATA,I),I=1,N),Y(NDATA),',
0137 'YCALC(NDATA),DELTAY(NDATA),ERROR(PERCENT)',//)
0138 FORMAT(30X,' PLOT OF ERROR(I) VERSUS YEXPT(I)',//)
0139 FORMAT(30X,' PLOT OF YCALC(I) VERSUS YEXPT(I)',//)
0140 END

```

```

0001 SUBROUTINE DER(RES,ARG,AP,N)
0002 DIMENSION AP(20)
0003 SUM=AP(2)
0004 DO 1 I=3,N
0005 AI=I
0006 IF(ARG-0.01 2.1,1
0007 1 SUM=SUM+(AI-1.0)*AP(I)*ARG**(AI-2.0)
0008 RES=SUM
0009 2 RETURN
0010 END

```

```

0001 SUBROUTINE EVBET(ARG,RES,C1,VM,C,PO)
0002 ARG=ARG/PO
0003 T1=ARG*((1.-ARG**C1)-C1*ARG**C1*(1.-ARG))/((1.-ARG)*(1.-ARG))
0004 T2=ARG*(1.-ARG**C1)/(1.-ARG)
0005 RES=VM*C*T1/(1.+C*T2)
0006 ARG=ARG*PO
0007 RETURN
0008 END

```

APPENDIX V

CALCULATION OF THE CHARACTERISTIC PARAMETERS OF THE ANALOG
OF THE REDLICH-KWONG EQUATION USING DE BOER'S METHOD

This program was used to calculate the values of a and β of the Redlich-Kwong analog with the method proposed by de Boer (33) using experimental adsorption data of each pure constituents.

The input data are read in the following order:

- 1) Title
- 2) Temperature
- 3) a_{id} , β_{id} (ALFA, BETA)
- 4) Pressure, $P(I)$, moles of gas adsorbed, $A(I)$, and $\pi A/RT$, $PI(I)$ for 15 incremental values of pressures.

The results are summarized in Table IV.4.

VEL 20

MAIN

DATE = 73100

01/11/09

```

DENIS GRAVELLE, CHEMICAL ENGINEERING
VAN DER WAALS EQUATION OF STATE
DIMENSION P(20),PI(20),A(20),X(20),Y(20),TITLE(20)
8 READ(5,1,END=10) (TITLE(I),I=1,20)
1 FORMAT(20A4)
WRITE(6,2) (TITLE(I),I=1,20)
2 FORMAT(1H1,20A4)
CONVT1=6.022
CONVT2=CONVT1**2.0*2.3901*(1.0E-02)
READ(5,20) T
R=1.98717
RT =R*T*(1.0E-03)
READ(5,20) ALPHA,BETA
BETA=BETA*CONVT1
ALPHA=ALPHA*CONVT2
AREA=722.9
N=15
AN=N
20 FORMAT(5F10.0)
DO 3 I=1,N
READ(5,20) P(I),A(I),PI(I)
READ(1,53) P(I),A(I),PI(I)
P(I)=P(I)/10.
PI(I)=RT*PI(I)/AREA
3 A(I)=AREA/A(I)
53 FORMAT(F10.0,20X,2F10.0)
9 FORMAT(F10.0,40X,F10.0)
11 FORMAT(1H0,I2.7E15.4)
BETA=30.
DO 4 J=1,8
BETA=BETA+10.0
4 DO 5 I=1,N
X(I)=BETA/A(I)
Y(I)=ALOG(P(I)*(1.-X(I))/X(I))-X(I)/(1.0-X(I))
X(I)=X(I)/(1.+X(I))-ALOG(1./(1.+X(I)))
5 CONTINUE
WRITE(6,12)
CALL LEASQ(X,Y,N,AA,B)
ALPHAC=-AA*RT*BETA/2.0
ALPHAC=-AA*RT*SQRT(T)*BETA
FACTOR=ALPHAC/ALPHA
AKTWO=EXP(B)
WRITE(6,12)
12 FORMAT(1H1,' VAN DER WAALS EQUATION OF STATE ANALYSIS'////)
12 FORMAT(1H1,' REDLICH-KWONG EQUATION OF STATE ANALYSIS'////)
WRITE(6,14) BETA,ALPHAC,AKTWO,FACTOR
14 FORMAT(1H0,'FOR A VALUE OF BETA=',F10.4,3X,' THE CALCULATED VALUE FOR
10R ALPHA IS ',F10.4,/, ' AND THE VALUE OF K IS ',F10.4,3X, 'FACTO

```

VEL 20

MAIN

DATE = 73100

01/11/09

```

3R =*,F10.4//)
WRITE(6,15)
15 FORMAT(1H0,'FRACTION ADSORBED, OBSERVED PRESSURE, CALCULATED PRESSURE
1E, DIFFERENCE AND PERCENT DEVIATION'//)
S=0.
DO 6 I=1,N
X(I)=BETA/A(I)
PC=AKTWO*X(I)/(1.0-X(I))*EXP(X(I)/(1.0-X(I)))*EXP(-2.*ALPHAC*X(I)/RT/BETA)
1RT/BETA)
PC=AKTWO*X(I)/(1.-X(I))*EXP(X(I)/(1.-X(I)))
PC=PC*EXP(-ALPHAC/BETA/RT/SQRT(T)*(X(I)/(1.+X(I))-ALOG(1./(1.+X(I))))
1))))
DEL=PC-P(I)
S=S+DEL*DEL
PER=DEL/P(I)*100.
6 WRITE(6,11) I,X(I),P(I),PC,DEL,PER
WRITE(6,7) N,S
7 FORMAT(1H0,' FOR',I5,3X,' THE SUM OF DEVIATION SQUARED IS ',E10.4)
WRITE(6,52)
52 FORMAT(1H1,' SPREADING PRESSURE CALCULATION ')
S=0.0
DO 51 I=1,N
PIC=RT/(A(I)-BETA)-ALPHAC/A(I)/A(I)
PIC=RT/(A(I)-BETA)-ALPHAC/A(I)/(A(I)+BETA)/SQRT(T)
DEL=PIC-PI(I)
S=S+DEL*DEL
PER=DEL/PI(I)*100.
51 WRITE(6,11) I,X(I),PI(I),PIC,DEL,PER
WRITE(6,7) N,S
4 CONTINUE
GO TO 8
10 RETURN
END

```

LEVEL 20

LEASQ

DATE = 73100

01/11/09

```
SUBROUTINE LEASQ(X,Y,N,A,B)
DIMENSION X(20),Y(20)
S1=0.0
S2=0.0
S3=0.0
S4=0.0
DO 1 I=1,N
S1=S1+Y(I)
S2=S2+X(I)*X(I)
S3=S3+X(I)*Y(I)
S4=S4+X(I)
1 CONTINUE
AN=N
D=AN*S2-S4*S4
A=(AN*S3-S4*S1)/D
B=(S1*S2-S3*S4)/D
WRITE(6,3) N,A,B
S1=0.0
S2=0.0
DO 2 I=1,N
6 YC=A*X(I)+B
7 DEL=Y(I)-YC
PER=DEL*100./YC
S1=S1+ABS(DEL)
S2=S2+ABS(PER)
WRITE(6,3) I,Y(I),YC,DEL,PER
2 CONTINUE
AVDEV=S1 /AN
AVPER=S2 /AN
WRITE(6,3) I,AVDEV,AVPER
3 FORMAT(1H0,20X,I2,4F10.4)
RETURN
END
```

APPENDIX VI

CALCULATION OF THE CHARACTERISTIC PARAMETERS OF THE ANALOG OF
THE REDLICH-KWONG EQUATION BY EXTENDING THE METHOD OF CHANG-LU
PROPOSED IN V.L.E. CALCULATIONS

This program was used to calculate the values of a and β of the Redlich-Kwong analog using experimental adsorption data.

The input data are read in the following order:

- 1) Title
- 2) Temperature, T
- 3) Pressure, P(I), moles of gas adsorbed, X(I,1),
 $\tau A/RT$ for gas 2, Y(I,2) for 15 incremental values
of pressure.

The output data are listed in Tables IV.5 of Appendix

I.

DATA INPUT

ETHANE - ETHYLENE - SILICA GEL AT 25.0 DEG. CENTIGRADE

298.16 305.5 48.5 282.66 49.98 0.0142 0.0381

50.0000	0.0655	0.0672	0.1559	0.1716
100.0000	0.1239	0.1315	0.2701	0.3163
150.0000	0.1773	0.1920	0.3638	0.4441 ₅
200.0000	0.2265	0.2498	0.4457	0.5602
250.0000	0.2722	0.3053	0.5198	0.6677
300.0000	0.3148	0.3588	0.3883	0.7686
350.0000	0.3547	0.4102	0.6519	0.2641
400.0000	0.2922	0.4602	0.7112	0.9551
450.0000	0.4275	0.5024	0.7668	1.0421
500.0000	0.4609	0.5552	0.2126	1.1256
550.0000	0.4925	0.6007	0.2669	1.2059
600.0000	0.5225	0.6442	0.9112	1.2233
650.0000	0.5510	0.6272	0.9526	1.3580
700.0000	0.5782	0.7297	0.9925	1.4301
750.0000	0.6041	0.7705	1.0287	1.4992

C CALCULATION OF OMEGA1 AND OMEGA2 WITH REDLICH-KWONG EQUATION
 C I=PRESSURE
 C K=COMPONENT
 C JJ=TEMPERATURE

```

0001 DIMENSION X(15,2),Y(15,2),TITLE(20),TC(2),PC(2),P(15),HK(2),
      1YA(14),YB(14),XT(14),YET(14),ERRCR(14),W(14)
0002 KK=2
0003 KK=1
0004 AREA=698.
0005 AREA=601.4
0006 AREA=695.4
0007 AREA=722.9
0008 TOL=.00005
0009 N=15
0010 AN=N
0011 JJ=0
0012 1 READ(5,2,END=4) (TITLE(I),I=1,20)
      C NM=14
      C 1 IF(JJ-NM)19,20,20
      C 19 READ(5,2) (TITLE(I),I=1,20)
0013 2 FORMAT(20A4)
      C WRITE(7,34) (TITLE(I),I=1,20)
0014 34 FCRMAT(20A4)
0015 READ(5,6) T,TC(1),PC(1),TC(2),PC(2),HK(1),HK(2)
0016 READ(5,6) DUM
0017 READ(5,6) DUM
0018 READ(5,6) DUM
0019 RT=1.987*T/1000.
0020 DO 3 I=1,15
0021 3 READ(5,6) P(I),X(I,1),Y(I,1),X(I,2),Y(I,2)
0022 6 FCRMAT(7F10.0)
0023 DO 35 K=1,2
0024 WRITE(6,50)
0025 50 FORMAT(1H1,////)
0026 WRITE(6,5) (TITLE(I),I=1,20)
0027 5 FORMAT(1H0,10X,20A4,/)
0028 WRITE(6,7)
0029 7 FCRMAT(1H0,10X,
      1, 'I',4X,'J',8X,'N',7X,'PI',8X,'Z',11X,'ALFA',7 X,
      1 'ALFA',7X,'BETA',//)
0030 JJ=JJ+1
0031 DO 30 I=1,N
0032 L=-1
0033 H=.98
      C I=N
0034 ADMOLE=X(I,K)
0035 PIAORT=Y(I,K)
0036 SIG=AREA /ADMOLE

```

```

0037      ZL=PIAORT/ADMOL
0038      PI=PIAORT*1.987*T/AREA./1000.
0039      HK(K)=X(KK,K)/P(KK)*10.
0040      HK(K)=HK(K)-0.03 *HK(K)
0041      32 Z1=P(I)*HK(K)*ZL*1.987*T/1000./10./PI/AREA
0042      THIV=1.0
0043      J=0
0044      40 CONTINUE
0045      IH=0
0046      41 IF(H.LT.1.0) GO TO 42
0047      H=H-0.05
0048      IH=IH+1
0049      IF(IH.LT.20) GO TO 41
0050      43 H=0.98
0051      42 J=J+1
0052      IF(H-0.0) 47,47,49
0053      47 IF(L-0) 46,30,30
0054      46 H=.1
0055      L=1
0056      WRITE(6,48)
0057      48 FORMAT(1HC,' H WAS NEGATIVE')
0058      GO TO 40
0059      49 RH =(1.-ZL*(1.-H))*(1.+H)*ALOG(1.+H)/H/(1.-H)
0060      FFH=ALOG(Z1*THIV)+1.0-ZL+ALOG(1.-H)+RH
0061      DFFH=-1./(1.0-H)+RH*(ZL/(1.-ZL*(1.-H)))
0062      TEST=FFH/DFFH
0063      H=H-TEST/2.0
0064      IF(J.GT.90) GO TO 45
0065      IF(ABS(TEST/H).GT.TOL) GO TO 40
0066      45 CONTINUE
0067      B=H*ZL/PI
0068      A2=B*(1.0/(1.0-H)-ZL)*(1.0+H)/H
0069      WA=A2*PC(K)*T**2.5/TC(K)**2.5
0070      WB=B*PC(K)*T/TC(K)
0071      ZCAL=1./(1.-H)-A2/B*(H/(1.+H))
0072      A=A2*1.987**2.*T**2.5/1000000.
0073      B=B*1.987*T/1000.
0074      R=B/SIG
0075      R1=-A/B/1.987/T/SQRT(T)*1000.
0076      R2=R/(1.-R)
0077      R3=R/(1.+R)
0078      R4=ALOG(1.+R)
0079      AK=HK(K)/AREA
0080      AK=1./AK/B
0081      PCAL=AK*R2*EXP(R2)*EXP(R1*(R3+R4))
0082      PICAL=RT/(SIG-B)-A/SQRT(T)/SIG/(SIG+B)
0083      PICAL=PICAL*1000.

```

```
0084          PI=PI*1000.  
0085          WRITE(6,202) I,J,ADMCLC,PIAORT,ZL,A,B  
0086          202 FORMAT(1H0,6X  
          1          ,2I5,3F10.4,3X,2F10.2)  
          C      WRITE(7,33) P(I),ADMCLC,PIAORT,WA,WE,A,B  
0087          33 FORMAT(F10.1,2F10.4,4F12.4)  
0088          30 CONTINUE  
          C      WRITE(7,36) HK(K)  
0089          36 FCRMAT(F10.6)  
0090          35 WRITE(6,31) HK(K)  
0091          31 FORMAT(1H0,/,/.12X, 'LIMITING SLOPE=',F7.5)  
0092          GO TO 1  
0093          4 RETURN  
          C/GO.FT07F001 DD SYSGLT=B  
0094          END
```

APPENDIX VII

PREDICTION OF PHASE EQUILIBRIA IN MIXTURES USING THE ANALOG OF THE REDLICH-KWONG EQUATION WHOSE COEFFICIENTS HAVE BEEN CALCULATED BY THE METHOD EMPLOYED IN V.L.E. CALCULATIONS PROPOSED BY CHANG AND LU

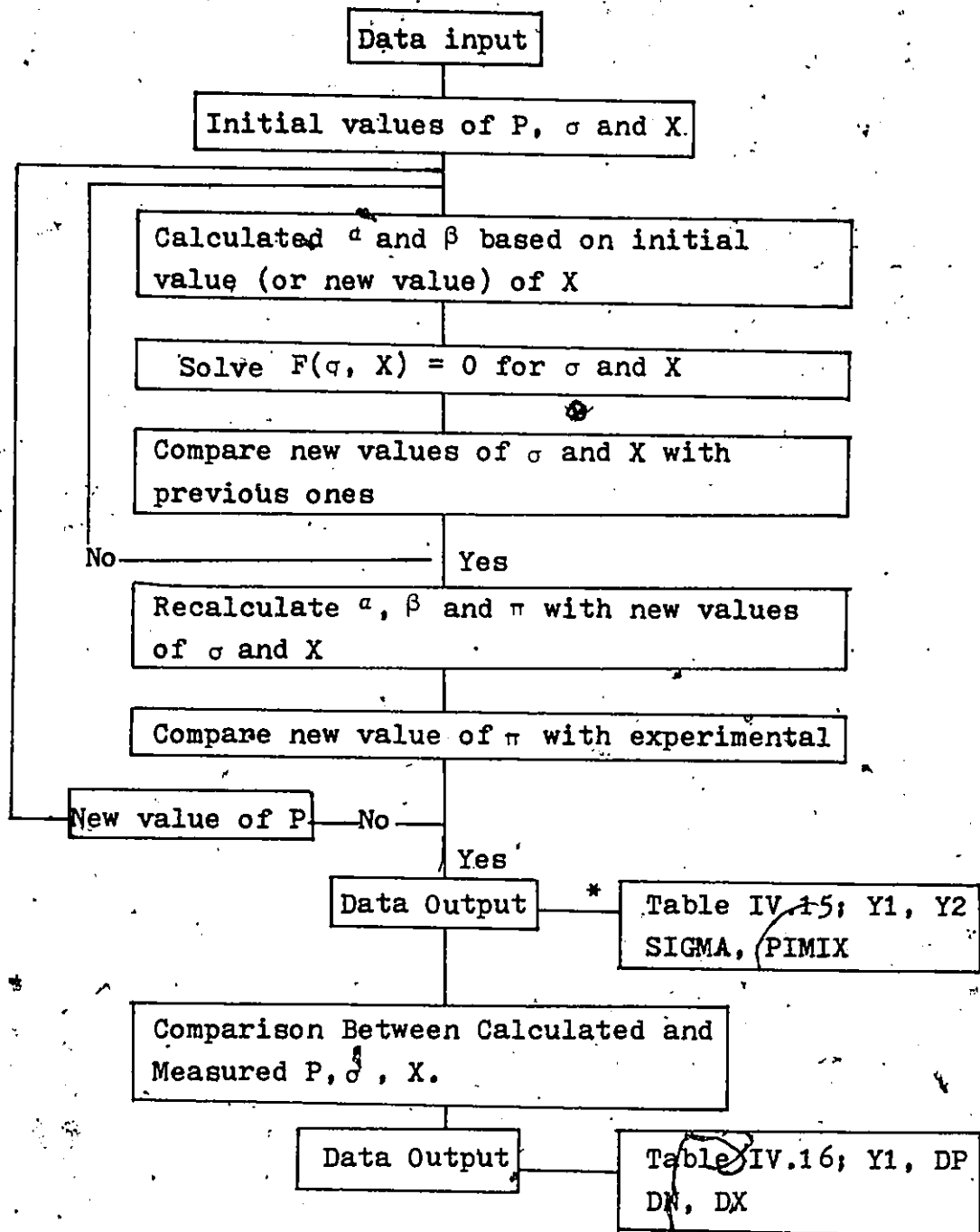
This program was used to calculate the values of σ and X of a binary mixture adsorbed using the analog of the Redlich-Kwong equation of state.

The input data are read in the following order:

- 1) k_{ij}
- 2) C_{ij}
- 3) P_c, V_c, T_c, ω for each pure component
- 4) T , the 3 compositions in the gas phase investigated
- 5) Title
- 6) T, K_1, K_2
- 7) $P, n, \pi A/RT, \alpha_i, \beta_i$ for each pure component
- 8) P, n, X ; experimental data for each composition in the gas phase considered (3 sets).

The output data are listed in Tables IV.15 and IV.16.

The iteration scheme employed to solve for the roots and X using incremental values of P is illustrated below:



* Results of Table IV.16 are obtained for equal intervals of gas phase molar compositions.

DATA INPUT

0.0				
-0.1				
49.98	127.64	282.7	0.085	
48.5	141.72	305.5	0.105	
0.2635	0.5042	0.7547		

ETHANE - ETHYLENE - SILICA GEL AT 25.0 DEG. CENTIGRADE

298.16	0.03024	0.01271		
27.0	0.225	0.25	24200.0	1300.0
200.0	0.228	0.25	11301.0	870.0
136.2	0.2216	0.486		
106.7	0.2142	0.6902		
90.17	0.2241	0.8786		
300.0	0.589	0.7705	5090.0	460.0
750.0	0.6041	0.7705	2513.8	361.7
526.5	0.614	0.4679		
414.4	0.5947	0.6888		
363.3	0.5989	0.7838		
435.0	0.75	1.014	2710.0	342.0
1000.0	0.75	1.014	2514.0	362.0
750.0	0.7673	0.4684		
586.4	0.7579	0.6865		
517.6	0.7616	0.8708		

```
C      TO CALCULATE MOLAR AREA AND ADSORBED PHASE COMPOSITION
      DIMENSION AD(15),ALFA(2),BETA(2),HK(2),TITLE(20),PIAORT(2)
      DIMENSION ARK(2),BRK(2),W(2),PC(2),VC(2),TC(2)
      DIMENSION X1(15),X2(15),Y1(15),Y2(15),SIGMA(15),P(10)
      DIMENSION PIT(15),TP(3),TN(3),TX(3)
      NP=10
      NP=3
      1 READ(5,19,END=17) AKIJ
      READ(5,19) CIJ
      READ(5,19) (PC(I),VC(I),TC(I),W(I),I=1,2)
      READ(5,21) (Y1(I),I=1,3)
      DO 23 I=1,3
      23 Y2(I)=1.-Y1(I)
      32 READ(5,2) (TITLE(I),I=1,20)
      READ(5,19) T, HK(1),HK(2)
      AREA=722.9
      AK=1.98717*(1.0E-03)
      AKT=AK*T
      HK1=HK(1)
      HK2=HK(2)
      DO 16 I=1,2
      16 HK(I)=HK(I)/AREA
      DO 3 KK=1,3
      READ(5,5) (P(I),AD(I),PIAORT(I),ALFA(I),BETA(I),I=1,2)
      60 FORMAT(2F10.0)
      READ(5,21) (TP(I),TN(I),TX(I),I=1,3)
      DO 56 I=1,3
      TP(I)=TP(I)/10.
      56 TN(I)=AREA/TN(I)
      P(1)=P(1)/10.
      P(2)=P(2)/10.
      SIG1=AREA /AD(1)
      SIG2=AREA /AD(2)
      T1=SIG1
      T2=SIG2
      PI=PIAORT(1)*AKT/AREA
      P1=AK*T/((SIG1-BETA(1))-ALFA(1)/SIG1/((SIG1+BETA(1)))/SQRT(T)
      P2=AK*T/((SIG2-BETA(2))-ALFA(2)/SIG2/((SIG2+BETA(2)))/SQRT(T)
      READ(5,31) BETA(1),BETA(2),ALFA(1),ALFA(2),HK(1),HK(2)
      31 FORMAT(20X,6F10.0)
      DO 9 I=1,2
      ARK(I)=ALFA(I)*PC(I)/AK**2.0/TC(I)**2.5
      9 BRK(I)=BETA(I)*PC(I)/AK/TC(I)
      9 HK(I)=1./((HK(I))*BETA(I))
      6 FORMAT(1H0,10F10.4)
      IF(NP.LT.10) GO TO 24
      Y1(1)=.1
      Y2(1)=.9
```

```

DO 18 I=2,9
  AI=I.
  Y1(I)=0.05+0.1*(AI-1.)
18 Y2(I)=1.-Y1(I)
  Y1(10)=.9
  Y2(10)=.1
24 CONTINUE
  CONST=(ARK(1)+ARK(2))*(VC(1)**(1./3.)+VC(2)**(1./3.))**3.0*
  1 (SQRT(TC(1)*TC(2)))**1.5*AK**2.0/(4.656-0.64*(W(1)+W(2)))/82.06
  ALFA12=CONST*(1.-AKIJ)**1.5
C   CIJ=1.-CONST*(1.-AKIJ)**1.5/SQRT(ALFA(1)*ALFA(2))
C   CIJ=1.0-ALFA12/SQRT(ABS(ALFA(1))*ABS(ALFA(2)))
  DO 3 K=1,1
  WRITE(6,34)
  WRITE(6,57)
  WRITE(6,4) (TITLE(I),I=1,20)
  WRITE(6,20) T,PI,P1,P2,P(1),P(2),T1 ,T2 ,HK1,HK2,(I,ALFA(I),I,BE
1TA(I),I=1,2)
  CIJ=0.0
  ALFA12=(ALFA(1)+ALFA(2))/2.*(1.-CIJ)
  ALFA12=SQRT(ABS(ALFA(1))*ABS(ALFA(2)))*(1.-CIJ)
  AN=0.
  PIAV=0.
  SIGAV=0.
22 DO 15 I=1,NP
  X1(I)=Y1(I)*HK(1)/(Y1(I)*HK(1)+Y2(I)*HK(2))
  X2(I)=1.-X1(I)
  PP=P(2)
40 PP=P(1)
  SIGMA(I)=X1(I)*SIG1+X2(I)*SIG2
  SIGMA(I)=X1(I)*BETA(1)+X2(I)*BETA(2)+X1(I)/HK(1)/Y1(I)/PP
  IP=0
36 IT=0
  IP=IP+1
  8 IT=IT+1
  IF(IT-20) 10,10,15
10 BMX=X1(I)*BETA(1)+X2(I)*BETA(2)
  IF(X1(I)-0.0) 15,15,27
27 IF(X2(I)-0.0) 15,15,28
28 AMX=X1(I)**2.*ALFA(1)+2.*X1(I)*X2(I)*ALFA12+X2(I)**2.*ALFA(2)
  EZ1=SIGMA(I)+BMX
  EZ2=SIGMA(I)-BMX
  IF(EZ2-0.0) 15,15,29
29 RT=1.987*T**1.5*BMX/1000.
  A1=-ALOG(EZ2)
  A2=BETA(1)/EZ2
  A3=-2.*(X1(I)*ALFA(1)+X2(I)*ALFA12)*ALOG(EZ1/SIGMA(I))/RT
  A4=AMX*BETA(1)*(ALOG(EZ1/SIGMA(I))-BMX/EZ1)/RT/BMX

```

```

43 FX1=ALOG(HK(1)*PP *Y1(I)/X1(I))
   FSIG1=A1+A2+A3+A4
   X=X1(I)
   SIG=SIGMA(I)
   X1(I)=X1(I)*FSIG1/FX1
   SIG1 =SIGMA(I)*FX1/FSIG1
42 A2=BETA(2)/EZ2
   A3=-2.*(X2(I)*ALFA(2)+X *ALFA12)*ALOG(EZ1/SIGMA(I))/RT
   A4=AMX*BETA(2)*(ALOG(EZ1/SIGMA(I))-BMX/EZ1)/RT/BMX
46 FX2=ALOG(HK(2)*PP *Y2(I)/X2(I))
   FSIG2=A1+A2+A3+A4
   X2(I)=X2(I)*FSIG2/FX2
   SIG2 =SIGMA(I)*FX2/FSIG2
   X1(I)=X1(I)/(X1(I)+X2(I))
   X2(I)=1.-X1(I)
   SIGMA(I)=(SIG1+SIG2)/2.0
45 EX1=X1(I)-X
   ESIG=SIGMA(I)-SIG
   ERX1=ABS(EX1)/X
   ERSIG=ABS(ESIG)/SIG
   IF(ERX1-.005 ) 11,11,8
11 IF(ERSIG-.005 ) 12,12,8
12 AMX=X1(I)**2.*ALFA(1)+2.*X1(I)*X2(I)*ALFA12+X2(I)**2.*ALFA(2)
   BMX=X1(I)*BETA(1)+X2(I)*BETA(2)
   P12=AK*T/(SIGMA(I)-BMX)-AMX/SIGMA(I)/(SIGMA(I)+BMX)/SQRT(T)
   EPI=ABS(P12-PI)
   ERPI=EPI/PI
   PIT(I)=PP
   IF(ERPI-0.005) 50,35,35
35 R=BMX/SIGMA(I)
   R1=-AMX/BMX/AKT/SQRT(T)
   R2=R/(1.-R)
   R3=R/(1.+R)
   R4=ALOG(1.+R)
   HKM=X1(I)*HK(1)+X2(I)*HK(2)
   HKM=1./HKM/BMX
C PP =HKM*R2*EXP(R2)*EXP(R1*(R3+R4))
   PP=PP+.1
   IF(PP-P(2)) 37,15,15
37 IF(IP-500)36,36,50
50 WRITE(6,13) I,PP,Y1(I),X1(I),SIGMA(I),P12
   SIGAV=SIGAV+SIGMA(I)
   PIAV=PIAV+P12
   AN=AN+1.
15 CONTINUE
   IF(AN.LE.0.0) GO T O 3
   PIAV=PIAV/AN
   SIGAV=SIGAV/AN

```

```

WRITE(6,14) CIJ,ALFA12,SIGAV,PIAV
IF(NP.GT.3) GO TO 3
WRITE(6,34)
WRITE(6,53)
WRITE(6,4) (TITLE(I),I=1,20)
WRITE(6,54) T,PI,P1,P2,P(1),P(2),T1 ,T2 ,HK1,HK2,(I,ALFA(I),I,BE
1TA(I),I=1,2)
S1=0.
S2=0.
S3=0.
DO 51 I=1,3
DP=ABS(TP(I)-PIT(I))/PIT(I)*100.
DN=ABS(TN(I)-SIGMA(I))/SIGMA(I)*100.
DX=ABS(TX(I)-X1(I))/X1(I)*100.
WRITE(6,52) Y1(I),DP,DN,DX
S1=S1+DP
S2=S2+DN
S3=S3+DX
51 CONTINUE
S1=S1/3.
S2=S2/3.
S3=S3/3.
WRITE(6,55)S1,S2,S3
WRITE(6,14) CIJ,ALFA12,SIGAV,PIAV
3 CONTINUE
READ(5,33) ICHEK
33 FORMAT(I1)
IF(ICHEK.GE.1) GO TO 1
GO TO 2
17 RETURN
21 FORMAT(3F10.0)
2 FORMAT(20A4)
13 FORMAT(1H0,10X,I5,F10.1,F10.2,F10.4,F10.2,F12.6)
19 FORMAT(4F10.0)
5 FORMAT(5F10.0)
34 FORMAT(1H1,////)
4 FORMAT(1H0,10X,20A4,/)
57 FORMAT(1H0,25X,' PREDICTION OF PHASE EQUILIBRIUM DATA',/)
20 FORMAT(1H0,10X,' TEMPERATURE=' ,F6.2,10X,' SPREADING PRESSURE=' ,F8.
16,/,10X,' CALCULATED SPREADING PRESSURE PI1=' ,F8.6,5X,'PI2=' ,
2F8.6,/,10X,' PURE ADSORBATE PRESSURE P1=' ,F7.2,5X,'P2=' ,F7.2,
3/,10X,' PURE MOLAR AREA SIG1=' ,F7.2,5X,'SIG2=' ,F7.2,/,10X,' L
4IMITING SLOPE K1=' ,F9.5,5X,'K2=' ,F9.5,/,10X,2(' ALFA'
5 ,I1,F10.4,5X,'BETA',I1,F10.4 ,/,10X ),/,15X,'
6I', 7X,'P ',7X,'Y1',7X,'X1' ,6X,'SIGMA', 6X,'PIMIX',/)
14 FORMAT(1H0,10X,' CIJ=' ,F6.3,5X,'ALFA12=' ,F10.4 ,/,10X,' SIGAV=' ,F
17.2,5X,'PIAV=' ,F10.6)
53 FORMAT(1H0,10X,' COMPARISON BETWEEN EXPERIMENTAL AND CALCULATED PH

```

```
1ASE EQUILIBRIUM DATA, //)
54 FORMAT(1H0,10X, 'TEMPERATURE=',F6.2,10X, ' SPREADING PRESSURE=',F8.
16, //,10X, ' CALCULATED SPREADING PRESSURE  PI1=',F8.6,5X, 'PI2=',
2F8.6, //,10X, ' PURE ADSORBATE PRESSURE  P1=',F7.2,5X, 'P2=',F7.2,
3 //,10X, ' PURE MOLAR AREA  SIG1=',F7.2,5X, 'SIG2=',F7.2, //,10X, ' L
4IMITING SLOPE  K1=',F9.5,5X, 'K2=',F9.5, //,10X, 2(' ALFA'
5      ,I1,F10.4,5X, 'BETA',I1,F10.4      , //,10X      ), //,15X, '
6  Y1      DP      DN      DX', //)
52 FORMAT(1H0,10X,F10.4,3F10.2)
55 FORMAT(1H0,11X, 'AVG.  DEV',3F10.2)
END
```